

**NEW INTERFACES TO ADVANCE
POINT-OF-CARE BIOSENSOR DIAGNOSTICS**

A Dissertation
Presented to
The Academic Faculty

by

Yan Zhang

In Partial Fulfillment
of the Requirements for the Degree
Doctor of Philosophy in the
School of Chemical & Biomolecular Engineering

Georgia Institute of Technology
August 2022

COPYRIGHT © 2022 BY YAN ZHANG

**NEW INTERFACES TO ADVANCE
POINT-OF-CARE BIOSENSOR DIAGNOSTICS**

Approved by:

Dr. Mark P. Styczynski, Advisor
School of Chemical & Biomolecular
Engineering
Georgia Institute of Technology

Dr. John Blazeck
School of Chemical & Biomolecular
Engineering
Georgia Institute of Technology

Dr. Julie Champion
School of Chemical & Biomolecular
Engineering
Georgia Institute of Technology

Dr. Pamela Peralta-Yahya
School of Chemistry & Biochemistry
Georgia Institute of Technology

Dr. Shuichi Takayama
Wallace H. Coulter Department of
Biomedical Engineering
Georgia Institute of Technology

Date Approved: June 07, 2022

ACKNOWLEDGEMENTS

Words cannot describe my gratitude to my thesis advisor, Dr. Mark Styczynski, who has been instrumental in my growth as a scientist. He has continued to challenge me to think critically and creatively during my Ph.D. journey. I also had a tremendous amount of creative freedom in my research under his mentorship, which gave me the courage and confidence to aim higher than I had ever before in my career goals.

I am deeply appreciative of my thesis committee members – Dr. Blazeck, Dr. Champion, Dr. Peralta-Yahya, and Dr. Takayama. Their unique perspectives brought valuable insights that influenced different parts of this work, and their questions made me look at my research more critically, all of which helped me to build a stronger thesis research project.

I am also grateful for the opportunity to work with many wonderful collaborators – Dr. Taisuke Kojima, Ge-ah Kim, Tasdiq Ahmed, Dr. Shreyas Dahotre, Aaron Silva Trenkle, Dr. Liangjun Zhao, Dr. M.G. Finn, and Dr. Gabriel Kwong. These collaborations enabled me to gain new knowledge and skills in many different fields of study. These experiences gave me numerous creative insights that helped my thesis research and side project ideas.

I would also like to thank all members of the Styczynski Lab for thought-stimulating conversations and collaborations. Many thanks to Dr. Monica McNerney for training me in cell-free systems and collaborating with me on several projects. I also had the pleasure

of working with Dr. April Miguez, Fernanda Piorino, and Megan McSweeney on different side projects that extended the research boundaries of this thesis.

I also need to thank my phenomenal team of undergraduate students – Niya Ford, Paige Steppe, Maxwell Kazman, and Vidhya Mallikarjunan. Thank you for entrusting me to serve as your research mentor. Your passion for science is highly contagious, and your dedication to research was instrumental in transforming exploratory project ideas I had in my mind into reality. It was an honor to mentor bright young scientists like you.

Lastly, I want to thank my friends, family, and my partner for their unwavering love and support in my academic journey. I could not have done this without you by my side.

TABLE OF CONTENTS

ACKNOWLEDGEMENTS	iii
LIST OF TABLES	viii
LIST OF FIGURES	ix
LIST OF SYMBOLS AND ABBREVIATIONS	xii
SUMMARY	xiv
CHAPTER 1. INTRODUCTION	1
1.1 Bacterial Biosensors for Point-of-Care Diagnostics	1
1.2 Cell-Free Expression System Enables Point-of-Care Biosensing	4
1.3 New Interfaces to Advance Point-of-Care Cell-Free Biosensors	7
1.3.1 Polymer aqueous two-phase systems for simultaneous detection of diverse analytes	7
1.3.2 Coupling CFE biosensors with personal glucose monitor for analyte quantification	9
1.3.3 Interfacing CFE biosensors with immunoassays for sensitive protein detection	11
1.4 Contribution of this Thesis	14
CHAPTER 2. PROTOCELL ARRAYS FOR SIMULTANEOUS DETECTION OF DIVERSE ANALYTES	15
2.1 Introduction	15
2.2 Materials and Methods	18
2.2.1 Bacterial strains	18
2.2.2 Genetic parts assembly and plasmid preparation	18
2.2.3 Preparation of in-house CFE lysate	19
2.2.4 CFE reactions	20
2.2.5 Protocell CFE reactions	21
2.2.6 Data acquisition and analysis	23
2.2.7 Trigger preparations	24
2.2.8 STEC toehold switch development	24
2.2.9 Human serum processing	25
2.2.10 Lyophilization	25
2.3 Results	26
2.3.1 Compartmentalization of CFE protein expression in ATPS-formed protocells	26
2.3.2 Multiplexed detection of model small molecule and nucleic acid systems	30
2.3.3 Multi-modal detection of clinically relevant targets in a human serum matrix	35
2.3.4 Toward a field-deployable, equipment-free diagnostic platform	42
2.4 Discussion	45

CHAPTER 3. POINT-OF-CARE ANALYTE QUANTIFICATION VIA LYSATE-BASED CELL-FREE BIOSENSORS INTERFACED WITH PERSONAL GLUCOSE MONITORS	51
3.1 Introduction	51
3.2 Materials and Methods	54
3.2.1 Bacterial strains and plasmid preparation	54
3.2.2 Crude E. coli cell-free lysate preparation	55
3.2.3 CFE reactions	56
3.2.4 PGM quantification	57
3.2.5 Serum processing	58
3.2.6 Trigger preparation	58
3.3 Results	59
3.3.1 Lysate-based CFE reaction producing LacZ enzyme can convert lactose to measurable glucose	59
3.3.2 Repurposing a PGM to quantify micronutrients in human serum	63
3.3.3 Extending PGM applications to the detection of bacterial infections	68
3.4 Discussion	72
CHAPTER 4. INTERFACING CELL-FREE EXPRESSION PLATFORMS WITH IMMUNOASSAYS FOR SENSITIVE DETECTION OF PROTEIN BIOMARKERS	75
4.1 Introduction	75
4.2 Materials and Methods	77
4.2.1 DNA preparation	78
4.2.2 DNA-antibody conjugate preparation	78
4.2.3 Sandwich immunoassay for spike protein detection	79
4.2.4 Crude E. coli lysate preparation	80
4.2.5 PURE system and lysate-based CFE reaction preparations	81
4.2.6 Data collection	82
4.3 Results	82
4.3.1 Antibody-conjugated DNA barcodes activate reporter expression in CFE systems	82
4.3.2 Antigen dose-response modulated activation of reporter expression	84
4.3.3 Optimizing PURE system-based CFE platform to reduce background signal	86
4.3.4 Designing a two-enzyme duplex platform to distinguish SARS variants	87
4.3.5 Demonstrating barcode-modulated enzyme activation in CFE systems	91
4.3.6 Demonstrating barcode-modulated enzyme activation in lysate-based CFE systems	92
4.3.7 Toward a duplex SARS-CoV-1 and SARS-CoV-2 detection platform	95
4.4 Discussion	96
CHAPTER 5. CONCLUSIONS AND FUTURE DIRECTIONS	99
5.1 Novelty of This Thesis Research	99
5.1.1 Novelty of protocell arrays	100
5.1.2 Novelty of personal glucose monitor-mediated CFE biosensor quantification	101
5.1.3 Novelty of CFE-coupled immunoassays	102

5.2	Next Steps and Future Directions	103
5.2.1	Next steps for protocell arrays	103
5.2.2	Future directions for protocell arrays	105
5.2.3	Next steps for personal glucose monitor-mediated CFE biosensor quantification	107
5.2.4	Future directions for personal glucose monitor-mediated CFE biosensor quantification	108
5.2.5	Next steps for CFE-coupled immunoassays	109
5.2.6	Future directions for CFE-coupled immunoassays	110
5.3	Concluding Remarks	111
APPENDIX A. Supplementary information for CHAPTER 2: Protocell Arrays for Simultaneous Detection of Diverse Analytes		113
A.1	Initial Validation of <i>B. Theta</i>, Stx1, and Stx2 Switch Activation in CFE Reactions	113
A.2	Sequence Information	115
A.3	Protocell and CFE Reaction Conditions	125
A.4	Primers for Trigger DNA Amplification	128
APPENDIX B. Supplementary information for CHAPTER 3: Point-of-care analyte quantification via lysate-based cell-free biosensors interfaced with personal glucose monitors		130
B.1	Assessment of Batch-to-Batch Variability in Cell-Free Lysates	130
B.2	Sequence Information	132
B.3	CFE Reaction Conditions	138
B.4	Primers for Trigger DNA Amplification	139
APPENDIX C. Supplementary information For CHAPTER 4: Interfacing cell-free expression platforms with immunoassays for sensitive detection of protein biomarkers		141
C.1	Sequence Information	141
C.2	CFE Reaction Conditions	148
REFERENCES		150

LIST OF TABLES

Table 1	Description of plasmid parts and DNA sequences used in CHAPTER 2	115
Table 2	Description of lysate, plasmid concentrations, and reaction additives present in protocell sensors or CFE reactions in each figure in CHAPTER 2	125
Table 3	Primers used for trigger DNA amplification in CHAPTER 2	128
Table 4	Description of plasmid parts and DNA sequences used in CHAPTER 3	132
Table 5	Description of lysate, plasmid concentrations, and reaction additives present in CFE reactions in each figure in CHAPTER 3	138
Table 6	Primers for trigger DNA amplification from <i>E. coli</i> O157: H7 genomic DNA template in CHAPTER 3	139
Table 7	Description of plasmid parts and DNA sequences used in CHAPTER 4	141
Table 8	Description of CFE system, plasmid concentrations, and reaction additives present used for each figure in CHAPTER 4	148

LIST OF FIGURES

Figure 1-1	Mechanisms of transcription factor, riboswitch, and toehold switch biosensors	3
Figure 1-2	Schematic of a lysate-based CFE reaction assembled from crude cell extract, plasmid DNA encoding genetic information to be expressed, and necessary reaction mixtures	5
Figure 1-3	Schematic of multiplexed ATPS-ELISA	9
Figure 1-4	Schematic of Xiang and Lu's work in repurposing the PGM to detect analytes other than glucose	11
Figure 1-5	Schematic of different approaches linking DNA molecules to detection antibodies to accomplish immuno-PCR	13
Figure 2-1	Schematic of the membrane-less protocell array platform for simultaneous detection of multiple analytes	16
Figure 2-2	Injection-molded polystyrene plates used in protocell array reactions	22
Figure 2-3	Characterization of protein expression and reaction compartmentalization in membrane-less protocells	28
Figure 2-4	Characterization of CFE reaction compartmentalization and protein production in PEG-Ficoll and PEG-dextran ATPS	30
Figure 2-5	Simultaneous detection of multiple model small molecules in membrane-less protocell arrays	31
Figure 2-6	Simultaneous detection of multiple model nucleic acid sequences in membrane-less protocell arrays	33
Figure 2-7	Co-expression of triggers B and H in single-phase CFE reactions mutually represses their outputs	35
Figure 2-8	Protocell array setup for simultaneous detection of zinc and vitamin B12 in protocell arrays	36
Figure 2-9	Protocell array setup for simultaneous detection of BT and STEC bacteria	38

Figure 2-10	Simultaneous detection of multiple clinically relevant biomarkers across multiple molecular classes in water and 20% human serum matrices	40
Figure 2-11	Protocell array output can be interpreted without equipment.	43
Figure 2-12	A membrane-less protocell array meets key criteria for a minimal-equipment, field-deployable multiplexed assay	44
Figure 3-1	Schematic of glucose monitor-mediated measurement of an analyte present in the biological sample	53
Figure 3-2	Characterization of glucose production and depletion in CFE reactions	60
Figure 3-3	Characterization of naproxen quenching in CFE reactions. Error bars in each sub-panel represent standard deviations of CFE reaction triplicates	62
Figure 3-4	Application of PGM-mediated quantification of zinc in CFE reactions	65
Figure 3-5	Endogenous metabolism in CFE reactions readily removed a wide range of glucose spiked into human serum without impacting protein expression	67
Figure 3-6	Application of PGM-mediated quantification of nucleic acids in CFE reactions	69
Figure 4-1	Schematic of the sandwich immunoassay interfaced with a CFE system	77
Figure 4-2	Activity comparison of free DNA barcode (Free) and antibody-conjugated DNA barcode (Conj) to express LacZ alpha fragment in the PURE <i>frex</i> ® system	84
Figure 4-3	Sensitivity of sandwich immunoassay interfaced with the PURE <i>frex</i> ® platform	85
Figure 4-4	Background LacZ contamination assessment in PURE <i>frex</i> ® and PURE <i>Express</i> ® systems	86
Figure 4-5	Schematic of the proposed duplex platform to detect SARS-CoV-1 and SARS-CoV-2 infection in a single test	88

Figure 4-6	Assessment of enzyme activities and the impact of iron cofactors in PURExpress® reactions	89
Figure 4-7	The addition of antioxidants prevented Fe ²⁺ oxidation in PURExpress®	91
Figure 4-8	Low sensitivity of trigger barcode-activated enzyme expression in PURExpress® systems	92
Figure 4-9	Linear DNA protection capabilities of χ DNA endonuclease inhibitor	93
Figure 4-10	Two toehold switches (B and S2) specifically activated their respective enzymes to produce visually distinct colors in crude cell lysate systems	94
Figure 4-11	Development of a sandwich, duplex immunoassay to detect and distinguish Spike/RBD proteins from SARS-CoV-1 and SARS-CoV-2	96
Figure 12	<i>B. Theta</i> , Stx1, and Stx2 Switch Activation in Response to Their Cognate Triggers in CFE Reactions	113
Figure 13	Assessment of lysate batch-to-batch variability in target quantification	130

LIST OF SYMBOLS AND ABBREVIATIONS

ATP	Adenosine Triphosphate
ATPS	Aqueous Two-Phase System
BT	<i>Bacteroides thetaiotaomicron</i>
CFE	Cell-Free Expression
CLIA	Clinical Laboratory Improvement Amendments
CoA	Coenzyme A
COVID	Coronavirus Disease
CPR	Chlorophenol Red
CPRG	Chlorophenol Red- β -D-Galactopyranoside
CTP	Cytidine Triphosphate
DNA	Deoxyribonucleic Acid
EA	Ethanolamine
EC	<i>Escherichia coli</i>
ELISA	Enzyme-linked Immunosorbent Assay
GFP	Green Fluorescent Protein
GTP	Guanosine Triphosphate
HPLC	High Performance Liquid Chromatography
ICP-MS	Inductively Coupled Plasma Mass Spectrometry
IPTG	Isopropyl β -D-1-Thiogalactopyranoside
LFA	Lateral Flow Assay
MG	Malachite Green
MGA	Malachite Green Aptamer

NAD	Nicotinamide Adenine Dinucleotide
NASBA	Nucleic Acid Sequence-Based Amplification
NHS	N-Hydroxysuccinimide
OD	Optical Density
PBS	Phosphate Buffered Saline
PCR	Polymerase Chain Reaction
PEG	Polyethylene Glycol
PEP	Phosphoenolpyruvic acid
PGM	Personal Glucose Monitor
PURE	Protein synthesis Using Recombinant Elements
RBD	Receptor Binding Domain
RNA	Ribonucleic Acid
RNAP	RNA Polymerase
RT-RPA	Reverse Transcription-Recombinase Polymerase Amplification
SARS	Severe Acute Respiratory Syndrome
SDS-PAGE	Sodium Dodecyl Sulfate-Polyacrylamide Gel Electrophoresis
STEC	Shiga toxin-producing <i>E. coli</i>
TL	Translation
TX	Transcription
UTP	Uridine Triphosphate
X-Gal	5-Bromo-4-Chloro-3-Indolyl- β -D-Galactoside
YTP	Yeast Tryptone Phosphate

SUMMARY

Inexpensive and field-deployable diagnostics that can detect and characterize different analyte concentrations at the point of care have the potential to enable efficient disease diagnosis and monitoring, leading to better patient outcomes. Cell-free biosensors, which harness living cells' sense and response capabilities to accomplish the same reactions outside of cells, have emerged as an enabling technology to implement point-of-care diagnostics due to their simplicity, portability, and affordability. To date, numerous cell-free biosensors have been developed and demonstrated in the field to detect pathogens, environmental contaminants, and clinically relevant micronutrients. However, critical gaps in areas of simultaneous detection of multiple analytes (multiplexed detection), point-of-care analyte quantification, and protein biomarker identification still exist and have limited the reach of cell-free diagnostics for point-of-care use.

This thesis describes my work in exploring new interfaces to augment current cell-free biosensor designs and endow them with new sets of analyte detection and quantification capabilities. Specifically, I developed the first-of-its-kind protocell arrays system interfacing cell-free biosensors with polymer aqueous two-phase system, enabling multiplexed detection of analytes spanning multiple molecular classes from a single sample. I also linked cell-free biosensor outputs with ubiquitous personal glucose monitors for point-of-care analyte quantification without the need for bulky analytical instruments. Lastly, I demonstrated that immunoassays detecting protein biomarkers could be coupled to cell-free biosensors, with emerging applications to enable affordable and accessible virus subtyping using protein biomarkers. Taken together, this work presents several

approaches aiming to address the current limitations in point-of-care cell-free diagnostics and provides highly generalizable design frameworks for rapid test reconfiguration toward other analytes.

CHAPTER 1. INTRODUCTION

Cell-derived biosensors responding to diverse classes of analytes and biomarkers are promising candidates for use in point-of-care diagnostics. Implementing these biosensors in cell-free expression systems, which extract the core cellular machinery to accomplish the same sensing reactions outside of cells, further extends the reach of biosensors to field deployment due to the simplicity, portability, and affordability of cell-free systems. To date, numerous cell-free biosensors have been developed in the lab with potential applications in disease diagnosis and environmental monitoring programs. However, significant improvements in cell-free biosensor designs are still needed for impactful uses of these diagnostics in clinical and point-of-care environments. This work explores new interfaces (polymer aqueous two-phase systems, personal glucose monitors, and immunoassays) augmenting cell-free biosensor designs to address current shortcomings in point-of-care analyte detection and unlock the translational potential of cell-free biosensor diagnostics.

1.1 Bacterial Biosensors for Point-of-Care Diagnostics

Rapid and widely accessible disease diagnosis can be a powerful tool for improving patient outcomes, informing public health decisions, and efficiently allocating medical resources. However, current diagnostic tools cannot meet this need: most of them require extensive sample processing, shipping, and off-site analysis, all of which introduce high costs and long wait times for results. As seen in the ongoing COVID-19 pandemic, long wait times and inaccurate test results can frustrate public health policymaking and contribute to overloaded healthcare systems, resulting in otherwise preventable outbreaks

and deaths. To maximize testing efficiency and best inform clinical care, diagnostic tools should produce accurate results for all desired biomarkers in a timely manner, ideally at the testing location.

Bacterial biosensors can meet the need for point-of-care diagnostics. Living cells have extensive capabilities to sense and respond to diverse classes of analytes, from ions to small molecules, to nucleic acids, and proteins, *via* genetic regulators such as transcription factors and riboregulators.

A transcription factor-based biosensor typically consists of a transcription factor protein that specifically binds to a biomolecular ligand (or analyte), resulting in a conformation change in the protein's DNA binding domain (Figure 1-1)¹. This conformation change alters the transcription factor's ability to bind to its respective promoter/operator site, thereby modulating the transcription levels of downstream reporter genes. Despite the simplicity of the analyte-activated regulation of transcription factors, bacteria have evolved at least 50 transcription factor families capable of recognizing a wide variety of analyte classes (amino acids, sugars, metal ions, fatty acids, aromatic compounds, and antibiotics)¹, with emerging applications to global health and environmental monitoring programs. For analyte detection and quantification, transcription factor-based biosensors produce differential reporter signal outputs in response to a range of analyte concentrations. The reporter signal output can then be used to infer the presence and concentration of analytes without using labor-intensive and expensive analysis techniques such as high-performance liquid chromatography (HPLC) or inductively coupled plasma mass spectrometry (ICP-MS), enabling bacterial biosensors to be implemented in resource-limited environments.

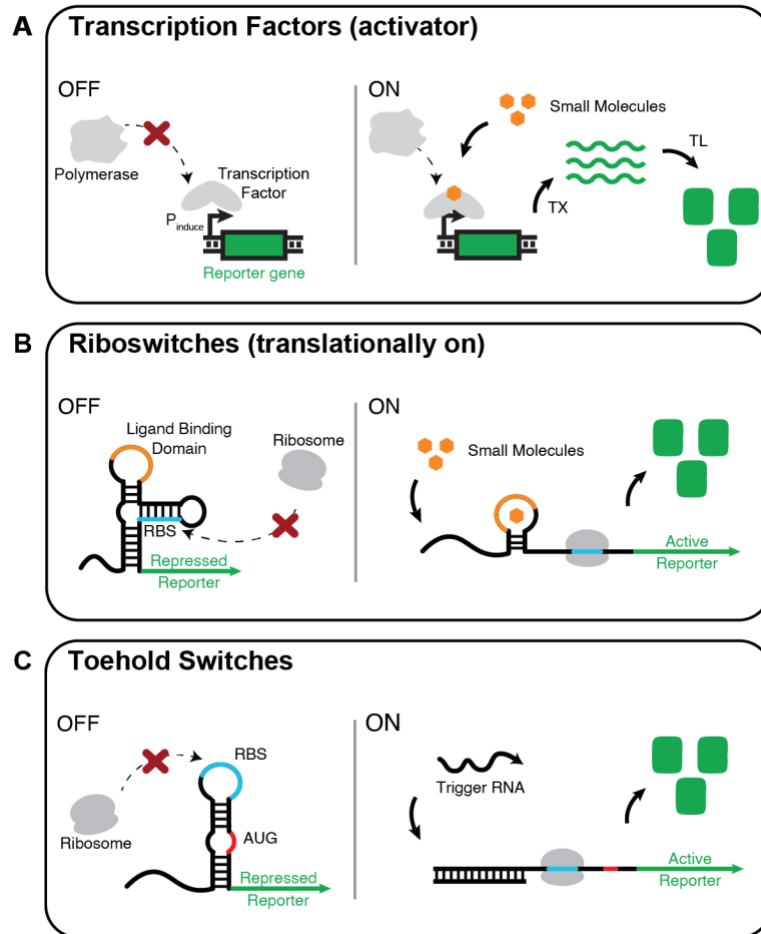


Figure 1-1 Mechanisms of transcription factor, riboswitch, and toehold switch biosensors. (A) A representative activator-type transcription factor regulating reporter transcription. Addition of small molecules alters the protein conformation of the transcription factor, allowing polymerase recruitment to the promoter site (P_{induce}) for reporter gene transcription (TX) and translation (TL). (B) A representative cis-acting riboswitch is activated by a small molecule ligand to regulate translation. Small molecule binding to the riboswitch's ligand-binding domain changes the secondary structure of the riboswitch, exposing the ribosome binding site for reporter protein translation. (C) Toehold switches are de novo designed riboregulators to activate translation in response to a trans-acting trigger RNA. In the presence of trigger RNA, the toehold region of the switch RNA preferentially base pairs with trigger RNA and unwinds the inhibitory hairpin, allowing for downstream translation of the reporter protein.

In addition to transcription factor-based biosensors, riboregulators (in the form of riboswitches and toehold switches) have recently emerged as prominent synthetic biology tools for developing tailormade biosensors. A riboswitch is a regulatory RNA molecule

with a ligand-binding domain (aptamer) that can bind to small molecule analytes², causing a secondary structure change that results in downstream reporter protein production. Analyte-responsive riboswitches may already exist in nature (such as the folate³ and vitamin B₁₂⁴ riboswitches), or they can be directly evolved in laboratories to bind new analytes with user-defined sensitivity and specificity⁵. Like transcription factor-based biosensors, riboswitches also produce differential reporter outputs to a range of analyte concentrations, enabling analyte detection and quantification in resource-limited settings.

For nucleic acid detection, toehold switches have been developed with a toehold-mediated RNA strand displacement motif to unwind inhibitory hairpin structure blocking downstream gene translation⁶. Toehold switches can be designed to detect arbitrary nucleic acid sequences (or “triggers”) and generate downstream reporter proteins. The generalizability of the toehold switch design also enabled its rapid adaptation to detect rapidly emerging infectious diseases⁷⁻⁹, accelerating the timeline from test development to field implementation.

1.2 Cell-Free Expression System Enables Point-of-Care Biosensing

While numerous bacterial biosensors have been developed to detect a wide variety of analytes¹⁰⁻¹⁴, critical challenges in assay portability, turnaround time, and containment exist to implement cellular biosensors in the field¹⁵. The emergence of cell-free expression (CFE) systems in the past decade was the critical advance that enabled the field implementation of biosensor diagnostics. CFE systems harvest the core transcription and translation machinery from living cells to perform the same biological function *in vitro* but with reduced complexity¹⁵. A typical CFE reaction consists of only three components: a

cell extract containing gene expression machinery, a reaction buffer optimized for gene expression, and DNA encoding the genetic program (Figure 1-2). The gene expression machinery is either derived from purified proteins necessary for gene expression (PURE systems) or crude lysates harvested from living cells¹⁵.

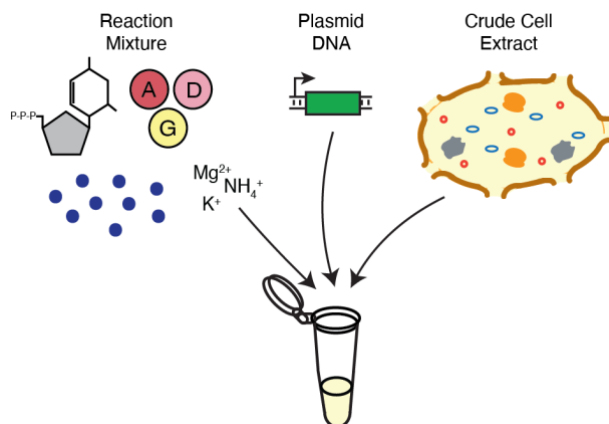


Figure 1-2 Schematic of a lysate-based CFE reaction assembled from crude cell extract, plasmid DNA encoding genetic information to be expressed, and necessary reaction mixtures (nucleotides, amino acids, salts, and cofactors).

Of the various types of lysate systems developed from different organisms (bacteria, yeast, wheat germ, insect cells, etc.), *Escherichia coli* lysate remains the most well-characterized, fastest to prepare, and cheapest to manufacture¹⁵. A typical method to harvest *E. coli* lysate for CFE systems is to grow a strain optimized for production (such as the BL21 strain family) in a rich-medium (2xYTP) and harvest cells in the mid-exponential phase. The resulting cell pellets are washed several times in either glutamate- or acetate-salt buffer and then lysed to extract crude transcription and translation machinery. Cell lysis can be done *via* methods including homogenization¹⁶, sonication¹⁷, and bead-beating¹⁸ for low-cost preparations. For all lysis methods, it is critical to precisely tune the mechanical input to achieve effective cell lysis without denaturing the protein machinery. To enhance transcriptional activity from endogenous *E. coli* polymerases,

additional processing steps such as “run-off” reactions and dialysis into a suitable storage buffer can be performed¹⁹.

Following cell-lysate preparation, a mixture of “energy buffer” mimicking the *E. coli* cytoplasmic environment (salts, cofactors, energy source, and crowding agents) along with the necessary building blocks of protein synthesis (nucleotides and amino acids) are added to the lysate to complete the CFE reaction²⁰. From here, plasmids or DNA fragments encoding for gene expression can be added to the CFE reaction and exogenous reaction additives (such as macromolecular crowders, nuclease inhibitors, or analytes for a biosensing reaction) for reaction activation or improvement.

Using CFE systems to implement biosensors has several advantages over living cells. First, CFE systems remove cell growth and survival burdens, eliminating the trade-off between a cell’s need to proliferate and an engineer’s need to program biological reaction networks. Furthermore, analytes otherwise toxic to living cells can now be detected in CFE systems without inhibiting biosensing reactions²¹. Removing cell growth and cell membrane also accelerate the response time of biosensing reactions; a CFE system can generate signal detection response in as quickly as 20 minutes⁷. Since there is no cell membrane in CFE systems, transport limitations associated with importing DNA programs and macromolecular analytes in living cells are eliminated, providing test engineers open access to precisely design and optimize the reactions. Lastly, compared to whole-cell biosensors, CFE systems can be easily lyophilized for ambient temperature storage and re-activated by sample addition to provide results within an hour⁷, improving test accessibility and turnaround time at the point of care.

These advances in CFE systems have stimulated the development of numerous CFE biosensors to detect diverse classes of analytes in resource-limited environments and at the point of care. Of note, cell-free toehold switch biosensors have been developed to detect infectious viruses^{7,8} and pathogenic bacteria⁹. Transcription factor-based sensing networks have also been implemented in CFE systems to detect environmental contaminants²¹⁻²⁴ and essential micronutrients (zinc)²⁵ in the field.

1.3 New Interfaces to Advance Point-of-Care Cell-Free Biosensors

While the number of CFE biosensors designed for point-of-care use has steadily risen in recent years, key limitations exist in current CFE biosensor designs and have constrained the translational potential of CFE biosensors¹⁵. Bringing in new interfaces to augment current CFE biosensors can endow new capabilities in simultaneous detection of diverse classes of analytes, numerical quantification of analyte concentration in the field, and protein antigen detection in resource-limited settings.

1.3.1 Polymer aqueous two-phase systems for simultaneous detection of diverse analytes

Current sensing and diagnostic tools, especially those designed for use at the point of need, typically only detect one type of analyte at a time, which places significant limitations on the number and the type of tests that can be done on each sample²⁶. To detect all relevant analytes, multiple CFE reactions would need to be run in parallel using multiple aliquots of the sample, introducing handling challenges for onsite testing and collection challenges for samples that are often only available in small volumes. Existing strategies for multiplexed testing, which is the simultaneous detection of different analytes from a single sample, usually require a library of orthogonal reporters, cannot measure analytes

from diverse molecular classes (i.e., both nucleic acid sequences and small molecules), or cannot be used in minimal-equipment settings²⁶⁻³¹.

Arrays of phase-separated biosensors formed by polymer-based aqueous two-phase systems (ATPS) and CFE reactions have the potential to address current limitations in point-of-need measurement multiplexing. Mixing two immiscible aqueous polymer solutions can lead to spontaneous liquid-liquid phase separation, which in appropriate ratios yields “droplets” in a “bulk phase.” The co-existing polymer phases have different entropic properties that allow selective partitioning of biomolecules across phases, enabling selective enrichment, compartmentalization, and reducing unwanted side reactions^{32,33}.

To date, ATPS systems composed of polyethylene glycol (PEG)-dextran polymers and PEG-Ficoll polymers have already been successfully applied to multiplex enzyme-linked immunosorbent assays (ELISAs) to minimize antibody crosstalk^{34,35}. By confining different capture and detection antibodies to phase-separated dextran or Ficoll polymers, protein antigens added in the PEG bulk phase can partition into the dextran or Ficoll polymer phases and bind to their respective capture and detection antibody pairs. The compartmentalization of antibodies in phase-separated polymer environments also enabled otherwise incompatible antibody pairs to co-exist spatially separated in the same environment to minimize cross-reactivity. This approach enabled multiplexed ELISAs to be performed within just one hour of antigen incubation and one wash step to remove unbound detection antibodies for result interpretation (Figure 1-3)³⁶.

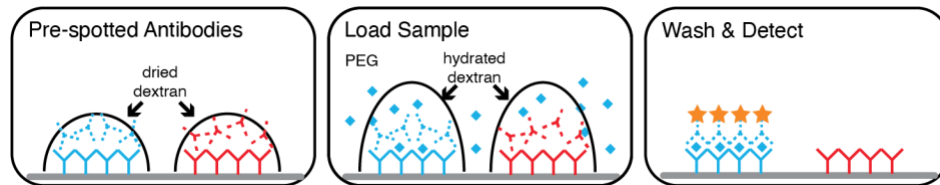


Figure 1-3 Schematic of multiplexed ATPS-ELISA. Different pairs of capture (solid antibody symbol) and detection (dashed antibody symbol) antibodies are mixed with dextran polymer, spotted onto their designated locations inside the microwell, and dried overnight. For antigen detection, the bulk phase polymer (PEG) containing the protein sample is added to the microwell. After a period of incubation and removal of unbound antibodies, different proteins in the same sample can be detected by tracking which microwell location produced the signal.

Studies have shown that similar partitioning and compartmentalization also occur for CFE systems placed in polymer ATPS environment^{37,38}. However, these efforts have focused on using polymer ATPS to create protocell-like model systems to study membrane-less compartmentalization of biochemical reactions for RNA and protein synthesis and catalysis. We envision that arraying biosensing “protocells” formed by polymer ATPS with CFE biosensors in a micro-well can enable simultaneous detection of diverse classes of analytes (from small molecules to nucleic acids and proteins) from just a single sample, leading to a new class of diagnostic platform that is deployable to the point of need.

1.3.2 Coupling CFE biosensors with personal glucose monitor for analyte quantification

For many diseases (such as micronutrient deficiencies), the analyte concentration, rather than its presence or absence, is the basis for diagnosis. However, limited access to analytical instruments has precluded accurate analyte quantification at the point of care. Quantitatively measuring analyte concentrations at the point of care can empower patients and healthcare workers to make faster and better medical choices. This pursuit drives

significant research and industry interest in developing quantitative sensors and electronic devices that enable rapid, affordable, accessible analyte quantification.

Despite numerous advances in the development of quantitative point-of-care diagnostics, few portable devices can match the simplicity and robustness of personal glucose monitors (PGMs)³⁹. Decades of development have made PGMs one of the most widely used analytical sensing platforms; PGMs are inexpensive, ubiquitous, and quantitative. Being able to interface PGMs with biosensor outputs (engineering biosensors to produce glucose in response to analyte concentrations) can enable facile analyte quantification at the point of care³⁹.

Since PGMs can only detect glucose, the challenge in repurposing PGMs to detect other analytes is in linking analyte signals to glucose production that the PGM can measure. The first work to repurpose PGM to quantify non-glucose analytes biomarkers was from Xiang and Lu⁴⁰. The authors devised a clever strategy for the analyte-induced release of the invertase enzyme, which catalyzes the conversion of sucrose to glucose, producing an analyte dose-modulated signal that can be read on the PGM. In this strategy, the DNA aptamer-conjugated invertases were immobilized to magnetic beads *via* DNA strand hybridization (Figure 1-4), and analyte binding to DNA aptamer released invertases from the magnetic beads. After removing the magnetic beads from the solution, sucrose is added to start the conversion to glucose and then measured on the PGM to infer the analyte concentration. This successful demonstration has stimulated many research efforts toward applying this strategy to sense a variety of analytes, including mycotoxins, DNA, enzymes, metal ions, and pathogenic bacteria³⁹.

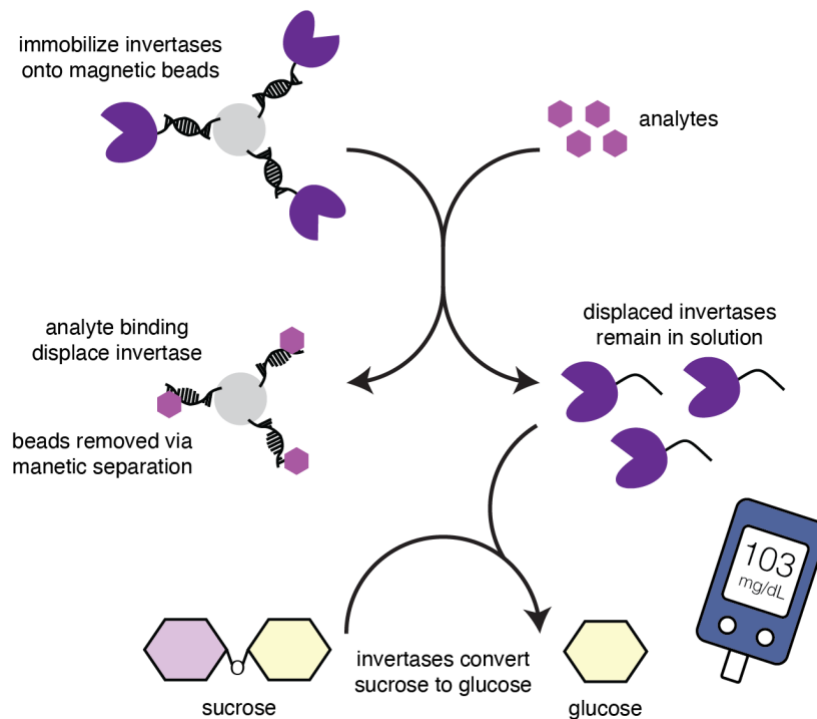


Figure 1-4 Schematic of Xiang and Lu’s work⁴⁰ in repurposing the PGM to detect analytes other than glucose. DNA-invertase conjugates are first immobilized to magnetic beads by hybridizing to a portion of the analyte-binding aptamer. The addition of analytes displaces invertases by competitive binding to the aptamer sequence. The magnetic beads are then removed *via* magnetic separation, and the displaced invertases remain in the solution to convert sucrose into glucose for PGM measurement.

However, nearly all of these methods require extensive assay processing steps to load and remove glucose-converting enzymes, which makes such strategies challenging to implement at the point of need. To this end, using a CFE system and analyte-responsive biosensing sensing circuit could enable glucose converting enzyme production *in situ*, reduce the required assay processing steps to simplify test implementation, and allow numerical quantification of diverse analytes with digital readouts at the point of care.

1.3.3 Interfacing CFE biosensors with immunoassays for sensitive protein detection

The vast majority of CFE biosensors are used to detect nucleic acids and small molecule analytes, with very few used to detect proteins. While aptamers have been used for cell-free protein detection, evolving suitable protein-binding sequences using methods such as SELEX is a non-trivial task and must be done for each new protein target⁴¹. Moreover, when the lab-evolved protein-binding aptamers are placed in the context of CFE reactions (either in the chemical environment or in gene expression contexts – next to a promoter, ribosomal binding sites, or reporter proteins), the sensitivity and signal-to-noise ratio of the aptamer drops significantly and limits their uses for protein detection⁴².

The current gold standard for protein detection is immunoassay, which uses antibodies to recognize specific epitopes of protein targets. To this end, the enzyme-linked immunosorbent assay (ELISA) has been shown to detect protein analytes with high specificity and sensitivity. A typical sandwich ELISA requires the protein (antigen) capture antibodies to be immobilized on a microwell surface first, followed by a wash step to remove unbound antibodies and a blocking step before the sample containing antigens is added to a microwell. After a period of incubation, any unbound antigens are washed away before an enzyme-linked detection antibody is added to the microwell. The detection antibodies bind to the antigen immobilized on the microwell, and the unbound antibodies are removed in the subsequent wash step. The enzyme-linked detection antibodies remaining in the well can now report on the presence and concentration of protein antigen *via* enzymatic reactions on chromogenic or chemiluminescent substrates.

Coupling immunoassays to polymerase chain reactions (immuno-PCR) further improves the sensitivity of protein detection by combining the protein antigen-recognition capabilities of immunoassays and exponential levels of amplification in PCR reactions. In

this case, a DNA oligonucleotide-conjugated detection antibody is used in place of an enzyme-linked detection antibody. The oligonucleotide signal serves as the template for the subsequent quantitative-PCR amplification step with fluorescent probes, enabling a 10- to 1000-fold increase in detection sensitivity compared to ELISA⁴³.

The DNA signal can be conjugated onto detection antibodies in various ways. The initial demonstration of DNA and antibody linkage used the avidin⁴⁴ or streptavidin⁴³ protein to link biotinylated DNA and antibodies together *via* the biotin-(strept)avidin binding affinity (Figure 1-5A). Seminal advances in DNA synthesis and crosslinking techniques also made direct conjugation of DNA to antibodies easier to produce at scale⁴⁵. DNA oligonucleotides can now be functionalized with terminal amine groups, reacting with an N-hydroxysuccinimidyl (NHS)-ester functionalized antibody to produce antibody-DNA conjugates (Figure 1-5B)⁴⁵.

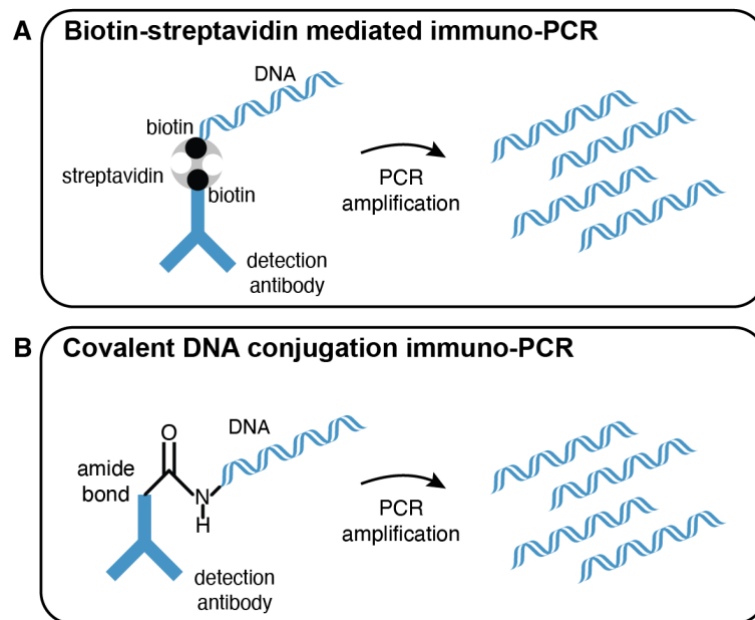


Figure 1-5 Schematic of different approaches linking DNA molecules to detection antibodies to accomplish immuno-PCR. (A) Biotin-streptavidin mediated assembly of DNA-antibody conjugate. Biotinylated detection antibodies and DNA are linked

together *via* affinity binding to tetrameric streptavidin. (B) Covalent conjugation of DNA to antibody. DNA functionalized with terminal amine groups reacts with NHS-ester functionalized detection antibody to form a covalent amide bond, linking DNA and antibody together.

Rather than using PCR to amplify the DNA signal linked to detection antibodies, a CFE biosensing system could be used to interpret the genetic signals carried on DNA. Instead of using direct amplification of DNA as in PCR, CFE systems can amplify genetic information encoded in conjugated DNA *via* transcription, translation, and enzymatic amplification (if an enzymatic reporter is used). Interfacing immunoassays with DNA-conjugated detection antibodies in a CFE system also allows for signal multiplexing *via* genetic circuits. Detection antibodies targeting distinct protein epitopes can be conjugated to different DNA signals orthogonally activating the expression of their respective reporter proteins, allowing facile translation to detect and distinguish multiple protein targets.

1.4 Contribution of this Thesis

In this dissertation, I developed methods to couple CFE systems with new interfaces to address current limitations in point-of-care biosensor diagnostics. I have created the first-of-its-kind “protocell array” system capable of simultaneous detection of diverse classes of analytes by embedding biosensors into multiple discretized, phase-separated “protocells” formed by polymer liquid-liquid phase separations. I have also expanded the repertoire of field-friendly diagnostics from presence-or-absence reporting to numerical analyte quantification by coupling biosensor output with a personal glucose monitor. Lastly, I interfaced immunoassay outputs with a CFE system to enable sensitive and accessible detection of protein antigens with emerging applications to identify virus variants near the point of care.

CHAPTER 2. PROTOCELL ARRAYS FOR SIMULTANEOUS DETECTION OF DIVERSE ANALYTES

Portions of this chapter are reproduced from my publication “ProtoCell Arrays for Simultaneous Detection of Diverse Analytes” in *Nature Communications*⁴⁶.

2.1 Introduction

Simultaneous detection of multiple analytes from a single sample (“multiplexing”), particularly when done at the point of need, can guide complex decision-making without increasing the required sample volume or cost per test. Despite recent advances, multiplexed analyte sensing still typically faces the critical limitation of measuring only one type of molecule (e.g., small molecules or nucleic acids) per assay platform. Here, we address this bottleneck with a customizable platform that integrates cell-free expression (CFE) system with polymer-based aqueous two-phase system (ATPS), producing membrane-less “protocells” containing transcription and translation machinery used for detection.

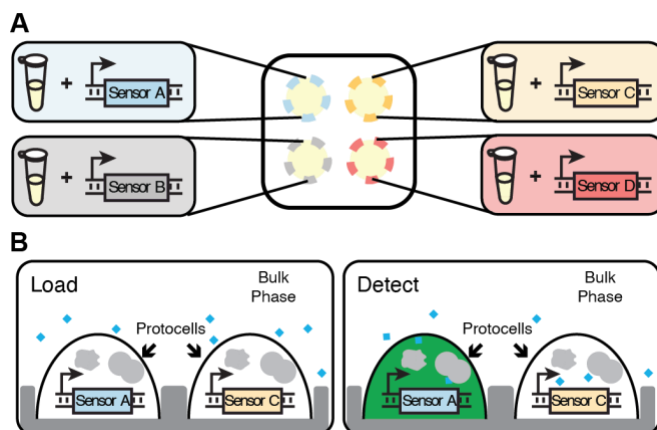


Figure 2-1 Schematic of the membrane-less protocell array platform for simultaneous detection of multiple analytes. The use of a spatially patterned array of phase-separated protocell sensors enables each microwell to provide measurements for multiple analytes using a single fluorescent or colorimetric reporter. (A) An overhead view of a microwell with 4 micro-basins. White area surrounding the micro-basins (yellow-shaded regions) represents the bulk phase formed by a PEG solution containing the analytes to be detected. Each micro-basin has a protocell containing a CFE reaction (represented by the microcentrifuge tube) with a different sensor plasmid or genetic circuit. (B) Side view of a microwell with micro-basins. Analytes in the bulk phase (blue diamonds) enter protocells to activate their cognate sensor (blue DNA construct), producing detectable reporter signals. Multiple analytes can be measured in parallel by tracking which protocell produces reporter signals (green color on the right).

Mixing two immiscible polymer solutions (polyethylene glycol (PEG) and Ficoll) at appropriate ratios leads to spontaneous liquid-liquid phase separation, creating Ficoll droplets in a PEG bulk phase. Adding biological machinery (like that of a CFE reaction) to the droplets yields what is essentially a membrane-less precursor of a cell (a “protocell”)^{38,47}, with genetic information and the capability to execute complex functions contained in a small, localized volume. Since many soluble macromolecules such as the proteins and nucleic acids that enable CFE-based sensing selectively partition from a PEG-rich phase to the dextran- or Ficoll-rich phase³³, the core of distinct biosensing machinery can stay compartmentalized in each ATPS-formed protocell.

We envision that multiple protocells, each performing a distinct sensing reaction, could be arrayed in the same microwell to detect chemically diverse targets from the same sample. For simultaneous detection of target analytes in a single sample, simple topographical placement of micro-basins inside a microwell can be used for stable positioning of distinct protocells^{34,35,48} each containing a different CFE sensor (Figure 2-1). The addition of a sample solution to the microwell initiates analyte uptake and compartmentalized detection reactions in multiple isolated membrane-less protocells. We

envisioned that an array of membrane-less protocell sensors formed by selective compartmentalization of CFE reactions in ATPS can facilitate simultaneous detection of multiple analytes beyond just proteins, leading to a new class of protocell array-based diagnostics that reports on diverse types of analytes, has a high degree of sensor customizability, and can be used at the point of need.

Toward this goal, here we first assess CFE transcription and translation capabilities in two protocell-forming polymer ATPS (PEG-Ficoll and PEG-dextran) with an in-house prepared *E. coli* lysate. We show that analytes (small molecules and nucleic acids) added to a microwell containing an array of CFE protocells selectively activate their cognate sensors confined to distinct protocells with comparable sensitivity to those in non-protocell CFE reactions. We highlight the utility of this platform for simultaneous, multi-modal biomarker detection *via* the detection of clinically relevant targets (e.g., nucleic acids from pathogenic bacteria and micronutrients) from the same sample and in a human serum matrix. Only one reporter (green fluorescent protein, GFP) is needed for multiplexed analyte measurement, which significantly reduces the complexity of test development and reconfiguration. Protocell arrays also meet key criteria for field-deployable sensors and diagnostics: we demonstrate that GFP reporters can be easily replaced with color-producing enzymatic reporters to enable equipment-free test interpretation, and we demonstrate parallel, simultaneous detection of multiple analytes using protocell arrays that have been lyophilized for storage at ambient temperature. Taken together, the presented protocell array platform both expands the reach of CFE biosensors and provides the foundation to develop advanced, customizable “diagnostic chips” for simultaneous detection of diverse types of analytes at the point of need.

2.2 Materials and Methods

2.2.1 Bacterial strains

E. coli strain DH10 β was used for all cloning and plasmid preparations. *E. coli* strain BL21 Star (DE3) $\Delta lacIZYA$ was created by lambda red recombination⁴⁹ and used for in-house cell-free lysate preparation. Genomic DNA from *E. coli* strains DH10 β and BL21 Star (DE3) were used as negative controls for target-specific amplification of Stx1 and Stx2 triggers. Genomic DNA from *B. thtaiotaomicron* (ATCC 29148D) and STEC O157:H7 (ATCC 51657GFP) were used for testing the detection of pathogenic bacteria.

2.2.2 Genetic parts assembly and plasmid preparation

Sequences of all parts used in this study are provided in Appendix A.2 Sequence Information. DNA oligonucleotides for cloning and sequencing were synthesized by Eurofins Genomics. Partial sequences for small molecule sensors and toehold switches were obtained from previously published sequences and were synthesized either as gene fragments or ssDNA-annealed oligonucleotides from Eurofins Genomics. Plasmids expressing regulators and reporter proteins were cloned using either Gibson Assembly⁵⁰ or blunt end ligation into plasmid backbone pJL1. Assembled constructs were transformed into DH10 β cells, and isolated colonies were grown overnight in LB with antibiotics. Plasmid DNA from overnight cultures was purified using EZNA miniprep columns (OMEGA Bio-Tek). Plasmid sequences were verified with Sanger DNA sequencing (Eurofins Genomics).

Plasmid DNA used for all CFE and protocell reactions were purified from EZNA midiprep columns (OMEGA Bio-Tek), followed by isopropanol and ethanol precipitation. The purified DNA pellet was reconstituted in the elution buffer, measured on a Nanodrop 2000 for concentration, and stored at -20 °C.

Genomic DNA for *B. thetaiotaomicron* (ATCC 29148D) used for pathogen detection was purchased from American Type Culture Collection (ATCC). Genomic DNA for STEC O157:H7 (ATCC 51657GFP) used for pathogen detection was obtained from an overnight culture grown in tryptic soy broth supplemented with 1% glucose at 37 °C. DNA was extracted using an Invitrogen PureLink Microbiome DNA Purification Kit (A29790). Genomic DNA for DH10 β and BL21 Star (DE3) were obtained from a 5 mL overnight culture grown in LB medium and were extracted using Quick-DNA Plus Kit (Zymo Research) according to the manufacturer's protocol.

2.2.3 Preparation of in-house CFE lysate

Cellular lysate for all experiments was prepared as described by Sun *et al.*¹⁸ with a few protocol modifications. Briefly, BL21 Star (DE3) $\Delta lacIZYA$ cells were grown in 2 \times YTP medium at 37 °C and 220 rpm to an optical density (OD) between 1.5-2.0, corresponding to the mid-exponential growth phase. Lysate prepared for toehold switch expression had an additional IPTG (0.4 mM) induction step when the OD reached 0.4 to activate expression of T7 RNA polymerase, creating a T7 RNAP-enriched lysate. Cells were centrifuged at 2700 xg and washed *via* resuspension with S30A buffer (50 mM tris, 14 mM magnesium glutamate, 60 mM potassium glutamate, 2 mM dithiothreitol, and pH-corrected to 7.7 with acetic acid). These centrifugation and wash steps were repeated twice

for a total of three S30A washes. After the final centrifugation, the wet cell mass was determined, and cells were resuspended in 1 mL of S30A buffer per 1 g of wet cell mass. The cellular resuspension was divided into 1 mL aliquots. Cells were lysed using a Q125 sonicator (Qsonica) at a frequency of 20 kHz and 50% of amplitude. Cells were sonicated on ice with cycles of 10 s on and 10 s off, delivering approximately 200-250 J, at which point the cells appeared visibly lysed. An additional 4 mM dithiothreitol was added to each tube, and the sonicated mixture was then centrifuged at 12,000 xg and 4°C for 10 min. After centrifugation, the supernatant was removed, divided into 0.5 mL aliquots, and incubated at 37 °C and 220 rpm for 80 min. After this runoff reaction, the cellular lysate was centrifuged at 12,000 xg and 4 °C for 10 min. The supernatant was removed and loaded into a 10 kDa molecular weight cutoff dialysis cassette (Thermo Fisher). Lysate was dialyzed in 1 liter of S30B buffer (14 mM magnesium glutamate, 60 mM potassium glutamate, 1 mM dithiothreitol, and pH-corrected to 8.2 with tris) at 4 °C for 3 hours. Dialyzed lysate was removed and centrifuged at 12,000 xg and 4 °C for 10 min. The supernatant was removed, aliquoted, flash-frozen in liquid nitrogen, and stored at -80 °C for future use.

2.2.4 CFE reactions

CFE reactions were assembled as described by Kwon and Jewett¹⁷. Briefly, reaction mixtures were composed of 27 v/v% of in-house prepared lysate, 2 mM each proteinogenic amino acid, 1.2 mM ATP, 0.85 mM each of GTP, CTP, and UTP, 0.2 mg/mL tRNA, 0.27 mM CoA, 0.33 mM NAD, 0.068 mM folinic acid, 1.5 mM spermidine, 33 mM PEP, 130 mM potassium glutamate, 10 mM Ammonium glutamate, 12 mM magnesium glutamate, 4 mM sodium oxalate, and specified concentrations of plasmids (described in

A.3 Protocell and CFE Reaction Conditions), RNA triggers, and small molecules. For experiments with RNA triggers, Rnase Inhibitor Murine (New England Biolabs) was added to the bulk phase at 0.5 v/v%. Each assembled CFE reaction was 10 μ L in volume and placed in a black-bottomed 384-well plate (Greiner Bio-One) and incubated at 37 °C for 3 hours for GFP expression. A clear adhesive film was used to cover the plate and prevent evaporation.

2.2.5 *Protocell CFE reactions*

Polymers used to establish ATPS-based membrane-less protocells were prepared by dissolving either 400k Ficoll, 500k dextran, or 35k PEG into nuclease-free water. The bulk phase at the time of preparation and before the addition of Ficoll or dextran protocells consisted of 5 v/v% of 35k PEG, 1x concentration of all reagents added for CFE reactions (excluding lysate), specified concentrations of small molecules or nucleic acids, and nuclease-free water to a final volume of 200 μ L for the 4-plex system or 100 μ L for the 9-plex system (Figure 2-2). For experiments with RNA triggers, Rnase Inhibitor Murine (New England Biolabs) was added to the bulk phase at 0.5 v/v%. For experiments containing human serum, RNase Inhibitor Murine (New England Biolabs) was added to a concentration of 1.5 v/v% in the bulk phase to decrease serum Rnase activity. For colorimetric output in CFE reactions, color substrates were added to the bulk phase to a final concentration of 0.6 mg/mL for CPRG or 0.2 mg/mL for X-gal.

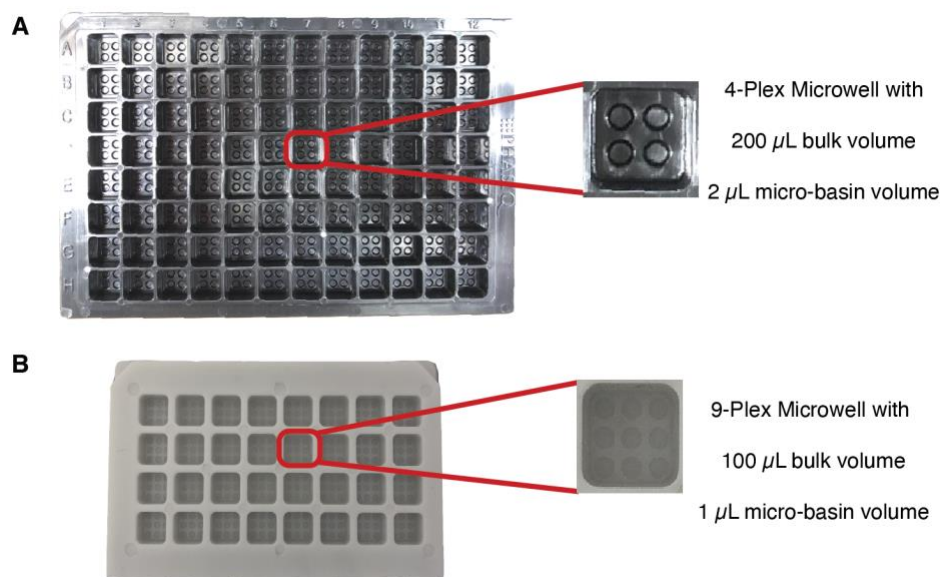


Figure 2-2 Injection-molded polystyrene plates used in protocell array reactions. Microwell layout and spacing are based on 96-well microplate standards from the Society for Laboratory Automation and Screening. (A) Black microwell plate with 2x2 arrays of 2 μL volume micro-basins for protocell placement. (B) White microwell plate with 3x3 arrays of 1 μL volume micro-basins for protocell placement. All microwell plates used in this study were manufactured by PHASIQ, Inc (Ann Arbor, Michigan).

Each protocell sensor consisted of 10 v/v% Ficoll or 5 v/v% dextran polymers, 27 v/v% cell-free lysate, 1x concentration of CFE reagents, specific concentrations of plasmid DNA (either provided in figures or in Appendix A.3 Protocell and CFE Reaction Conditions), and water to a final volume of 2 μL for the 4-plex system or 1 μL for the 9-plex system. The assembled protocell solution was then vortexed at a medium-high setting to ensure homogenous mixing. Protocells for detection of linear DNA also contained 2 μM of χDNA to protect linear DNA against endonucleases present in the CFE lysate.

To assemble the protocell arrays, a bulk phase solution containing specified concentrations of targets was first pipetted into the custom-made microwell plate (PHASIQ) to fill up each microwell. Protocell droplets were then pipetted into the bulk

phase solution at their designated micro-basins. Unless otherwise noted, microwells containing assembled protocell arrays were incubated at 37 °C for 3 hours before imaging on a ChemiDoc MP (Bio-Rad) imaging system. A clear adhesive film was used to cover the plate and prevent evaporation.

2.2.6 *Data acquisition and analysis*

For CFE reactions, endpoint GFP readings were taken using a plate reader (Synergy4, BioTek) with its companion Gen 5 software. The excitation and emission wavelengths were 485 and 528 nm, with a gain setting of 70. Data acquired from Gen 5 software was exported to Microsoft Excel files for further analysis. For protocell array reactions with fluorescent reporters, the ChemiDoc MP imaging system (Bio-Rad) was used for fluorescent plate imaging. Image Lab software (Bio-Rad) was used for image collection with settings of 0.5 s exposure time, grayscale image color, 530/28 filter for GFP detection, and Blue Epi illumination as a light source. An image transform procedure was uniformly applied to all images in Image Lab (with high, low, and gamma values of 10000, 0, and 1, respectively) before exporting files for analysis. For image analysis, each image was first converted to an 8-bit grayscale image. An image processing software, Fiji, was used to manually extract signal intensities from each 1.5 mm diameter micro-well (pixel size 50) for data analysis. The signal intensities were recorded and analyzed using Microsoft Excel. For colorimetric protocell array reactions, all pictures were taken with an iPhone X (Apple) in a light-controlled setting⁵¹. Adobe Photoshop was used to crop individual wells for data presentation. A brightness adjustment was uniformly applied to all colorimetric ATPS photos to make them better resemble their appearance to the naked eye.

2.2.7 *Trigger preparations*

DNA encoding each trigger RNA used in experiments was either amplified from cloned plasmid or from genomic DNA of specified species of bacteria by PCR with Q5 DNA polymerase (New England Biolabs). Primers were designed to create linear DNA with a T7 promoter and additional protective sequences on the 5' and 3' ends of the linear template. Sequences for primers used to amplify triggers from DNA templates or genomic DNA are provided in Appendix A.4 Primers for Trigger DNA Amplification. After PCR amplification, all products were run on a 2 w/v% agarose gel to verify successful amplification of targets and then purified using a PCR purification kit (Omega Bio-Tek). The prepared linear DNA was either directly used in CFE and protocell reactions or used as a template for *in vitro* transcription.

RNA triggers were transcribed from linear DNA templates using T7 polymerase according to the manufacturer's protocol (New England Biolabs). Following RNA synthesis, Dnase I (Zymo Research) was added to degrade the linear DNA template. The RNA products were then purified using an RNA Clean and Concentrator kit (Zymo Research) according to the manufacturer's protocol. Following purification, RNA concentration was measured on a Nanodrop 2000, sub-aliquoted to reduce freeze-thaw cycles, and stored -20 °C.

2.2.8 *STEC toehold switch development*

Toehold switches targeting gene sequences of Shiga toxin proteins (Stx1 and Stx2) in STEC O157:H7 were designed using NUPACK with series B toehold switch design⁶ and cloned into a pJL1 plasmid containing a GFP reporter. Trigger sequences were

synthesized by Eurofins Genomics as gene fragments containing a T7 promoter and 30-35 bp of protective sequences before and after the actual trigger sequence and were cloned onto the pJL1 plasmid backbone to facilitate sensor screening. Trigger/sensor pairs were then tested in CFE reactions containing 2.5 nM toehold switch sensor-GFP reporter plasmid and 5 nM of trigger plasmid to verify successful sensor activation and orthogonality (data in Appendix A.1 Initial Validation of *B. Theta*, Stx1, and Stx2 Switch Activation in CFE Reactions Figure 12). Following trigger/sensor pair validation, primers used to amplify different trigger sequences from genomic DNA were verified for specificity toward their targets using PCR reactions with non-target templates.

2.2.9 *Human serum processing*

Pooled human serum was purchased from Corning (Corning, NY). Endogenous zinc was removed from serum through Chelex-100 treatment. In total, 1 g of Chelex-100 resin was added to 100 mL of serum, and the mixture was vigorously stirred for 2 hrs at room temperature. Resin was then isolated from the serum through centrifugation followed by syringe filtering. All serum samples were aliquoted to minimize freeze-thaw cycles and stored at -20 °C until use.

Measurement of successful zinc removal from serum was conducted at the University of Georgia Laboratory for Environmental Analysis. Samples were digested with concentrated acid and analyzed on ICP-MS according to EPA method 3052.

2.2.10 *Lyophilization*

Protocell sensors (1 μL) containing 55 v/v% lysate, specified concentrations of plasmid DNA, and 10 v/v% Ficoll were spotted into micro-basins, and the plate was stored at $-80\text{ }^{\circ}\text{C}$ to freeze for at least 5 hours. Bulk phase solutions (360 μL per bulk phase condition, 120 μL per technical replicate) containing 5% PEG, 0.2 mg/mL X-gal, and 1x CFE energy buffer were prepared in 2-mL Eppendorf tubes and stored at $-80\text{ }^{\circ}\text{C}$ to freeze for at least 5 hours. Frozen plates and bulk phase solutions were transferred to a pre-chilled Labconco Fast-Freeze flask as quickly as possible to prevent reagent thawing. The flask was connected to a Labconco benchtop lyophilizer and lyophilized at $-50\text{ }^{\circ}\text{C}$ and 0.05 mbar overnight (> 14 hrs).

Freeze-dried reactions were taken out of the lyophilizer the following day. For the bulk phase, water mixed with 50 nM of specified bacterial triggers was used to reconstitute the lyophilized bulk phase solution to 360 μL (120 μL per technical triplicate). 1 μL of water was used to rehydrate the freeze-dried protocells, and the plate was placed at room temperature for 5 minutes for protocells to congeal, thereby reducing the potential for protocell sensors to float into neighboring wells during rehydration. Reconstituted bulk phase solutions were added to microwells before incubating at $37\text{ }^{\circ}\text{C}$. A clear adhesive film was used to cover the plate and prevent evaporation.

2.3 Results

2.3.1 Compartmentalization of CFE protein expression in ATPS-formed protocells

While CFE-based protocells have previously been described^{37,38}, their application to analyte detection has not. To use membrane-less CFE protocells for simultaneous measurement of multiple analytes, the sensor plasmids and core machinery for

transcription and translation must retain activity in an ATPS environment and stay compartmentalized inside the protocell. We first verified that CFE reactions based on an in-house prepared *E. coli* lysate could maintain transcription and translation function in the context of an ATPS. CFE reactions constitutively producing GFP were tested in two ATPS environments: a 5% 35k PEG – 5% 500k dextran system and a 5% 35k PEG – 10% 400k Ficoll system. These pairs of polymers were selected based on the following criteria: their ability to separate into two liquid phases without pre-equilibration to create a metastable system with mass transfer enhancements from convective mixing⁵²; our past experience indicating their stability in dehydrated ATPS systems^{36,52}; and previously reported evidence that these polymers are compatible with CFE machinery^{37,38,53}. Polymer concentrations required to form biphasic separation were selected based on previously characterized binodal curves^{52,54}. Additional rheological data are also available in the literature^{52,54}. PEG constitutes the bulk phase for both ATPS environments, while dextran or Ficoll constitutes the protocell (Figure 2-3A). Individual protocells were first formed by mixing CFE reactions with Ficoll or dextran polymer until homogenous and pipetting a 2 μ L droplet into a bulk phase PEG solution. No protein production was observed after 3 hours of incubation at 37 °C (Figure 2-3B), perhaps due to the necessary salts and building blocks for protein synthesis (nucleotides and amino acids originally in the protocell) not remaining strongly partitioned in the protocell but instead diffusing into the bulk phase and thus diluting their concentrations. Supplementing CFE energy buffer in the PEG bulk phase enabled CFE protein synthesis (Figure 2-3B).

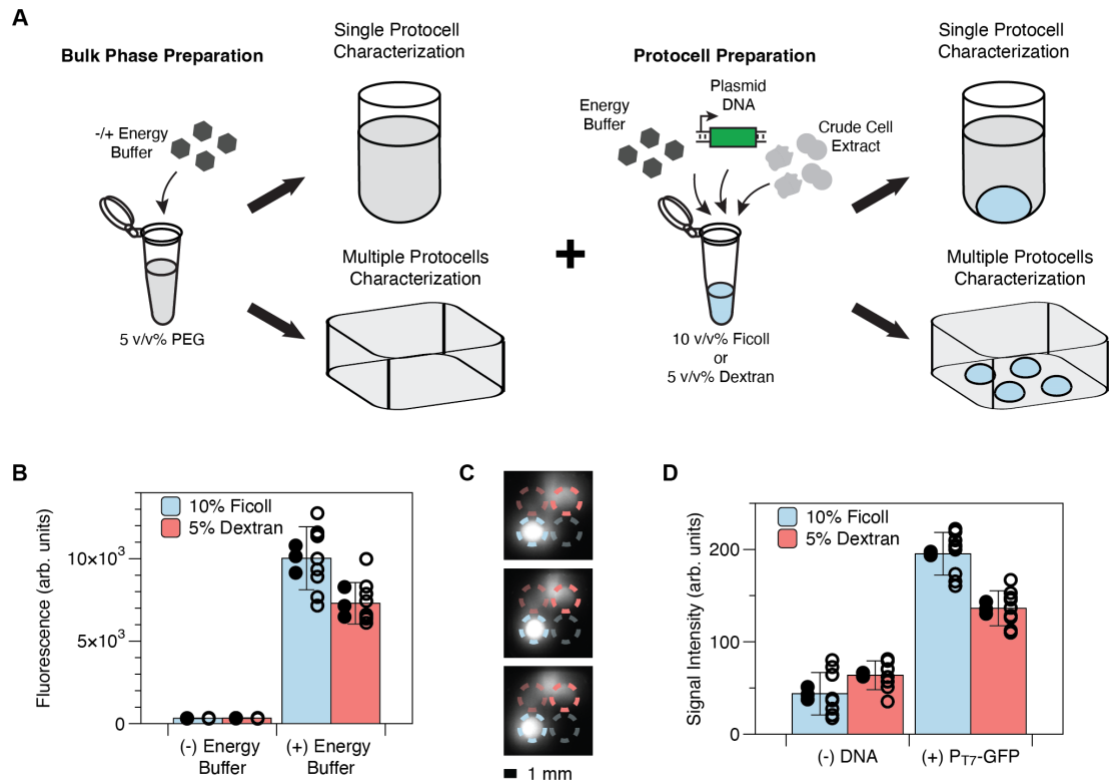


Figure 2-3 Characterization of protein expression and reaction compartmentalization in membrane-less protocells. (A) Schematic of single-well and multi-well protocell reactions and their preparation methods. A small volume of Ficoll or dextran solution containing reagents for cell-free GFP expression was pipetted into a bulk phase solution of PEG to form a protocell. Subsequent reactions were incubated at 37 °C for 3 hours. (B) Fluorescence of Ficoll and dextran protocell reactions in single-protocell format were measured with a plate reader with 485/528 nm excitation/emission wavelengths. For detectable protein expression, energy buffer must be supplemented in the bulk phase. (C) Fluorescence image of protocell arrays obtained by a ChemiDoc MP imager (0.5 s exposure time, 530/28 nm filter) for 3 biological replicates. Contents of individual protocells are indicated with colored circles: blue for Ficoll polymer-encapsulated reactions, red for dextran-encapsulated reactions. Bright colors indicate CFE reactions containing GFP plasmid for expression, and faded colors indicate negative controls with no plasmid. Scale bar is 1 mm. (D) Quantitative assessment of fluorescence image in C, with pixel intensity quantified by image processing software (Fiji). Data are presented as mean values \pm SD of 9 replicates (3 biological replicates \times 3 technical replicates). Solid-filled circles represent the mean of each biological triplicate, and hollow circles represent all data points. Note, due to different measurement instruments being used for B and D, the arbitrary units on the y-axes are different scales.

We next validated that ATPS-formed protocells compartmentalize multiple CFE reactions, such that reporter plasmids and proteins remain in their phase-separated droplets in a membrane-less protocell array. We performed CFE reactions in a custom-designed 96-well plate where each microwell contains 4 micro-basins for protocell placement, with the bulk phase supplemented with energy buffer. CFE reactions with or without a plasmid coding for GFP were combined with dextran or Ficoll, loaded into the micro-basins (Figure 2-3A), and incubated at 37 °C for 3 hours. A fluorescence imager (ChemiDoc MP) was used to measure protein production in the protocell array in this custom microwell plate. GFP-producing Ficoll protocells were better localized in their designated micro-basins compared to those of dextran protocells (Figure 2-3C-D), demonstrating that cell-free lysate, plasmids, and reporter proteins are better compartmentalized in the PEG-Ficoll environment. This result also suggests that multiple protocells expressing different biosensors could be arrayed in the same microwell, enabling a platform for parallel, simultaneous detection of multiple targets. We note that GFP diffusion from high GFP-producing protocells is visible in the fluorescence images at later time points for both PEG-dextran and PEG-Ficoll systems (Figure 2-4). Since typical CFE sensing reactions are on the order of 0.5-3 hours, such issues at later time points in PEG-Ficoll protocells should be less problematic for detection applications, though some degree of non-specific crosstalk due to these limitations is possible.

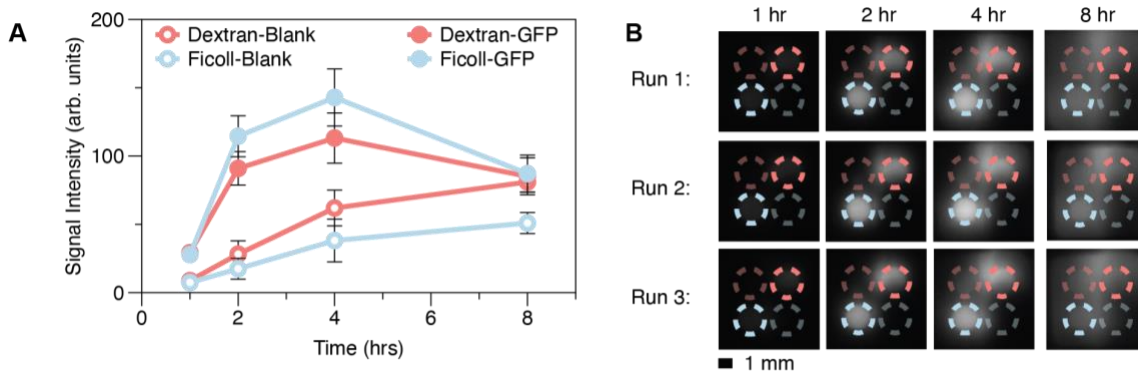


Figure 2-4 Characterization of CFE reaction compartmentalization and protein production in PEG-Ficoll and PEG-dextran ATPS. (A) Time course quantification of 10% Ficoll and 5% dextran CFE protocells with and without plasmid encoding for GFP expression. Disruption of the biphasic partitioning of GFP was observed beyond 4 hours. This could be caused by GFP diffusion from protocell to the bulk phase^{34,36}. Typical CFE sensing reactions are on the order of 1 to 3 hours, making issues at longer time scales less relevant. Data are presented as mean values \pm SD of 9 replicates (3 biological replicates \times 3 technical replicates). Each biological replicate represents an independently assembled reaction on a different day. (B) Representative time-course fluorescence image of compartmentalized CFE reactions in protocell arrays for each biological replicate. Blue circles indicate Ficoll-formed protocell with a plasmid coding for GFP expression (bright blue) and without plasmid (faded blue). Red circles indicate dextran-formed protocell with a plasmid coding for GFP expression (bright red) and without plasmid (faded red). Scale bar is 1 mm.

2.3.2 Multiplexed detection of model small molecule and nucleic acid systems

To demonstrate that these membrane-less CFE protocell arrays can be used for simultaneous detection of multiple analytes, we incorporated sensors that respond to multiple model small molecules. Plasmids encoding each sensor system were embedded in different protocells, with analytes added to the bulk phase to diffuse into the protocells to activate their cognate sensor proteins. To evaluate small molecule detection, we tested an isopropyl β -D-1-thiogalactopyranoside (IPTG)-inducible LacI-P_{T7lacO} circuit and an arabinose-inducible AraC-P_{BAD} circuit (Figure 2-5A)⁵⁵. In each biosensing circuit, the small molecule inducer modulates the activity of its corresponding transcriptional regulator (IPTG derepresses LacI and arabinose activates AraC), allowing transcription of GFP

reporter from its respective promoter (P_{T7lacO} or P_{BAD}). The arabinose CFE sensor uses a single plasmid encoding constitutive AraC expression and P_{BAD} -regulated GFP expression from the same divergent promoter. The IPTG sensor uses one plasmid to express GFP from a P_{T7lacO} promoter and another to express LacI constitutively. When IPTG and arabinose were individually added to the bulk phase, only the appropriate sensor reactions were activated, with minimal signal crosstalk (Figure 2-5B). This result demonstrates that protocell arrays can successfully detect multiple small molecule signals simultaneously.

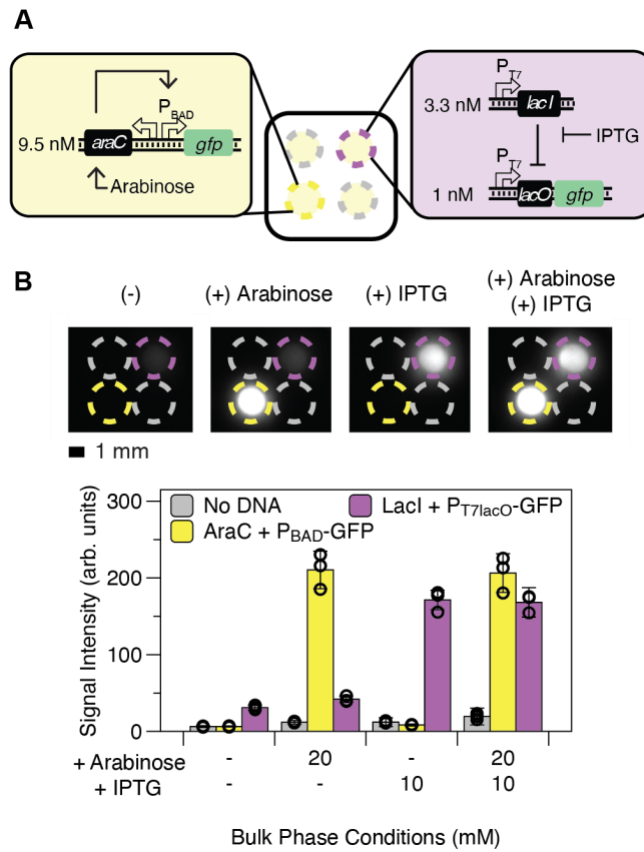


Figure 2-5 Simultaneous detection of multiple model small molecules in membrane-less protocell arrays. (A) Schematic of protocell array setup for simultaneous detection of two small molecules. Yellow and purple circles indicate micro-basins containing arabinose and IPTG sensors, respectively. Gray circles are micro-basins containing CFE protocells without plasmids. The circuit diagrams and plasmid concentrations used for the arabinose and IPTG sensors are shown in the insets. (B) Representative fluorescence images and their quantification results after 3 hours of

incubation at 37 °C. Small molecules added to the bulk phase for each experiment are indicated above each image. Circle colors are as in a. Each protocell sensor is only activated when its cognate small molecule (10 mM IPTG, 20 mM arabinose, or both) is present in the bulk phase. Data are presented as mean values \pm SD of 9 replicates (3 biological replicates x 3 technical replicates) for protocell sensors and 18 replicates (3 biological replicates x 6 technical replicates) for controls with no plasmid (3 biological replicates x 6 technical replicates). Hollow circles represent the mean of each biological triplicate. Scale bar is 1 mm.

We next demonstrated that protocell arrays could also enable simultaneous detection of multiple RNA targets using previously reported model toehold switches to control the output of CFE reactions⁸. A toehold switch is a *de novo* designed RNA regulator that forms an inhibitory hairpin to prevent translation of a downstream protein⁶. Addition of a “trigger” RNA with sequence complementarity to part of the switch unfolds the hairpin, turning on reporter expression (Figure 2-6A). We constructed plasmids in which two previously characterized orthogonal toehold switches (B and H)⁸ are constitutively expressed from a T7 promoter, and used these sensor plasmids in the protocell array (Figure 2-6B). GFP expression for a given protocell sensor was only observed when the cognate RNA trigger for the switch in that protocell was present in the bulk phase, demonstrating that protocell arrays can successfully detect multiple RNA targets in parallel (Figure 2-6C, D).

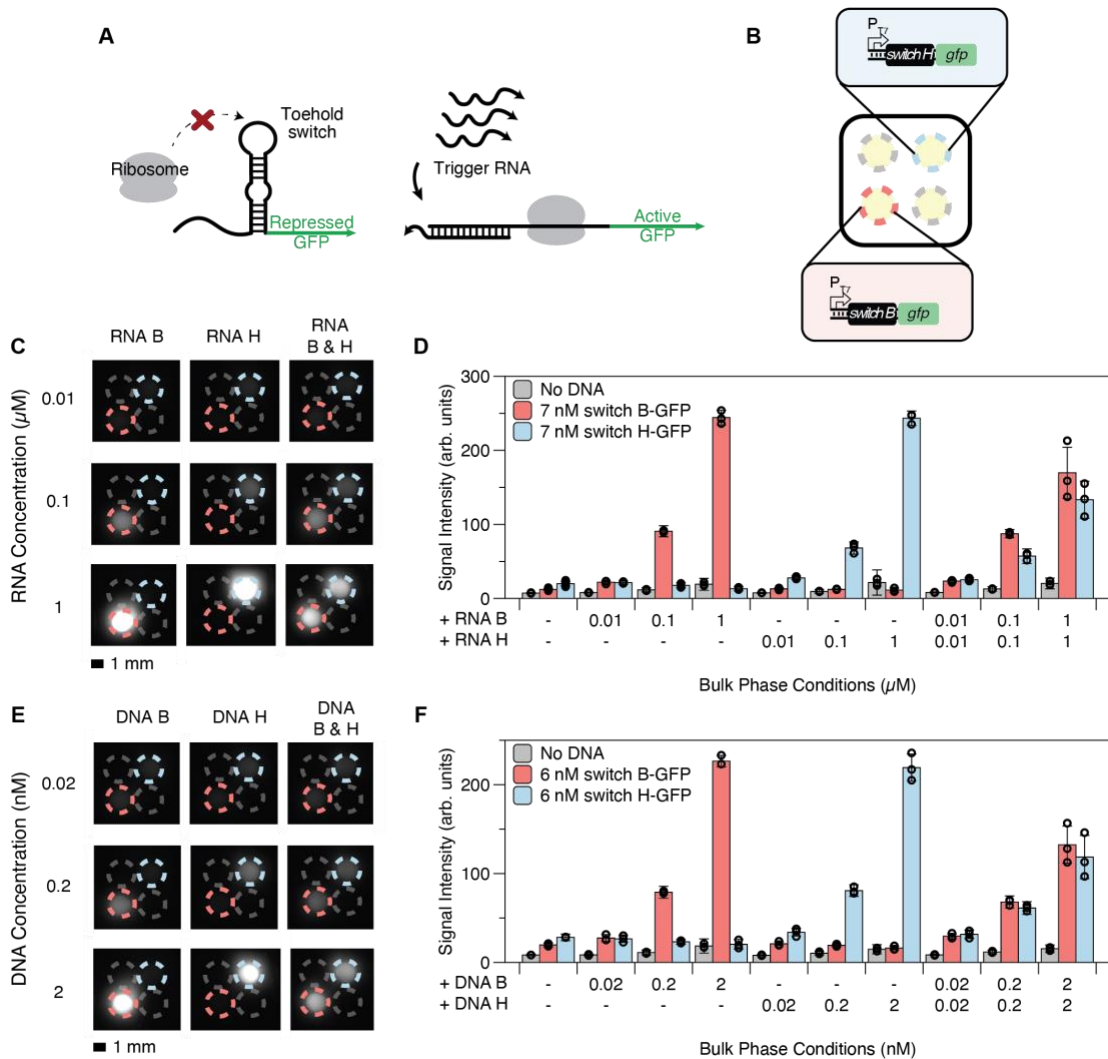


Figure 2-6 Simultaneous detection of multiple model nucleic acid sequences in membrane-less protocell arrays. Reactions were incubated at 37 °C for 3 hours. **(A)** Schematic of toe-hold switch mechanism. Without trigger RNA, the switch mRNA forms an inhibitory hairpin blocking the translation of a reporter (GFP). Addition of trigger RNA unwinds the switch hairpin, allowing GFP translation. **(B)** Schematic of protocell array setup for simultaneous detection of multiple nucleic acid sequences. Red and blue circles indicate micro-basins containing toe-hold switches B and H, respectively. Gray circles indicate CFE protocells without plasmids. **(C)** Representative fluorescence image of RNA detection from 10 nM to 1 μM . Images in the same column have the same RNA trigger(s) added. Images in the same row have the same concentration of trigger(s) added. Circle colors are as shown in B. **(D)** Quantification of fluorescence images in C and their replicates. Addition of both RNA triggers mutually represses their outputs, but this effect is specific to these triggers. **(E)** Representative fluorescence image of linear DNA detection from 20 pM to 2 nM. Images in the same column have the same DNA trigger(s) added. Images in the same row have the same concentration of DNA trigger(s) added. Circle colors are as shown in B. Addition of both DNA triggers also mutually represses their outputs. **(F)**

Quantification of fluorescence images in e and their replicates. For experiments where the bulk phase had no triggers, data are presented as mean values \pm SD of 27 replicates for protocells containing toehold switch sensors (9 biological replicates x 3 technical replicates) and 54 replicates for reactions with no DNA (9 biological replicates x 6 technical replicates). For experiments with triggers (RNA or DNA), data are presented as mean values \pm SD of 9 replicates for protocells containing toehold switch sensors (3 biological replicates x 3 technical replicates) and 18 replicates for reactions with no DNA (3 biological replicates x 6 technical replicates). Hollow circles represent the mean of each biological replicate. Scale bar is 1 mm.

Since DNA is more stable than RNA and can serve as a template for producing many RNA molecules, we hypothesized that protocell sensors could respond more sensitively to triggers expressed from a DNA template. RNA can be readily converted into DNA using reverse-transcriptase mediated isothermal amplification techniques like Nucleic Acid Sequence-Based Amplification (NASBA) or Reverse Transcription Recombinase Polymerase Amplification (RT-RPA)^{56,57}, making the detection of DNA-templated RNA a viable strategy for field-deployable detection of RNA targets. Just 0.2 nM of linear DNA (expressing RNA under the control of a T7 promoter) added to the bulk phase strongly activated GFP expression, with slight activation detectable upon adding just 20 pM of linear DNA (Figure 2-6E, F). While the simultaneous presence of both triggers B and H caused some suppression of both signals compared to either one alone (Figure 2-6D, F), this effect was also observed in single-phase CFE reactions and was found to be specific only to triggers B and H (Figure 2-7), suggesting adverse base-pair interactions among trigger sequences that are independent of protocell array-based sensing.

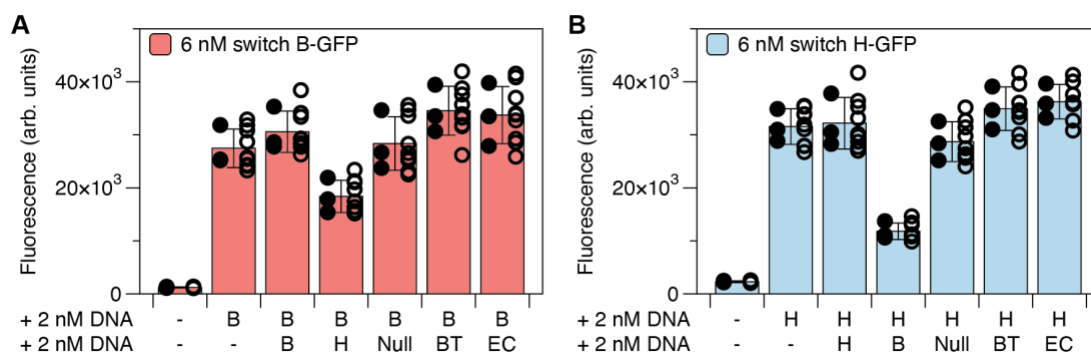


Figure 2-7 Co-expression of triggers B and H in single-phase CFE reactions mutually represses their output. This inhibition effect is specific to the combination of triggers B and H, as evidenced by the lack of repression when random (Null) and previously characterized trigger sequences (*Bacteroides thetaiotaomicron* and *Escherichia coli*, BT and EC respectively)⁹ are also added to the CFE reactions. This effect occurs for any CFE sensing reaction, not just in protocell arrays. (A) Trigger B was co-expressed with different linear DNA transcribing RNA triggers. Only the addition of trigger H significantly reduced GFP production from the switch B-GFP plasmid. (B) Trigger H was co-expressed with different linear DNA transcribing RNA triggers, and only the addition of trigger B reduced GFP production from the switchH-GFP plasmid. Reactions were incubated at 37 °C for 3 hours before fluorescent measurement on a plate reader. Data are presented as mean values \pm SD of 9 replicates (3 biological replicates \times 3 technical replicates). Each biological replicate is an independently assembled reaction on a different day. Solid-filled circles represent the average of each biological replicate, and hollow circles represent all data points.

2.3.3 Multi-modal detection of clinically relevant targets in a human serum matrix

Having demonstrated the multiplexing capabilities of protocell arrays, we next used this platform to detect multiple types of clinically relevant biomarker molecules with public health relevance: ions/minerals, small molecules, RNA, and DNA. The ions and small molecules we chose for detection were two micronutrients, zinc and vitamin B₁₂ (adenosylcobalamin), that are important sensing targets for global health applications and for which our group has previous experience developing CFE biosensors^{11,25}. The zinc sensor uses the activator ZntR, which activates expression from its cognate promoter P_{ZntA} when zinc is present. The B₁₂ sensor uses the activator EutR, which activates expression from its

cognate promoter P_{EutS} when both B_{12} and the cofactor ethanolamine (EA) are present. We characterized these micronutrient biosensors together in protocell arrays to confirm sensor performance (Figure 2-8).

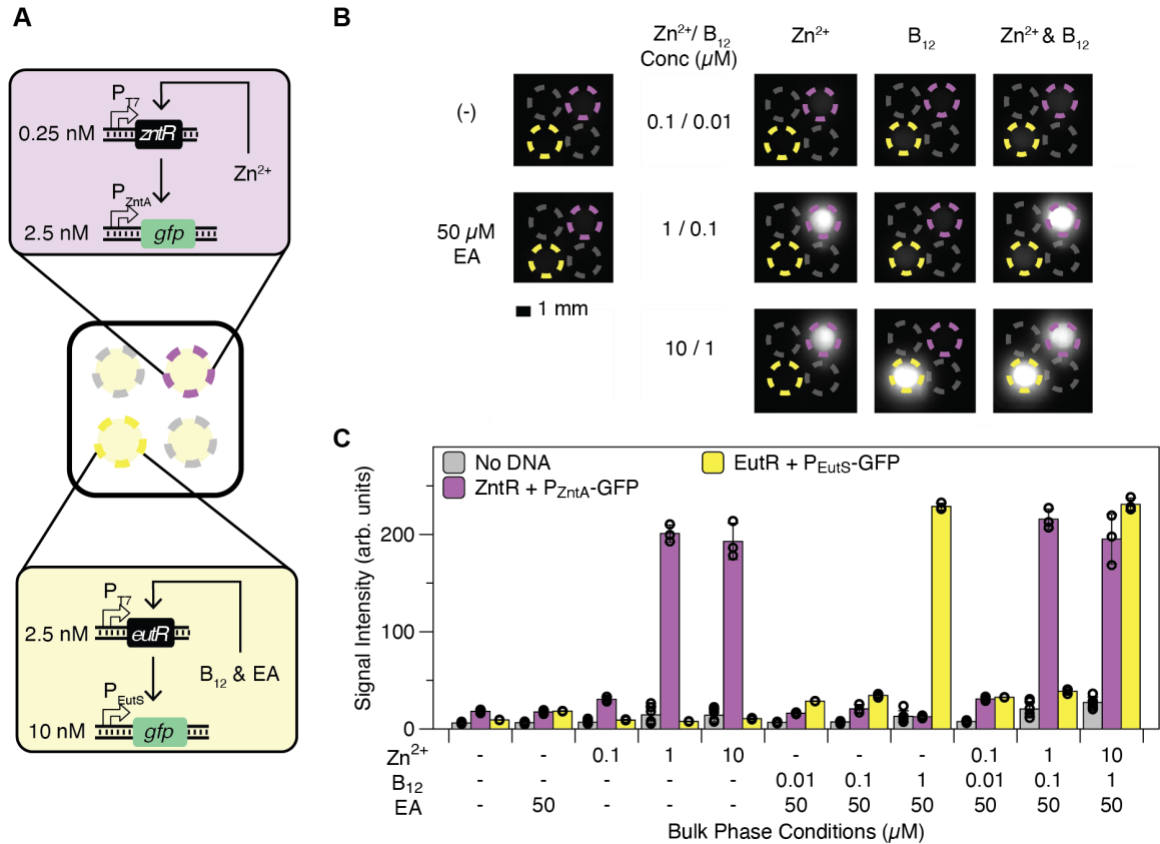


Figure 2-8 Protocell array setup for simultaneous detection of zinc and vitamin B_{12} in protocell arrays. Reactions were incubated at $37\text{ }^{\circ}\text{C}$ for 3 hours. (A) Schematics of zinc and vitamin B_{12} sensors and their concentrations. Zinc modulates GFP expression by binding to the transcriptional regulator ZntR, which in turn activates transcription from its cognate promoter P_{zntA} (purple schematic). Vitamin B_{12} modulates GFP expression by binding to the transcriptional regulator EutR with ethanolamine (EA) as a cofactor. EutR then activates transcription from its cognate promoter P_{EutS} (yellow schematic). Gray circles represent protocells with CFE reactions without plasmid DNA. (B) Representative fluorescence images of simultaneous detection of small molecules at different input and concentration conditions. (-) indicates neither zinc nor vitamin B_{12} was added in the bulk phase, and $50\text{ }\mu\text{M}$ EA indicates a bulk phase condition with only the cofactor for vitamin B_{12} sensor. Zinc was tested at $0.1 - 10\text{ }\mu\text{M}$. Vitamin B_{12} was tested at $0.01 - 1\text{ }\mu\text{M}$. All micro-wells containing vitamin B_{12} in the bulk phase also have $50\text{ }\mu\text{M}$ EA as a cofactor for sensor activation. Scale bar is 1 mm. (C) Quantification of fluorescence images in

B and their replicates. Data are presented as mean values \pm SD of 3 technical replicates for sensing reactions and 6 technical replicates for protocells with no DNA. Hollow circles represent all data points.

For nucleic acid detection, we developed and used toehold switch sensors that detect nucleic acid sequences from two bacterial pathogens: Shiga toxin-producing *E. coli* (STEC), which is a foodborne pathogen that causes life-threatening gastrointestinal symptoms⁵⁸, and *Bacteroides thetaiotaomicron* (BT), which is linked to increased virulence of STEC⁵⁹. We used a previously developed toehold switch for BT⁹ but had to design new switches for STEC, as previously published *E. coli* switches would cross-react with non-pathogenic *E. coli* strains⁹. We developed two STEC switches targeting genomic sequences of toxin proteins: Shiga toxin I (S1) and Shiga toxin II (S2)⁶⁰. When different combinations of linear DNA coding for BT, S1, and S2 triggers amplified from the genomic DNA of BT and STEC O157:H7 were added to the bulk phase of a microwell containing protocell arrays, all protocell sensors showed orthogonal trigger detection with minimal reaction crosstalk (Figure 2-9), demonstrating that protocell arrays can reliably detect multiple pathogenic bacteria nucleic acid sequences in parallel.

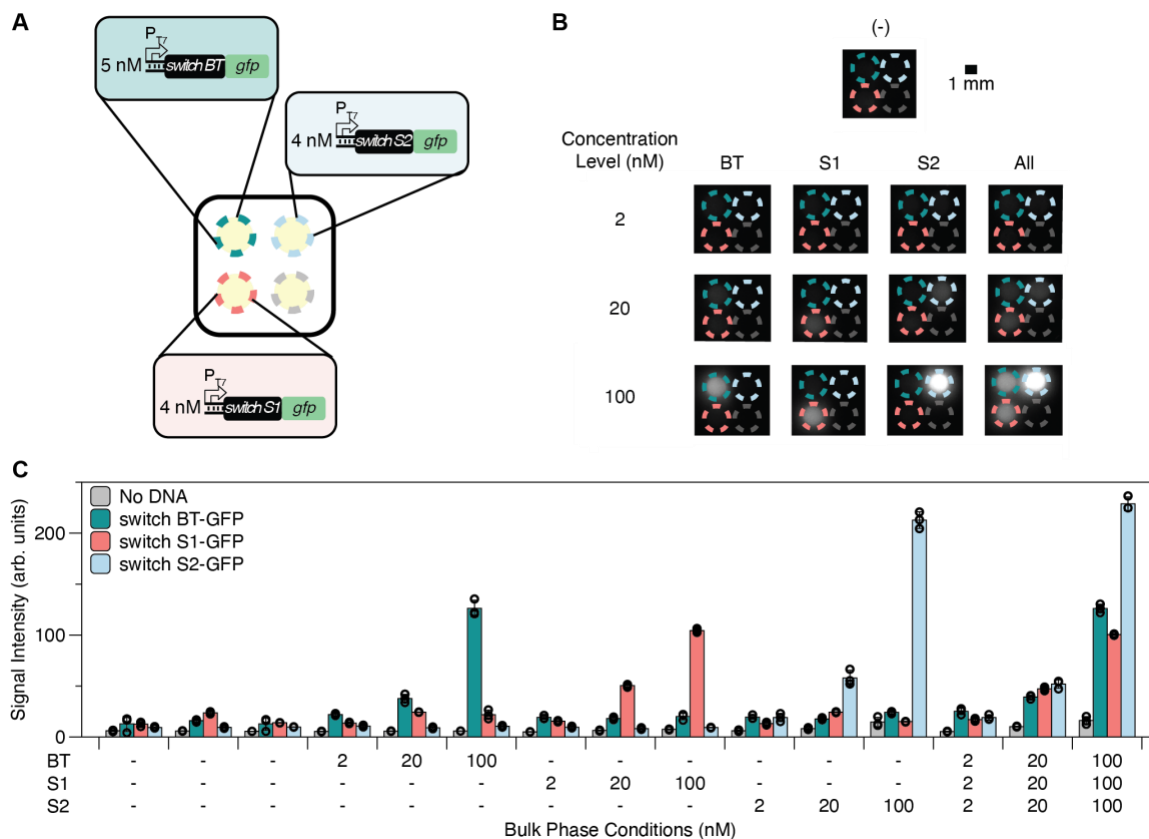


Figure 2-9 Protocell array setup for simultaneous detection of BT and STEC bacteria. Reactions were incubated at 37 °C for 3 hours. (A) Teal, red, and blue circles represent protocells containing toehold switch sensors to detect BT, S1, and S2 triggers, respectively. The gray circle represents a CFE protocell without plasmid DNA. (B) Representative fluorescence image of simultaneous nucleic acid detection at different input and concentration conditions. Location and color of each bacterial sensor as shown in A. Linear DNA for expression of triggers was amplified from genomic DNA of each bacterium and added to the bulk phase at concentrations of 2, 20, and 100 nM. Scale bar is 1 mm. (C) Quantification of fluorescence images from b and their replicates. Data are presented as mean values \pm SD of 3 technical replicates. Hollow circles represent all data points.

We then combined the validated micronutrient and bacterial sensors to demonstrate multi-modal detection of diverse classes of analytes in a chemically defined sample and a contrived human serum sample. A protocell array containing sensors for zinc, B₁₂, S1, and S2 was deposited to the microwell along with different combinations of analytes (zinc, B₁₂, S1 trigger RNA, and linear DNA for S2 trigger expression) in the bulk phase (Figure

2-10A). Each protocell sensor produced GFP only when its cognate analyte was present, demonstrating successful multiplexed detection spanning multiple molecular classes (ion, small molecule, RNA, and DNA) from a single sample (Figure 2-10B). Notably, the protocells used for micronutrient and bacterial sensors compartmentalized different CFE lysates – micronutrient sensors used *E. coli* lysate with basal level T7 RNAP and bacterial sensors used lysate enriched in T7 RNAP. The S2-sensing protocell also contained 2 μ M χ DNA to protect S2 trigger DNA from exonuclease degradation by CFE lysate once it entered the protocell to activate reporter production⁶¹. Because other protocells did not have χ DNA, the competition for transcriptional machinery from S2 trigger that had diffused into those protocells was thus minimized, as that linear DNA would get rapidly degraded in those protocells⁶¹. This showcases the fact that multiple customized sensing reactions can coexist in the same protocell array without negatively impacting neighboring protocell reactions.

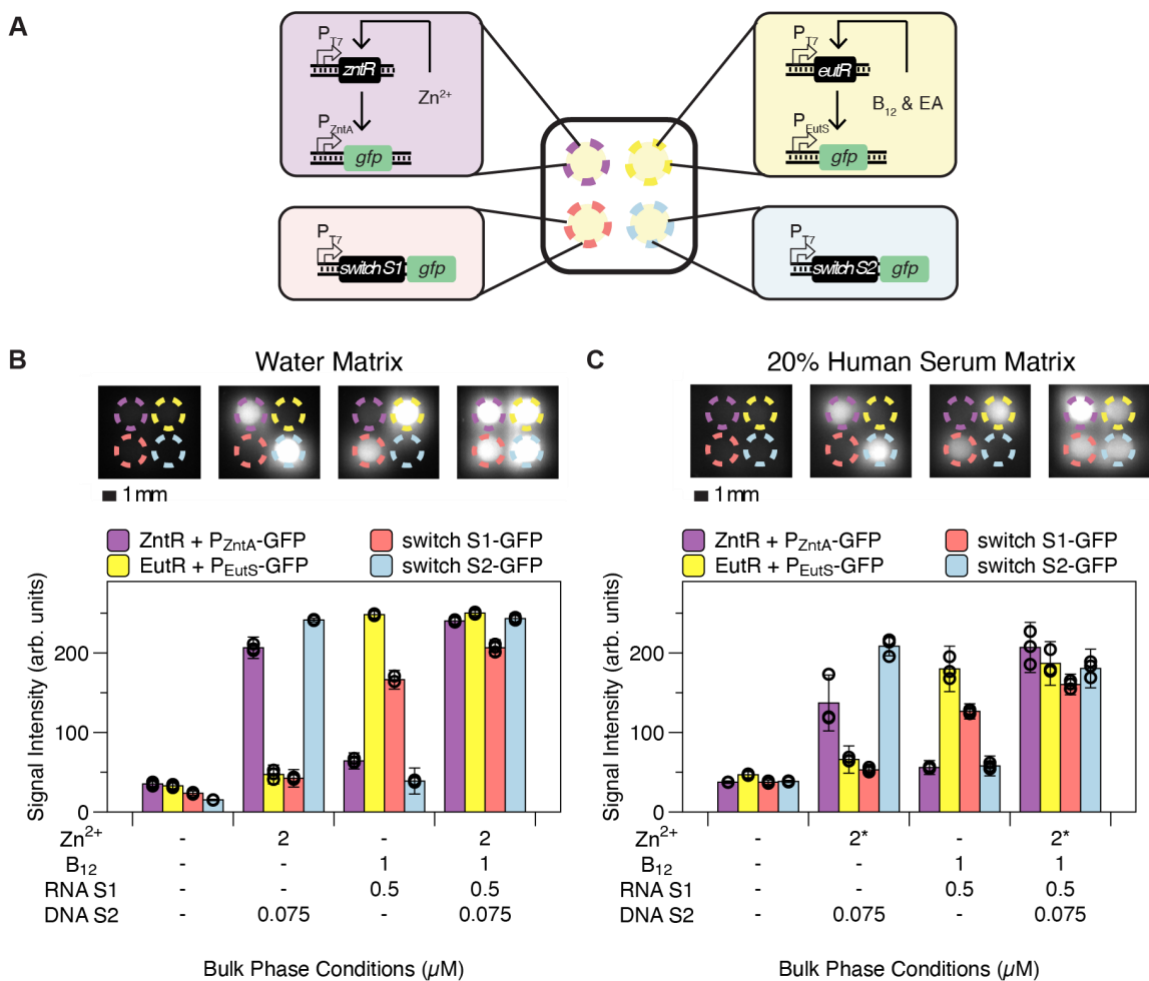


Figure 2-10 Simultaneous detection of multiple clinically relevant biomarkers across multiple molecular classes in water and 20% human serum matrices. Reactions were incubated at 37 °C for 3 hours. (A) Schematic of membrane-less protocell array setup for multi-modal, simultaneous detection of diverse classes of clinically relevant biomarkers. Purple and yellow circles indicate micro-basins containing zinc and vitamin B₁₂ sensors, respectively. Red and blue circles indicate micro-basins containing S1 and S2 toehold switches, respectively. (B) Representative fluorescence image (top) and pixel quantification of its replicates (bottom), demonstrating multi-modal target measurement using protocell arrays with simultaneous detection of ion, small molecule, RNA, and DNA targets from the same bulk phase. (C) Multi-modal target detection in a 20% human serum matrix. Representative fluorescence image (top) and quantification of fluorescence of representative image and its replicates (bottom) demonstrating the robustness of protocell arrays to a complex sample matrix. The asterisk (*) next to the zinc concentration indicates the total zinc concentration is 2 μM in the bulk phase after accounting for the zinc remaining in chelated human serum. Of note, the sensor plasmid concentrations were increased in C compared to B to yield comparable output signal; this tuning was necessary due to the decrease in protein expression that occurs in human serum²⁵. Data are presented

as mean values \pm SD of 9 replicates (3 biological replicates x 3 technical replicates). Hollow circles indicate the mean of each biological replicate. Scale bar is 1 mm.

With this multi-modal, multiplexed analyte sensing platform established, we next sought to verify that detection with protocell arrays remains robust even in complex samples such as human serum. We increased sensor plasmid concentrations to compensate for nuclease activity in serum^{62,63} and spiked 20% human serum with target molecules at levels similar to those used in our previously published CFE efforts²⁵. With these contrived serum samples as the bulk phase, we observed target-specific activation from all protocell sensors (Figure 2-10C), demonstrating our platform's translational potential for assessment of biomarkers in patient samples.

We note that the presence of S1 RNA and B₁₂ in the bulk phase caused a slight increase in overall expression from the zinc sensor (both in basal expression levels in the +S1 +B₁₂ case compared to the null case, and in activated levels in the +all case compared to the +S2 +Zn²⁺ case, Figure 2-10). This is a prototypical example of a “matrix effect”, where analytes other than a sensor's target analyte that are present in the same sampling matrix can cause changes in a sensor's response⁶⁴⁻⁶⁶. Matrix effects are a widely-encountered analytical issue that must be addressed for almost any quantitative sensor or diagnostic in a complex sample matrix^{25,64-66}.

In addition to matrix effects due to different target analytes, the presence of human serum also has inhibitory effects on CFE protein production²⁵ (Figure 2-10). Serum's negative impact on CFE protein production is potentially caused by nuclease activity^{62,63}. As a result, we increased the plasmid concentrations of biosensors to counteract the loss in protein production and provide comparable signal output in a serum matrix.

2.3.4 *Toward a field-deployable, equipment-free diagnostic platform*

To be useful as a minimal-equipment, point-of-care sensing and diagnostic tool, the membrane-less protocell array platform should produce test results that can be visually interpreted without the aid of equipment like plate readers or fluorescence imagers. Toward this goal, we replaced the GFP reporter protein with β -galactosidase (LacZ), an enzyme that catalyzes the production of a colorimetric readout. We tested two colorimetric substrates, chlorophenol red-beta-D-galactopyranoside (CPRG) and 5-Bromo-4-chloro-3-indolyl β -D-galactopyranoside (X-gal), that are substrates for LacZ and are widely used for CFE diagnostics and molecular biology assays, respectively^{7-9,25,67}. We also used a new white microwell design to improve pigment visualization, reduce the bulk phase volume requirement, and increase the number of micro-basins in a microwell to include more reactions (Figure 2-2B). We found that, while LacZ could produce visible color change 30 minutes faster when cleaving CPRG than when cleaving X-gal, the product of CPRG cleavage rapidly diffused from the protocell to the surrounding bulk phase (Figure 2-11). This diffusion would obscure result interpretation if readings were not taken within 30 minutes of color change, which could be an issue if different multiplexed sensors have different characteristic response times. As a result, we chose to use X-gal for subsequent test development based on its stable localization of pigments, despite a longer reaction time.

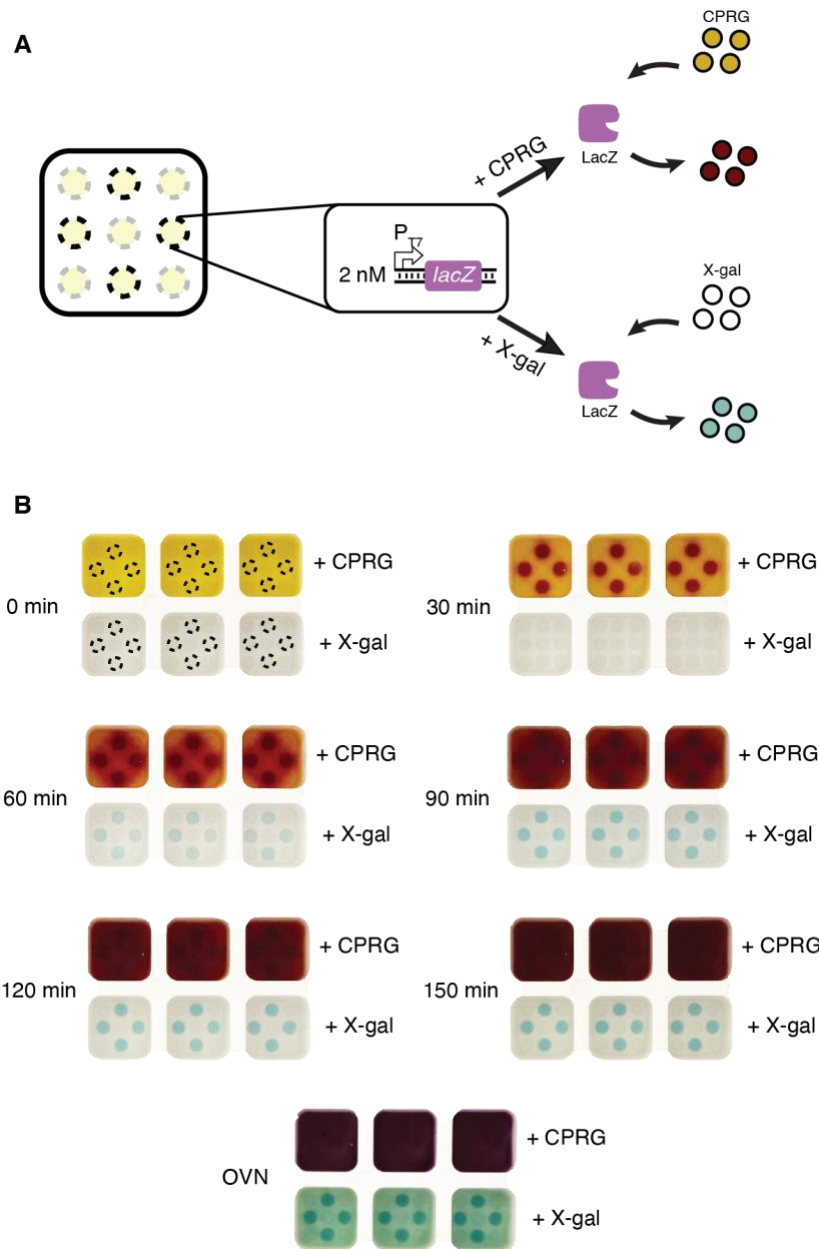


Figure 2-11 Protocell array output can be interpreted without equipment. (A) Schematic of visually interpretable protocell array sensing reactions. Black circles represent micro-basins containing protocells that constitutively produce LacZ. The bulk phase contains either 0.6 mg/mL CPRG (yellow in panel B) or 0.2 mg/mL X-gal (colorless in panel B) as the substrate for pigment production. Once produced, the LacZ enzyme either cleaves CPRG to form chlorophenol red (CPR, red) or cleaves X-gal to form a blue precipitate. (B) Time course pigment production from two substrates. The bulk phase containing CPRG yields visible color change within 30 minutes of incubation, but the pigment readily diffuses into the bulk phase at later time points, making test results uninterpretable. The bulk phase containing X-gal produces visible color more slowly, with visible color change occurring at 1 hour.

However, the color remains localized over the entire incubation period and is still mostly localized even after overnight incubation (> 14 hrs). Images presented are 3 technical replicates derived from the same reagent master mix.

We next used this colorimetric reporter to detect the presence of nucleic acid sequences characteristic of pathogenic bacteria. A protocell array with toehold switch-based sensors for BT, S1, and S2 was loaded into micro-basins, and the bulk phase contained combinations of linear DNA coding for expression of cognate triggers amplified from the genomic DNA of BT and STEC O157:H7 (Figure 2-12A). All protocell sensors turned visibly blue to accurately report on the presence of the triggers within 2 hours with minimal pigment leakage to neighboring reactions (Figure 2-12B).

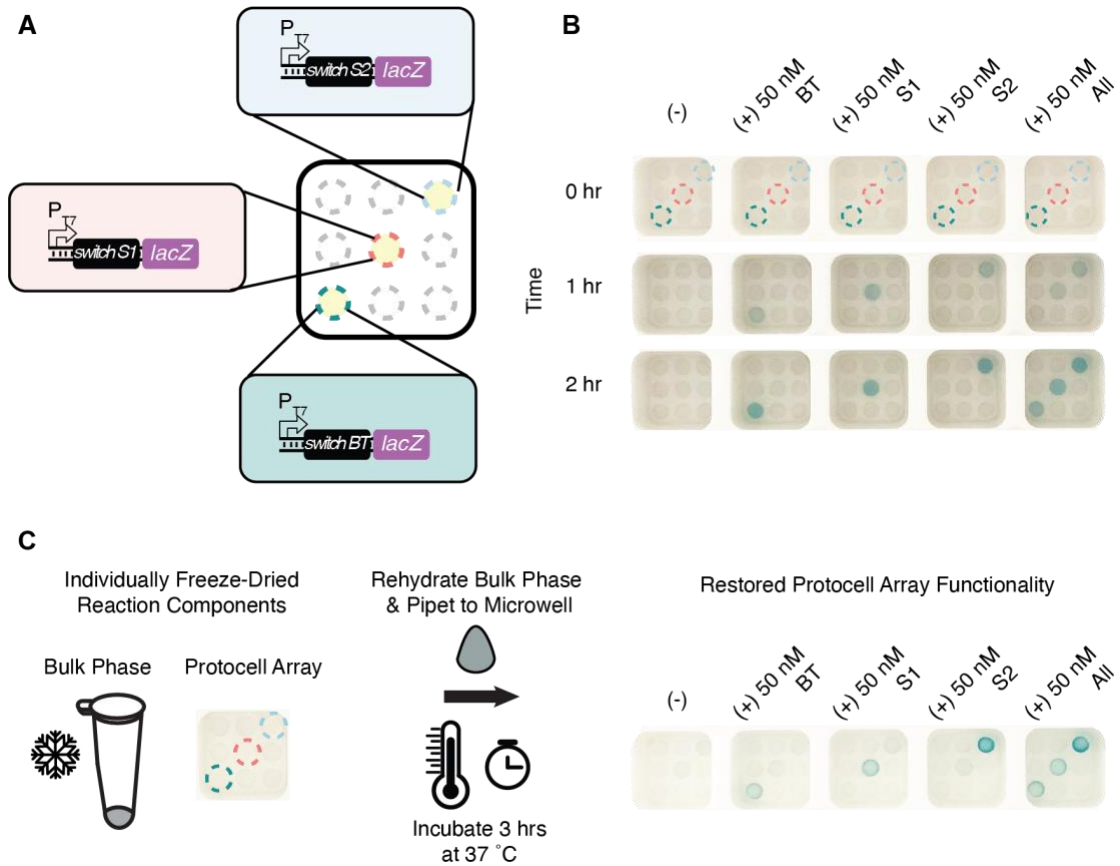


Figure 2-12 A membrane-less protocell array meets key criteria for a minimal-equipment, field-deployable multiplexed assay. (A) Schematic of colorimetric protocell array setup for simultaneous detection of multiple nucleic acid sequences.

Teal, red, and blue circles indicate micro-basins containing BT, S1, and S2 protocell sensors, respectively. Gray circles indicate empty micro-basins without CFE reactions. (B) Representative sensor activation and pigment production in different bulk phase conditions and at different time points. Images in the same row were taken at the same incubation time. The concentration and the type of DNA trigger(s) used are indicated above each image. Dashed circles indicate micro-basins containing protocell sensors, as shown in A. (C) Protocell array functions after lyophilization. Protocells containing CFE reactions coding for sensors of bacterial nucleic acid sequences were lyophilized in micro-basins within microwells, and bulk phase solutions were lyophilized separately. Addition of sample-reconstituted bulk phase to microwells formed the protocells *via* liquid-liquid phase separation and revived CFE sensing reactions leading to pigment production after 3 hours of incubation at 37 °C.

Additionally, a field-deployable protocell array-based sensing platform must be compatible with storage and transportation at ambient temperature for easy distribution to the point of need. To demonstrate our system's ability to meet this criterion, we lyophilized arrays of Ficoll CFE sensors containing different bacteria nucleic acid sensors in micro-basins and separately lyophilized the bulk phase solution (containing PEG, X-gal, and CFE energy buffer). We show that the addition of water- or trigger-reconstituted bulk phase to the array formed the protocells *via* liquid-liquid phase separation and activated the CFE sensors in the protocell arrays. All bacteria-sensing protocells remained compartmentalized in their micro-basins, produced visible color change within 3 hours of incubation at 37 °C, and accurately reported the triggers added to the bulk phase (Figure 2-12C). This result suggests the possibility of a simple-to-operate multiplexed assay that can be performed by minimally trained staff, which is critical for point-of-need use in the field of environmental or epidemiological surveillance.

2.4 Discussion

In recent years, membrane-less protocell models have been used for various scientific and engineering applications, including cell-like functionalities such as selective nucleic

acid retention^{47,68}, reaction acceleration^{69,70}, and droplet division⁷¹. Despite being membrane-less, these phase-separated droplets are quite robust, maintaining their structure through dehydration and rehydration cycles⁷² and enabling potentially impactful downstream uses. One example is the acoustically-trapped protocell patterning technique that enables different enzymatic reactions to occur in adjacent protocells⁷³. However, such a strategy requires complex equipment and extensive optimization of reaction environments, making it challenging to implement at the point of need.

Our approach using polymer ATPS to construct protocell arrays can address current limitations in bringing multiplexed analyte measurement to field applications. We show that topographical micro-basin features patterned on the floor of standardized 96-well plate format microwells (Figure 2-2) enable multiple protocells to coexist spatially separated without any external input to maintain separation. The membrane-less aspect of protocells formed by ATPS also facilitates minimally-hindered analyte diffusion (and even concentration for some analytes with favorable partitioning behaviors^{33,38,74}) into the protocells. Furthermore, these protocells can compartmentalize custom-designed CFE reactions that can detect diverse classes of analytes, remain robust to complex sample environments, and retain their sensing capabilities after lyophilization for on-demand, simultaneous measurement of multiple analytes at the point of need.

The embedding of CFE reactions in ATPS-formed protocells is uniquely poised to meet many key challenges in biosensing applications, as this platform can be customized to detect diverse sets of analytes by reprogramming the DNA sequence of plasmids used as the basis for sensing. Previous work has demonstrated that CFE can be used to detect metabolites *via* incorporation of genetically encoded metabolic transducers^{29,75}, proteins

via genetically encoded aptamers^{42,76}, and nucleic acids *via* genetically encoded synthetic regulators^{7,9,77}. These different sensing systems often require differently optimized CFE reactions (e.g., lysate preparations or macromolecular reaction additives), but these individually optimized sub-systems can all be used together in parallel to measure different targets in the same sample. Of note, the protocells sensing nucleic acids in Figure 2-10 used a T7 RNAP-enriched lysate, while protocells sensing small molecules did not. Moreover, only the protocell expressing S2 switch contained χ DNA for linear DNA protection, which helped to minimize competition for transcription resources in the other protocells as the linear DNA coding for S2 trigger would be degraded in the other protocells. Selectively tuning an individual sensor's performance without negatively impacting other sensors is an enabling advance for simultaneous, parallel measurement of multiple analytes, made possible by encapsulating individual sensors into discrete, phase-separated protocells. The compartmentalization of protocell sensors eliminates the need for multiple, orthogonal, or target-specific reporter systems, allowing all sensors in the same microwell to be developed with the same reporter system. This facilitates rapid development of test panels, as newly developed sensors can be readily incorporated into existing protocell arrays with obsolete sensors easily replaced.

An array of spatially separated gene networks that sense and respond to different analytes in the same environment has many potential applications. One such example is in agricultural and environmental surveillance²¹, where a small environmental sample can indicate the presence of a pollutant, excessive fertilizer, or even an animal or plant pathogen. Another example would be to study crosstalk between protocells. While interactions between sensor protocells would be construed as a problem for developing

diagnostics, the ability for individual protocells to produce small molecules that could diffuse to other protocells in the array could be used as a platform for prototyping chemical communication networks among synthetic cells^{78,79}. Each protocell could be separately programmed with a different function, allowing for the investigation of different communication networks at the single-(proto)cell level. In addition, the physical arrangement of protocell arrays—a reaction phase with an interface to a bulk liquid where diffusion of small molecules can occur freely between the two liquids—is similar to a CFE reaction operating in dialysis mode, which has been shown to extend CFE reaction lifetime⁸⁰. In dialysis operation, toxic molecules produced in CFE reactions can diffuse out of the reaction volume, potentially improving CFE yield. Thus, protocells could provide a new way to accrue the benefits of dialysis mode reactions without expensive dialysis membranes or cassettes.

Perhaps the most impactful application of these membrane-less protocell arrays is for point-of-care diagnostics with simultaneous, parallel detection of multiple clinically relevant biomarkers in human biofluids. Many diseases and disorders that clinicians and researchers seek to identify in the field are not diagnosed based on just one biomarker but by the combination of multiple test results, often spanning multiple classes of biomolecules. The protocell array formed by CFE and ATPS is an enabling platform for these needs. It is compatible with complex sample matrices and withstands lyophilization for intact functionality upon rehydration, enabling flexible test development and deployment to the point of need without expensive cold chain requirements. However, in our efforts to demonstrate serum compatibility with protocell arrays, we found that serum proteins formed cloudy precipitates when added to a PEG-rich bulk phase. While serum

protein precipitation did not obstruct biphasic polymer separation and detection of GFP signal, it hindered micro-basin and pigment visualization in colorimetric reactions. One possible way to resolve this might be to use clear-bottomed plates such that pigments can be visualized from the bottom³⁴.

The results in Figure 2-10 demonstrate our platform's translational potential for assessment of biomarkers in patient samples. We achieved zinc detection at 2 μM , which is within the clinically relevant range for zinc deficiency (1.7-2.3 μM in 20% human serum)^{25,81}. Unfortunately, there is currently no CFE-based B₁₂ sensor with a limit of detection in the clinically relevant range for B₁₂ deficiency (15 - 80 pM in 20% serum)^{11,82}. Activation of the B₁₂ sensor at 1 μM nonetheless offers a proof-of-concept toward simultaneous detection of diverse classes of analytes in a complex human serum matrix. In addition, since pathogen nucleic acids are typically present at femtomolar concentrations^{7,9,83}, nucleic acid amplification methods such as NASBA or RT-RPA would need to be integrated into the sample workup or directly into protocell arrays to bring these targets into the sensor response range. This input amplification (common to nearly all current CFE nucleic acid sensors^{7,9,30,77}) does, however, increase the level of complexity of the test and require trained operators to execute. Fortunately, ongoing research efforts are moving toward eliminating the need for upstream input amplification⁸⁴. Given the demonstrated modularity and easily reconfigurable format of our platform, those resulting amplification-free CFE systems could be incorporated into our protocell array and enable one-pot detection of clinically relevant biomarker levels. Nonetheless, one would still need to ensure that any upstream processing does not alter levels of other targeted biomarkers present in the sample.

In conclusion, we have demonstrated that arrays of polymer ATPS-formed, membrane-less protocells with compartmentalized DNA transcription and RNA translation machinery can perform simultaneous detection of diverse classes of analytes. Such a protocell system survives lyophilization to enable test storage and distribution at ambient temperature. Rehydration with an analyte-containing polymer solution reestablishes phase separation, allows uptake of analytes by the resulting protocell sensors, and revives compartmentalized transcription- and translation-mediated detection reactions. These arrays of membrane-less protocells provide modular, field-deployable, multi-modal, multiplexed diagnostic potential. Interfacing CFE reactions with membrane-less protocells addresses the current limitation in simultaneous detection of diverse analytes from a single sample and opens new opportunities for implementing diagnostic panels for use at the point of care.

CHAPTER 3. POINT-OF-CARE ANALYTE QUANTIFICATION VIA LYSATE-BASED CELL-FREE BIOSENSORS INTERFACED WITH PERSONAL GLUCOSE MONITORS

Portions of this chapter are reproduced from my publication “Point-of-care analyte quantification and digital readout *via* lysate-based cell-free biosensors interfaced with personal glucose monitors” in *ACS Synthetic Biology*⁸⁵.

3.1 Introduction

Field-deployable diagnostics based on cell-free expression (CFE) systems have advanced greatly, but on-site quantification of target analytes remains a challenge. Most of the current on-site CFE detection strategies use enzymatic reporters to generate visible color pigment for either a binary, yes-or-no result readout^{7,8} or a semi-quantitative measurement of target concentration using transient color changes²⁵. Others have used custom-built, portable electronic devices in place of bulky plate readers for result interpretation and quantification^{7,8,21}. While these efforts represent promising strides toward quantitative analyte measurement at the sampling site, few of these approaches or devices can match the simplicity, quantification, and digital readout offered by a personal glucose monitor (PGM). As a result, there has been significant research effort to engineer biosensors that can be read by a glucose monitor^{39,40,86-92} rather than trying to engineer entirely new quantification devices that match the PGM’s portability and reliability. Recent efforts have even successfully interfaced glucose monitors with CFE system-based biosensors, though they were subject to significant limitations.

The first-ever reported use of CFE systems with a glucose monitor was limited to using reagent complementation strategies⁸⁶, such that it was only used to measure analytes that were required components of the CFE reaction. A more recent report demonstrated detection of the presence and absence of targets (nucleic acid sequences) but did not aim for analyte quantification⁸⁷. In addition, the demonstration used an expensive, purified protein expression system (PURExpress, at almost \$10 per sample) and required a separate, overnight enzymatic conversion step to remove confounding glucose that is present in the sample. The glucose removal step that was used required the user to know in advance the sample glucose levels and then add sample-specific volumes of reagents to clear native glucose from samples without causing unwanted degradation of the glucose generated by the sensing reaction. All of these requirements decrease that approach's potential viability for field-deployable applications. While that report was a significant step forward, the use of a PGM for qualitative, presence/absence diagnosis rather than quantitative measurement meant the strategy did not fully exploit one of the most critical and impactful capabilities offered by PGMs. Even more importantly, for most clinically relevant biomarkers for conditions other than infectious disease, it is the biomarkers' concentration—not merely their presence or absence—that is the criterion for diagnosis^{25,93-95}. For these target analytes, quantification at the point of need is critical and digital readout enables straightforward result interpretation.

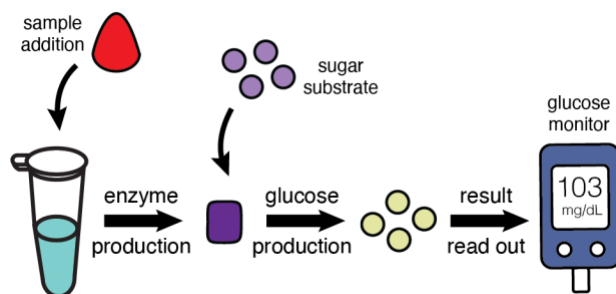


Figure 3-1 Schematic of glucose monitor-mediated measurement of an analyte present in the biological sample. The biosensor produces a sugar-converting enzyme (LacZ) in response to different concentrations of the analyte. LacZ then converts a complex sugar substrate (lactose) into glucose measurable on a glucose monitor.

Here, we aim to expand the repertoire of glucose monitor-mediated analyte detection to include quantification of diverse sets of analytes *via* lysate-based CFE systems. We first showed that a genetic circuit constitutively expressing the enzyme β -galactosidase (LacZ) in the CFE lysate reaction successfully allows LacZ conversion of lactose to glucose and yields measurable PGM outputs (Figure 3-1). We then demonstrated analyte-modulated LacZ production and glucose conversion *via* different biosensing circuits. We successfully used a zinc-responsive transcription factor to generate dose-dependent expression of LacZ to identify zinc deficiency in a human serum matrix at clinically relevant concentrations. We further showed that the same detection strategy could be used to detect and quantify nucleic acid biomarkers from pathogenic *E. coli* by merely substituting the zinc transcriptional control elements with RNA regulatory elements (toehold switches). In developing these diagnostic sensors, we found that the metabolic pathways active in lysate-based CFE systems⁹⁶⁻¹⁰⁰ readily deplete glucose in reactions. As a result, we decoupled LacZ production from glucose conversion and capitalized on this lysate metabolism for one-pot removal of glucose that may be initially present in a complex sample environment (like human serum or other biofluids), thereby eliminating a separate processing step to

remove endogenous glucose required in current PGM-mediated analyte quantification methods^{87,91,92}. Taken together, our work showcases a broadly applicable and modular strategy for rapid and reliable quantification of target analytes at the point of need, expanding the repertoire of PGM-mediated biomarker detection with biosensors expressed in lysate-based CFE systems.

3.2 Materials and Methods

3.2.1 Bacterial strains and plasmid preparation

E. coli strain DH10 β was used for all cloning and plasmid preparations. *E. coli* strain BL21 Star (DE3) $\Delta lacIZYA$ was created by lambda red recombination and used for in-house cell-free lysate preparation. Genomic DNA from *E. coli* O157: H7 (ATCC 51657GFP) was used as a template for *stx1* and *stx2* trigger amplification.

Sequences for all DNA and plasmid parts used in this study are provided in Appendix

B.2 Sequence Information. Eurofins Genomics synthesized DNA oligonucleotides for cloning and sequencing. Plasmid DNA used for all CFE reactions was purified from EZNA midiprep columns (OMEGA Bio-Tek) followed by isopropanol and ethanol precipitation. The purified DNA pellets were reconstituted in the elution buffer, measured on a Nanodrop 2000 for concentration, and stored at -20 °C until use.

3.2.2 *Crude E. coli cell-free lysate preparation*

Cellular lysate for all experiments was prepared as described by Sun *et al*¹⁸. with a few protocol modifications. Briefly, BL21 Star (DE3) $\Delta lacIZYA$ cells were grown in 2× YTP medium at 37 °C and 220 rpm to an optical density (OD) of 0.3-0.5 for IPTG induction at 0.4 mM to activate expression of T7 RNAP Polymerase. The cells were grown further until the OD was 1.5-2.0, corresponding to the mid-exponential growth phase. Cells were centrifuged at 2700 rcf and washed three times with S30A buffer (50 mM tris, 14 mM magnesium glutamate, 60 mM potassium glutamate, 2 mM dithiothreitol, and pH-corrected to 7.7 with acetic acid). After the final centrifugation, the wet cell mass was determined, and cells were resuspended in 1 mL of S30A buffer per 1 g of wet cell mass. The cellular resuspension was divided into 1 mL aliquots. Cells were lysed using a Q125 sonicator (Qsonica) at a frequency of 20 kHz and 50% amplitude. Cells were sonicated on ice with cycles of 10 s on and 10 s off, delivering approximately 200 J, at which point the cells appeared visibly lysed. An additional 4 mM dithiothreitol was added to each tube, and the sonicated mixture was then centrifuged at 12,000 rcf and 4 °C for 10 min. After centrifugation, the supernatant was removed, divided into 100 μ L aliquots, and stored at -80 °C until use.

An additional runoff reaction and dialysis were performed in lysate used for expression of toehold switches and malachite green aptamer. Briefly, the centrifuged sonication product was incubated at 37 °C and 220 rpm for 80 min. After this runoff reaction, the cellular lysate was centrifuged at 12,000 rcf and 4 °C for 10 min. The supernatant was removed and loaded into a 10 kDa molecular weight cutoff dialysis cassette (Thermo Fisher). The lysate was dialyzed in 1 liter of S30B buffer (14 mM magnesium glutamate, 60 mM potassium glutamate, 1 mM dithiothreitol, and pH-corrected to 8.2 with tris) at 4 °C for 3 hours. Dialyzed lysate was removed and centrifuged at 12,000 rcf and 4 °C for 10 min. The supernatant was removed, aliquoted in volumes of 100 µL, and stored at -80 °C for future use.

3.2.3 CFE reactions

The CFE reaction composition was as previously described by Kwon and Jewett¹⁷. All lysate and reagent master mixes were thawed on ice and had fewer than 3 freeze-thaw cycles. All reactions were assembled on ice and in PCR tube strips. The reaction master mix containing lysate was vortexed briefly at a medium-high setting to ensure homogenous mixing before being aliquoted into individual reactions. All CFE reactions, except reactions expressing toehold switches or malachite green aptamers, used crude lysate without post lysate processing steps such as run-off reactions and dialysis. Dialyzed lysate was used for toehold switch and malachite green aptamer reactions due to its enhanced transcriptional capacity¹⁹.

For reactions measured with a plate reader, each CFE reaction was 10 µL in volume and pipetted into a black-bottomed 384-well plate (Greiner Bio-One) for fluorescence

measurement or a clear-bottomed 384-well plate (Greiner Bio-One) for absorbance measurement. Kinetic reads were performed in a plate reader (Synergy4, BioTek) at 37 °C for 1 hr. The filter setting for GFP measurement was 485/510 nm excitation/emission wavelengths, with the gain set at 70. The filter setting for malachite green measurement was 615/650 nm excitation/emission wavelengths, with the gain set at 100. For chlorophenol red- β -D-galactopyranoside (CPRG) measurement, sample absorbance was measured at 580 nm. All plates were sealed with a transparent, adhesive film to prevent evaporation.

For reactions read on a PGM, each assembled CFE reaction was 9 μ L in volume and placed in a PCR tube with the cap on to prevent evaporation. Reactions were incubated at 37 °C in a thermocycler for the specified amount of time before glucose measurement. For reactions quenched with the naproxen-lactose mix, 1 μ L of the 10x quench mix (100 mM naproxen sodium and 400 mM lactose) was added to each reaction and the mixture was vortexed at medium-high setting, settled to the bottom of the tube using a mini centrifuge, and incubated at 37 °C for 15 minutes before measurement on a PGM. The same concentration of the naproxen-lactose mix was added to all CFE reactions.

3.2.4 PGM quantification

A glucose oxidase-based PGM (OneTouch Ultra 2 Blood Glucose Monitoring System, LifeScan Inc) and accompanying test strips (OneTouch Ultra Test Strips, LifeScan Inc) were used for glucose measurement. Once the glucose-generating step of the reaction was completed, 2 μ L of each reaction was spotted on the test strip and measured with the

PGM. Because the PGM's readout range is from 20 to 600 mg/dL, values below or above the meter threshold were assigned a value of 20 mg/dL or 600 mg/dL, respectively.

3.2.5 *Serum processing*

Pooled human serum was collected from donors as approved in Institutional Review Board protocol number H17489. Venous blood was collected in 6 mL of BD Vacutainer collection tubes for trace element testing, and tubes were left on ice for about 30 min to clot. Blood was transferred to a 50 mL conical tube and centrifuged at 2700 rcf for 30 min at 4 °C. Serum was removed, and an aliquot of untreated human serum was saved for zinc baseline analysis. The remaining serum was treated with Chelex 100 resin by adding 1 mg resin per 1 mL of serum and vigorously stirred for 2 hrs at room temperature. The resin was isolated from samples through centrifugation and syringe filtering. All serum samples were aliquoted to minimize free-thaw cycles and stored at -20 °C until use.

Measurement of successful zinc removal from serum was done at the University of Georgia Laboratory for Environmental Analysis. Samples were digested with concentrated acid and analyzed on ICP-MS according to EPA method 3052.

3.2.6 *Trigger preparation*

DNA encoding each trigger RNA used in experiments was amplified from the genomic DNA of *E. coli* O157: H7 via PCR with Q5 DNA polymerase (New England Biolabs). Sequences for primers used to amplify triggers from DNA template or genomic DNA are provided in the supplementary table of the manuscript. After PCR amplification,

products were run on a 2 w/v% agarose gel to verify strain-specific amplification of targets and then purified using a PCR purification kit (Omega Bio-Tek). The prepared linear DNA was either directly used in CFE reactions or used as a template for *in vitro* transcription.

RNA triggers were transcribed from a linear DNA template using T7 polymerase according to the manufacturer's protocol (New England Biolabs). Following RNA synthesis, Dnase I (Zymo Research) was added to degrade the linear DNA template. The RNA products were then purified using an RNA Clean and Concentrator kit (Zymo Research) according to the manufacturer's protocol. Following purification, RNA concentration was measured on a Nanodrop 2000, aliquoted, and stored at -20 °C.

3.3 Results

3.3.1 Lysate-based CFE reaction producing LacZ enzyme can convert lactose to measurable glucose

The first step toward PGM-mediated analyte quantification using lysate-based CFE reactions was to confirm that the CFE reagents are compatible with commercial PGMs. To verify reagent compatibility and glucose stability, we incubated D-(+)-glucose (hereafter referred to as glucose) at concentrations of 0-25 mM in CFE reactions to span the full PGM detection range and tracked their respective value readouts over time. Compared to glucose standards prepared in water, we observed a slight decrease in signal output for immediate measurement of the same glucose concentration in the CFE matrix (Figure 3-2A). We also found significant glucose consumption in CFE reactions over time (Figure 3-2A). This finding was perhaps unsurprising, as previous reports have observed and characterized significant endogenous glycolytic metabolic activity in CFE lysates⁹⁶⁻¹⁰⁰; we attributed the

loss in signal output over time to enzyme-catalyzed conversion of glucose to glucose-6-phosphate due to residual glycolytic activity in the lysate.

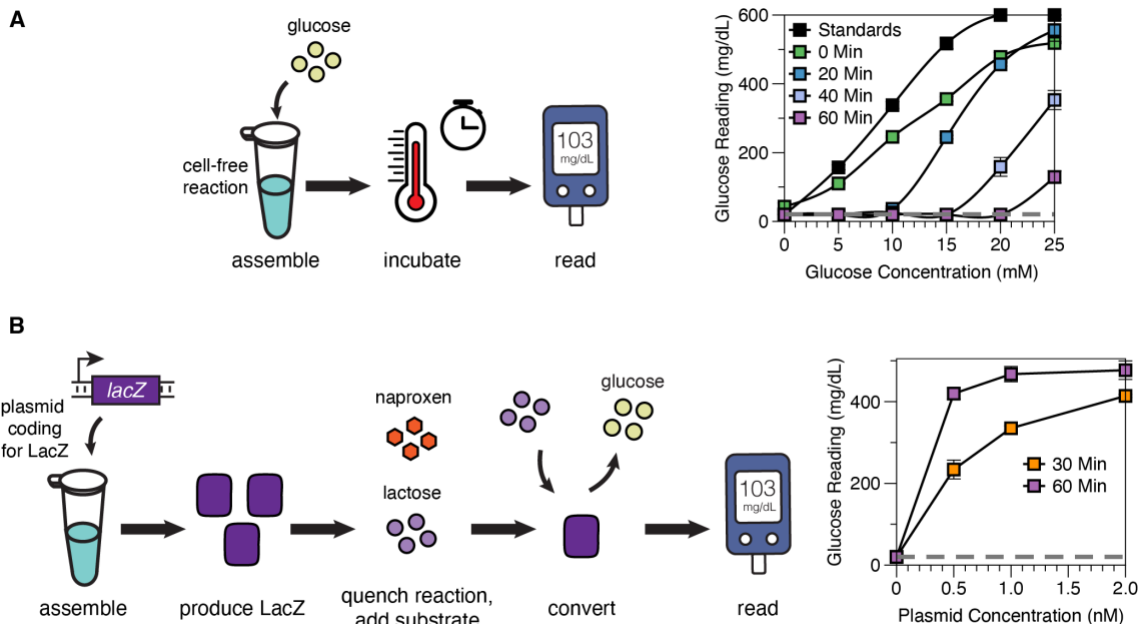


Figure 3-2 Characterization of glucose production and depletion in CFE reactions. (A) Verification of CFE compatibility with PGM and time-course measurement of glucose depletion in reactions. A slight decrease in PGM output was observed for the same concentration of glucose in the CFE matrix and no incubation time compared to glucose in a water solution (“Standards”). Rapid depletion of glucose signal was observed in all CFE reactions over time. Error bars represent the standard deviation of CFE reaction triplicates. Dashed gray line represents PGM’s lowest reading threshold, 20 mg/dL. (B) Decoupling enzyme production and glucose conversion in CFE reactions enabled dose-dependent PGM signal output. CFE reactions containing varying concentrations of plasmid constitutively expressing LacZ were incubated for 30 to 60 minutes before each reaction was quenched by naproxen-lactose mix to shift the reaction from enzyme production to glucose conversion. Plasmid concentration-modulated glucose production was detected using the PGM after 15 minutes of incubation. Error bars represent the standard deviation of CFE reaction triplicates. Dashed gray line represents PGM’s lowest reading threshold, 20 mg/dL.

Endogenous glycolytic activity in crude *E. coli* lysate could pose serious problems for CFE-mediated analyte quantification using PGMs, since glucose molecules generated by the reporter enzyme in the CFE reaction would be readily depleted, and thus desired

signal would be lost. To address this issue, we chose to decouple reporter enzyme production from enzyme-catalyzed glucose production. To assess how fast glucose can be produced for detection by the PGM, we added a plasmid for constitutive expression of the enzyme LacZ to the CFE reaction for 30 to 60 minutes. Following this incubation, a mixture consisting of naproxen and lactose was added to the CFE reaction to terminate transcription in the CFE system (*via* naproxen), slow down lysate metabolism (*via* naproxen), and start glucose production *via* LacZ conversion of lactose to glucose. Different concentrations of plasmid that constitutively express LacZ were used as a testbed model for our eventual goal of LacZ expression that increases based on the amount of analyte present. After 15 minutes of incubation, we observed plasmid dose-modulated glucose signal production on the PGM (Figure 3-2B). Naproxen was used here due to its effectiveness at inhibiting CFE reactions without impairing LacZ activity²⁵ (Figure 3-3A-D). We anticipate that other small molecule inhibitors added at high concentrations could also be capable of halting the CFE reaction, but we chose naproxen here due to its minimal effects on LacZ-mediated glucose production, its inhibition of endogenous glucose depletion (Figure 3-3E), and our previous experience using naproxen with CFE biosensors²⁵.

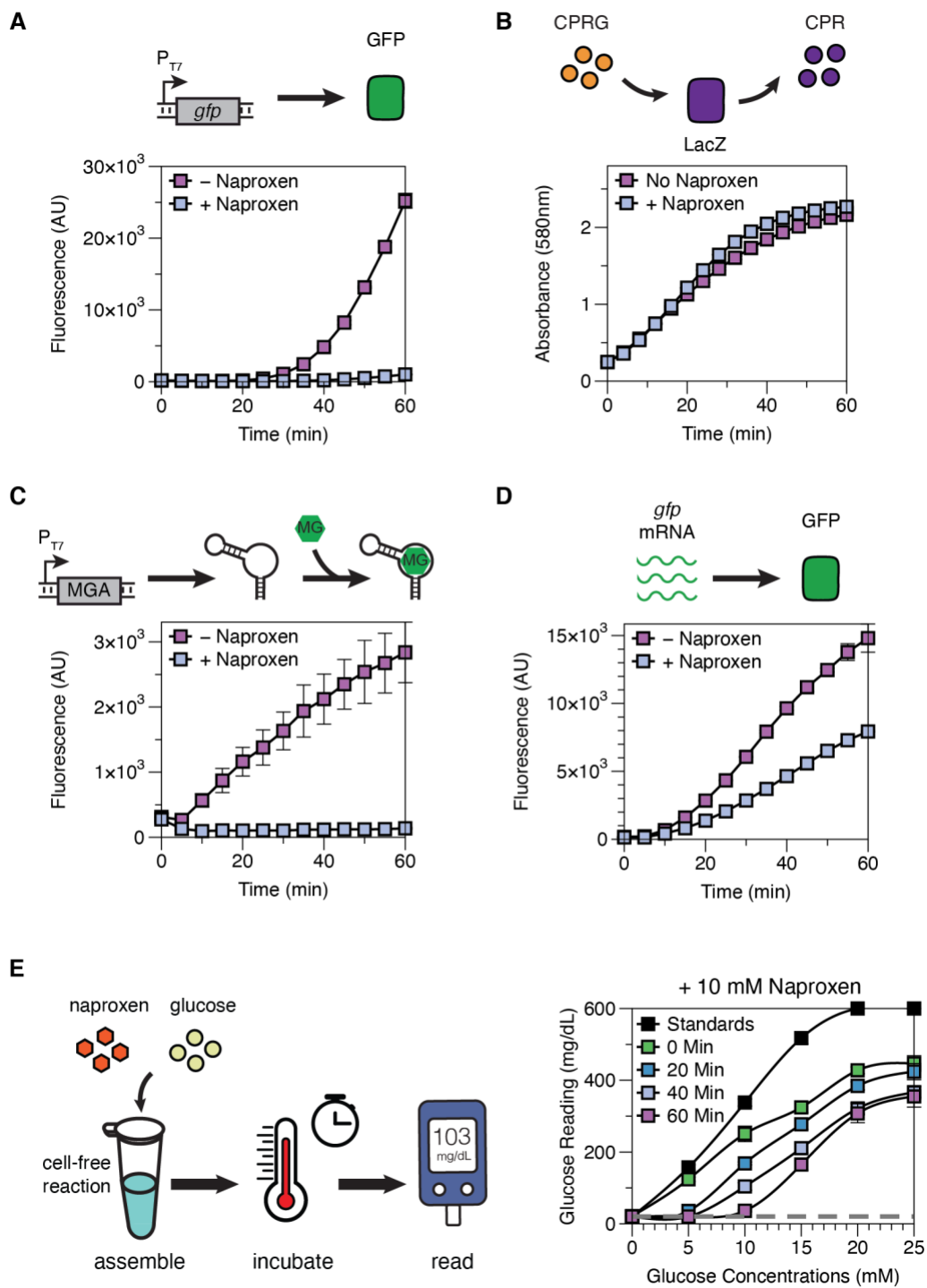


Figure 3-3 Characterization of naproxen quenching in CFE reactions. Error bars in each sub-panel represent standard deviations of CFE reaction triplicates. (A) Plasmid encoding for GFP expression was added to each reaction for fluorescent signal production to characterize naproxen's cumulative impact on protein transcription

and translation. Addition of naproxen sodium at the beginning of the CFE reaction inhibits GFP expression. (B) BL21 Star (DE3) lysate containing LacZ enzyme was dosed into a CFE reaction at 5% volume. LacZ activity was measured by its ability to cleave chlorophenol red- β -D-galactopyranoside (CPRG) to chlorophenol red. Addition of naproxen sodium did not significantly impact LacZ activity. (C) Plasmid encoding for malachite green RNA aptamer (MGA) expression and malachite green dye (MG) were added to each reaction for fluorescent signal production to characterize transcription. Addition of naproxen sodium at the beginning of the CFE reaction prevents transcription. (D) RNA transcripts coding for GFP translation were added to each CFE reaction for fluorescent signal production. Addition of naproxen sodium resulted in ~46% repression of translation. (E) Addition of 10 mM naproxen slowed down endogenous glucose consumption in CFE reactions, with glucose readings (especially at later time points) higher in the presence of naproxen than in Figure 3-2A. Standards presented here are the same set of data presented in Figure 3-2A.

3.3.2 Repurposing a PGM to quantify micronutrients in human serum

After successfully verifying plasmid dose-dependent glucose production in CFE systems, we tested whether small molecule inducers could modulate dose-dependent glucose readings on PGMs. We chose zinc as our target analyte for PGM-mediated quantification due to its global health relevance (zinc deficiency is responsible for the deaths of 100,000 children under the age of five worldwide every year)^{81,101} and our group's previous experience in developing a semi-quantitative zinc biosensor²⁵. The zinc sensor used here constitutively expresses (from the promoter P_{T7}) a transcription factor ZntR, which in turn controls the expression of LacZ based on the concentration of zinc. Zinc binding activates ZntR, which turns on expression from its cognate promoter P_{ZntA} for LacZ production (Figure 3-4A).

Because the human physiologically relevant zinc concentration spans from 2 to 20 μM ^{25,81}, we first tested for zinc-modulated glucose production in a water matrix across this range (Figure 3-4B). Using the same strategy to decouple analyte detection from glucose

conversion, we incubated CFE reactions for 45 minutes for LacZ production before quenching reactions with naproxen-lactose mix and incubating for another 15 minutes for glucose production. Although we have demonstrated that 30 min of reaction can generate enough LacZ to produce detectable glucose signals on the PGM, we extended the reaction to 45 min to account for the lag time associated with the expression of sufficient zinc-responsive transcription factor to enable expression of LacZ, an additional step not present in our initial experiments from Figure 3-2. In just 1 hour of total assay time (including glucose production), we observed a linear increase in glucose readout over a range spanning 0-10 μ M zinc, above which the response of zinc sensor starts to saturate at increasing zinc concentrations²⁵. Further, we observed consistent glucose production across different reactions assembled on different days, demonstrating that PGM-mediated analyte quantification could be a reliable method for daily monitoring of micronutrient status.

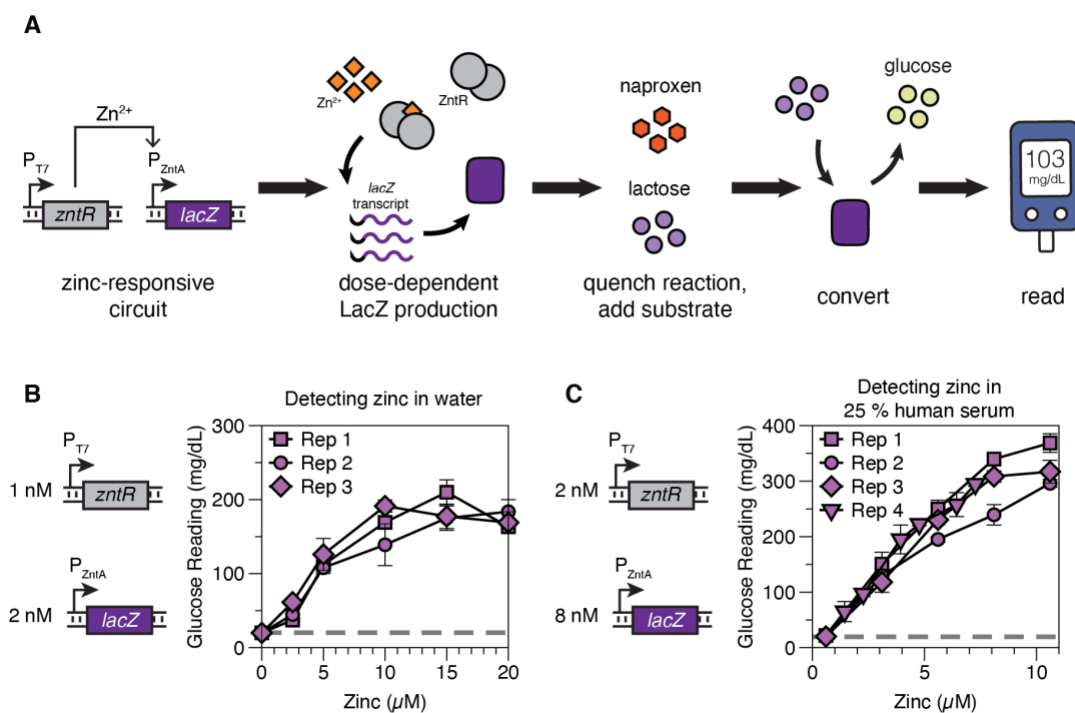


Figure 3-4 Application of PGM-mediated quantification of zinc in CFE reactions. (A) Schematic of zinc-modulated glucose production and PGM-mediated target quantification in CFE reaction. Zinc modulates LacZ production by binding to the constitutively expressed transcription factor ZntR, thereby activating transcription from the ZntR-responsive promoter P_{ZntA} . Following 45 min of LacZ production, a mixture of the naproxen-lactose solution was added to quench the CFE reaction and to start lactose conversion for 15 min. The converted glucose was then read on the PGM for target analyte quantification. **(B)** Dose-dependent glucose production in CFE reaction with zinc in a water matrix. The same experiment was replicated on different days to verify consistency in glucose output. Replicates (Rep) represent independently assembled reactions and error bars represent the standard deviation of CFE reaction triplicates in each replicate. Dashed gray line represents PGM's lowest reading threshold, 20 mg/dL. **(C)** Dose-dependent glucose production in CFE reaction with zinc in 25% pooled human serum. X-axis zinc concentrations reflect the total zinc in the reaction after accounting for the remaining zinc in chelated serum (Figure 3-5D). The same experiment was replicated on different days and with an independently assembled reaction to verify consistency in glucose output. Error bars represent the standard deviation of CFE reaction triplicates in each replicate. Dashed gray line represents PGM's lowest reading threshold, 20 mg/dL.

We then focused on the linear response range of zinc concentrations, re-optimized plasmid concentrations for increased signal, and tested the compatibility of our approach with human serum samples (Figure 3-4C). Because zinc is endogenously present in serum

and the samples were from otherwise healthy volunteers, the baseline level of zinc in the pooled serum sample would prevent us from assessing the assay's ability to detect deficient zinc levels. To address this issue, we first removed endogenous zinc from the pooled serum samples *via* chelation (Figure 3-5D) and then spiked different concentrations of zinc back into the serum. In CFE reactions containing 25% pooled human serum, we observed a consistent dose-dependent glucose signal readout over a range spanning 0.6-10.6 μM zinc across different days (Figure 3-4C), reflecting 2.4-42.4 μM zinc in non-diluted human serum and thus spanning a broad range of clinically relevant concentrations to detect zinc deficiency and toxicity. The common clinical reference range for zinc deficiency is between 8.5-11.5 μM (or 2.1-2.9 μM in 25% serum)^{25,81}. Since our assay can accurately measure zinc in this range, our approach can be easily deployed for a quantitative micronutrient monitoring test at home or in resource-limited environments.

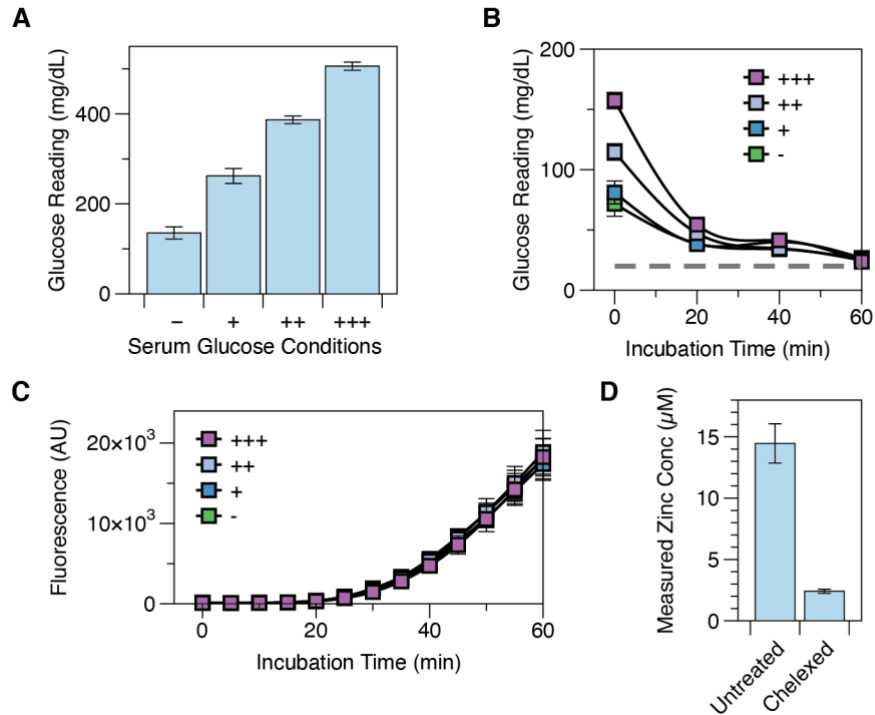


Figure 3-5 Endogenous metabolism in CFE reactions readily removed a wide range of glucose spiked into human serum without impacting protein expression. (A) Glucose was added to human serum to span the full detection range of the glucose monitor (OneTouch Ultra 2). Error bars in each sub-panel represent standard deviations of technical triplicates. (B) Human serum containing various amounts of glucose was added to a CFE reaction (with no LacZ expression) at 25% volume, and significant depletion of glucose was observed in the first 20 minutes for all reactions. Error bars in each sub-panel represent standard deviations of reaction triplicates. (C) GFP expression was unaffected in CFE reactions containing 25% human serum at a wide range of glucose concentrations. Error bars in each sub-panel represent standard deviations of two independently assembled experimental replicates, each with CFE reaction triplicates. (D) Verification *via* ICP-MS of serum zinc removal after treatment with Chelex-100 resin.

We further highlight that endogenous glucose present in human serum did not interfere with our PGM readout since the metabolic reactions active in cell-free lysate readily removed serum glucose without impacting protein production (Figure 3-5A-C). Previous efforts using PGMs for sensing in serum matrices have required additional steps to remove the confounder of serum glucose from reporter measurements^{91,92}, since serum glucose would be expected to vary from patient to patient—the very reason the PGM

exists—and thus interfere with the quantitative interpretation of the biosensor readout. Some of the previously reported approaches to solving this problem would be infeasible for practical field application. With our approach, the glucose consumption that was initially a potential obstacle in the use of lysate-based CFE biosensors has been repurposed as a distinct advantage that allows quantification across highly variable patient sample matrices.

Furthermore, our strategy of using a transcription factor-based, small molecule inducible genetic circuit is modular and easily generalizable to detect other small molecule targets. To develop a quantitative assay for another target molecule, one simply needs to replace the transcription factor and promoter and adjust the reaction conditions to achieve the desired output level. This only needs to be done once for each new sensor being developed, and is typically best accomplished *via* systematic variation of plasmid levels to achieve the desired dynamic range of output in the same short assay time, followed by variations of CFE reaction time and/or lactose conversion time if necessary to further increase output signal. The quantification workflow stays unchanged and remains robust to complex samples.

3.3.3 *Extending PGM applications to the detection of bacterial infections*

We next tested if PGM-mediated analyte quantification could be extended to quantify targets other than small molecules, as well as if the approach could use genetic circuits based on regulators other than transcription factors. We chose to use toehold switches recognizing Shiga toxin 1 and 2 genes (*stx1* and *stx2*) to detect pathogenic *E. coli* due to the clinical relevance of the problem⁵⁸ and our previous work in developing these

switches⁴⁶. Toehold switches work by RNA-RNA strand hybridization and displacement⁶ for sensitive and fairly specific detection of target sequences. The addition of a trigger sequence complementary to the toehold and partial stem region of the switch unwinds the inhibitory switch hairpin that would otherwise block translation, thereby allowing reporter enzyme expression (Figure 3-6A).

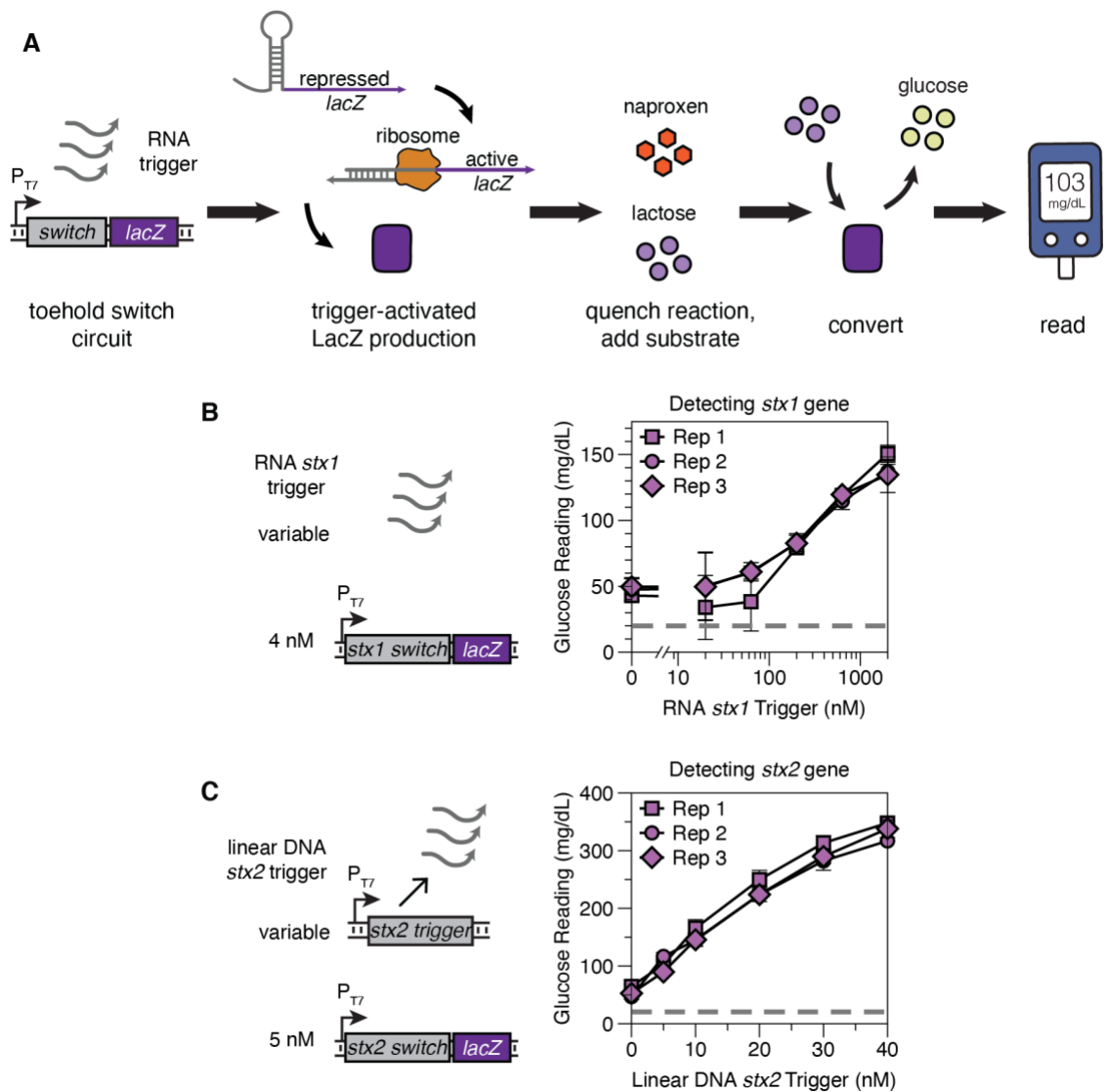


Figure 3-6 Application of PGM-mediated quantification of nucleic acids in CFE reactions. (A) Schematic of toehold switch-modulated LacZ production and LacZ-catalyzed lactose conversion to glucose output. Following 45 min of LacZ production caused by RNA trigger activating a toehold switch to allow translation of LacZ, a

mixture of the naproxen-lactose solution was added to quench the CFE reaction and to start lactose conversion for 15 min. The converted glucose was then read on the PGM for target analyte quantification. (B) Activation of *stx1* toehold switch and glucose output by RNA *stx1* trigger. Linear glucose response was observed with a logarithmic increment of RNA triggers from 20 to 2000 nM. The same experiment was replicated on different days to verify consistency in glucose output. Replicates (Rep) represent independently assembled reactions and error bars represent the standard deviation of CFE reaction triplicates in each replicate. Dashed gray line represents PGM's lowest reading threshold, 20 mg/dL. (C) Activation of *stx2* toehold switch and glucose output by linear DNA coding for *stx2* trigger, which can transcribe RNA *stx2* trigger in CFE reaction. Linear glucose response was observed with linear increments of DNA *stx2* trigger from 5 to 40 nM. Replicates (Rep) represent independently assembled reactions and error bars represent the standard deviation of CFE reaction triplicates in each replicate. Dashed gray line represents PGM's lowest reading threshold, 20 mg/dL.

Using the same strategy and assay times, we first demonstrated RNA-modulated glucose output over time using a *stx1* toehold switch with a LacZ reporter (Figure 3-6B). DNA of *stx1* triggers was amplified from the genomic DNA of Shiga toxin-producing *E. coli* O157:H7 and served as a template for *in vitro* transcription to produce RNA *stx1* triggers. A linear increase in glucose output was observed over logarithmic increments of RNA *stx1* triggers ranging from 20 nM to 2 μ M, behavior consistent with RNA trigger-activated toehold switch output in previous reports^{7,9,25}. Because RNA could also be made from a linear DNA template coding for trigger transcription, we next tested if adding linear DNA could modulate glucose production. We added linear DNA encoding RNA *stx2* trigger amplified from genomic DNA of *E. coli* O157:H7 to activate an *stx2* toehold switch with a LacZ reporter. We observed higher glucose conversion and a lower detection limit than for *stx1* (Figure 3-6 C).

Compared to the zinc sensor, the toehold switches used here exhibited higher background leakiness, as evidenced by the baseline (0 nM) readouts being approximately 50 mg/dL instead of the PGM's minimum reading (20 mg/dL). This increased background

is due to the use of a dialyzed CFE lysate with enhanced transcriptional activity for this application, as well as due to optimizing switch plasmid concentrations for improved fold-change in glucose readings over the range of trigger concentrations tested, both intentional design decisions for this sensor. It is important to assess the background noise level during the development of any new PGM-based sensor and then compensate for this noise *via* reaction optimization to whatever extent is feasible. Ideally, background noise would be below the PGM's detection threshold, and reduction of sensor concentration, reaction time, or lactose substrate concentrations could help achieve this goal, although sometimes other design goals may conflict with this objective and constraint those reaction parameters. Alternatively, a t-test could be done during development to establish the limit of detection for distinguishing signal from noise, allowing identification of the corresponding PGM readings that indicate only background noise. Nevertheless, our results demonstrate that a lysate-based CFE reaction coupled to PGM quantification is a highly generalizable platform compatible with multiple types of analyte inputs and multiple types of genetic regulators.

Although our current nucleic acid sensors could not detect targets at physiologically relevant concentrations (typically attomolar to femtomolar levels), an upstream amplification step can be implemented to bring initial nucleic acid concentrations up to the detection limit^{7,9,87}. Previous work has shown robust concentration-dependent toehold switch activation with femto- to pico-molar of triggers amplified *via* isothermal amplification techniques⁹. Further, we note that although for detection of infectious diseases (such as COVID-19, Zika, and Ebola virus), a binary yes/no result may often be sufficient for diagnosis^{7,8,102}, there are many cases where continuous monitoring and

quantification of viral load is essential for assessing treatment efficacy and determining disease prognosis¹⁰³. Having a low-cost, portable, and reliable quantification device can empower patients and healthcare workers to make faster and better medical decisions at the point of need.

3.4 Discussion

Our work demonstrates that CFE lysate-based biosensors can be easily coupled to a PGM for rapid and reliable analyte quantification at the point of need. The resulting platform is highly generalizable, with demonstrated compatibility with different genetic regulators, analyte types, and sample matrices. Previous efforts repurposing PGMs for small molecule quantification have often used invertase-conjugated antibodies and DNA oligomers, or reagent drop-out methods^{39,40,86,88-92}, which have limitations in sensor sensitivity, specificity, and generalizability toward the detection of other targets. Here we show that interfacing synthetic circuits in CFE reactions adds an extensive library of developed biosensors to PGM sensor design and allows users to fine-tune individual sensing reactions with genetic regulators and signaling cascades. Indicative of the modularity and generalizability of this approach, each of the sensing circuits used here was originally developed in the context of different biosensors, but all could be directly integrated into a PGM-based readout with some basic assay optimization (e.g., adjustment of plasmid concentrations and reaction time). The modular utility of the transcription and translation reactions used to transduce signals in CFE reactions means that diverse target analytes can be detected with high sensitivity and specificity while providing critical quantification.

We further highlight that the CFE-based approach is an enabling platform for improved test accessibility and use at the point of need. CFE biosensing reactions have been demonstrated to retain their function after lyophilization^{7,8,22,24,25,46}, including those based on lysates. As a result, these tests can be stored and shipped to testing sites without the cold-chain requirements of PGM-mediated diagnostics that use invertase conjugated antibody or aptamer approaches^{40,88-92}, significantly enabling CFE-based diagnostics' deployment to the point of need. Moreover, the use of lysate-based CFE in this work rather than purified protein expression systems (like PURExpress) can reduce the cost of CFE reagents by almost an order of magnitude^{8,87}, making such an approach more feasible for wide-scale deployment and more accessible to the developing world as well as to consumers in developed countries. We also show that CFE metabolism can be exploited to remove endogenous glucose initially present in complex samples (like human serum) in a one-pot format, thereby eliminating an upstream processing step to remove endogenous glucose that would otherwise be a requirement of a PGM-based method. At the point of use, the operator simply needs to rehydrate the freeze-dried test reaction with sampled fluid to activate the sensing reaction, incubate the sample for a set amount of time, and then add the naproxen-lactose solution to shift the reaction to glucose production. A commercial PGM strip would be used to measure the glucose produced, immediately generating a numerical output on the PGM for result interpretation.

It is worth noting that for successful field deployment of these PGM-based sensors, additional investigation will be necessary. One area that such investigations should focus on is the reduction of batch-to-batch variability in crude lysate and reagent preparation. Interlaboratory variability in cell-free lysate, reagent, and reaction preparation is known to

potentially have an impact on quantitative outputs of CFE reactions¹⁰⁴. When we assessed the PGM's ability to accurately quantify targets using CFE reactions from five crude lysate batches, the inter-lysate variability was found to be low, though the variability due to batches of CFE reagents was a bit higher (Appendix B.1 Assessment of Batch-to-Batch Variability in Cell-Free Lysates, Figure 13). This suggests the importance of standardization, quality assurance, and quality control if this process were to be scaled up for manufacturing and distributed use. Another area worth further investigation is the sensitivity of assay results to perturbations in the time and temperature during the LacZ production and glucose conversion steps. If sensitivity to such perturbations is high, one potential mitigating strategy would be to use a set of standards that could be run in parallel with the test reaction for additional validation²⁵; we note that some PGMs already require some degree of calibration by the user. Another possibility could be to engineer a companion device to automate reagent dispensing and regulate reaction temperature and timing. Prototypes for automated, sequential introduction of reagents^{105,106} and portable incubators⁸⁷ have been developed by different labs for point-of-care diagnostics. Though these additions would increase the capital cost of the equipment and the cost per assay, thus limiting its potential use in low-resource environments, it would still be sufficiently accessible for patient at-home use and clinic use in the developed world.

Nevertheless, our work provides an enabling advance toward inexpensive, point-of-care sample quantification with simpler transportation and operator requirements and fast result turnaround in 1 hr. We demonstrate that interfacing synthetic biology and CFE to PGM-mediated analyte detection has the potential to enable accessible, affordable, and reliable quantification of diverse analytes at the point of need.

CHAPTER 4. INTERFACING CELL-FREE EXPRESSION PLATFORMS WITH IMMUNOASSAYS FOR SENSITIVE DETECTION OF PROTEIN BIOMARKERS

This work was done in collaboration with Dr. Shreyas Dahotre, Aaron D. Silva Trenkle, and Dr. Liangjun Zhao, under the supervision of Dr. M.G. Finn, Dr. Gabriel A. Kwong, and Dr. Mark P. Styczynski. Dr. Shreyas Dahotre and Aaron D. Silva Trenkle played a significant role in DNA-antibody conjugation. Dr. Liangjun Zhao played a significant role in DNA barcode synthesis and conceptual design.

4.1 Introduction

The novel coronavirus (SARS-CoV-2) disease has highlighted the need for scalable and rapidly reconfigurable diagnostics to track and contain the disease and its variants. Virus mutations resulting in the Delta, Omicron, and other variants of concern could alter the transmission rate and evade detection in current diagnostic tests¹⁰⁷⁻¹⁰⁹. As a result, there is a critical need to develop sensitive and accessible diagnostic tests to detect and distinguish the original SARS-CoV-2 strain and the circulating variants to better inform medical treatment and public health policies.

Currently, all identification of SARS-CoV-2 variants is done by genome sequencing and constrained to hospitals and specialized clinical laboratories, making these assays cost-prohibitive to implement at the population scale¹¹⁰. Since SARS-CoV-2 variants of concern carry a series of mutations on the spike protein^{107-109,111}, an antigen-based diagnostic

targeting distinct mutated epitopes of spike proteins could enable large-scale virus strain tracking at or near the point of care.

However, there are critical challenges in implementing antigen-based variant subtyping assays. First, sensitive and specific spike epitope detection antibodies need to be raised to recognize distinct epitopes of the wildtype SARS-CoV-2 from variants of concern. Since specific antibodies have been raised successfully to distinguish spike proteins from SARS-CoV-1 and SARS-CoV-2 at the beginning of the pandemic¹¹², there exists the possibility to raise specific antibodies capable of distinguishing distinct spike protein epitopes of SARS-CoV-2 and its variants of concern. Another critical roadblock is the lack of sensitivity in antigen-based diagnostics compared to nucleic acid-based diagnostics¹¹³, as the latter can go through exponential nucleic acid amplification cycles. As a result, improving the sensitivity of current immunoassays can drastically increase clinical adoption and expand the accessibility of SARS-CoV-2 and variant detection diagnostics.

We envision that cell-free expression (CFE) systems can respond to the result of an immunoassay by simply labeling the detection antibody with a piece of DNA barcode with genetic information¹¹⁴. The genetic information embedded in the DNA barcode can then be transcribed and translated in the CFE reaction, producing reporter enzymes with colorimetric outputs (Figure 4-1). The resulting assay platform can endow immunoassays with higher sensitivity by enabling multiple signal amplification steps, including transcription, translation, and enzymatic conversion. Moreover, the resulting platform can be highly reconfigurable and scalable to detect multiple protein targets in the same sample

simply by adding new detection antibodies with unique barcodes for more sensitive detection in a CFE system.

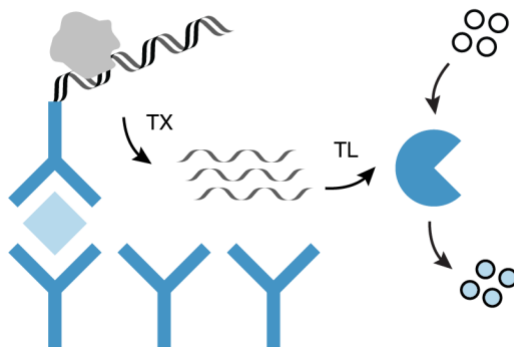


Figure 4-1 Schematic of the sandwich immunoassay interfaced with a CFE system. In this setup, protein antigen binding to the capture and detection antibodies allows retention of DNA barcode in wells after the wash steps. CFE reactions can then be added to transcribe (TX) and translate (TL) the genetic information embedded in the DNA barcode. Once the reporter enzyme is produced, it can cleave a colorimetric substrate and produce visually detectable outputs.

In this work, I assessed the feasibility of relaying protein detection signals from immunoassays to CFE systems *via* conjugation of DNA barcodes onto detection antibodies. I then demonstrated successful coupling of immunoassay and protein detection reporting *via* DNA-barcode mediated reporter complementation and pigment production in CFE systems. The possibility of multiplexing protein detection with the development of a duplex immunoassay was explored. I demonstrated DNA barcode-mediated activation of beta-galactosidase (LacZ) and catechol-2,3-dioxygenase (C23DO) enzymes to produce distinct colors (blue and yellow, respectively) in CFE systems, with emerging applications for identifying different strains of coronaviruses.

4.2 Materials and Methods

4.2.1 DNA preparation

Sequences for all DNA constructs and plasmids used in this study are provided in the C.1 Sequence Information. DNA oligonucleotides used for DNA-antibody conjugation were synthesized by Integrated DNA Technologies with amine modification (AmC6) at the 5' end. Linear, double-stranded DNA encoding LacZ alpha fragment or RNA triggers used in experiments were amplified from plasmid template either by PCR with Q5 DNA Polymerase (New England Biolabs). Amplified DNA was run on a 2 w/v% agarose gel to verify successful amplification of targets and then purified using a PCR purification kit (Omega Bio-Tek).

E. coli strain DH10 β was used for all cloning and plasmid preparations. Eurofins Genomics synthesized DNA oligonucleotides for cloning and sequencing. Plasmid DNA used for all CFE reactions was purified from EZNA midiprep or maxiprep columns (OMEGA Bio-Tek), followed by isopropanol and ethanol precipitation. The purified DNA pellets were reconstituted in the elution buffer, measured on a Nanodrop 2000 for concentration, and stored at -20 °C until use.

4.2.2 DNA-antibody conjugate preparation

Detection antibody for conjugation was mixed with 50-fold excess succinimidyl-6-hydrazino-nicotinamide (S-HyNic from Solulink) crosslinker. Amine-functionalized DNA barcodes were mixed with 20-fold excess succinimidyl-4-formylbenzamide (S-4FB) crosslinker in a separate tube. Both reactions were incubated at room temperature for 4 hours before citrate buffer exchange (50 mM sodium citrate, 150 mM NaCl, pH 6) to remove excess linkers in the Ab-linker reaction and DNA-linker reaction using 0.5 mL

Amicon spin filters at 30K and 10K, respectively. Functionalized DNA was combined with antibodies at a 5:1 ratio and reacted overnight. The conjugated products were purified the following morning on a Superdex 200 Increase 10/300 GL column using an AKTA Pure FPLC (GE Healthcare). Purified conjugation products were verified by SDS-PAGE with Coomassie staining.

4.2.3 *Sandwich immunoassay for spike protein detection*

Capture antibodies (3F2¹¹², gift of Dr. Goldstein at the Center for Disease Control (CDC), for SARS-CoV-2 Spike/RBD protein detection or 40150-D003, Sino Biological, for SARS-CoV-1/2 Spike/RBD proteins detection) were diluted to 2 µg/mL in 50 mM carbonate/bicarbonate buffer at pH 9.6 and added to high binding 96-well half-area microplates (Corning) at 100 µL per microwell. The microplate was sealed with an adhesive plate cover and incubated overnight at 4 °C. The coating solution was removed the following day, and the wells were washed 4 times with 125 µL of Wash Buffer (PBS with 0.05% Tween-20) to remove unbound antibodies.

Following the wash step, 125 µL of Blocking Buffer (PBS with 1 % w/v Casein) was added to each well. The plate was sealed with a plate cover and incubated for 1 hr at room temperature. The Blocking Buffer was then removed, and 100 µL of samples containing different concentrations of Spike/RBD proteins (40634-V08B for SARS-CoV-1, Sino Biological, and the gift of Dr. Goldstein at CDC for SARS-CoV-2 Spike/RBD) diluted in the Blocking Buffer were added to the microwell and incubated for 1 hr at room temperature with shaking. The samples were then removed, and the wells were washed 4 times with 125 µL of Wash Buffer.

After the wash step, oligo-conjugated detection antibodies (3A7¹¹² for SARS-CoV-2 Spike/RBD protein detection, or 40150-MM08 and 40592-R001 (Sino Biological) for SARS-CoV-1/2 Spike/RBD proteins detection, respectively) were diluted to 1 µg/mL in Blocking Buffer and added to each microwell at 100 µL. The plate was incubated at room temperature for 1 hr with shaking. The antibody solution was then removed, and the wells were washed 4 times with 125 µL of Wash Buffer. After the final wash step, the remaining oligo-conjugated detection antibodies become the templates of CFE reaction or isothermal nucleic acid amplification.

4.2.4 Crude *E. coli* lysate preparation

Cellular lysate for all experiments was prepared as described by Sun *et al.*¹⁸ with a few protocol modifications. Briefly, BL21 Star (DE3) $\Delta lacIZYA$ cells were grown in a 2× YTP medium at 37 °C and 220 rpm to an optical density (OD) of 0.3-0.5 for IPTG induction at 0.4 mM to activate the expression of T7 RNAP Polymerase. The cells were grown further until the OD was 1.5-2.0, corresponding to the mid-exponential growth phase. Cells were centrifuged at 2700 rcf and washed three times with S30A buffer (50 mM tris, 14 mM magnesium glutamate, 60 mM potassium glutamate, 2 mM dithiothreitol, and pH-corrected to 7.7 with acetic acid). After the final centrifugation, the wet cell mass was determined, and cells were resuspended in 1 mL of S30A buffer per 1 g of wet cell mass. The cellular resuspension was divided into 1 mL aliquots. Cells were lysed using a Q125 sonicator (Qsonica) at 20 kHz and 50% amplitude. Cells were sonicated on ice with cycles of 10 s on and 10 s off, delivering approximately 200 J, at which point the cells appeared visibly lysed. An additional 4 mM dithiothreitol was added to each tube, and the sonicated mixture was then centrifuged at 12,000 rcf and 4 °C for 10 min. After centrifugation, the supernatant

was removed and incubated at 37 °C and 220 rpm for 80 min for lysate runoff reaction. After this runoff reaction, the cellular lysate was centrifuged at 12,000 rcf and 4 °C for 10 min. The supernatant was removed and loaded into a 10 kDa molecular weight cutoff dialysis cassette (Thermo Fisher). The lysate was dialyzed in 1 liter of S30B buffer (14 mM magnesium glutamate, 60 mM potassium glutamate, 1 mM dithiothreitol, and pH-corrected to 8.2 with tris) at 4 °C for 3 hours. Dialyzed lysate was removed and centrifuged at 12,000 rcf and 4 °C for 10 min. The supernatant was removed, aliquoted in volumes of 100 µL, and stored at -80 °C for future use.

4.2.5 *PURE system and lysate-based CFE reaction preparations*

CFE reactions using PURE systems, PURE $_{flex}$ ® (Gene Frontier) and PURE $_{Express}$ ® (New England Biolabs), were assembled according to manufacturers' protocols. Specific concentrations of plasmid DNA are provided in Appendix C.2 CFE Reaction Conditions. For colorimetric reactions, chlorophenol red- β -D-galactopyranoside (CPRG) substrate was added at 0.6 mg/mL, 5-Bromo-4-chloro-3-indolyl β -D-galactopyranoside (X-gal) substrate was added at 0.4 mg/mL, and catechol substrate was added at 4 mM. All reactions were assembled on ice, and the reaction master mix was vortexed at a medium-high setting to ensure homogenous mixing before being aliquoted into individual reactions.

The CFE reaction composition was as previously described by Kwon and Jewett¹⁷. All lysate and reagent master mixes were thawed on ice and had no more than 3 freeze-thaw cycles. All reactions were assembled on ice and in PCR tube strips. The reaction

master mix containing lysate was vortexed briefly at a medium-high setting to ensure homogenous mixing before being aliquoted into individual reactions.

4.2.6 *Data collection*

For reactions measured with a plate reader, each CFE reaction was 5-10 μL in volume and pipetted into a clear-bottomed 384-well plate (Greiner Bio-One) for fluorescence and absorbance measurement. Kinetic reads were performed in a plate reader (Synergy4, BioTek) at 37 °C for 1-2 hr. The filter setting for GFP measurement was 485/510 nm excitation/emission wavelengths, with the gain set at 70. The Alexa Fluor 488 measurement filter setting was 485/528 nm excitation/emission wavelengths, with the gain set at 100. For Alexa Fluor 595, measurement was at 590/620 nm excitation/emission wavelengths, with the gain set at 150. The absorbance measurement wavelength for reactions with CPRG was at 580 nm, X-gal at 615 nm, and catechol at 385 nm. All plates were sealed with a transparent, adhesive film during incubation to prevent evaporation.

All images were taken using either iPhone X or iPhone 13 (Apple) with the default photography application in a light-controlled setting. A brightness filter was uniformly applied to all photos to reflect their visual appearance to the naked eye, and the background of images was cropped in Adobe Photoshop.

4.3 **Results**

4.3.1 *Antibody-conjugated DNA barcodes activate reporter expression in CFE systems*

One critical consideration in CFE-mediated detection of spike protein antigen is whether the genetic information embedded in the DNA barcodes can be successfully

interpreted after conjugation onto detection antibodies. We first verified the CFE system's capability to decode DNA barcodes *via* a 200-mer double-stranded DNA conjugated to a detection antibody. The 200-mer DNA carries the genetic information to transcribe and translate the alpha fragment of the LacZ enzyme. Once translated, the alpha fragment reassembles with the omega fragment of LacZ and becomes a fully active enzyme¹¹⁵. The reassembled LacZ enzyme activity was assessed by its ability to cleave the CRPG substrate to chlorophenol red (CPR), producing color changes from yellow to purple²⁵. The intensity of the color change depends on the concentration of DNA barcodes in a CFE reaction.

A reconstituted CFE platform (PURE*flex*®) was used to improve the stability of the linear DNA barcodes in reaction. Compared to lysate-based CFE platforms, a reconstituted system of purified proteins (PURE) lacks endonucleases that would otherwise degrade linear DNA, ensuring the stability of antibody-conjugated DNA barcode for expressing LacZ alpha fragment⁶¹. To assess the functionality of antibody-conjugated DNA barcodes, free and conjugated DNA barcodes were added to a CFE reaction constitutively expressing the LacZ omega fragment. In the range of LacZ alpha fragment DNA concentration tested (50 fM – 5 nM), it was found that antibody-conjugated DNA barcodes could be successfully expressed in CFE systems but lost one order of magnitude in sensitivity compared to free barcodes (Figure 4-2). Furthermore, significant background activity of the PURE*flex*® system was observed and investigated further in Section 4.3.3.

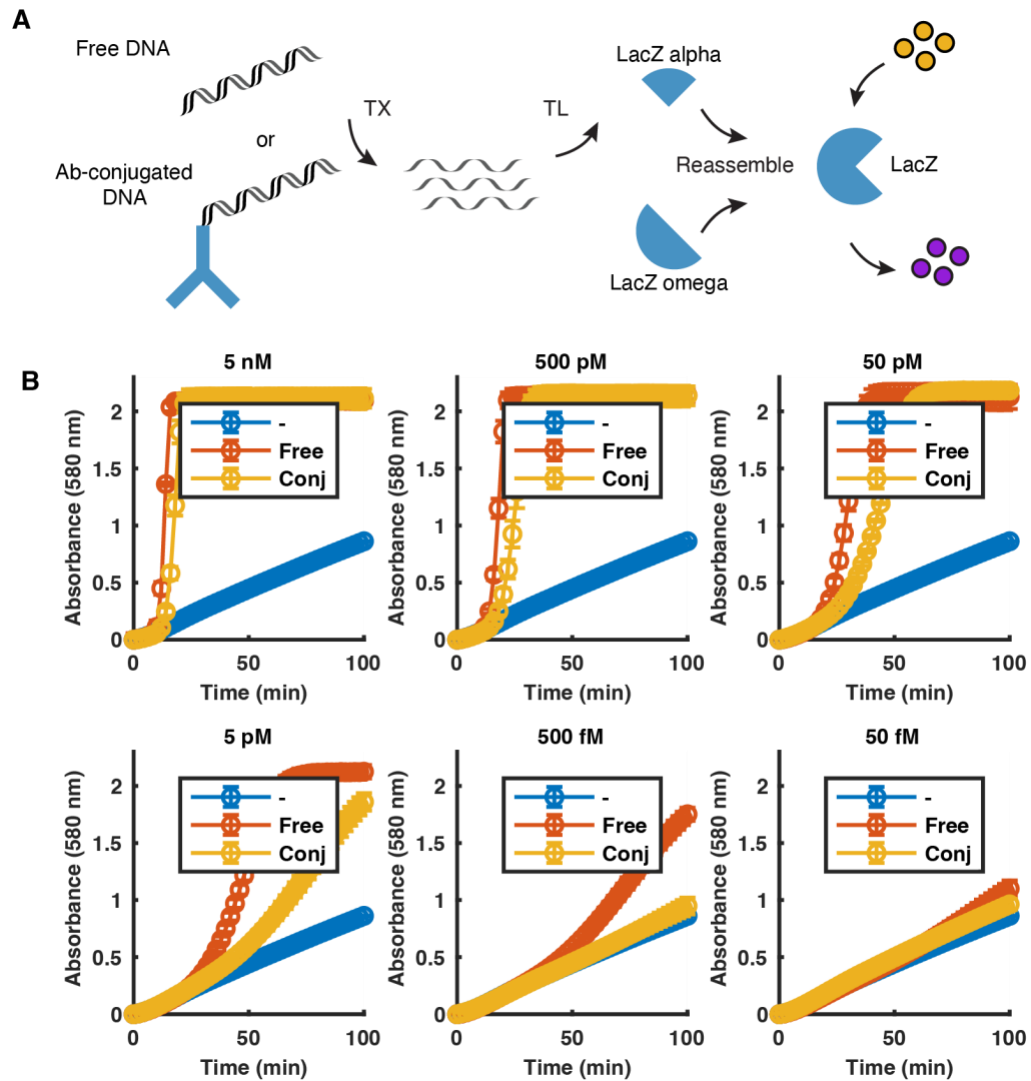


Figure 4-2 Activity comparison of free DNA barcode (Free) and antibody-conjugated DNA barcode (Conj) to express LacZ alpha fragment in the PUREflex® system. (A) Schematic of free and conjugated DNA-activated enzyme expression and enzymatic catalyzed CPRG conversion. DNA barcode expresses the alpha fragment of the LacZ enzyme. The alpha fragment can then reassemble with the LacZ omega fragment and catalyze CPRG conversion to CPR. (B) Conjugated DNA barcodes have slower activity and lose one order of magnitude in sensitivity compared to unconjugated, free barcodes. A negative control without DNA expressing LacZ alpha fragment (-) was included to characterize the reaction background. Reactions were run on a plate reader at 37 °C for 100 min, with purple pigment absorbance read at 580 nm every 2 min. The error bar represents the standard deviation of reaction triplicates.

4.3.2 Antigen dose-response modulated activation of reporter expression

Following successful expression of antibody-conjugated DNA in CFE system, immunoassay-coupled barcode expression and color change in CFE reaction were demonstrated. In this setup, antigen detection was performed similarly to a conventional ELISA (see Section 4.2.3). The detection antibody is conjugated to a DNA barcode to express the LacZ alpha fragment in the CFE reaction. The LacZ alpha fragment expression levels are indirectly modulated by the concentration of the SARS-CoV-2 Spike/RBD proteins complexed to the capture and detection antibodies. The more Spike/RBD antigens complexed, the more detection antibodies with DNA barcodes present in the CFE reaction, producing more LacZ enzyme to catalyze the conversion of CPRG to purple pigment. The assay was able to detect 1 ng/mL of the Spike/RBD antigen using a plate reader and 16 ng/mL *via* visual detection. (Figure 4-3). This demonstrates that the developed CFE platform can successfully interface with conventional immunoassays to produce colorimetric outputs for equipment-free detection of SARS-CoV-2.

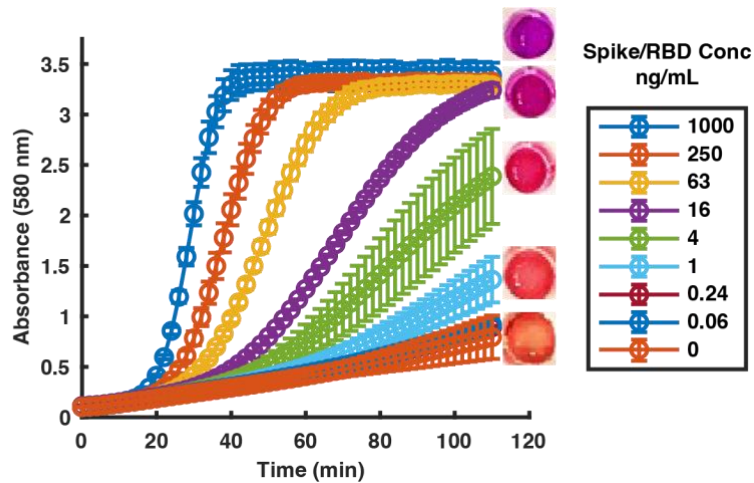


Figure 4-3 Sensitivity of sandwich immunoassay interfaced with the PUREflex® platform. The developed assay has a 1 ng/mL Spike/RBD protein detection limit on the plate reader and a 16 ng/mL visual detection limit. Sandwich immunoassay was performed at room temperature, and CFE reactions were tracked on a plate reader at 37 °C. Purple pigment absorbance was measured every 2 minutes at 580 nm. Error

bars indicate biological duplicates. Photos indicate the terminal reaction color at 2 hours.

4.3.3 Optimizing PURE system-based CFE platform to reduce background signal

In carrying out these assays, significant background LacZ activities were observed in reactions without any LacZ alpha fragments (Figure 4-2 and Figure 4-3). This was found to be caused by LacZ enzyme contamination of PURE*flex*[®] systems (Figure 4-4), possibly from the protein purification process. If used for a sensor designed to be visually interpretable, this background contamination could make it difficult to detect color changes at low Spike/RBD protein concentrations. To address this issue, the level of background LacZ activity of the PURE*flex*[®] system with another commercial PURE system, PURE*express*[®], was compared (Figure 4-4). It was found that PURE*express*[®] had lower LacZ background contamination, making it a better CFE platform for downstream assay development.

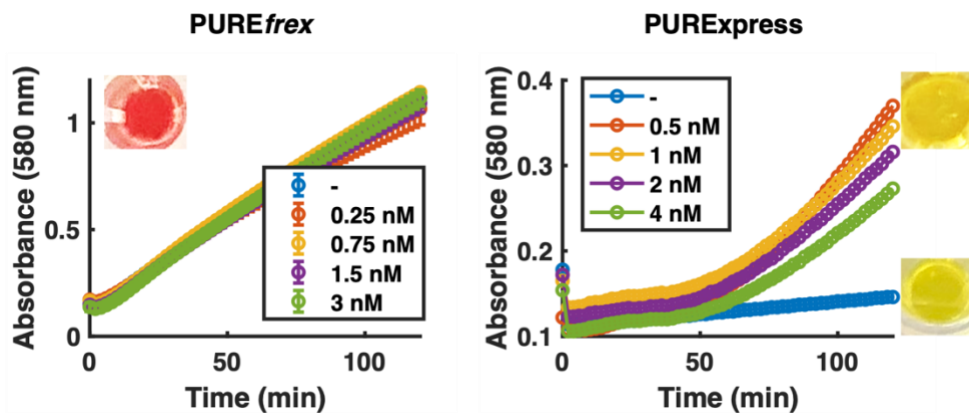


Figure 4-4 Background LacZ contamination assessment in PURE*flex*[®] and PURE*express*[®] systems. Each CFE reaction was supplemented with a range of DNA coding for LacZ omega fragment expression, which should have minimal activity for cleaving CPRG to CPR without complementation of the alpha fragment. Negative control reactions (-) without any DNA increased in pigment conversion in the

PUREflex® system (left). The negative control reaction (-) in PURExpress® did not substantially increase pigment conversion, indicating minimal LacZ background contamination (right). Reactions were incubated on the plate reader at 37 °C for 2 hours. Absorbance measurements were taken every 2 minutes at 580 nm. Error bars in PUREflex® reactions represent reaction triplicates. PURExpress® reactions shown are single reactions. Photos indicate terminal reaction color at 2 hours.

4.3.4 *Designing a two-enzyme duplex platform to distinguish SARS variants*

After verifying gene expression from antibody-conjugated DNA barcodes in a sandwich ELISA format, I proceeded to reconfigure the assay platform for antigen multiplexing. Because antibodies specifically targeting distinct, mutated epitopes of SARS-CoV-2 variants of concern are not currently available, detection of different strains of coronaviruses (SARS-CoV-1 and SARS-CoV-2) was used as a proof of principle (Figure 4-5A). To distinguish and report on the presence of either strain of the coronaviruses, unique DNA barcodes were attached to different detection antibodies targeting SARS-CoV-1 and SARS-CoV-2.

Each DNA barcode was a different toehold switch trigger designed to activate a different color-converting enzyme. Toehold switches design was adopted here due to their shorter length for antibody conjugation (under 200 nucleotides). DNA barcode conjugated to SARS-CoV-1 antibody is a trigger that activates the LacZ expression under its respective toehold switch, converting a colorless substrate, X-gal, to a blue precipitate⁴⁶. The barcode on the SARS-CoV-2 antibody is another trigger sequence to activate catechol-2,3-dioxygenase (C23DO), which converts a colorless catechol substrate to a bright yellow pigment⁷⁷ (Figure 4-5C, D). Although unlikely in a clinical sample, the presence of both SARS-CoV-1 and SARS-CoV-2 would activate substrate conversion for both enzymes, leading to a third, distinct, green color output. Successful duplexed detection of these two

strains of coronaviruses would provide proof of principle of our assay's ability to identify SARS-CoV-2 and its variants of concern in a single test, given the availability of variant-specific antibodies.

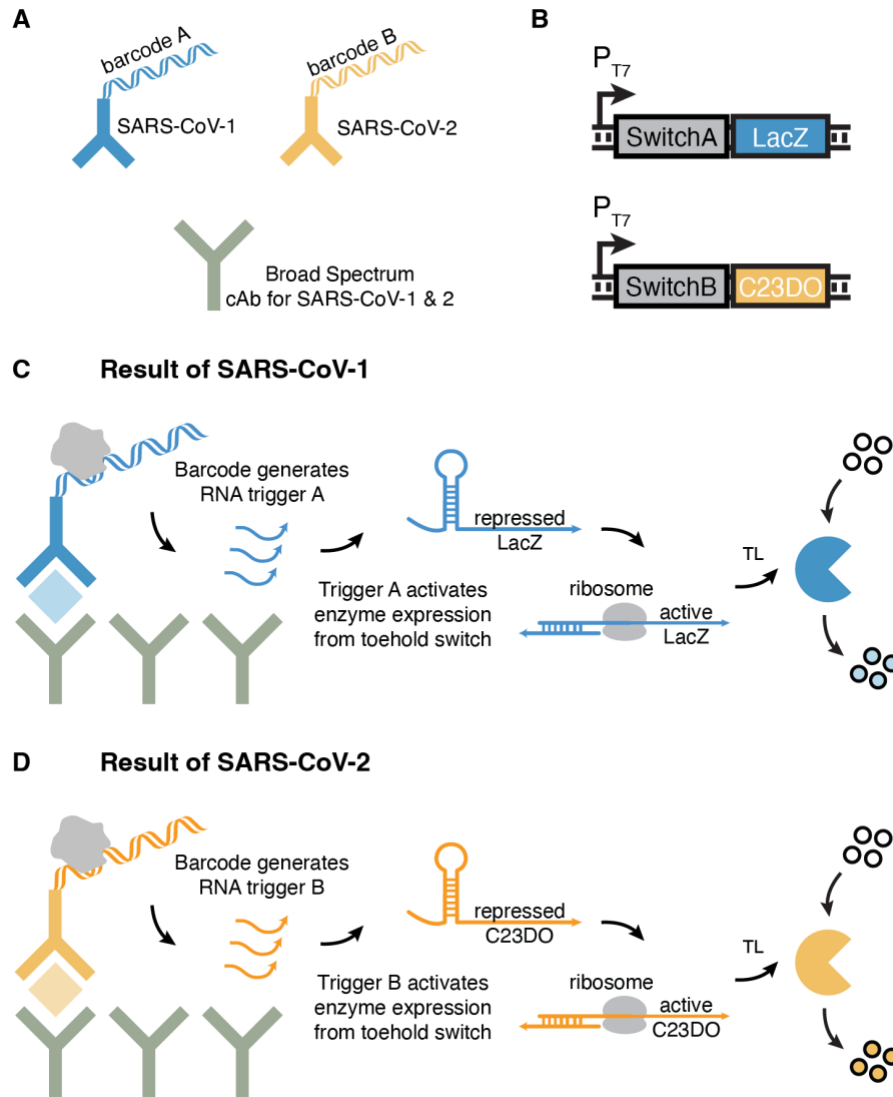


Figure 4-5 Schematic of the proposed duplex platform to detect SARS-CoV-1 and SARS-CoV-2 infection in a single test. (A) Unique DNA barcodes A and B are conjugated to detection antibodies targeting Spike/RBDs of SARS-CoV-1 and SARS-CoV-2, respectively. A broad-spectrum capture antibody will be used to enable Spike/RBD protein detection in duplex format. (B) Two orthogonal toehold switches are used to express LacZ and C23DO reporter proteins in the presence of RNA triggers A and B, respectively. (C-D) CFE expression of RNA triggers encoded in

barcodes A and B their respective enzymes, LacZ and C23DO, to produce visually distinguishable blue and yellow colors.

I first prototyped catechol conversion to yellow pigment by the C23DO enzyme in PURExpress®. Surprisingly, no catechol conversion was observed in 2 hours of reaction time (Figure 4-6A) despite being demonstrated to work in a lysate-based CFE system⁷⁷. Upon further investigation, it was found that Fe²⁺ is an essential cofactor for C23DO-mediated catalysis of catechol¹¹⁶ and possibly depleted in the protein purification process to make PURE systems, resulting in the inability of C23DO to catalyze catechol conversion. By supplementing the reactions with 1 mM of Fe²⁺, C23DO-catalyzed yellow pigment production was restored (Figure 4-6B).

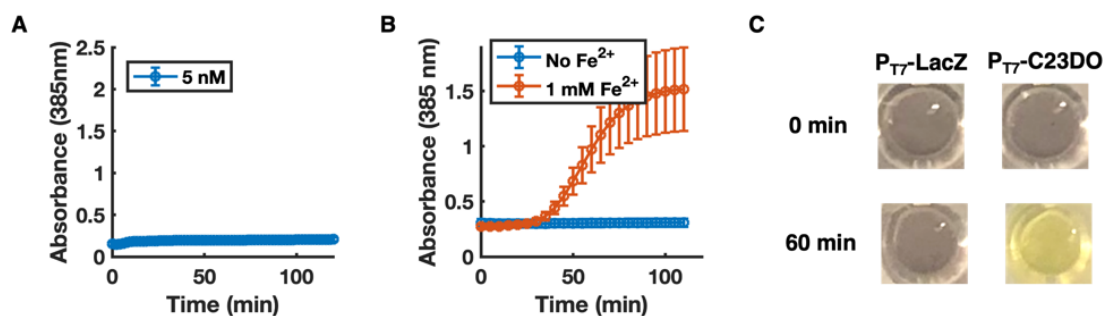


Figure 4-6 Assessment of enzyme activities and the impact of iron cofactors in PURExpress® reactions. (A) 5 nM of DNA constitutively expressing C23DO enzyme could not catalyze yellow color production without supplementation of Fe²⁺ cofactor. (B) Supplementation of 1 mM Fe²⁺ enabled C23DO catalyzed conversion of catechol. Reactions were monitored for 2 hours on a plate reader at 37 °C, and the yellow pigment was monitored at 385 nm. Error bars represent the standard deviation of reaction triplicates. (C) Direct supplementation of 1 mM Fe²⁺ in PURExpress® resulted in visible iron precipitate. While this precipitate is resolubilized in reaction expressing C23DO for clear visualization of yellow pigment after 1-hour incubation at 37 °C, the precipitate obscured blue pigment visualization from reaction expressing LacZ enzyme.

However, the addition of millimolar levels of Fe²⁺ into the PURE reaction resulted in the oxidation of Fe²⁺ to Fe³⁺ and precipitation of Fe³⁺ in reactions. While the dark purple

Fe³⁺ precipitate could be resolubilized in reactions expressing C23DO, this color remained in reactions expressing the LacZ enzyme and obscured the blue pigments generated (Figure 4-6C). As a result, different additives to prevent Fe²⁺ to Fe³⁺ oxidation in PURE reactions were explored to minimize Fe³⁺ precipitation and color interference.

Vitamin C (ascorbic acid) and citric acid are two well-known antioxidants that could minimize Fe²⁺ oxidation to Fe³⁺ in the CFE reaction environment, thereby reducing the color interference that occurs at the current level of iron supplemented¹¹⁷. 1 mM of each additive was supplemented in PURExpress® reactions constitutively expressing the C23DO enzyme. When both vitamin C and citric acid were added to the reaction, just 50 µM of Fe²⁺ could catalyze the production of yellow color pigment in under 30 minutes, and the pigment was more strongly produced than vitamin C alone (Figure 4-7). Addition of both vitamin C and citric acid significantly reduced the amount of Fe²⁺ required (20-fold reduction from 1 mM to 50 µM) and minimized purple Fe³⁺ precipitation in the reaction to enable clear visualization of blue pigments produced by the LacZ enzyme.

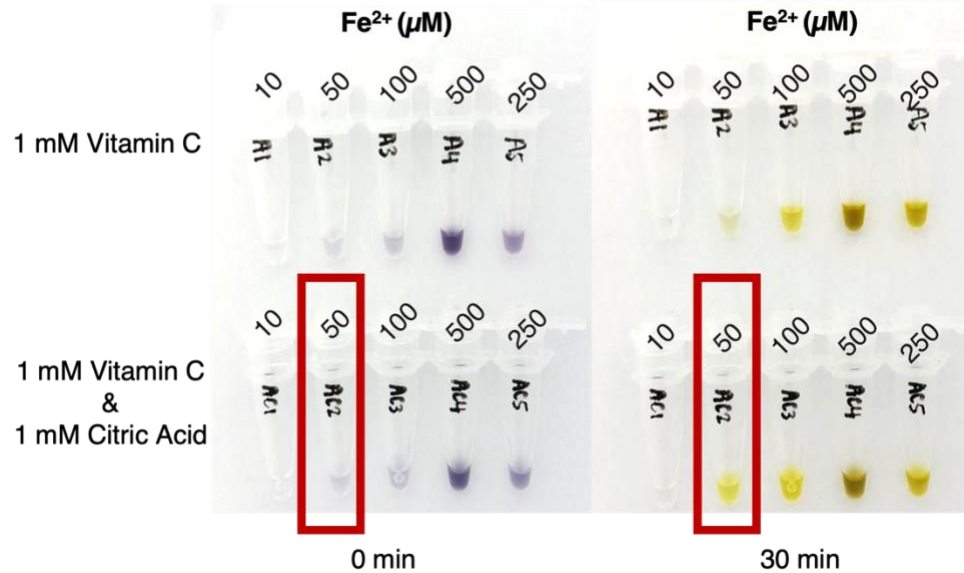


Figure 4-7 The addition of antioxidants prevented Fe²⁺ oxidation in PURExpress®. Fe²⁺ was supplemented in reactions expressing C23DO enzyme over a range of concentrations from 10 – 500 μM. Adding vitamin C (Vit C) and citric acid significantly reduced the required Fe²⁺ and unwanted oxidation compared to reactions without antioxidants (Figure 4-6), producing the desired bright yellow pigment. Reactions were incubated at 37 °C for 30 minutes.

4.3.5 Demonstrating barcode-modulated enzyme activation in CFE systems

After successfully establishing C23DO-mediated yellow pigment production in PURExpress®, I proceeded to verify the barcode-modulated activation of LacZ and C23DO enzymes in the reaction. In this design, each barcode is a linear DNA fragment encoding 30-36 nucleotides of RNA triggers. Once transcribed in the reaction, individual RNA triggers hybridize to their respective toehold switches and activate downstream enzyme expression⁶.

For this demonstration, I used two previously developed orthogonal toehold switches^{6,46}. I first tested RNA trigger-activated C23DO expression from its cognate toehold switch. Surprisingly, no trigger-mediated activation of C23DO was observed in

PURExpress® reactions. Specifically, I found that toehold switches were severely transcriptionally limited in PURE systems compared to lysate-based systems^{46,85}. Although PURE systems were initially selected for improved stability of linear DNA barcodes in the reaction, transcriptional limitations in PURE systems significantly inhibited enzyme expression modulated by toehold switches. In fact, previous demonstrations of toehold switch activation in commercial PURExpress® reactions all required RNA triggers to be prepared from separate *in vitro* transcription reactions and added at high nanomolar to micromolar concentrations⁷⁻⁹. As a result, the dual-color antigen duplex test was developed in a lysate-based CFE system moving forward.

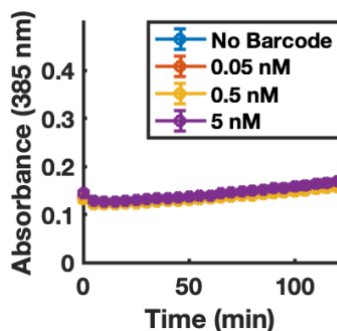


Figure 4-8 Low sensitivity of trigger barcode-activated enzyme expression in PURExpress® systems – 5 nM DNA barcodes coding for RNA triggers could not elicit detectable enzyme production. Reactions were incubated at 37 °C with absorbance monitored at 385 nm every 5 minutes. Error bars represent the standard deviation of reaction triplicates.

4.3.6 Demonstrating barcode-modulated enzyme activation in lysate-based CFE systems

In a lysate-based CFE system, endonucleases (such as the RecBCD complex) can rapidly degrade linear DNA barcodes⁶¹. This degradation could be problematic for our assay because these linear DNA barcodes are the templates to generate RNA triggers to activate enzyme production. Endonuclease inhibitors such as χ DNA can be added to protect

these DNA barcodes. I began by first titrating different χ DNA concentrations in CFE reactions and observed that 5 μ M of χ DNA is sufficient for linear DNA barcode protection (Figure 4-9).

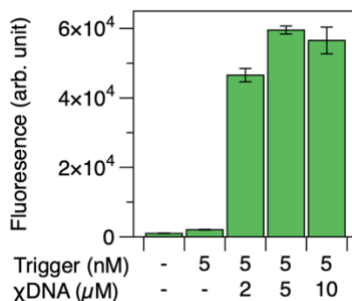


Figure 4-9 Linear DNA protection capabilities of χ DNA endonuclease inhibitor. Different concentrations of χ DNA were tested for the ability to protect 5 nM of DNA barcode to produce RNA trigger expression to activate green fluorescent protein (GFP) expression. 5 μ M χ DNA offered the best barcode protection in the range of concentrations tested. GFP fluorescence was measured on a plate reader (485 nm excitation, 510 nm emission) after incubation at 37 °C for 2 hours. Error bars represent the standard deviation of reaction triplicates.

After optimizing the lysate-based CFE system, I proceeded to verify DNA barcode-activated expression of the individual enzymes to be used. Two switch configurations were tested. In the first configuration, trigger B activates LacZ enzyme production from switch B, and trigger S2 activates C23DO enzyme production from switch S2 (Figure 4-10A). The toehold switches activating each enzyme were then swapped, with trigger S2 activating LacZ and trigger B activating C23DO (Figure 4-10B). Successful switch activation and color generation in lysate-based CFE systems were observed with 5 nM of triggers.

Furthermore, there was sufficient Fe²⁺ cofactor in the cell lysate to enable C23DO catalysis without adding antioxidants in both configurations. Pigment production in the first configuration was also less impacted by co-expression of both enzymes in the switch

concentrations tested and was selected to be the more optimal configuration to use going forward. It is possible for the second configuration to behave similarly to the first with additional optimization of different switch concentrations.

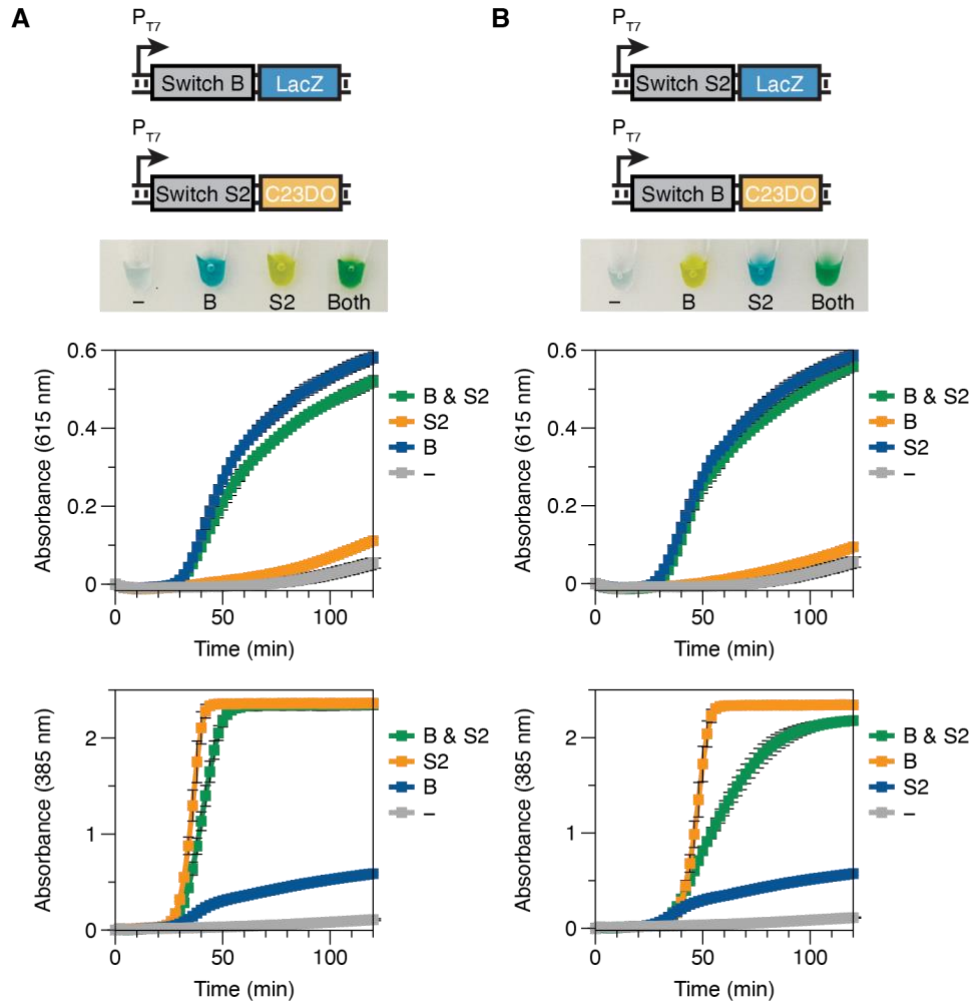


Figure 4-10 Two toehold switches (B and S2) specifically activated their respective enzymes to produce visually distinct colors in crude cell lysate systems. (A) The addition of triggers B, S2, or both strongly activated the expression of LacZ, C23DO, and both enzymes, respectively. (B) The switches were swapped for enzyme activation. The addition of triggers S2, B2, or both strongly activated the expression of LacZ, C23DO, or both enzymes, respectively. Compared to the configuration shown in (A), co-expression of both triggers significantly impacted yellow pigment generation. Yellow pigment production was monitored at 385 nm, and blue pigment production was monitored at 615 nm. Reactions were incubated at 37 °C for 2 hours, with absorbances monitored every 2 minutes. Error bars represent reaction

triplicates. Photo depicts terminal reaction colors in different trigger addition scenarios after 2 hours of incubation.

4.3.7 Toward a duplex SARS-CoV-1 and SARS-CoV-2 detection platform

After optimizing the necessary CFE framework for a two-color antigen test, the next step was to validate the duplex immunoassay to be interfaced with the CFE system. I first identified a broad-spectrum antibody (40150-D003 from Sino Biological) capable of binding to Spike/RBD proteins from both strains of coronaviruses to serve as the capture antibody in the sandwiched immunoassay format. The sensitivity and specificity of a mixture of detection antibodies targeting the spike/RBD proteins SARS-CoV-1 and 2 (40150-MM08 and 40592-R001 from Sino Biological, respectively) in a sandwich immunoassay format with fluorescent secondary antibodies were then assessed.

Since the two detection antibodies are raised on different animal isotypes (mouse and rabbit), a mixture of fluorescently-labeled anti-mouse and anti-rabbit secondary antibodies could be used to report on the detection antibody complexed in the immunoassay. The proposed duplex immunoassay to detect and distinguish SARS-CoV-1 and 2 was successfully validated by tracking the fluorescence intensity of bound secondary antibodies measured on the plate reader (Figure 4-11). The current assay detects SARS-CoV-1 Spike/RBD protein at 1 $\mu\text{g/mL}$ and SARS-CoV-2 at 0.1 $\mu\text{g/mL}$. Significant improvements in antigen sensitivity are anticipated once this immunoassay is interfaced with CFE reactions having transcription, translation, and enzymatic amplification. Nevertheless, this immunoassay platform established the necessary framework to detect different protein antigens with colorimetric result generation using CFE reactions.

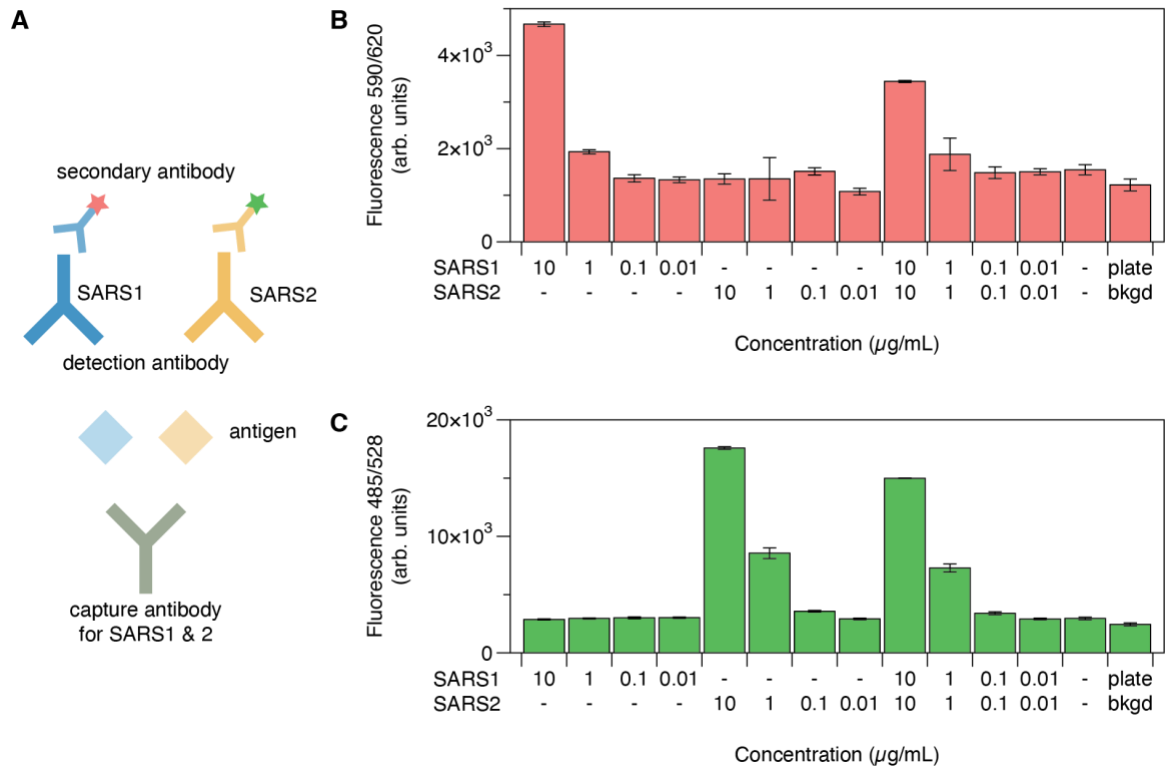


Figure 4-11 Development of a sandwich, duplex immunoassay to detect and distinguish Spike/RBD proteins from SARS-CoV-1 and SARS-CoV-2. (A) Schematic of the sandwich immunoassay format. A broad-spectrum capture antibody is used to bind Spike/RBD proteins from both strains of coronavirus. A mixture of SARS-CoV-1 and SARS-CoV-2 detection antibodies enables specific binding to the respective Spike/RBD proteins immobilized on capture antibodies. Fluorescence-labeled secondary antibodies were used to report the detection of antibody binding to the immobilized antigen. (B-C) SARS-CoV-1 Spike/RBD binding is detected at 590/620 nm (excitation/ emission), and SARS-CoV-2 is detected at 485/528 nm. Sandwich immunoassay was carried out at room temperature. Error bars represent reaction triplicates.

4.4 Discussion

In this work, I have successfully interfaced immunoassays detecting protein antigens with CFE systems. I showed that DNA barcodes conjugated to detection antibodies could transduce protein detection signals from immunoassays to activate reporter generation in CFE systems. I demonstrated successful immunoassay detection of SARS-CoV-2

Spike/RBD protein with colorimetric CFE reaction outputs using DNA barcode-conjugated detection antibodies.

I further developed and optimized the necessary components for a two-color duplex antigen test that can be extended to detect SARS-CoV-2 variants. I first characterized different CFE systems (PURE and cell lysate) for their compatibility with LacZ and C23DO enzyme expression and their ability to sensitively interpret DNA signals linking protein detection events to reporter production *via* toehold switches. In doing so, I found that while commercialized PURE systems were often regarded as more reliable and better in performance, they are deficient in necessary metal cofactors and are less amenable to customizations possible for in-house prepared bacterial cell lysates. In particular, it was found that the PURE system is deficient in Fe^{2+} , which is vital for the C23DO enzyme-mediated catalysis of catechol to produce yellow pigments. Moreover, I found that toehold switches are severely transcriptionally limited in PURE systems – 5 nM of trigger DNA strongly activated C23DO enzyme production in lysate-based systems, but no activation was observed in PURE.

These findings were quite surprising: we previously thought that PURE systems would allow significantly more sensitive detection than lysates due to their deficiency in nucleases that destroys linear DNA templates and RNA signals⁶¹. The results showed the contrary. Despite containing RecBCD nucleases rapidly degrading linear DNA templates, lysate-based systems can still strongly express linear DNA signals when supplemented with nuclease-stalling χ DNA. To address transcriptional limitation in toehold switches, cell-free lysates could be enriched with T7 RNA polymerases *via* IPTG induction on *E. coli* BL21 Star (DE3) cells during lysate preparation steps (Methods 4.2.4)^{46,85}. Direct

supplementation of purified T7 RNAP into PURE reactions did not yield improvements in toehold switch sensitivity (data not shown).

For multiple protein detection, given that antibodies specifically targeting distinct, mutated epitopes of SARS-CoV-2 variants of concern are not currently available, successful detection of SARS-CoV-1 and SARS-CoV-2 would be the closest proof-of-principle. We created a duplex immunoassay using a broad-spectrum capture antibody binding to spike/RBD proteins from SARS-CoV-1 and SARS-CoV-2 along with coronavirus strain-specific detection antibodies to report on spike/RBD binding. Immediate next steps would be to conjugate the DNA trigger barcodes developed in this chapter onto different coronavirus detection antibodies to relay the barcode signal to the CFE reaction. The CFE reaction could then produce a colorimetric output based on the DNA barcode and identify coronavirus strains and variants.

Following the successful demonstration of duplexed antigen detection, the next step would be to validate the assay's sensitivity to targets. The assay's sensitivity would be compared to commercial antigen rapid tests and clinically relevant antigen concentrations. Additional DNA amplification strategies (such as Recombinase Polymerase Amplification, RPA⁵⁶) could be used to amplify DNA barcodes from antigen-bound detection antibodies for ultrasensitive detection and identification of coronavirus strains and variants. Taken together, this work provides the proof-of-principle for CFE system interfaced detection of protein antigens, with emerging applications for more widely-deployable variant subtyping for SARS-CoV-2.

CHAPTER 5. CONCLUSIONS AND FUTURE DIRECTIONS

In this thesis, I have augmented CFE biosensors with various interfaces to address their current shortcomings for implementation in clinical and point-of-care settings. In this chapter, I will discuss the novelty and contribution of this thesis in advancing the point-of-care implementation of CFE biosensors. I will also discuss some remaining steps necessary for field implementation and future directions.

5.1 Novelty of This Thesis Research

While CFE biosensors have been developed to detect diverse classes of analytes, one limitation to their potential long-term impact is that they can only detect one analyte at a time⁴⁶. Biological samples clinicians seek to detect in the field typically have complex analyte profiles spanning multiple classes of biomarkers^{26,118}, requiring multiple tests to be ordered and multiple samples being acquired for accurate diagnosis. In addition to lacking multiplexed detection capabilities, an overwhelming majority of CFE biosensors designed for point-of-care use can only test for the presence-or-absence of analytes, not their concentrations^{25,85}. Yet, accurate quantification of biomarkers is critical for diagnosing many diseases and assessing treatment efficacy. Lastly, very few CFE biosensors can detect protein biomarkers. While lateral flow immunoassays have been developed for protein detection and used for at-home rapid tests, these assays lack sensitivity and detect only one protein biomarker¹¹³. Coupling immunoassays to a field-friendly CFE biosensing platform can provide additional signal amplification and multiplexed detection, enabling sensitive detection of multiple proteins near the point of care.

5.1.1 Novelty of protocell arrays

CFE systems have been implemented in multiple liquid-liquid phase-separated systems to study membrane-less protocells^{37,38}, but their applications in multiplexed analyte detection have not been explored. I demonstrate that individual membrane-less, phase-separated protocells compartmentalizing CFE biosensors can co-exist in the same environment to detect multiple analytes from the same sample. This resulted in a highly customizable platform for the development of diagnostic panels. The phase separation of protocell biosensors reduced undesirable crosstalk among multiple gene circuits expressing different biosensors, which has been a common obstacle in multiplexed biosensor designs. Additionally, phase separation of protocell arrays enabled selective optimization of individual CFE biosensing reactions in protocells by using differently prepared crude-cell lysates or incorporating necessary protein or nucleic acid additives, minimizing their impacts on neighboring protocell sensors.

I also show that topographical micro-basin features patterned on the floor of standardized 96-well plate format microwells enabled the simple spatial separation of coexisting protocell biosensors. This spatial separation allows for multiple biosensors to use the same reporter for signal readout, drastically reducing the complexity of diagnostic panel development. The test user simply needs to match the location of the reporter signal to the corresponding sensor location to interpret the test result.

Phase and spatial separation of protocell biosensors also enhance the test customizability and reconfigurability. As demonstrated in CHAPTER 2, each CFE biosensor is prototyped independently of the other and functions similarly when combined

with other protocell cell sensors. This indicates that a customizable protocell array testing panel can be rapidly assembled from existing protocell sensors. To update the testing panel, one can simply replace the existing sensor or remove it without impacting other protocell sensors in the same environment, which is typically not possible in conventional cell-free multiplexing approaches²⁸⁻³⁰.

Furthermore, conventional multiplexed analyte detection assay can only detect one class of analytes (only small molecules or only nucleic acids)²⁶. To report on multiple classes of molecules, multiple instruments (such as different mass spectrometry and polymerase chain reaction machines) are required for sample analysis. I show that coupling aqueous two-phase systems with CFE biosensors can be easily configured to detect diverse classes of analytes from ions to small molecules to nucleic acids by merely reprogramming the DNA sequence coding for different biosensors. Taken together, my work expands the reach of CFE biosensors and provides the foundation for developing customizable “diagnostic chips” for simultaneous detection of diverse analytes.

5.1.2 Novelty of personal glucose monitor-mediated CFE biosensor quantification

Numerous CFE biosensors have been developed to detect analytes, but rapid and reliable analyte quantification using CFE systems at the point of care remains a challenging feat. I have shown that CFE biosensors can produce glucose as a reporter and interface with a personal glucose monitor to provide digital quantification of analytes at the testing site. Compared to conventional approaches to building portable electronic plate readers⁷ and illumination chambers²¹, the personal glucose monitor provides a more intuitive and easily interpretable interface to assess analyte concentrations. The commercialization and

ubiquity of personal glucose monitors also make this device easily deployable to almost anywhere, significantly increasing the reach of PGM-coupled CFE biosensors.

Previous demonstrations of biosensors interfaced with glucose monitors were limited in their compatibility with blood samples and field deployability. For example, previous reports required additional sample processing steps to remove endogenous sample glucose^{87,91,92}. I showed that endogenous lysate metabolism present in cell-free extracts could be capitalized to remove sample glucose at the beginning of the reaction. This is accomplished by decoupling analyte-activated enzymatic reporter production from reporter-catalyzed glucose conversion. In fact, endogenous lysate metabolism can remove nearly all glucose present in human serum samples spiked with excessive amounts of glucose during the reporter production step. When the reaction shifts to reporter-catalyzed glucose conversion, the only glucose signal remaining is what was produced from the analyte, not what is naturally present in human serum samples. Taken together, I demonstrate that CFE-based genetic circuitries and biosensors can be easily coupled to PGMs for rapid and reliable analyte quantification in a complex sample matrix at the point of need.

5.1.3 Novelty of CFE-coupled immunoassays

Nearly all CFE biosensors detect either small molecules or nucleic acids rather than protein antigens. The current gold standard for protein detection is *via* sandwich immunoassays with capture and detection antibodies raised to recognize different epitopes of the protein antigen. To report on the presence of protein antigens, the detection antibodies are linked to either fluorescence or enzymatic reporters (*via* direct conjugation

or secondary antibodies) for signal generation. As seen in the COVID-19 pandemic, antigen-based rapid tests are valuable for enabling affordable and accessible detection of SARS-CoV-2 at the point of care. But these antigen tests have limited sensitivity compared to nucleic acid tests to detect early SARS-CoV-2 infections¹¹³, as nucleic acid-based detection can go through exponential cycles of DNA amplification.

I showed that nucleic acids coding for gene expression can be conjugated to detection antibodies to relay protein antigen detection events in immunoassays to enzymatic signal generation in CFE systems. The conjugated nucleic acid signals can be further amplified *via* transcription and translation in CFE reactions, potentially improving immunoassay sensitivity. Because different SARS strains and variants carry a series of mutations on their Spike/RBD proteins¹¹¹, different detection antibodies targeting specific strains or variants can carry different nucleic acid signals activating the expression of different reporter proteins. Combining CFE systems with immunoassays carrying DNA barcodes enables facile identification of SARS-CoV-1 and SARS-CoV-2 strains near the point of care. Taken together, this work demonstrates that augmenting immunoassays with CFE platforms enables sensitive and specific detection of viral protein antigens, creating an affordable and accessible test for population-scale implementation.

5.2 Next Steps and Future Directions

5.2.1 Next steps for protocell arrays

To further advance the protocell array platform to design customizable diagnostic panels spanning multiple classes of molecules, additional characterization of ATPS is necessary. As seen in the initial characterization of cell-free protein synthesis in the ATPS environment, significant diffusion of GFP signal from protocells to the surrounding bulk environment was observed after 3 hours (Figure 2-4). Moreover, while plasmid DNA was strongly partitioned in the Ficoll polymer, significant partitioning of RNA and short, double-stranded DNA was not observed. Further characterization of different protein and nucleic acid partitioning behaviors in the ATPS environment, on parameters such as polymer concentrations, pH, and CFE reagent concentrations will likely impact the effectiveness of protocell reactions, compartmentalization, and stability of partitioning.

The selection of PEG and Ficoll polymer concentrations to enable membrane-less compartmentalization of CFE reactions could also benefit from detailed reagent characterizations. The original binodal was constructed using polymers dissolved in phosphate-buffered saline (PBS) solution^{52,54}. While specific concentrations of polymers prototyped in the cell-free environment worked well, additional characterization of the specific PEG-Ficoll and PEG-dextran liquid-liquid phase separation binodal in the environment of CFE reagents could enable further platform optimization. For example, the protocell sensor polymer concentrations (Ficoll or dextran) could be individually tuned to favor the partitioning of a particular class of analyte. And for uses where long-term protocell stability is critical, polymer concentration needs to be increased to improve CFE reaction encapsulation without inhibiting the reaction.

5.2.2 *Future directions for protocell arrays*

Nearly all CFE-mediated nucleic acid detection assays require an upstream sample amplification step to bring expected attomolar concentrations of samples to the nanomolar detection range of current nucleic acid sensors^{7,9,30,83,87}. All current nucleic acid amplification steps take place separately from CFE sensing reactions, possibly due to reagent incompatibility. However, requiring reaction steps to happen in different locations creates additional sample handling steps that can be difficult to execute in resource-limited environments. These amplification steps assays are also extremely prone to sample cross-contamination¹¹⁹, necessitating extensive operator training and assay handling to ensure test accuracy.

For the protocell array diagnostic platform to be field-deployable for the detection of nucleic acids, developing methods for one-pot amplification and detection of nucleic acid analytes is critical. To this end, the coexistence of DNA replication and protein expression machinery has been previously demonstrated in reconstituted CFE reactions from purified proteins (PURE systems)^{120,121}. This suggests that it is possible for a protocell reaction to have coexisting DNA replication and biosensing machinery to carry out one-pot sample amplification and detection. Additional characterization of CFE and CFE protocell systems interfaced with DNA replication machinery could enable significant improvement of the field-deployability of protocell array systems.

Another research direction to improve protocell arrays is to incorporate protein detection. Most CFE biosensors detect small molecules and nucleic acids, with very few detecting proteins. Since ATPS was initially developed to multiplex ELISAs, it is likely

that antibody-based detection of protein analytes could be compatible with the protocell array environment. Capture and detection antibodies can be compartmentalized in Ficoll or dextran polymer droplet and added to a designated micro-basin in a 4-plex or 9-plex well. Since the phase separation of protocells allows selective tuning of different reaction environments, antibody-detection polymer droplets can coexist with CFE biosensing protocells with minimized reaction interference.

However, all ATPS ELISAs require at least one wash step to remove unbound detection antibodies for signal reporting, which could preclude the implementation of CFE biosensing reactions in the same test³⁶. In particular, reporters produced in CFE reactions generally don't have surface immobilization capabilities and may be removed in the wash step. A possible mitigating strategy is to have special surface treatments on micro basins. Anti-reporter capture antibodies (anti-GFP or anti-LacZ) can be pre-spotted onto micro basins to immobilize reporters produced in CFE biosensors and retain reporter signals after washes. The micro basin surfaces can also be manufactured to have nickel coatings, and reporters can be expressed with Histidine tag to maximize surface binding and retention after washes. As biomedical samples of clinical relevance have complex sample profiles spanning multiple classes of molecules, simultaneous measurement of biomarkers from diverse molecular classes in one test, using a single sample, can revolutionize healthcare delivery at the point of care. The future of diagnostics can now happen at home or in resource-limited areas using a fully customizable diagnostic panel of the size of a dime rather than a collection of bulky analytical instruments.

5.2.3 *Next steps for personal glucose monitor-mediated CFE biosensor quantification*

Rapid, scalable, and affordable distribution of test kits is critical to field deployment of point-of-care testing. Lyophilization, which dehydrates reactions into a powder form, can be used to make CFE biosensing reactions shelf-stable for test storage and shipment at ambient temperature^{7-9,25,46,83}. Demonstrating that biosensors can still reliably produce consistent glucose outputs between different lyophilized samples will be a necessary next step in bringing glucose-monitor mediated quantification of CFE biosensors to field implementation. In addition to variability assessments between multiple lyophilization runs, it is also essential to assess the stability of reagents when stored at ambient temperature. Ideal periods of assessments should span from weeks to months. For impactful application of CFE biosensor tests in the field, the lyophilized reactions should be shelf-stable for at least a year.

Biological variability in human serum samples leading to variability in test output, a phenomenon known as “matrix effects”, can preclude accurate analyte quantification using an established range of values²⁵. This test only assessed pooled human serum samples for target quantification and did not assess potential quantification differences in single-donor serum samples. An important next step would be to determine the robustness of our quantification on single-donor serum samples. In particular, identifying the possible source of biological variability (whether they arise from differences in blood glucose levels, hydration, etc.) and steps to mitigate deviations (collecting samples first thing in the morning) should be assessed. Ideally, quantification results should be evaluated on tens to hundreds of single-donor serum samples to make conclusions sufficiently generalizable. If variability across single-donor serum samples is high, an alternative strategy using a

sample-specific calibration of reference reactions could be used to control for matrix effects²⁵.

5.2.4 Future directions for personal glucose monitor-mediated CFE biosensor quantification

Once the glucose monitor-mediated CFE biosensing approach passes the initial criteria for field deployment (shelf-stable and low inter-individual quantification variability), an important next step is to improve the test's ease of use. The current assay requires two incubation steps (45 minutes of reporter production and 15 minutes of glucose conversion) and three hands-on reagent steps (addition of samples to rehydrate the test, addition of small molecule inhibitor and lactose mixture, and sampling reacted solution on glucose monitor strips for glucose meter measurement). For field use, it is best to minimize the number of hands-on pipetting steps to minimize operator-induced variability and errors. Ideally, the operator should only need to add samples into the reaction, wait for reactions to complete, and then read off a number on the glucose monitor that directly translates to the concentration of a target analyte.

Paper-based microfluidic devices that manipulate reagent flows can be designed to meet this goal. For example, microfluid paper-based analytical devices (μ -PADs) have been developed for sequential addition or withdrawal of reagents with reduced operator manipulation^{105,106,122}. These devices can be connected with electronic circuits for result interpretation on a glucose monitor or smartphone device^{105,106}. Furthermore, advances in paper-fluidic devices have successfully separated whole blood into plasma with minimal operator manipulation¹²³. A fully integrated paper-fluidic device that takes in a drop of a

patient's blood, performs automated whole-blood separation to extract serum or plasma from the sample, rehydrates the biosensing reaction, converts lactose into glucose for interpretation, and outputs quantitative results on the glucose monitor would have tremendous translational potential in point-of-care diagnostics.

5.2.5 Next steps for CFE-coupled immunoassays

In this work, I demonstrated that DNA-barcode conjugated detection antibodies could relay protein antigen signals in immunoassays. The next step is to apply this DNA barcoding and signal detection strategy to specific detection antibodies recognizing Spike/RBD protein epitopes on SARS-CoV-1 and SARS-CoV-2 strains as a proof-of-principle. Additional validation using inactivated virus particles rather than purified, recombinant Spike/RBD proteins would be essential for test validation. In fact, using inactivated virus samples may actually lead to sensitivity improvements as the outer surface of the coronaviruses have 24-40 Spike/RBD proteins expressed¹²⁴. This means that, for every SARS-CoV-1 or 2 virus particles bound to the capture antibody, 24-40 detection antibodies can bind the virus and relay this DNA barcode signal for cell-free amplification, resulting in an ultra-sensitive diagnostic assay.

However, the vast majority of current antigen-based SARS-CoV-2 diagnostics lyse the lipid membrane of the virus in the sample collection step, which could potentially cause Spike/RBD proteins to misfold in the process¹²⁵. Although sample lysis is necessary as these rapid tests detect the nucleocapsid proteins rather than the Spike/RBD protein and the collected sample must inactivate the virus for biocontainment purposes, further assessment of virus inactivation methods that allows viral particles and Spike/RBD

proteins to stay intact to bind capture and detection antibodies would be necessary for bringing this test closer to clinical implementation.

5.2.6 Future directions for CFE-coupled immunoassays

The current test design involving numerous sample transfer steps can at best be implemented in Clinical Laboratory Improvement Amendment (CLIA) certified laboratories, necessitating significant improvements to the test and reagent handling strategies in order to bring CFE coupled immunoassays for point-of-care and at-home implementation. The immunoassay step is the most problematic area, requiring extensive wait time and wash steps. Implementing the antibody capture and detection on a lateral flow assay (LFA) strip may be a potentially more field-friendly solution. Rather than using gold nanoparticle-conjugated detection antibodies on the LFA, DNA barcode-conjugated detection antibodies can be used and immobilized to a designated location on the LFA strip *via* antigen binding. Following immobilization, that area of the LFA strip can be cut out and placed in the CFE reaction for assay interpretation. For facile interpretation of assay signals, a companion smartphone application can be designed to analyze colorimetric results produced by the CFE reaction.

Additional areas that warrant further investigation are the DNA barcode synthesis and conjugation to detection antibodies. One of the reasons short oligo fragments such as LacZ alpha fragments and toehold switch trigger sequences were chosen to relay antigen signals is due to the set of current limitations in oligo synthesis. Commercial DNA synthesis is limited to synthesizing at most 200-nucleotides of DNA, placing a size limitation on the DNA signal used to relay information from immunoassays to CFE

reactions. As a result, DNA conjugates were limited to using either a split reporter system (a 45-amino acid LacZ alpha fragment) or toehold switch triggers (30-35 nucleotide sequences) to make the signal relay sequences as short as possible. Being able to attach larger DNA fragments to detection antibodies could significantly expand the design space of signal relay modules. Generating larger DNA fragments is possible *via* PCR with amine-functionalized primers, but the process becomes cost-prohibitive at a large scale – at least 650 μg of 200-nt DNA is needed for a 150- μg scale of antibody conjugation, but typical PCR reaction makes only 2.5 μg (260-fold less).

However, even when large-scale DNA synthesis is no longer a problem, challenges remain in purifying conjugated antibodies from unreacted large DNA fragments after conjugated reactions due to similarity in sizes to be separated from column chromatography. To this end, using biotinylated antibodies and DNA fragments may remove this purification problem, as DNA fragments and detection antibodies can be joined together by affinity binding to streptavidin⁴³. Further advancements in DNA synthesis, conjugation of DNA to antibodies, and protein purification methods would endow CFE-coupled immunoassays with more capabilities for impactful use in clinical diagnostics.

5.3 Concluding Remarks

In this thesis, I have described my efforts to connect CFE biosensors to new interfaces to improve their translational potential. In interfacing CFE biosensor expression systems with polymer aqueous two-phase systems, I developed the first-of-its-kind multiplexed detection platform to screen diverse classes of molecules from a single sample. In augmenting CFE reporter production with personal glucose monitors, I accomplished

digital quantification of analyte concentrations in resource-limited settings. Lastly, in coupling immunoassays with CFE platforms, I demonstrated that CFE reactions could report on antigen binding in immunoassays and enable multiplexed detection of different SARS strains. The body of work presented in this thesis indicates that CFE systems are a modular and versatile platform for implementing point-of-care diagnostics. While there are still gaps in bringing these products to clinical adoption and field implementation, this work has laid the foundation and established future directions for further test and device optimization.

APPENDIX A. SUPPLEMENTARY INFORMATION FOR CHAPTER 2: PROTOCELL ARRAYS FOR SIMULTANEOUS DETECTION OF DIVERSE ANALYTES

A.1 Initial Validation of *B. Theta*, Stx1, and Stx2 Switch Activation in CFE Reactions

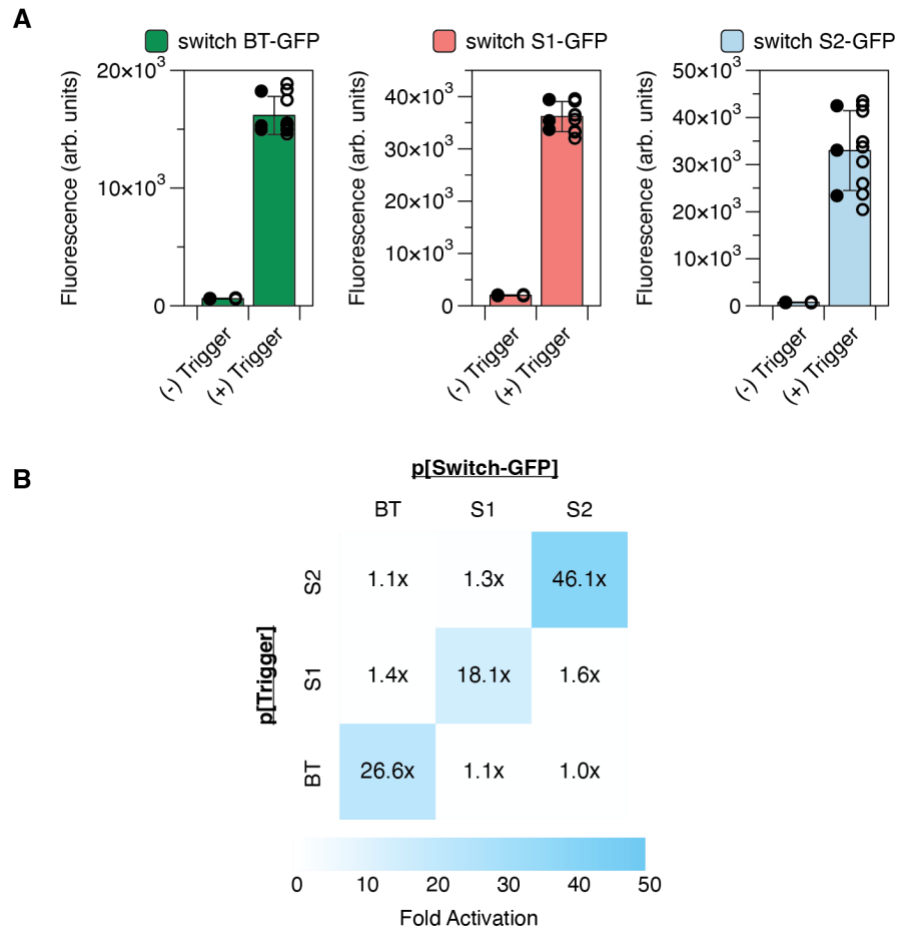


Figure 12 *B. Theta*, Stx1, and Stx2 switch activation in response to their cognate triggers in CFE reactions. Reactions were incubated at 37 °C for 3 hours. (A) All triggers and switches were expressed from plasmids. Data are presented as mean values \pm SD of 9 replicates (3 biological replicates \times 3 technical replicates). Each biological replicate is an independently assembled reaction on a different day. Solid-filled circles represent the mean of each biological replicate, and hollow circles represent all data points. (B) Specificity assessment of previously developed *B. theta*

toehold switch and newly developed Stx1 and Stx2 toehold switches. Only correctly paired triggers and switches showed high levels of GFP activation. Fold change shown represent average fold activation from 9 replicates (3 biological replicates x 3 technical replicates).

A.2 Sequence Information

Table 1. Description of plasmid parts and DNA sequences used in CHAPTER 2

Name	Construct Description
pJL1	Relevant part of the plasmid encoding superfolder GFP expression under P _{T7} promoter with strong ribosomal binding site
P_{T7} Promoter-Stability Hairpin-StrongRBS-<i>sfgfp</i>-T7 Terminator	
<pre> taatacgactcactatagggaga ccacaacgggtttccctctagaaataatTTTTGTTTAACTTTAAGAAGG agatatacatATGAGCAAAGGTGAAGAACTGTTTACCGCGTGTGCGGATTCTGGTGGAACTGGATGGC GATGTGAACGGTCACAAATTCAGCGTGCCTGGTGAAGGTGAAGGCGATGCCACGATTGGCAAACCTGACGC TGAAATTTATCTGCACCACCGCAAACCTGCCGGTGCCTGGCCGACGCTGGTGACCACCCTGACCTATGG CGTTTCAGTGTTTTAGTCGCTATCCGGATCACATGAAACGTCACGATTTCTTTAAATCTGCAATGCCGGAA GGCTATGTGCAGGAACGTACGATTAGCTTTAAAGATGATGGCAAATATAAAACGCGCGCCGTTGTGAAAT TTGAAGGCGATACCCTGGTGAACCGCATTGAACTGAAAGGCACGGATTTTAAAGAAGATGGCAATATCCT GGGCCATAAACTGGAATACAACCTTAAATAGCCATAATGTTTATATTACGGCGGATAAACAGAAAAATGGC ATCAAAGCGAATTTTACCGTTCGCCATAACGTTGAAGATGGCAGTGTGCAGCTGGCAGATCATTATCAGC AGAATACCCCGATTGGTGTATGGTCCGGTGTCTGCCGATAATCATTATCTGAGCACGCAGACCCGTTCT GTCTAAAGATCCGAACGAAAAAGGCACGCGGGACCACATGGTTCTGCACGAATATGTAATGCGGCAGGT ATTACGTGGAGCCATCCGCAGTTCGAAAAATAAgtcgaccggctgctaacaagcccgaaggaagctga gttggctgctgccaccgctgagcaataac tagcataacccttggggcctctaaacgggtcttgaggggt TTTTG </pre>	
P _{T7} - <i>lacI</i>	Relevant part of the plasmid encoding LacI expression under P _{T7} promoter with strong ribosomal binding site
P_{T7} Promoter-Stability Hairpin-StrongRBS-<i>lacI</i>-T7 Terminator	
<pre> taatacgactcactatagggaga ccacaacgggtttccctctagaaataatTTTTGTTTAACTTTAAGAAGG agatatacatATGAAACCAGTAACGTTATACGATGTCGCAGAGTATGCCGGTGTCTTATCAGACCGTT TCCCGCGTGGTGAACCAGGCCAGCCACGTTTCTGCGAAAACGCGGGAAAAAGTGAAGCGGCGATGGCGG AGCTGAATTACATTCCTCAACCGCGTGGCACAACAACCTGGCGGGCAAACAGTCGTTGCTGATTGGCGTTGC CACCTCCAGTCTGGCCCTGCACGCGCCGTCGCAAATGTGCGCGGCGATTAAATCTCGCGCCGATCAACTG GGTGCCAGCGTGGTGGTGTGATGGTGAACGAAGCGGCGTGAAGCCTGTAAAGCGGCGGTGCACAATC TTCTCGCGCAACGCGTCAGTGGGCTGATCATTAACTATCCGCTGGATGACCAGGATGCCATTGCTGTGGA AGCTGCCTGCACTAATGTTCCGGCGTATTTCTTGATGTCTCTGACCAGACACCCATCAACAGTATTATT TTCTCCCATGAAGACGGTACGCGACTGGGCGTGGAGCATCTGGTTCGATTGGGTCAACAGCAAAATCGCGC TGTTAGCGGGCCCATTAAGTCTGTCTCGGCGCTCTGCTGCTGGCTGGCTGGCATAAAATATCTCACTCG CAATCAAATTCAGCCGATAGCGGAACGGGAAGGCGACTGGAGTGCCATGTCCGTTTTTCAACAAACATG CAAATGCTGAATGAGGGCATCGTTCCTCCACTGCGATGCTGGTTGCCAACGATCAGATGGCGCTGGGCGCAA TGCGCGCCATTACCGAGTCCGGGCTGCGCGTTGGTGCAGATATCTCGGTAGTGGGATACGACGATACCGA AGACAGCTCATGTTATATCCCGCCGTTAACCACCATCAAACAGGATTTTCGCTGCTGGGGCAAACCAGC GTGGACCGCTTGTGCAACTCTCTCAGGGCCAGGCGGTGAAGGGCAATCAGCTGTTGCCCGTCTCACTGG TGAAAAGAAAAACCACCCTGGCGCCAATACGCAAACCGCCTCTCCCCGCGGTTGGCCGATTCAATTAAT GCAGCTGGCAGCAGAGTTTCCCGACTGGAAAGCGGGCAGTGATAAgtcgaccggctgctaacaagccc gaaaggaagctgagttggctgctgccaccgctgagcaataac tagcataacccttggggcctctaaacg ggtcttgaggggtTTTTG </pre>	

<i>P_{T7}lacO-sfgfp</i>	Relevant part of the plasmid encoding superfolder GFP expression under <i>P_{T7}lacO</i> promoter with strong ribosomal binding site
<i>P_{T7}</i> Promoter-<i>lacO</i>-Stability Hairpin-StrongRBS-<i>sfgfp</i>- T7 Terminator	
<pre> taatacgcactcactatagggagatgtgagcgggataaacaaccacaacgggtttccctctagaaataattttg ttaaactttaagaaggagatatacatATGAGCAAAGGTGAAGAACTGTTTACCGGCGTTGTGCCGATTCT GGTGAACCTGGATGGCGATGTGAACGGTCACAAATTCAGCGTGCCTGGTGAAGGTGAAGGCGATGCCACG ATTGGCAAACCTGACGCTGAAATTTATCTGCACCACCGCAAACCTGCCGGTGCCGTGGCCGACGCTGGTGA CCACCCTGACCTATGGCGTTTTCAGTGTCTTAGTTCGCTATCCGGATCACATGAAACGTCACGATTTCTTTAA ATCTGCAATGCCGGAAGGCTATGTGCAGGAACGTACGATTAGCTTTAAAGATGATGGCAAATATAAAACG CGCGCCGTTGTGAAATTTGAAGGCGATACCCTGGTGAACCGATTGAACTGAAAGGCGACGGATTTTAAAG AAGATGGCAATATCCTGGGCCATAAACTGGAATAACAACCTTAATAGCCATAATGTTTATATTACGGCGGA TAAACAGAAAAATGGCATCAAAGCGAATTTTACCCTTCGCCATAACGTTGAAGATGGCAGTGTGCAGCTG GCAGATCATTATCAGCAGAATACCCGATTGGTGTGCTGCCGGTGTGCTGCCGATAATCATTATCTGA GCACGCAGACCGTTTCTGTCTAAAGATCCGAACGAAAAAGGCACGCGGGACCACATGGTTCTGCACGAATA TGTGAATGCGGCAGGTATTACGTGGAGCCATCCGCAGTTCGAAAAATAAgtcgcaccggctgctaacaaga cccgaaggaagctgagttggctgctgccaccgctgagcaataactagcataacccttggggcctctaa acgggtcttgaggggttttttg </pre>	

<i>araC-P_{BAD}-sfgfp</i>	Relevant part of the plasmid with divergent <i>P_{BAD}</i> promoter for constitutive AraC expression and arabinose modulated superfolder GFP expression.
<i>araC</i>-<i>P_{BAD}</i>-Stability Hairpin-StrongRBS-<i>sfgfp</i>- T7 Terminator	
<pre> TTATGACAACCTTGACGGCTACATCATTCACTTTTTCTTCCACAACCGGCACGGAACTCGCTCGGGCTGGCC CCGGTGCATTTTTTAAATACCCGCGAGAAATAGAGTTGATCGTCAAACCAACATTGCGACCGACGGTGG CGATAGGCATCCGGGTGGTGTCTCAAAGCAGCTTCGCCTGGCTGATACGTTGGTCTCGCGCCAGCTTAA GACGCTAATCCCTAAGTGTGGCGGAAAAGATGTGACAGACGCGACGGCGACAAGCAAACATGCTGTGCG ACGCTGGCGATATCAAATTTGCTGTCTGCCAGGTGATCGCTGATGACTGACAAGCCTCGCGTACCCGAT TATCCATCGGTGGATGGAGCGACTCGTTAATCGCTTCCATGCGCCGACGTAACAATTGCTCAAGCAGATT TATCGCCAGCAGCTCCGAATAGCGCCCTTCCCTTGGCCGGCGTTAATGATTTGCCCAAACAGGTGCGTG AAATGCGGCTGGTGCCTTCATCCGGGCGAAAGAACCCTGATTGGCAAATATTGACGGCCAGTTAAGCC ATTCATGCCAGTAGGCGCGCGGACGAAAGTAAACCCACTGGTGATACCATTCGCGAGCCTCCGGATGACG ACCGTAGTGATGAATCTCTCTGGCGGGAACAGCAAATATCACCCGGTCCGCAAACAATTTCTCGTCCC TGATTTTTACCACCCCTGACCGCAATGGTGAGATTGAGAATATAACCTTTCCATTTCCAGCGTCCGT CGATAAAAAATCGAGATAACCGTTGGCTCAATCGCGGTTAAACCCGCCACCAGTGGGCATTAACGA GTATCCCGGCAGCAGGGGATCATTGCGCTTCAGCCATacttttcatactcccgccattcagagaagaa accaattgtccatattgcatcagacattgcccgtcactgctcttttactggtcttctcgttaaccaaac cggtaaccccgcttattaaaagcattctgtaacaaagcgggaccaaagccatgacaaaaacgcgtaacaa aagtgtctataatcacggcagaaaagtcacacattgattatgtgacggcgtcacactttgctatgccata gcatttttatccataagattagcggatcctacctgaagctttttatcgcaactctctactgtttctccat accggtttttttgggctagccacaacgggtttccctctagaaataattttgtttaactttaagaaggaga tatacatATGAGCAAAGGTGAAGAACTGTTTACCGGCGTTGTGCCGATTCTGGTGAACCTGGATGGCGAT GTGAACGGTCACAAATTCAGCGTGCCTGGTGAAGGTGAAGGCGATGCCACGATTGGCAAACCTGACGCTGA AATTTATCTGCACCACCGCAAACCTGCCGGTGCCGTGGCCGACGCTGGTGAACCCCTGACCTATGGCGT TCAGTGTCTTAGTTCGCTATCCGGATCACATGAAACGTCACGATTTCTTTAAATCTGCAATGCCGGAAGGC TATGTGCAGGAACGTACGATTAGCTTTAAAGATGATGGCAAATATAAAACGCGCGCCGTTGTGAAATTTG AAGGCGATACCCTGGTGAACCGCATTGAACTGAAAGGCACGGATTTTAAAGAAGATGGCAAATATCCTGGG CCATAAACTGGAATACAACCTTTAATAGCCATAATGTTTATATTACGGCGGATAAACAGAAAAATGGCATC AAAGCGAATTTTACCCTTCGCCATAACGTTGAAGATGGCAGTGTGCAGCTGGCAGATCATTATCAGCAGA ATACCCCGATTGGTGTGCTGCCGTGCTGCCGGATAATCATTATCTGAGCACGCAGACCGTTCTGTCT TAAAGATCCGAACGAAAAAGGCACGCGGGACCACATGGTTCTGCACGAATATGTGAATGCGGCAGGTATT ACGTGGAGCCATCCGCAGTTCGAAAAATAAgtcgcaccggctgctaacaagaagcccgaaggaagctgagtt </pre>	

ggctgctgccaccgctgagcaataac tagcataacccttggggcctctaaacgggtcttgaggggtttt
ttg

P_{T7}-trigger B
Linear DNA encoding expression of RNA trigger B under a P_{T7} Promoter. Additional nucleotides (>20bp) are included in 5' and 3' end as extra protection against nuclease degradation.

P_{T7} Promoter-trigger B-T7 Terminator
aacgccagcaacgcgatcccgcgaaat taatacgcactcactatagggaga GGGATGCCCGTAGTTCATTC
TACGGGCATGAATAACGACATACAGCAAGCGATTTACTTATACTA tagcataacccttggggcctctaa
acgggtcttgaggggttttttgtttgctgaaagccaattctgatta

P_{T7}-switch B-*sfgfp*
Relevant part of the plasmid encoding superfolder GFP expression under P_{T7} promoter and toehold switch B

P_{T7} Promoter-switch B-*sfgfp*-TrnB-T7 Terminator
taatacgcactcactatagggaga GGGTATAAGTAAATCGCTTGCTGTATGTCGTTAAACAGAGGAGATAA
CGAATGACAGCAAGCAACCTGGCGGCAGCGCAAAAG ATGAGCAAAGGTGAAGAAGTGTTCACGGCGTTG
TGCCGATTCTGGTGGAACTGGATGGCGATGTGAACGGTCACAAATTCAGCGTGCGTGGTGAAGGTGAAGG
CGATGCCACGATTGGCAAACCTGACGCTGAAATTTATCTGCACCACCGCAAACCTGCCGGTGCCGTGGCCG
ACGCTGGTGACCACCCTGACCTATGGCGTTTTCAGTGTTCAGTGTTCAGTGTTCAGTGTTCAGTGTTCAGT
ATTTCTTTAAATCTGCAATGCCGGAAGGCTATGTGCAGGAACGTACGATTAGCTTTAAAGATGATGGCAA
ATATAAAACGCGCGCGTTGTGAAATTTGAAGGCGATACCCTGGTGAACCGCATTGAAGTAAAGGCAAG
GATTTTAAAGAAGATGGCAATATCCTGGGCCATAAACTGGAATACAACCTTAATAGCCATAATGTTTATA
TTACGGCGGATAAACAGAAAAATGGCATCAAAGCGAATTTTACCGTTCGCCATAACGTTGAAGATGGCAG
TGTGCAGCTGGCAGATCATTATCAGCAGAATACCCCGATTGGTGTATGGTCCGGTGTCTGCTGCCGATAAT
CATTATCTGAGCACGCAGACCCTTCTGTCTAAAGATCCGAACGAAAAAGGCACGCGGGACCACATGGTTC
TGCACGAATATGTGAATGCGGCAGGTATTACGTGGAGCCATCCGCAGTTCGAAAAATAA ggatctgaagc
ttgggcccgaacaaaaactcatctcagaagaggatctgaatagcgcgctcgaccatcatcatcatcatca
ttgagtttaaacgggtctccagcttggtgttttggcggatgagagaagattttcagcctgatacagatta
aatcagaacgcagaagcggcttgataaaacagaatttgctggcggcagtagcgcggtggtcccacctga
ccccatgccgaactcagaagtgaacgcgctagcgcgcatggttagtggtgggtctccccatgagagagta
gggaactgccaggcatcaataaaacgaaaggctcagtcgaaagactgggcctttcgttttatctgttgt
ttgtcgggtgaact ggatcgtcgaccggctgctaacaagcccgaaggaagctgagttggctgctgccac
cgctgagcaataac tagcataacccttggggcctctaaacgggtcttgaggggtttttt

P_{T7}-trigger H
Linear DNA encoding expression of RNA trigger H under a P_{T7} Promoter. Additional nucleotides (>20bp) are included in 5' and 3' end as extra protection against nuclease degradation.

P_{T7} Promoter-trigger H-T7 Terminator
aacgccagcaacgcgatcccgcgaaat taatacgcactcactatagggaga GGGACCGTGGACCGCATGAG
GTCCACGGTAAACATAACTATAACAAGCCTACAATTCATTCAAAC tagcataacccttggggcctctaa
acgggtcttgaggggttttttgtttgctgaaagccaattctgatta

P_{T7}-switch H-*sfgfp*
Relevant part of the plasmid encoding superfolder GFP expression under P_{T7} promoter and toehold switch H

P_{T7} Promoter-switch H-*sfgfp*-TrnB-T7 Terminator

taatacgcactcactatagggagaGGGTGAATGAATTGTAGGCTTGTATAGTTATGAACAGAGGAGACAT
 AACATGAACAAGCCTAACCTGGCGGCAGCGCAAAAGATGAGCAAAGGTGAAGAAGCTGTTTACC
 TGCCGATTCTGGTGGAACTGGATGGCGATGTGAACGGTCACAAATTCAGCGTGCCTGGTGAAGGTGAAGG
 CGATGCCACGATTGGCAAACCTGACGCTGAAATTTATCTGCACCACCGCAAACCTGCCGGTGCCTGGCCG
 ACGCTGGTGACCACCCTGACCTATGGCGTTTCACTGTTTTAGTCGCTATCCGGATCACATGAAACGTCACG
 ATTTCTTTAAATCTGCAATGCCGGAAGGCTATGTGCAGGAACGTACGATTAGCTTTAAAGATGATGGCAA
 ATATAAACGCGCGCCGTTGTGAAATTTGAAGGCGATAACCCTGGTGAACCGCATTGAACTGAAAGGCACG
 GATTTTAAAGAAGATGGCAATATCCTGGGCCATAAACTGGAATACAACCTTAATAGCCATAATGTTTATA
 TTACGGCGGATAAACAGAAAAATGGCATCAAAGCGAATTTTACCGTTCGCCATAACGTTGAAGATGGCAG
 TGTGCAGCTGGCAGATCATTATCAGCAGAATACCCCGATTGGTGTGATGGTCCGGTGTCTGCTGCCGATAAT
 CATTATCTGAGCACGCAGACCGTTCTGTCTAAAGATCCGAACGAAAAAGGCACGCGGGACCACATGGTTC
 TGCACGAATATGTGAATGCGGCAGGTATTACGTGGAGCCATCCGCAGTTCGAAAAATAAaggatctgaagc
 ttgggcccgaacaaaaactcatctcagaagaggatctgaatagcgcgctcgaccatcatcatcatcatca
 ttgagtttaaacgggtctccagcttggtggtggttggcggtgagagaagatcttcagcctgatacagatta
 aatcagaacgcagaagcgggtctgataaaacagaatttgccctggcggcagtagcggggtggtcccacctga
 ccccatgccgaactcagaagtgaacgcgctagcgcgcatggttagtgtggggtctcccacatgagagagta
 ggaactgccaggcatcaataaaacgaaaggctcagtcgaaagactgggccttctggtttatctgttgtg
 ttgtcgggtgaactggatcgctgcaccggctgctaacaaagcccgaaggaagctgagttggctgctgccac
 cgctgagcaataactagcataacccttggggcctctaaacgggtcttgaggggttttttg

P_{T7}-zntR	Relevant part of the plasmid encoding ZntR expression under P _{T7} promoter with strong ribosomal binding site
PT7 Promoter-Stability Hairpin-StrongRBS-zntR-T7 Terminator	
<p> taatacgcactcactatagggagaccacaacgggtttccctctagaaataattttggtttaacttttaagaagg agatatacatATGTATCGCATTGGTGTAGCTGGCAAAAATGGCGGAAGTAACACCCGACACGATTTCGTTAT TACGAAAAACAGCAGATGATGGAGCATGAAGTGCCTACTGAAGGTGGGTTTCGCCTATATACCGAAAGCG ATCTCCAGCGATTGAAATTTATCCGCCATGCCAGACAACCTAGGTTTCACTGCTGGAGTCGATCCGCGAGTT GCTGTGATCCGCATCGATCCTGAACACCATAACCTGTGAGGAGTCAAAGGCATTGTGCAGGAAAGATTG CAGGAAGTCAAGCACGGATAGCCGAGTTGCAGAGTATGCAGCGTTTCTTGCAACGCCTTAACGATGCCT GTTGTGGGACTGCTCATAGCAGTGTATTATTGTTTCGATTCTTGAAGCTCTTGAACAAGGGGCGAGTGGCGT TAAGAGTGGTTGTTGATAAgtcgaccggctgctaacaaagcccgaaggaagctgagttggctgctgccac cgctgagcaataactagcataacccttggggcctctaaacgggtcttgaggggttttttg </p>	

P_{ZntA}-<i>sfgfp</i>	Relevant part of the plasmid encoding superfolder GFP expression under ZntR regulated P _{ZntA} promoter
P_{ZntA}-Stability Hairpin-StrongRBS-<i>sfgfp</i>-T7 Terminator	
<p> CTGTATCTCTGATAAAACTTGACTCTGGAGTCGACTCCAGAGTGTATCCTTCGGTTAAATccacaacgggtt tccctctagaaataattttggtttaacttttaagaaggagatatacatATGAGCAAAGGTGAAGAAGCTGTTT ACCGCGTTGTGCCGATTCTGGTGGAACTGGATGGCGATGTGAACGGTCACAAATTCAGCGTGCCTGGTGAAGGTGAAGGCGATGCCACGATTGGCAAACCTGACGCTGAAATTTATCTGCACCACCGCAAACCTGCCGGT GCCGTGGCCGACGCTGGTGACCACCCTGACCTATGGCGTTTCACTGTTTTAGTCGCTATCCGGATCACATG AAACGTCACGATTTCTTTAAATCTGCAATGCCGGAAGGCTATGTGCAGGAACGTACGATTAGCTTTAAAG ATGATGGCAAATATAAAACGCGCGCCGTTGTGAAATTTGAAGGCGATAACCCTGGTGAACCGCATTGAACT GAAAGGCACGATTTTAAAGAAGATGGCAATATCCTGGGCCATAAACTGGAATACAACCTTAATAGCCAT AATGTTTATATTACGGCGGATAAACAGAAAAATGGCATCAAAGCGAATTTTACCGTTCGCCATAACGTTG AAGATGGCAGTGTGCAGCTGGCAGATCATTATCAGCAGAATACCCCGATTGGTGTGATGGTCCGGTGTCTGCT GCCGGATAATCATTATCTGAGCACGCAGACCGTTCTGTCTAAAGATCCGAACGAAAAAGGCACGCGGGAC CACATGGTTCTGCACGAATATGTGAATGCGGCAGGTATTACGTGGAGCCATCCGCAGTTCGAAAAATAAg tcgaccggctgctaacaaagcccgaaggaagctgagttggctgctgccaccgctgagcaataacttagca taacccttggggcctctaaacgggtcttgaggggttttttg </p>	

P_{T7} - <i>eutR</i>	Relevant part of the plasmid encoding EutR expression under P_{T7} promoter with strong ribosomal binding site.
P_{T7} Promoter- Stability Hairpin - StrongRBS - <i>eutR</i> - T7 Terminator	
<pre> taatacgactcactatagggagaccacaacgggtttccctctagaaataattttggtttaactttaagaagg agatatacatATGAAAAAGACCCGTACAGCCAATTTGCACCATCTTTATCATGAACCCCTTACCCGAAAAC CTGAAGCTCACGCCGAAGGTCGAAGTGGATAATGTTCATCAACGACAGACAACGGATGTCTATGAACATG CTTTAACGATTACCGCCTGGCAGCAGATTTACGATCAGCTGCATCCGGGCAAGTTTCATGGTGAATTTAC GGAAATCTACTCGATGATATTCAGGTTTTTCGTGAATACACCGGTCTGGCGCTGCGTCAGTCGTGCCTG GTCTGGCCGAACTCGTTCTGGTTTGGCATTCCGGCAGCGCGGTGAGCAGGGATTTATCGGTTCCGAAT GTCTGGGAAGCGCGAAATCGCCACCCGCCCTGGTGGCACTGAATTTGAACTGAGCAGCAGCCGGATGATTA CAGTACCTGGGCGTGGTGCTTTCTGAAGATGTCATCACCCGGCAGGCTAACTTTTTGCATAACCCGGAT CGGGTATTACATATGTTGCGTAACCAGTCGGCGCTGGAAGTGAAAGAGCAGCATAAAGCCGCGCTGTGGG GCTTTGTCCAACAGGCGCTGGCGACGTTTTGCGAGAATCCGGAAAATCTCCATCAGCCAGCAGTGCGAAA AGTGCTGGGGGATAATTTGCTAATGGCGATGGGGGCCATGCTGGAAGAAGCGCAACCAATGGTGACGGCG GAAAGCATCAGTCATCAGAGTTACCGTCGATTGCTTTCCCGCGCCCGTGAATATGTGCTGGAAAACATGT CCGAACCGGTGACGGTGGTGGATTTGTGTAATCAACTGCATGTCAGCCGCCGACGCTACAAAACGCGTT TCACGCTATTTTAGGCATTGGCCCGAACGCGTGGCTGAAACGCATTCGCCTGAACGCCGTACGCCGCGAA CTGATAAGTCCGTGGTCGAAAGTATGACGGTAAAAGACGCCGCATGCAGTGGGGATTCTGGCATCTGG GGCAATTTGCCACGGATTACCAGCAGCTGTTTTCCGAGAAGCCGTACTGACGCTGCATCAGCGGATGCG GGAGTGGGGGTGAgtcgaccggctgctaacaaagcccgaaggaagctgagttggctgctgccaccgctg agcaataactagcataacccttggggcctctaaacgggtcttgagggggttttttg </pre>	

P_{EutS} - <i>sfgfp</i>	Relevant part of the plasmid encoding superfolder GFP expression under EutR regulated P_{EutS} promoter
P_{EutS} - Stability Hairpin - StrongRBS - <i>sfgfp</i> - T7 Terminator	
<pre> AACAGAGCGAAGTGGTGGCTTCAGCGTATGGCGATCAGGATCTGAGCTTTGGTCCGGAATACATCATTCC AAAACCGTTTGATCCGCGCTTGATCGTTAAGATCGCTCCTGCGGTGCTAAAGCCGCGATGGAGTCGGGC GTGGCGACTCGTCCGATTGCTGATTTTCAGCTCTACATCGACAAGCTGACTGAGTTCGTTTACAAAACCA ACCTGTTTATGAAGCCGATTTTTCTCCAGGCTCGCAAAGCGCCGAAGCGCGTGTGTTCTGCCGGAAGGGGA AGAGGCGCGCTTCTGCATGCCACTCAGGAACTGGTAACGCTGGGACTGGCGAAACCGATCCTTATCGGT CGTCCGAACGTGATCGAAATGCGCATTCAGAACTGGGCTTGCAGATCAAAGCGAGCGTTGATTTTTGAGA TCGTCAATAACGAATCCGATCCGCGCTTTAAAGAGTACTGGACCGAATACTTCCAGATCATGAAGCGTCG CGGCGTCACTCAGGAACAGGCGCAGCGGGCGCTGATCAGTAACCCGACAGTGATCGGCGCGATCATGGTT CAGCGTGGGGAAGCCGATGCAATGATTTGCGGTACGGTGGGTGATTATCATGAACATTTTAGCGTGGTGA AAAATGTCTTTGGTTATCGCGATGGCGTTCACACCGCAGGTGCCATGAACGCGCTGCTGCTGCCGAGTGG TAACACCTTTATTGCCGATACATATGTTAATGATGAACCGGATGCAGAAGAGCTGGCGGAGATCACCTTG ATGGCGGCAGAACTGTCCGTCGTTTTGGTATTGAGCCGCGCGTGTGTTTTGTTGTGCGACTCCAACCTTG GTTCTTCTGACTGCCCGTCGTCGAGCAAATGCGTCAGGCGCTGGAACTGGTCAGGGAACGTGCACCAGA ACTGATGATTGATGGTGAAATGCACGGCGATGCAGCGCTGGTGGAAGCGATTTCGCAACGACCGTATGCCG GACAGCTCTTTGAAAGGTTCCGCCAATATTCTGGTGATGCCGAACATGGAAGCTGCCCGCATTAGTTACA ACTTACTGCGTGTTCCAGCTCGGAAGGTGTGACTGTCGGCCCGGTGCTGATGGGTGTGGCGAAACCGGT TCACGTGTTAACGCCGATCGCATCGGTGCGTCGTATCGTCAACATGGTGGCGCTGGCCGTGGTTAGAAGCG CAAACCCAACCGCTGTAATTTTTTTAACTCTCACGCTTATCCTGAATATTCAGGGTAAGCAGTTTAGCT GCAATATATTAGTAAAGCTTATTACTGAGTTGCGAATAATAAAAAAAAAAGCAGTCTATATAATATCTCGA TATTATTTATTTATATTATCATGCGTTGCATAGAAAGTTTTATGCACCACAGCGAATATCTCCTCATTCTT AGTACTTACCTACCTTTTAAACGCGCTTGCCGAAATTTGTTATTACTCTGACGAAAAATTTGTCAGCA TACACGAAAGTTTTTACAGGCGGCGACTccacaacgggtttccctctagaaataattttggtttaacttt aagaaggagatatacatATGAGCAAAGGTGAAGAACTGTTTACCGCGTGTGGCCGATTCTGGTGGAACT GGATGGCGATGTGAACGGTCACAAATTCAGCGTGCCTGGTGAAGGTGAAGGCGATGCCACGATTGGCAA CTGACGCTGAAATTTATCTGCACCACCGGCAAACTGCCGGTGGCCGACGCTGGTGACCACCCTGA CCTATGGCGTTCAGTGTTTAGTCGCTATCCGGATCATGAAACGTCACGATTTCTTTAAATCTGCAAT </pre>	

```
GCCGGAAGGCTATGTGCAGGAACGTACGATTAGCTTTAAAGATGATGGCAAATATAAAACGCGCGCCGTT
GTGAAATTTGAAGGCATACCCTGGTGAACCGCATTGAACTGAAAGGCACGGATTTTAAAGAAGATGGCA
ATATCCTGGGCCATAAACTGGAATACAACCTTTAATAGCCATAATGTTTATATTACGGCGGATAAACAGAA
AAATGGCATCAAAGCGAATTTTACC GTTCGCCATAACGTTGAAGATGGCAGTGTGCAGCTGGCAGATCAT
TATCAGCAGAATACCCCGATTGGTGATGGTCCGGTGCTGCTGCCGGATAATCATTATCTGAGCACGCAGA
CCGTTCTGTCTAAAGATCCGAACGAAAAAGGCACGCGGGACCACATGGTTCTGCACGAATATGTGAATGC
GGCAGGTATTACGTGGAGCCATCCGCAGTTCGAAAAATAAgtcgaccggctgctaacaaagcccgaaagg
aagctgagttggctgctgccaccgctgagcaataac tagcataacccttggggcctctaaacgggtctt
gaggggttttttg
```

P _{T7} -trigger BT	Linear DNA encoding expression of RNA trigger BT under a P _{T7} Promoter. Additional nucleotides (~30bp) are included in 5' and 3' end as extra protection against nuclease degradation.
-----------------------------	---

P_{T7} Promoter-trigger BT

```
ggaaaaacgccagcaacgcgatcccgcgaaat taatacgactcactataggtcgacttcggaaacgcttat
AGAAAGGAGCAACACCACACAAGCCGGTCATACAGTAATTCAGCTACCGCATACGTTTCAaaaaaaaaac
gccgccttttcggcggcgtttg
```

P _{T7} -switch BT- <i>sfgfp</i>	Relevant part of the plasmid encoding superfolder GFP expression under P _{T7} promoter and toehold switch BT
--	---

P_{T7} Promoter-switch BT-*sfgfp*-TrmB-T7 Terminator

```
taatacgactcactatagggagaGTTACTGTATGACCGGCTTTGTGTGGTGTGCTCCTTGGACTTTAGA
ACAGAGGAGATAAAAGATGAAGGAGCAACACAACCTGGCGGCAGCGCAAAAAGATGAGCAAAGGTGAAGAAC
TGTTTACCGGCGTTGTGCCGATTCTGGTGGAACTGGATGGCGATGTGAACGGTCACAAATTCAGCGTGCG
TGGTGAAGGTGAAGGCGATGCCACGATTGGCAAACCTGACGCTGAAATTTATCTGCACCACCGGCAAACCTG
CCGGTGCCGTGGCCGACGCTGGTGACCACCCTGACCTATGGCGTTCAGTGTTTTAGTCGCTATCCGGATC
ACATGAAACGTACGATTTCTTTAAATCTGCAATGCCGGAAGGCTATGTGCAGGAACGTACGATTAGCTT
TAAAGATGATGGCAAATATAAAACGCGCGCCGTTGTGAAATTTGAAGGCATACCCTGGTGAACCGCATT
GAACTGAAAGGCACGGATTTTAAAGAAGATGGCAATATCCTGGGCCATAAACTGGAATACAACCTTTAATA
GCCATAATGTTTATATTACGGCGGATAAACAGAAAAATGGCATCAAAGCGAATTTTACC GTTCGCCATAA
CGTTGAAGATGGCAGTGTGCAGCTGGCAGATCATTATCAGCAGAATACCCCGATTGGTGATGGTCCGGTG
CTGCTGCCGGATAATCATTATCTGAGCACGCAGACCGTTCTGTCTAAAGATCCGAACGAAAAAGGCACGC
GGGACCACATGGTTCTGCACGAATATGTGAATGCGGCAGGTATTACGTGGAGCCATCCGCAGTTCGAAAA
ATAAaggatctgaagcttgggcccgaacaaaaactcatctcagaagaggatctgaatagcgccgctcgacca
tcatcatcatcattgagtttaaacggtctccagcttggctgTTTTggcggatgagagaagatTTTca
gctgatacagattaaatcagaacgcgagaagcggctctgataaaacagaatttgctggcggcagtagcgc
ggtggtcccacctgaccccatgccgaactcagaagtgaacgcgctagcgcgatggttagtggtgggtct
ccccatgagagtagggaactgccaggcatcaataaaaacgaaaggctcagtcgaaagactgggccttt
cgTTTTatctgttggTTTgtcggtgaactggatcgctcgaccggctgctaacaaagcccgaaaggaagctga
gttggctgctgccaccgctgagcaataac tagcataacccttggggcctctaaacgggtcttgaggggt
TTTTTg
```

P _{T7} -trigger S1	Linear DNA encoding expression of RNA trigger S1 under a P _{T7} Promoter. Additional nucleotides (~30bp) are included in 5' and 3' end as extra protection against nuclease degradation.
-----------------------------	---

P_{T7} Promoter-trigger S1

ggaaaaaacgccagcaacgcgatcccgcgaaat**taatacgcactcactatagg**ATAAATCGCCATTTCGTTGA
 CTACTTCTTATCTGGATTTAATGTGCGATAGTGGAACTCACTGACGCAGTCTGTGGCAAGAGCGATGTT
 ACGGTTTaaaaaaacgccgcctttcggcgccgctttg

P _{T7} -switch S1- <i>sfgfp</i>	Relevant part of the plasmid encoding superfolder GFP expression under P _{T7} promoter and toehold switch S1
--	---

P_{T7} Promoter-switch S1-*sfgfp*-TrnB-T7 Terminator

taatacgcactcactatagggagaGGGCGTCAGTGAGGTTCCACTATGCGACATTAATCCAGGGACTTTA
 GAACAGAGGAGATAAAGATGCTGGATTTAATTAACCTGGCGGCAGCGCAAAAGATGAGCAAAGGTGAAGA
 ACTGTTTACCGGCGTTGTGCGGATTCTGGTGGAACTGGATGGCGATGTGAACGGTCACAAATTCAGCGTG
 CGTGGTGAAGGTGAAGGCGATGCCACGATTGGCAAACCTGACGCTGAAATTTATCTGCACCACCGGCAAC
 TGCCGGTGGCGTGGCCGACGCTGGTGAACCCCTGACCTATGGCGTTCAGTGTTTAGTCGCTATCCGGA
 TCACATGAAACGTCACGATTTCTTTAAATCTGCAATGCCGGAAGGCTATGTGCAGGAACGTACGATTAGC
 TTTAAAGATGATGGCAAATATAAAACGCGCCGCTGTGAAATTTGAAGGCGATACCCTGGTGAACCGCA
 TTGAACGAAAGGCACGGATTTTAAAGAAGATGGCAATATCCTGGGCCATAAACTGGAATACAACCTTAA
 TAGCCATAATGTTTATATTACGGCGATAAACAGAAAAATGGCATCAAAGCGAATTTTACCGTTCGCCAT
 AACGTTGAAGATGGCAGTGTGCAGCTGGCAGATCATTATCAGCAGAATACCCCGATTGGTGATGGTCCGG
 TGCTGCTGCCGATAATCATTATCTGAGCAGCAGACCGTTCTGTCTAAAGATCCGAACGAAAAAGGCAC
 GCGGGACCACATGGTTCTGCACGAATATGTGAATGCGGCAGGTATTACGTGGAGCCATCCGCAGTTCGAA
 AAATAAaggatctgaagcctgggcccgaacaaaaactcatctcagaagaggatctgaatagcgccgctcgac
 catcatcatcatcatcattgagtttaaacggtctccagcctggctgTTTTGGCGGATGAGAGAAGATTTT
 cagcctgatacagattaaatcagaacgcagaagcggctctgataaaacagaatttgctggcgccagtagc
 gcggtggtcccacctgaccccatgccgaactcagaagtgaacgcctagcgcgatggttagtggtgggt
 ctccccatgcgagagttagggaactgccaggcatcaataaaaacgaaaggctcagtcgaaagactgggct
 ttcgTTTTatctgTTgTTgTcggtgaactggatcgctcgaccggctgctaacaagcccgaaggaagct
 gagttggctgctgccaccgctgagcaataac**tagcataacccttggggcctctaaccgggtcttgagggg**
 gTTTTTg

P _{T7} -trigger S2	Linear DNA encoding expression of RNA trigger S2 under a P _{T7} Promoter. Additional nucleotides (~30bp) are included in 5' and 3' end as extra protection against nuclease degradation.
-----------------------------	---

P_{T7} Promoter-trigger S2

ggaaaaaacgccagcaacgcgatcccgcgaaat**taatacgcactcactatagg**GTATCCTATTCGCGGGAGT
 TTACGATAGACTTTTCGACCCAACAAAGTTATGTCTCTTCGTTAAATAGTATACGGACAGAGATATCGAC
 CCCTCTTGAACATATATCaaaaaaacgccgcctttcggcgccgctttg

P _{T7} -switch S2- <i>sfgfp</i>	Relevant part of the plasmid encoding superfolder GFP expression under P _{T7} promoter and toehold switch S2
--	---

P_{T7} Promoter-switch S2-*sfgfp*-TrnB-T7 Terminator

taatacgcactcactatagggagaGGGATACTATTTAACGAAGAGACATAACTTTGTTGGGTCCGACTTTA
 GAACAGAGGAGATAAAGATGGACCCAACAAAGATGAGCAAAGGTGAAGAAGTGTTCACCGGCGTTGTGCC
 GATTCTGGTGGAACTGGATGGCGATGTGAACGGTCACAAATTCAGCGTGCCTGGTGAAGGTGAAGGCGAT
 GCCACGATTGGCAAACCTGACGCTGAAATTTATCTGCACCACCGGCAAACTGCCGGTGGCGTGGCCGACGC
 TGGTGACCACCCTGACCTATGGCGTTCAGTGTTTTAGTCGCTATCCGGATCACATGAAACGTCACGATTT
 CTTTAAATCTGCAATGCCGGAAGGCTATGTGCAGGAACGTACGATTAGCTTTAAAGATGATGGCAAATAT
 AAAACGCGCGCCGTTGTGAAATTTGAAGGCGATACCCTGGTGAACCGCATTGAACTGAAAGGCACGGATT

TTAAGAAGATGGCAATATCCTGGGCCATAAACTGGAATACAACCTTAATAGCCATAATGTTTATATTAC
GGCGGATAAACAGAAAAATGGCATCAAAGCGAATTTTACCGTTCGCCATAACGTTGAAGATGGCAGTGTG
CAGCTGGCAGATCATTATCAGCAGAATACCCCGATTGGTGTGGTCCGGTGCTGCTGCCGGATAATCATT
ATCTGAGCACGCAGACCGTTCTGTCTAAAGATCCGAACGAAAAAGGCACGCGGGACCACATGGTTCTGCA
CGAATATGTGAATGCGGCAGGTATTACGTGGAGCCATCCGCAGTTCGAAAAATAAaggatctgaagcttgg
gcccgaacaaaaaactcatctcagaagaggatctgaatagcgcgctcgaccatcatcatcatcattga
gtttaaaccggtctccagcttggctgttttggcggatgagagaagattttcagcctgatacagattaaatc
agaacgcagaagcggctctgataaaacagaatttgccctggcggcagtagcgcgggtgggtcccacctgacccc
atgcccgaactcagaagtgaacgcgctagcgcgcatggtagtgtggggctctccccatgagagagtaggga
actgcccaggcatcaaataaaacgaaaggctcagtcgaaagactgggcctttcgttttatctgttgttgg
cggatgaactggatcgctgacccggctgctaacaagcccgaaggaagctgagttggctgctgccaccgct
gagcaataac tagcataacccttggggcctctaaacgggtcttgaggggttttttg

<i>P_{T7}-lacZ</i>	Relevant part of the plasmid encoding β-galactosidase (LacZ) expression under P _{T7} promoter
P_{T7} Promoter- Stability Hairpin-StrongRBS-<i>lacZ</i>-T7 Terminator	
<p>taatacgactcactatagggagaccacaacgggtttccctctagaaataattttgtttaactttaagaagg agataatacatatgACCATGATTACGGATTCACTGGCCGTCGTTTTACAACGTCGTGACTGGGAAAACCCCT GGCGTTACCCAACCTTAATCGCCTTGAGCACATCCCCCTTCGCCAGCTGGCGTAATAGCGAAGAGGCC GCACCGATCGCCCTTCCCAACAGTTGCGCAGCCTGAATGGCGAATGGCGCTTTGCCTGGTTTTCCGGCACC AGAAGCGGTGCCGAAAGCTGGCTGGAGTGCATCTTCTGAGGCCGATACTGTGCTCGTCCCCTCAAAC TGGCAGATGCACGGTTACGATGCGCCCATCTACACCAACGTGACCTATCCCATTACGGTCAATCCGCCGT TTGTTCCACGGAGAATCCGACGGGTGTTACTCGCTCACATTTAATGTTGATGAAAGCTGGCTACAGGA AGGCCAGACCGCAATTTTTTGTATGGCGTTAACTCGGCGTTTCATCTGTGGTGCAACGGGCGCTGGGTC GGTTACGGCCAGGACAGTCGTTTGGCGTCTGAATTTGACCTGAGCGCATTTTTACGCGCGGAGAAAAAC GCCTCGCGGTGATGGTGTGCTGCGCTGGAGTGCAGGCAGTTATCTGGAAGATCAGGATATGTGGCGGATGAG CGGCATTTTTCCGTGACGTCTCGTTGCTGCATAAACCGACTACACAAATCAGCGATTTCCATGTTGCCACT CGCTTTAATGATGATTTTCAGCCGCGCTGTAAGTTCAGATGTGCGGCGAGTTGCGTGACT ACCTACGGGTAACAGTTTTCTTTATGGCAGGGTGAAACGCAGGTGCGCCAGCGGCACCGCGCTTTTCGGCGG TGAAATTATCGATGAGCGTGGTGGTTATGCCGATCGCGTCACACTACGTCTGAACGTGAAAACCCGAAA CTGTGGAGCGCCGAAATCCCGAATCTCTATCGTGCGGTGGTTGAACTGCACACCGCCGACGGCAGCGTGA TTGAAGCAGAAGCCTGCGATGTGCGTTTTCCGCGAGGTGCGGATTGAAAATGGTCTGCTGCTGTAACGG CAAGCCGTTGCTGATTCGAGGCGTTAACCGTCACGAGCATCATCCTCTGCATGGTCAGGTCATGGATGAG CAGACGATGGTGCAGGATATCCTGCTGATGAAGCAGAACAACCTTAACGCCGTGCGCTGTTCCGATTATC CGAACCATCCGCTGTGGTACACGCTGTGCGACCGCTACGGCCTGTATGTGGTGGATGAAGCCAATATTGA AACCACGGCATGGTGCCAATGAATCGTCTGACCGATGATCCGCGCTGGCTACCGGCATGAGCGAACGC GTAACCGCAATGGTGCAGCGCGATCGTAATACCCGAGTGTGATCATCTGGTCGCTGGGGAATGAATCAG GCCACGGCGCTAATCACGACGCGCTGTATCGCTGGATCAAATCTGTGATCCTTCCCGCCGGTGCAGTA TGAAGGCGGCGGAGCCGACACCACGGCCACCGATATTATTTGCCCGATGTACGCGCGCGTGGATGAAGAC CAGCCCTTCCC GGCTGTGCCGAAATGGTCCATCAAAAAATGGCTTTCGCTACCTGGAGAGACCGCGCCCGC TGATCCTTTGCGAATACGCCACGCGATGGGTAACAGTCTTGGCGGTTTCGCTAAATACTGGCAGGCGTT TCGTGATATCCCCGTTTACAGGGCGGCTTCGTCTGGGACTGGGTGGATCAGTCGCTGATTAATATGAT GAAAACGGCAACCCGTGGTGGCTTACGGCGGTGATTTGGCGATACGCCGAACGATCGCCAGTCTGTGA TGAACGGTCTGGTCTTTGCGGACCGCACCGCATCCAGCGCTGACGGAAGCAAAACACCGCAGCAGTT TTTCCAGTTCGGTTTTATCCGGGCAAACCATCGAAGTGACCAGCGAATACTGTTCCGTGATAGCGATAAC GAGCTCCTGCACTGGATGGTGGCGCTGGATGGTAAGCCGCTGGCAAGCGGTGAAGTGCCTCTGGATGTCG CTCCACAAGGTAAACAGTTGATTGAACTGCCTGAACTACCGCAGCCGAGAGCGCCGGGCAACTCTGGCT CACAGTACGCGTAGTGCAACCGAACGCGACCGCATGGTGCAGAAGCCGACACATCAGCGCCTGGCAGCAG TGGCGTCTGGCTGAAAACCTCAGCGTGACACTCCCCGCCGCGTCCCACGCCATCCCGCATCTGACCACCA GCGAAATGGATTTTTGCATCGAGCTGGGTAATAAGCGTTGGCAATTTAACGCCAGTCAGGCTTTCTTTTC ACAGATGTGGATTGGCGATAAAAAACAACCTGCTGACGCCGCTGCGCGATCAGTTCACCCGTGCACCGCTG GATAACGACATTGGCGTAAGTGAAGCGACCCGCATTGACCCTAACGCCTGGGTGCAACGCTGGAAGGCGG CGGGCCATTACCAGGCCGAAGCAGCGTTGTTGCAGTGCACGGCAGATACTTGTGATGCGGTGCTGAT TACGACCGCTCACGCGTGGCAGCATCAGGGGAAAACCTTATTTATCAGCCGAAAACCTACCGGATTGAT GGTAGTGGTCAAATGGCGATTACCGTTGATGTTGAAGTGGCGAGCGATAACCCGCATCCGGCGCGGATTG</p>	

```
GCCTGAACTGCCAGCTGGCGCAGGTAGCAGAGCGGGTAAACTGGCTCGGATTAGGGCCGCAAGAAAACCTA
TCCCGACCGCCTTACTGCCGCCTGTTTTGACCGCTGGGATCTGCCATTGTCAGACATGTATACCCCGTAC
GTCTTCCCGAGCGAAAACGGTCTGCGCTGCGGGACGCGCAATTGAATTATGGCCACACCAGTGGCGCG
GCGACTTCCAGTTCAACATCAGCCGCTACAGTCAACAGCAACTGATGGAAACCAGCCATCGCCATCTGCT
GCACGCGGAAGAAGGCACATGGCTGAATATCGACGGTTTTCCATATGGGGATTGGTGGCGACGACTCCTGG
AGCCCCTCAGTATCGGCGGAATTCCAGCTGAGCGCCGGTTCGCTACCATTACCAGTTGGTCTGGTGTCAA
AATAagtcgaccggctgctaacaagcccgaaggaagctgagttggctgctgccaccgctgagcaataa
ctagcataacccttggggcctctaaacgggtcttgaggggtttttt
```

χ DNA	DNA oligo containing 6 χ sites to stall endonuclease degradation on linear DNA templates.
FW:	TCACTTCACTGCTGGTGGCCACTGCTGGTGGCCACTGCTGGTGGCCACTGCTGGTGGCCACTGCTGGTGG CCACTGCTGGTGGCCA
RV:	TGGCCACCAGCAGTGGCCACCAGCAGTGGCCACCAGCAGTGGCCACCAGCAGTGGCCACCAGCAGTGGCC ACCAGCAGTGAAGTGA

P _{T7} -Null	Linear DNA encoding expression of random RNA sequences under a P _{T7} Promoter. Additional nucleotides (>20bp) are included in 5' and 3' end as extra protection against nuclease degradation.
P_{T7} Promoter-Null	aacgccagcaacgcgatcccgcgaaat taatac gactcactatagggaga GTCGACCGGCTGCTAACAAA GCCCGAAAGGAAGCTGAGTTGGCTGCTGCCACCGCTGAGCAATAACT tagcataacccttggggcctct a aacgggtcttgaggggtttttt gttggctgaaagccaattctga

P _{T7} -trigger EC	Linear DNA encoding expression of RNA trigger EC under a P _{T7} Promoter. Additional nucleotides (~20bp) are included in 5' and 3' end as extra protection against nuclease degradation.
P_{T7} Promoter-trigger EC	aacgccagcaacgcgatcccgcgaaat taatac gactcactatagggaga AAGACGGATATCTATTTTCGT TTCCACGTTTGAACCG tagcataacccttggggcctctaaacgggtcttgaggggttttttgttggctg aaagccaattctga

A.3 Protocell and CFE Reaction Conditions

Table 2. Description of lysate, plasmid concentrations, and reaction additives present in protocell sensors or CFE reactions in each figure in CHAPTER 2.

Figures	Detecting	Lysate Preparation	Plasmids	Reaction Additives
Figure 2-3 Figure 2-4		Uninduced T7 RNAP Batch U2	1.875 nM P _{T7} -GFP	
Figure 2-5	IPTG	Uninduced T7 RNAP Batch U2	3.33 nM P _{T7} -LacI 1 nM P _{T7} lacO-GFP	
Figure 2-5	Arabinose	Uninduced T7 RNAP Batch U2	9.5 nM AraC-P _{BAD} -GFP	
Figure 2-6	RNA B Trigger	Induced T7 RNAP Batch I2	7 nM P _{T7} -switchB-GFP	0.5 v/v% Rnase Inhibitor Murine in the bulk phase
Figure 2-6	RNA H Trigger	Induced T7 RNAP Batch I2	7 nM P _{T7} -switchH-GFP	0.5 v/v% Rnase Inhibitor Murine in the bulk phase
Figure 2-6 Figure 2-7	Linear DNA B Trigger	Induced T7 RNAP Batch I2	6 nM P _{T7} -switchB-GFP	2 μM χDNA in protocell
Figure 2-6 Figure 2-7	Linear DNA H Trigger	Induced T7 RNAP Batch I2	6 nM P _{T7} -switchH-GFP	2 μM χDNA in protocell
Figure 2-8	Zinc	Uninduced T7 RNAP Batch U1	0.25 nM P _{T7} -ZntR 2.5 nM P _{zntA} -GFP	
Figure 2-8	Vitamin B ₁₂	Uninduced T7 RNAP Batch U1	2.5 nM P _{T7} -EutR 10 nM P _{eutS} -GFP	
Figure 2-9	Linear DNA <i>B. theta</i> Trigger	Induced T7 RNAP Batch I1	5 nM P _{T7} - <i>B. theta</i> switch-GFP	2 μM χDNA in protocell 0.5 v/v% Rnase Inhibitor Murine in the bulk phase

Figure 2-9	Linear DNA Stx1 Trigger	Induced T7 RNAP Batch I1	4 nM P _{T7} -Stx1-GFP	10 μM GamS in protocell 0.5 v/v% Rnase Inhibitor Murine in the bulk phase
Figure 2-9	Linear DNA Stx2 Trigger	Induced T7 RNAP Batch I1	5 nM P _{T7} -Stx2-GFP	2 μM χDNA in protocell 0.5 v/v% Rnase Inhibitor Murine in the bulk phase
Figure 2-10	Zinc	Uninduced T7 RNAP Batch U3	0.15 nM P _{T7} -ZntR 2 nM P _{ZntA} -GFP	1.5 v/v% Rnase Inhibitor Murine in the bulk phase
Figure 2-10	Vitamin B ₁₂	Uninduced T7 RNAP Batch U3	1.5 nM P _{T7} -EutR 7.5 nM P _{EutS} -GFP	1.5 v/v% Rnase Inhibitor Murine in the bulk phase
Figure 2-10	RNA Stx1 Trigger	Induced T7 RNAP Batch I1	4 nM P _{T7} -Stx1 switch-GFP	1.5 v/v% Rnase Inhibitor Murine in the bulk phase
Figure 2-10	Linear DNA Stx2 Trigger	Induced T7 RNAP Batch I1	2.5 nM P _{T7} -Stx2 switch-GFP	1.5 v/v% Rnase Inhibitor Murine in the bulk phase 2 μM χDNA in protocell
Figure 2-10	Zinc	Uninduced T7 RNAP Batch U3	0.25 nM P _{T7} -ZntR 5 nM P _{ZntA} -GFP	1.5 v/v% Rnase Inhibitor Murine in the bulk phase
Figure 2-10	Vitamin B ₁₂	Uninduced T7 RNAP Batch U3	2.5 nM P _{T7} -EutR 10 nM P _{EutS} -GFP	1.5 v/v% Rnase Inhibitor Murine in the bulk phase
Figure 2-10	RNA Stx1 Trigger	Induced T7 RNAP Batch I1	7.5 nM P _{T7} -Stx1 switch-GFP	1.5 v/v% Rnase Inhibitor Murine in the bulk phase
Figure 2-10	Linear DNA Stx2 Trigger	Induced T7 RNAP Batch I1	7.5 nM P _{T7} -Stx2 switch-GFP	1.5 v/v% Rnase Inhibitor Murine in the bulk phase 2 μM χDNA in protocell
Figure 2-11	Cleave CPRG	Uninduced T7 RNAP Batch U1	2 nM P _{T7} -LacZ	0.6 mg/mL CPRG in the bulk phase
Figure 2-11	Cleave X-gal	Uninduced T7 RNAP Batch U1	2 nM P _{T7} -LacZ	0.2 mg/mL X-gal in the bulk phase

Figure 2-12	Linear DNA <i>B. theta</i> Trigger	Induced T7 RNAP Batch I1	1.5 nM P _{T7} - <i>B. theta</i> switch-LacZ	0.2 mg/mL X- gal in the bulk phase 2 μM χDNA in protocell
Figure 2-12	Linear DNA Stx1 Trigger	Induced T7 RNAP Batch I1	1.33 nM P _{T7} -Stx1- LacZ	0.2 mg/mL X- gal in the bulk phase 2 μM χDNA in protocell
Figure 2-12	Linear DNA Stx2 Trigger	Induced T7 RNAP Batch I1	1.33 nM P _{T7} -Stx2- LacZ	0.2 mg/mL X- gal in the bulk phase 2 μM χDNA in protocell
Figure 2-12	Linear DNA <i>B.</i> <i>theta</i> Trigger	Induced T7 RNAP Batch I1	4.5 nM P _{T7} - <i>B. theta</i> switch-LacZ	0.2 mg/mL X- gal in the bulk phase 2 μM χDNA in protocell
Figure 2-12	Linear DNA Stx1 Trigger	Induced T7 RNAP Batch I1	2.7 nM P _{T7} -Stx1- LacZ	0.2 mg/mL X- gal in the bulk phase 2 μM χDNA in protocell
Figure 2-12	Linear DNA Stx2 Trigger	Induced T7 RNAP Batch I1	3 nM P _{T7} -Stx2-LacZ	0.2 mg/mL X- gal in the bulk phase 2 μM χDNA in protocell
Figure 12	Plasmid <i>B. theta</i> Trigger	Induced T7 RNAP Batch I2	5 nM P _{T7} - <i>B. theta</i> trigger 2.5 nM P _{T7} - <i>B. theta</i> switch-GFP	
Figure 12	Plasmid Stx1 Trigger	Induced T7 RNAP Batch I2	5 nM P _{T7} -Stx1 trigger 2.5 nM P _{T7} -Stx1 switch-GFP	
Figure 12	Plasmid Stx2 Trigger	Induced T7 RNAP Batch I2	5 nM P _{T7} -Stx2 trigger 2.5 nM P _{T7} -Stx2 switch-GFP	

A.4 Primers for Trigger DNA Amplification

Table 3. Primers used for trigger DNA amplification in CHAPTER 2. Lowercase, unlabeled sequences are protective regions to decrease endonuclease degradation. Highlighted sequences indicate the T7 promoter, and uppercase sequences are primer annealing regions. Target-specific primers were designed to bind to >19 base pairs before and after the actual trigger sequence to prevent unintended primer activation of switches. The specificity of the developed switches was also validated on the genomic DNA of STEC O157: H7, *B. thetaiotaomicron*, and common laboratory *E. coli* strains DH10 β and BL21 Star (DE3)

Amplifying	Primer Sequence
B or H	<p>Fwd: aacgccagcaacgcgatcccgcgaaat TAATACGACTCACTATAGGGAGA</p> <p>Rev: taatcagaattggctttcagcaaaaAAACCCCTCAAGACCCGTT</p> <p>Template: T7-trigger B or T7-trigger H in A.2 Sequence Information</p>
<i>B. theta</i>	<p>Fwd: ggaaaaacgccagcaacgcgatcccgcgaaat taatacgactcactataggCCGAC TTCGGAACGCTTATAGA</p> <p>Rev: caaacgccgccgaaaggcggcggtttttttTGAACGTATGCGGTAGCTGAA</p> <p>Genomic Target: hypothetical protein SAMN029103 22_01913 ATGCATGCATACATTATCCAACAAC TAACAAGAATTATATTGTTTATCACTATCGG TTTGCCTATAGGACTAAAAAGTTTTGCCCAAGAAACAAAACGTTTCTATATGGAAC TGGACACTCCCCGCAATGGAGCCAAAGCAGGACAAGAGCTTGAATTAATAACATC AGCACAGCCGATTTTCGATTCTGTATCTCCACCCGACTTCGGAACGCTTATAGAAAC AGTTGAAGGAGCAACACCACACAAAGCCGGTCATACAGTAAAAACGGCATATTGA CAGATATCTACGAGCAGGGATTACGCTACCGCATACTTTCAAGAAGCCAGGAAAC ACCAAAC TACCTCTGGCATCCATCAAGGCAAACGAAAGGAATACGAAACACCTCT GACCAGTGTATGGGTACATCCGGTCGATACCAATATCGACAGTGTAAAATGCAGCA TTCAGCTGGAGGATTCTTATCGCAAAGGAGTTTTCACTGCCATCGGGATCTGTCTC TTAATCGCCTGGTTATTGATCCGCTTATCGTTTCAGAAACAAAAAATAAAGAGAC AGGATAA</p>
Stx1	<p>Fwd: ggaaaaacgccagcaacgcgatcccgcgaaat taatacgactcactataggATAAA TCGCCATTCGTTGACTACT</p> <p>Rev: caaacgccgccgaaaggcggcggtttttttAAACCGTAACATCGCTCTTGCCA</p> <p>Genomic Target: Shiga Toxin 1 Accession #: BA000007. Region: 2924904...2925851. ATGAAAATAATTATTTTTAGAGTGCTAACTTTTTTCTTTGTTATCTTTTCAGTTAA TGTGGTTGCGAAGGAATTTACCTTAGACTTCTCGACTGCAAAGACGTATGTAGATT</p>

	<p>CGCTGAATGTCATTTCGCTCTGCAATAGGTACTCCATTACAGACTATTTTCATCAGGA GGTACGTCTTTACTGATGATTGATAGTGGCACAGGGGATAATTTGTTTGCAGTTGA TGTCAGAGGGATAGATCCAGAGGAAGGGCGGTTTAATAATCTACGGCTTATTGTTG AACGAAATAATTTATATGTGACAGGATTTGTTAACAGGACAAATAATGTTTTTTAT CGCTTTGCTGATTTTTTACATGTTACCTTTCCAGGTACAACAGCGGTTACATTGTC TGGTGACAGTAGCTATAACCAGTTACAGCGTGTTCAGGGATCAGTCGTACGGGGA TGCAGATAAATCGCCATTTCGTTGACTACTTCTTATCTGGATTTAATGTGCGATAGT GGAACCTCACTGACGCAGTCTGTGGCAAGAGCGATGTTACGGTTTGTACTGTGAC AGCTGAAGCTTTACGTTTTTCGGCAAATACAGAGGGGATTTTCGTACAACACTGGATG ATCTCAGTGGGCGTTCCTATGTAATGACTGCTGAAGATGTTGATCTTACATTGAAC TGGGGAAGGTTGAGTAGTGTCTGCCTGATTATCATGGACAAGACTCTGTTCTGCTGT AGGAAGAATTTCTTTTGGGAAGCATTAAATGCAATTTCTGGGAAGCGTGGCATTAAATAC TGAATTGTCATCATCATGCATCGCGAGTTGCCAGAATGGCATCTGATGAGTTTCCT TCTATGTGTCCGGCAGATGGAAGAGTCCGTGGGATTACGCACAATAAAATATTGTG GGATTCATCCACTCTGGGGCAATTCTGATGCGCAGAACTATTAGCAGTTG</p>
<p>Stx2</p>	<p>Fwd: ggaaaaacgccagcaacgcgatcccgcgaaattaatacgcactcactataggGTATC CTATTCCTCCGGGAGTTTACGATAGACTTTTC</p> <p>Rev: caaacgcgcgcaagggcgcgcttttttttGATATATGTTCAAGAGGGGTCGATAT CTCTGTCCG</p> <p>Genomic Target: Shiga Toxin 2 Accession #: BA000007. Region: 1267107...1268066. ATGAAGTGTATATTATTTAAATGGGTACTGTGCCTGTTACTGGGTTTTTCTTCGGT ATCCTATTCCCAGGAGTTTACGATAGACTTTTCGACCCAACAAAGTTATGTCTCTT CGTTAAATAGTATACGGACAGAGATATCGACCCCTCTTGAACATATATCTCAGGGG ACCACATCGGTGTCTGTTATTAACACACCCACCAGGGCAGTTATTTTGTGTTGGA TATACGAGGGCTTGATGTCTATCAGGCGCGTTTTGACCATCTTCGTCTGATTATTG AGCAAAATAATTTATATGTGGCCGGGTTTCGTTAATACGGCAACAAATACTTTCTAC CGTTTTTTCAGATTTTACACATATATCAGTGCCCGGTGTGACAACGGTTTCCATGAC AACGGACAGCAGTTATAACACTCTGCAACGTGTGCGAGCGCTGGAACGTTCCGGAA TGCAAATCAGTCGTCCTCACTCACTGGTTTTCATCATATCTGGCGTTAATGGAGTTTCA GGTAATACAATGACCAGAGATGCATCCAGAGCAGTTCTGCGTTTTTGTCACTGTCAC AGCAGAAGCCTTACGCTTTCAGGCAGATACAGAGAGAATTTTCGTAGGCAGTGTCTG AAACTGCTCCTGTGTATACGATGACGCCGGGAGACGTGGACCTCACTCTGAACTGG GGGCGAATCAGCAATGTGCTTCCGGAGTATCGGGGAGAGGATGGTGTGAGAGTGGG GAGAATATCCTTTAATAATATATCAGCGATACTGGGGACTGTGGCCGTTATACTGA ATTGCCATCATCAGGGGGCGGTTCTGTTTCGCGCCGTGAATGAAGAGAGTCAACCA GAATGTCAGATAACTGGCGACAGGCCGTTATAAAAATAAACAATACATTATGGGA AAGTAATACAGCTGCAGCGTTTCTGAACAGAAAGTACAGTTTTTATATACAACGG GTAAATAAAGGAGTTAAGCATGAAGAAGATGTTTATGGCGGTTTTATTTGCATTAG CTTCTGTTAATGCAATGGCGGCGGATTGTGCTAAAGGTAAAATTGAGTTTTTCCAAG TATAATGAGGATGACACATTTACAGTGAAGGTTGACGGGAAAGAATACTGGACCAG TCGCTGGAATCTGCAACCGTTACTGCAAAGTGCTCAGTTGACAGGAATGACTGTCA CAATCAAATCCAGTACCTGTGAATCAGGCTCCGGATTTGCTGAAGTGCAGTTTAAAT AATGACTGA</p>

APPENDIX B. SUPPLEMENTARY INFORMATION FOR CHAPTER 3: POINT-OF-CARE ANALYTE QUANTIFICATION VIA LYSATE-BASED CELL-FREE BIOSENSORS INTERFACED WITH PERSONAL GLUCOSE MONITORS

B.1 Assessment of Batch-to-Batch Variability in Cell-Free Lysates

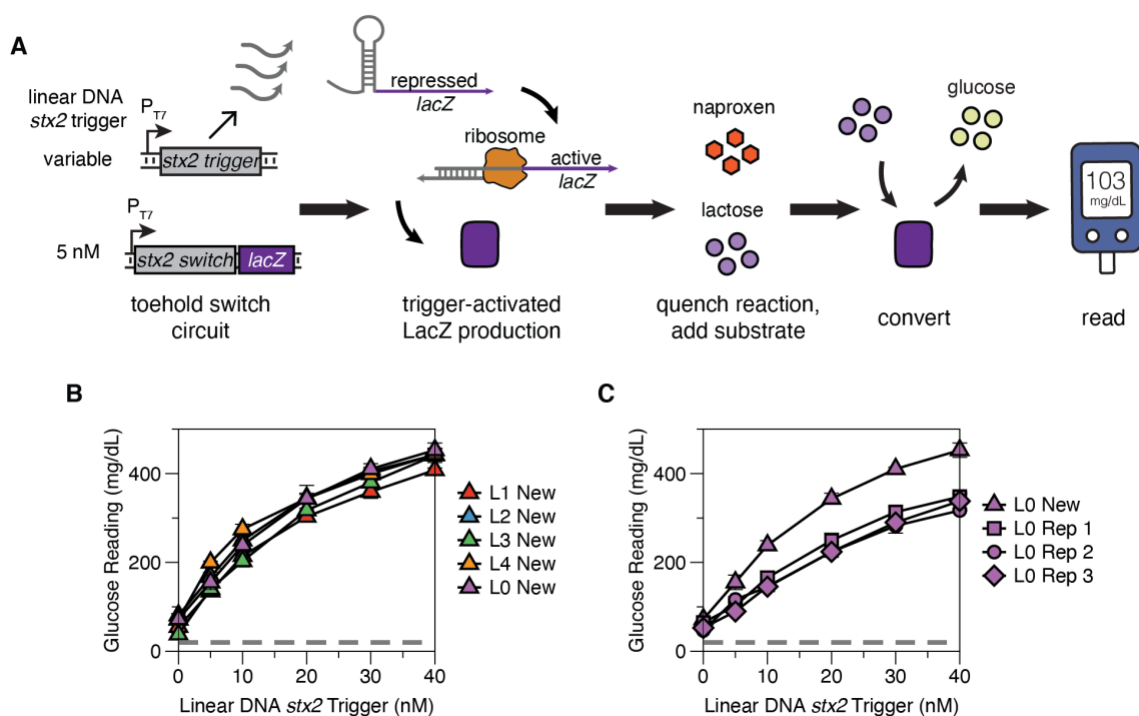


Figure 13 Assessment of lysate batch-to-batch variability in target quantification. (A) Schematic of toehold switch sensor used and process workflow. Linear DNA expressing the *stx2* trigger sequence was added at 0-40 nM to a CFE reaction containing 5 nM of the cognate *stx2* toehold switch. Experiment workflow is the same as Figure 3-6: reactions were incubated at 37 °C for 45 min before being quenched by a mixture of naproxen and lactose and incubated for another 15 min before PGM measurement. (B) Comparison of linear DNA quantification using different batches of lysate prepared using the same protocol. Low inter-lysate variability was observed across five batches of lysates. L0-2 were prepared over the course of 2019, and L3-4 were prepared in spring 2021. The “New” designation in the figure legend indicates a different batch of CFE reagent was used in data collection compared to that used

for the remainder of the figures (L0). Error bars represent the standard deviation of CFE reaction triplicates. Dashed gray line represents PGM's lowest reading threshold, 20 mg/dL. (C) Comparison of linear DNA quantification in the same lysate batch but different reagent batches or aliquots. L0 Rep 1-3 are the same set of data shown in Figure 3-6 using old reagents, while L0 New is the same lysate using a new batch of reagents. While the trend of signal production is preserved, the new batch of reagent generated higher glucose readings for the same amount of linear DNA input. Thus, there is the potential for batch-to-batch variability at multiple levels in these reactions that should be controlled for carefully.

B.2 Sequence Information

Table 4. Description of plasmid parts and DNA sequences used in CHAPTER 3

Name	Construct Description
<i>P_{T7}-lacZ</i>	Relevant part of the plasmid encoding β -galactosidase (LacZ) expression under the T7 promoter
T7 Promoter- Stability Hairpin-StrongRBS-<i>lacZ</i>-T7 Terminator	
<pre> taatacgcactcactatagggagaccacaacgggtttccctctagaaataattttgtttaactttaagaagg agatatacatatgACCATGATTACGGATTCACTGGCCGTCGTTTTACAACGTCGTGACTGGGAAAACCCCT GGCGTTACCCAACCTTAATCGCCTTGCGCACATCCCCCTTCGCCAGCTGGCGTAATAGCGAAGAGGCC GCACCGATCGCCCTTCCCAACAGTTGCGCAGCCTGAATGGCGAATGGCGCTTTGCCTGGTTCCGGCACC AGAAGCGGTGCCGAAAGCTGGCTGGAGTGCATCTTCTGAGGCCGATACTGTGTCGTCCCCTCAAAC TGGCAGATGCACGGTTACGATGCGCCCATCTACACCAACGTGACCTATCCCATTACGGTCAATCCGCCGT TTGTTCCCACGGAGAATCCGACGGGTTGTTACTCGCTCACATTTAATGTTGATGAAAGCTGGCTACAGGA AGCCAGACGCGAATTATTTTTGATGGCGTTAACTCGCGTTTTCATCTGTGGTGAACGGCGCTGGGTC GGTTACGGCCAGGACAGTCGTTTGCCTCTGAATTTGACCTGAGCGCATTTTTACGCGCCGGAGAAAACC GCCTCGCGGTGATGGTGCTGCGCTGGAGTGACGGCAGTTATCTGGAAGATCAGGATATGTGGCGGATGAG CGGCATTTTTCCGTGACGTCTCGTTGCTGCATAAACCGACTACACAAATCAGCGATTTCCATGTTGCCACT CGCTTTAATGATGATTTTCAGCCGCGCTGTACTGGAGGCTGAAGTTCAGATGTGCGGCGAGTTGCGTGACT ACCTACGGGTAACAGTTTCTTTATGGCAGGGTGAAACGCAGGTCGCCAGCGGCACCGCGCTTTCCGGCGG TGAAATTATCGATGAGCGTGGTGGTTATGCCGATCGCGTCACACTACGTCTGAACGTCGAAAACCCGAAA CTGTGGAGCGCCGAAATCCCGAATCTCTATCGTGCCTGGTTGAACTGCACACCGCCGACGGCAGCTGA TTGAAGCAGAAGCCTGCGATGTGCGTTTCCGCGAGGTGCGGATTGAAAATGGTCTGCTGCTGCTGAACGG CAAGCCGTTGCTGATTCGAGGCGTTAACCGTCACGAGCATCATCCTCTGCATGGTCAGGTCATGGATGAG CAGACGATGGTGCAGGATATCCTGCTGATGAAGCAGAACAACCTTAAACGCCGTGCGCTGTTCCGATTATC CGAACCATCCGCTGTGGTACACGCTGTGCGACCGCTACGGCCTGTATGTGGTGGATGAAGCCAATATTGA AACCACGGCATGGTGCCAATGAATCGTCTGACCGATGATCCGCGCTGGCTACCGGGATGAGCGAACGC GTAACGCGAATGGTGCGAGCGGATCGTAATCACCCGAGTGTGATCATCTGGTCGCTGGGGAATGAA TCAGGCCACGGCGCTAATCACGACGCGCTGTATCGCTGGATCAAATCTGTCGATCCTTCCC GCC CGGTGCAGTATGAAGCGGGCGGAGCCGACACCACGGCCACC GATATTTATTTGCCGATGTACGC GCGCGTGGATGAAGACCAGCCCTTCCCGCTGTGCCGAAATGGTCCATCAAAAAATGGCTTTCG CTACCTGGAGAGACGCGCCCGCTGATCCTTTGCGAATACGCCACGCGATGGGTAACAGTCTTG GCGGTTTCGCTAAATACTGGCAGGCGTTTCGTGAGTATCCCCGTTACAGGGCGGCTTCGTCTG GGACTGGGTGGATCAGTCGCTGATTAATATGATGAAAACGGCAACCCGTGGTGGCTTACGGC GGTGATTTTGGCGATACGCCGAACGATCGCCAGTTCTGTATGAACGGTCTGGTCTTTGCCGACC GCACGCCGATCCAGCGCTGACGGAAGCAAAACACCAGCAGCAGTTTTTCCAGTTCGTTTTATC CGGGCAAACCATCGAAGTGACCAGCGAATACCTGTTCCGTCATAGCGATAACGAGCTCCTGCAC TGGATGGTGGCGCTGGATGGTAAGCCGCTGGCAAGCGGTGAAGTGCCCTCTGGATGTCGCTCCAC AAGGTAAACAGTTGATTGAACTGCCTGAACTACCGCAGCCGGAGAGCGCCGGGCAACTCTGGCT CACAGTACGCGTAGTGCAACCGAACGCGACCGCATGGTCAGAAGCCGGACACATCAGCGCCTGG CAGCAGTGGCGTCTGGCTGAAAACCTCAGCGTGACACTCCCCGCCGCTCCACGCCATCCCCG ATCTGACCACCAGCGAAATGGATTTTTGCATCGAGCTGGGTAATAAGCGTTGGCAATTTAACCG CCAGTCAGGCTTCTTTTACAGATGTGGATTGGCGATAAAAAACAACCTGCTGACGCCGCTGCGC GATCAGTTCACCCGTGCACCGCTGGATAACGACATTGGCGTAAGTGAAGCGACCCGCATTGACC CTAACGCCTGGGTGCAACGCTGGAAGGCGGGCGGCCATTACCAGGCCGAAGCAGCGTTGTTGCA GTGCACGGCAGATACACTTGCTGATGCGGTGCTGATTACGACCGCTCACGCGTGGCAGCATCAG GGGAAAACCTTATTTATCAGCCGAAAACCTACCGGATTGATGGTAGTGGTCAAATGGCGATTA CCGTTGATGTTGAAGTGGCGAGCGATAACCGCATCCGGCGCGGATTTGGCCTGAACTGCCAGCT GGCGCAGGTAGCAGAGCGGGTAAACTGGCTCGGATTAGGGCCGCAAGAAAATATCCCAGCCG </pre>	

CTTACTGCCGCCTGTTTTGACCGCTGGGATCTGCCATTGTCAGACATGTATAACCCGTACGTCT
 TCCCGAGCGAAAACGGTCTGCGCTGCGGGACGCGGAATTGAATTATGGCCCACACAGTGGCG
 CGGCGACTTCCAGTTCAACATCAGCCGCTACAGTCAACAGCAACTGATGGAAACCAGCCATCGC
 CATCTGCTGCACGCGGAAGAAGGCACATGGCTGAATATCGACGGTTCCATATGGGGATTGGTG
 GCGACGACTCCTGGAGCCCGTCAGTATCGGCGGAATTCAGCTGAGCGCCGGTTCGCTACCATTA
 CCAGTTGGTCTGGTGTCAAAAAtaagtcgaccggctgctaacaaagcccgaaggaagctgagt
 tggctgctgccaccgctgagcaataac tagcataacccttggggcctctaaacgggtcttgag
 gggttttttg

<i>P_{T7}-zntR</i>	Relevant part of the plasmid encoding ZntR expression under T7 promoter with a strong ribosomal binding site
T7 Promoter-Stability Hairpin-StrongRBS-zntR-T7 Terminator	
<p>taatacgactcactatagggagaccacaacgggtttccctctagaaaataattttgtttaactttaagaagg agatatacatATGTATCGCATTGGTGTAGCTGGCAAAAATGGCGGAAGTAACACCCGACACGATTTCGTTAT TACGAAAAACAGCAGATGATGGAGCATGAAGTGCCTACTGAAGGTGGGTTTCGCTATATACCGAAAGCG ATCTCCAGCGATTGAAATTTATCCGCCATGCCAGACAAGTGGTTCAGTCTGGAGTCGATCCGCGAGTT GCTGTGATCCGCATCGATCCTGAACACCATACTGTGAGGAGTCAAAGGCATTGTGCAGGAAAGATTG CAGGAAGTCAAGCACGGATAGCCGAGTTGCAGAGTATGCAGCGTTTCTTGCAACGCCTTAACGATGCCT GTTGTGGGACTGCTCATAGCAGTGTATTATTGTTTCGATTCTTGAAGCTCTTGAACAAGGGGCGAGTGGCGT TAAGAGTGGTGTGATAAgtcgaccggctgctaacaaagcccgaaggaagctgagttggctgctgcca ccgctgagcaataac tagcataacccttggggcctctaaacgggtcttgaggggtttttt</p>	

<i>P_{ZntA}-lacZ</i>	Relevant part of the plasmid encoding LacZ expression under ZntR regulated P _{ZntA} promoter
P_{ZntA}-Stability Hairpin-StrongRBS-lacZ-T7 Terminator	
<p>CTGTATCTCTGATAAAAACCTTGAAGTCTGGAGTCTGACTCCAGAGTGTATCCTTCGGTTAAIccacaacgggtt tccctctagaaaataattttgtttaactttaagaaggagatatacatatgACCATGATTACGGATTCACTG CCCCTCGTTTTACAACGTCGTGACTGGGAAAACCCCTGGCGTTACCCAACCTAATCGCCTGCAGCACATC GCGTTTTCGCCAGCTGGCGTAATAGCGAAGAGGCCCGCCAGCCGATCGCCCTTCCCAACAGTTGCGCAGCCT GAATGGCGAATGGCGCTTTCCTGGTTTCCGGCACCAGAAGCGGTGCCGAAAGCTGGCTGGAGTGCAT CTTCTGAGGCCGATACTGTCGTGTCCTCCCTCAAACCTGGCAGATGCACGGTTACGATGCGCCCATCTACA CCAACGTGACCTATCCCATTACGGTCAATCCGCCGTTTTGTTCCACGGAGAATCCGACGGGTTGTTACTC GCTCACATTTAATGTTGATGAAAGCTGGCTACAGGAAGGCCAGACGCGAATTATTTTTGATGGCGTTAAC TCGGCGTTTTCATCTGTGGTGAACGGGCGCTGGGTTCGGTTACGGCCAGGACAGTTCGTTTGGCGTCTGAAT TTGACCTGAGCGCATTTTTACGCGCCGGAGAAAACCGCCTCGCGGTGATGGTGTGCGCTGGAGTGCAGG CAGTTATCTGGAAGATCAGGATATGTGGCGGATGAGCGGCATTTTTCCGTGACGTCTCGTTGCTGCATAAA CCGACTACACAAATCAGCGATTTCCATGTTGCCACTCGCTTTAATGATGATTTAGCCGCGCTGTACTGG AGGCTGAAGTTCAGATGTGCGGCGAGTTGCGTACTACCTACGGGTAACAGTTTCTTTATGGCAGGGTGA AACGCAGGTGCCAGCGGCACCGCGCCTTTCCGGCGGTGAAATTATCGATGAGCGTGGTGGTTATGCCGAT CGCGTCACACTACGTCTGAACGTCGAAAACCCGAAACTGTGGAGCGCCGAAATCCCGAATCTCTATCGTG CGGTGGTTGAACTGCACACCCGCCGACGGCAGCTGATTGAAGCAGAAGCCTGCGATGTGGTTTTCCGCGA GGTGCGGATTGAAAATGGTCTGCTGCTGCTGAACGGCAAGCCGTTGCTGATTTCGAGGCGTTAACCGTCA GAGCATCATCTCTGCATGGTCAGGTCATGGATGAGCAGACGATGGTGCAGGATATCCTGCTGATGAAGC AGAACAACTTTAAACCGCGTGCCTGTTTCGATTATCCGAACCATCCGCTGTGGTACACGCTGTGCGACCG CTACGGCCTGTATGTGGTGGATGAAGCCAATATTGAAACCCACGGCATGGTGCATGAATCGTCTGACC CGAGTGTGATCATCTGGTTCGCTGGGAATGAATCAGGCCAGCGCTAATCAGCAGCGCTGTATCGCTG GATCAAATCTGTGATCCTTCCGCGCGGTGCAGTATGAAGGCGGCGGAGCCGACACCACCGGCCACCGAT ATTATTTGCCGATGTACGCGCGCTGGATGAAGACCAGCCCTTCCGCGCTGTGCCGAAATGGTCCATCA AAAAATGGCTTTTCGCTACCTGGAGAGACGCGCCCGCTGATCCTTTGCGAATACGCCACGCGATGGGTAA CAGTCTTGGCGGTTTTCGCTAAATACTGGCAGGCGTTTTCGTCAGTATCCCCGTTTACAGGGCGGCTTCGTC</p>	

TGGGACTGGGTGGATCAGTCGCTGATTAATATGATGAAAACGGCAACCCGTGGTTCGGCTTACGGCGGTG
 ATTTTGGCGATACGCCGAACGATCGCCAGTTCTGTATGAACGGTCTGGTCTTTGCCGACCGCACGCCGCA
 TCCAGCGCTGACGGAAGCAAAACACCAGCAGCAGTTTTTCCAGTTCGGTTTATCCGGGCAAACCATCGAA
 GTGACCAGCGAATACCTGTTCCGTGCATAGCGATAACGAGCTCCTGCACTGGATGGTGGCGCTGGATGGTA
 AGCCGCTGGCAAGCGGTGAAGTGCCTCTGGATGTCGCTCCACAAGGTAAACAGTTGATTGAACTGCCTGA
 ACTACCGCAGCCGGAGAGCGCCGGGCAACTCTGGCTCACAGTACGCGTAGTGCAACCGAACGCGACCGCA
 TGGTCAGAAGCCGGACACATCAGCGCCTGGCAGCAGTGGCGTCTGGCTGAAAACCTCAGCGTGACACTCC
 CCGCCGCTCCCACGCCATCCCGCATCTGACCACCAGCGAAATGGATTTTGCATCGAGCTGGGTAATAA
 GCGTTGGCAATTTAACCGCCAGTCAGGCTTTCTTTACAGATGTGGATTGGCGATAAAAAACAACCTGCTG
 ACGCCGCTGCGCGATCAGTTCACCCGTGCACCGCTGGATAACGACATTGGCGTAAGTGAAGCGACCCGCA
 TTGACCCTAACGCCTGGGTGGAACGCTGGAAGGCGGGGCCATTACCAGGCCGAAGCAGCGCTTGTGCA
 TTGCACGGCAGATAACACTTGTGATGCGGTGCTGATTACGACCGCTCACGCGTGGCAGCATCAGGGGAAA
 ACCTTATTTATCAGCCGAAAACCTACCGGATTGATGGTAGTGGTCAAATGGCGATTACCGTTGATGTTG
 AAGTGGCGAGCGATACACCGCATCCGGCGCGGATTGGCCTGAACTGCCAGCTGGCGCAGGTAGCAGAGCG
 GGTAACCTGGCTCGGATTAGGGCCGCAAGAAAACCTATCCCGACCGCCTTACTGCCGCCTGTTTTGACCGC
 TGGGATCTGCCATTGTCAGACATGTATACCCCGTACGTCTTCCCGAGCGAAAACGGTCTGCGCTGCGGGA
 CGCGCGAATTGAATTATGGCCACACCAGTGGCGCGGCGACTTCCAGTTCAACATCAGCCGCTACAGTCA
 ACAGCAACTGATGGAAACAGCCATCGCCATCTGCTGCACGCGGAAGAAGGCACATGGCTGAATATCGAC
 GGTTTCCATATGGGGATTGGTGGCGACGACTCCTGGAGCCCGTCAGTATCGGCGGAATTCCAGCTGAGCG
 CCGGTCGCTACCATTACCAGTTGGTCTGGTGTCAAAAAatagtcgaccggctgctaacaaagccccgaaag
 gaagctgagttggctgctgccaccgctgagcaataac**tagcataacccttggggcctctaaacgggtct**
tgaggggttttttg

RNA <i>stx1</i> trigger	RNA <i>stx1</i> trigger
<i>stx1</i> trigger	
ATAAATCGCCATTTCGTTGACTACTTCTTATCTGGATTTAATGTTCGCATAGTGGAACCTCACTGACGCAGTCTGTGGCAAGAGCGATGTTACGGTTT	

P _{T7} - <i>stx1</i> switch- <i>lacZ</i>	Relevant part of the plasmid encoding LacZ expression under T7 promoter and <i>stx1</i> toehold switch
T7 Promoter-<i>stx1</i> switch-<i>lacZ</i>-TrnB-T7 Terminator	
<p>taatacagactcactatagggagaGGGCGTCAGTGAGGTTCCACTATGCGACATTAAATCCAGGGACTTTA GAACAGAGAGGAGATAAAGATGCTGGATTTAATTAACCTGGCGGCAGCGCAAAAGatgACCATGATTACGGA TTCACTGGCCGTCGTTTTACAACGTCGTGACTGGGAAAACCTGGCGTTACCCAACCTAATCGCCTTGCA GCACATCCCCCTTTTCGCCAGCTGGCGTAATAGCGAAGAGGCCCGCACCGATCGCCCTTCCCAACAGTTGC GCAGCCTGAATGGCGAATGGCGCTTTGCCTGGTTTTCCGGCACAGAAAGCGGTGCCGGAAGCTGGCTGGA GTGCGATCTTCTGAGGCCGATACTGTCGTCGTCCCCTCAAACCTGGCAGATGCACGGTTACGATGCGCCC ATCTACACCAACGTGACCTATCCATTACGGTCAATCCGCCGTTTGTTCACGGAGAATCCGACGGGTT GTTACTCGCTCACATTTAATGTTGATGAAAGCTGGCTACAGGAAGGCCAGACGCGAATTATTTTTGATGG CGTTAACTCGGCGTTTCATCTGTGGTGCAACGGGCGCTGGGTCCGTTACGGCCAGGACAGTCGTTTGCCG TCTGAATTTGACCTGAGCGCATTTTTACGCGCCGGAGAAAACCGCCTCGCGGTGATGGTGTGCGCTGGA GTGACGGCAGTTATCTGGAAGATCAGGATATGTGGCGGATGAGCGGCATTTTCCGTGACGTCTCGTTGCT GCATAAACCGACTACACAAATCAGCGATTTCCATGTTGCCACTCGTTTAAATGATGATTTACGCCGCGCT GTACTGGAGGCTGAAGTTCAGATGTGCGGGCAGTTGCGTGACTACCTACGGGTAACAGTTTCTTTATGGC AGGGTGAAACGCAGGTGCCAGCGGCACCGCGCCTTTCCGGCGGTGAAATTATCGATGAGCGTGGTGGTTA TGCCGATCGCGTCACACTACGTCTGAACGTCGAAAACCCGAAACTGTGGAGCGCCGAAATCCCGAATCTC TATCGTGCGGTGGTTGAACTGCACACCGCCGACGGCAGCTGATTGAAGCAGAAGCCTGCGATGTCGGTT TCCGCGAGGTGCGGATTGAAAATGGTCTGCTGCTGCTGAACGGCAAGCCGTTGCTGATTGAGGCGTTAA CCGTCACGAGCATCATCCTCTGCATGGTCAGGTCATGGATGAGCAGACGATGGTGCAGGATATCCTGCTG ATGAAGCAGAACAACCTTAAACCGCGTGCCTGTTTCGATTATCCGAACCATCCGCTGTGGTACACGCTGT GCGACCGCTACGGCCTGTATGTGGTGGATGAAGCCAATATTGAAACCCACGGCATGGTCCAATGAATCG</p>	

TCTGACCGATGATCCGCGCTGGCTACCGGCGATGAGCGAACCGGTAACGCGAATGGTGCAGCGCGATCGT
AATCACCCGAGTGTGATCATCTGGTCGCTGGGGAATGAATCAGGCCACGGCGCTAATCACGACGCGCTGT
ATCGCTGGATCAAATCTGTGATCCTTCCCGCCGGTGCAGTATGAAGGCGGCGGAGCCGACACCACGGC
CACCGATATTATTTGCCGATGTACGCGCGCGTGGATGAAGACCAGCCCTTCCCGGCTGTGCCGAAATGG
TCCATCAAAAAATGGCTTTTCGCTACCTGGAGAGACGCGCCCGCTGATCCTTTGCGAATACGCCACGCGA
TGGGTAACAGTCTTGGCGGTTTCGCTAAATACTGGCAGGCGTTCGTGATATCCCCGTTTACAGGGCGG
CTTCGTCTGGGACTGGGTGGATCAGTCGCTGATTAAATATGATGAAAACGGCAACCCGTTGGTTCGGCTTAC
GGCGGTGATTTTGGCGATACGCCGAACGATCGCCAGTTCTGTATGAACGGTCTGGTCTTTGCCGACCGCA
CGCCGCATCCAGCGCTGACGGAAGCAAAACACCAGCAGCAGTTCCTCAGTTCGGTTTATCCGGGCAAAC
CATCGAAGTGACCAGCGAATACCTGTTCCGTCATAGCGATAACGAGCTCCTGCATGGATGGTGGCGCTG
GATGGTAAGCCGCTGGCAAGCGGTGAAGTGCCTCTGGATGTCGCTCCACAAGGTAACAGTGTGATTGAAC
TGCTGAACTACCGCAGCCGGAGAGCGCCGGGCAACTCTGGCTCACAGTACGCGTAGTGCAACCGAACGC
GACCGCATGGTGAAGCCGGACACATCAGCGCCTGGCAGCAGTGGCGTCTGGCTGAAAACCTCAGCGTG
ACACTCCCGCCGCGTCCCACGCCATCCCGCATCTGACCACCAGCGAAATGGATTTTTGCATCGAGCTGG
GTAATAAGCGTTGGCAATTTAACCGCCAGTCAGGCTTTCTTTACAGATGTGGATTGGCGATAAAAAACA
ACTGCTGACGCCGCTGCGCGATCAGTTCACCCGTGCACCGCTGGATAACGACATTGGCGTAAGTGAAGCG
ACCCGCATTGACCCTAACGCCTGGGTGCAACGCTGGAAGGCGGCGGGCCATTACCAGGCCGAAGCAGCGT
TGTTGCAGTGCACGGCAGATACACTTGCTGATGCGGTGCTGATTACGACCGCTCACGCGTGGCAGCATCA
GGGAAAACCTTATTTATCAGCCGAAAACCTACCGGATTGATGGTAGTGGTCAAATGGCGATTACCGTT
GATGTTGAAGTGGCGAGCGATAACCCGCATCCGGCGCGGATTGGCCTGAACTGCCAGCTGGCGCAGGTAG
CAGAGCGGGTAAACTGGCTCGGATTAGGGCCGCAAGAAAACCTATCCCGACCGCCTTACTGCCGCTGTTT
TGACCGCTGGGATCTGCCATTGTGACATGTATACCCCGTACGTCTTCCCGAGCGAAAACGGTCTGCGC
TGCGGGACGCGCAATTGAATTATGGCCACACCAGTGGCGCGGCGACTTCCAGTTCAACATCAGCCGCT
ACAGTCAACAGCAACTGATGGAACCCAGCCATCGCCATCTGCTGCACGCGGAAGAAGGCACATGGCTGAA
TATCGACGGTTTCCATATGGGGATTGGTGGCGACGACTCCTGGAGCCCGTCAGTATCGGCGGAATTCCAG
CTGAGCGCCGGTTCGCTACCATTACCAGTTGGTCTGGTGTCAAAAAataaaggatctgaagcttgggccc
gaacaaaaactcatctcagaagaggatctgaatagcgccgtcgaccatcatcatcatcattgagttt
aaacggctctccagcttggctgttttggcggatgagagaagattttcagcctgatacagattaaatcagaa
cgcagaagcggcttgataaaacagaatttgctggcggcagtagcgcggtggtcccacctgaccccatgc
cgaactcagaagtgaacgcgctagcgcgcatggtagtgtggggctctcccacatgagagataggggaactg
ccagggcatcaataaaaacgaaaggctcagtcgaaagactgggccttttcgcttttatctgtttgtttgtcggt
gaactggatcgctcgaccggctgctaacaagccgaaaggaagctgagttggctgctgccaccgctgagc
aataacc

<p><i>P_{T7}-stx2 trigger</i></p>	<p>Linear DNA encoding expression of RNA <i>stx2</i> trigger under a T7 Promoter. Additional nucleotides (~30bp) were included in 5' and 3' end as extra protection against nuclease degradation.</p>
<p>T7 Promoter-<i>stx2</i> trigger</p> <p>ggaaaaacgccagcaacgcatcccgcgaaat</p> <p>taatacgactcactataggGTATCCTATTCCCGGGAGT TTACGATAGACTTTTCGACCCAACAAAGTTATGTCTCTTCGTTAAATAGTATACGGACAGAGATATCGAC CCCTCTTGAACATATATCaaaaaaaacgcccctttcggcggcgctttg</p>	

<p><i>P_{T7}-stx2 switch-lacZ</i></p>	<p>Relevant part of the plasmid encoding LacZ expression under T7 promoter and <i>stx2</i> toehold switch</p>
<p>T7 Promoter-<i>stx2</i> switch- <i>lacZ</i>- TrnB-T7 Terminator</p> <p>taatacgactcactatagggagaGGGATACTATTTAACGAAGAGACATAACTTTGTTGGGTCCGACTTTA GAACAGAGGAGATAAAGATGGACCCAACAAAGatgACCATGATTACGGATTCACTGGCCGTCGTTTTACA ACGTCGTGACTGGGAAAACCCCTGGCGTTACCCAACCTTAATCGCCTTGACGACATCCCCCTTTCGCCAGC TGGCGTAATAGCGAAGAGGCCCGCACCGATCGCCCTTCCCAACAGTTGCGCAGCCTGAATGGCGAATGGC GCTTTGCCTGGTTTCCGGCACCGAAGCGGTGCCGGAAAGCTGGCTGGAGTGCATCTTCTGAGGCCGA</p>	

TACTGTCGTCGTCCTCCAACTGGCAGATGCACGGTTACGATGCGCCCATCTACACCAACGTGACCTAT
 CCCATTACGGTCAATCCGCCGTTTGTCCACGGAGAATCCGACGGGTTGTTACTCGCTCACATTTAATG
 TTGATGAAAGCTGGCTACAGGAAGGCCAGACGCGAATTATTTTTGATGGCGTTAACTCGGCGTTTCATCT
 GTGGTGCAACGGGCGCTGGGTGCGTTACGGCCAGGACAGTCTGTTTCCGCTCTGAATTTGACCTGAGCGCA
 TTTTACGCGCCGGAGAAAACCGCCTCGCGGTGATGGTGCTGCGCTGGAGTGACGGCAGTTATCTGGAAG
 ATCAGGATATGTGGCGGATGAGCGGCATTTTCCGTGACGTCTCGTTGCTGCATAAACCGACTACACAAAT
 CAGCGATTTCCATGTTGCCACTCGCTTTAATGATGATTTTCAGCCGCGCTGTACTGGAGGCTGAAGTTCAG
 ATGTGCGGCGAGTTGCGTGACTACCTACGGGTAACAGTTTCTTTATGGCAGGGTAAAACGCAGGTCGCCA
 GCGGCACCGCGCCTTTCCGGCGGTGAAATTATCGATGAGCGTGGTGGTTATGCCGATCGCGTCACACTACG
 TCTGAACGTCGAAAACCCGAACTGTGGAGCGCCGAAATCCCGAATCTCTATCGTGCGGTGGTTGAACG
 CACACCTGCTGACGGCAGCTGATTGAAGCAGAAGCCTGCGATGTCGGTTTCCGCGAGGTGCGGATTGAAA
 ATGGTCTGCTGCTGCTGAACGGCAAGCCGTTGCTGATTCGAGGCGTTAACCGTCACGAGCATCCTCT
 GCATGGTCAGGTCATGGATGAGCAGACGATGGTGCAGGATATCCTGCTGATGAAGCAGAACAACCTTAAAC
 GCCGTGCGCTGTTTCGATTATCCGAACCATCCGCTGTGGTACACGCTGTGCGACCGCTACGGCCTGTATG
 TGGTGGATGAAGCCAATATTGAAACCCACGGCATGGTGCCAATGAATCGTCTGACCGATGATCCGCGCTG
 GCTACCGGCGATGAGCGAACCGGTAACCGCAATGGTGCAGCGCGATCGTAATCACCCGAGTGTGATCATC
 TGGTTCGCTGGGGAATGAATCAGGCCACGGCGTAATCACGACGCGCTGTATCGCTGGATCAAATCTGTGCG
 ATCCTTCCC GCCCGGTGCAGTATGAAGGCGGCGAGCCGACACCACGGCCACCGATATTATTTGCCCGAT
 GTACGCGCGCTGGATGAAGACCAGCCCTTCCGGCTGTGCCGAAATGGTCCATCAAAAAATGGCTTTCG
 CTACCTGGAGAGACGCGCCCGCTGATCCTTTGCGAATACGCCACGCGATGGGTAACAGTCTTGGCGGTT
 TCGCTAAATACTGGCAGGCGTTTCGTCAGTATCCCCGTTTACAGGGCGGCTTCGTCTGGGACTGGGTGGA
 TCAGTCGCTGATTAATATGATGAAAACGGCAACCCGTGGTTCGGCTTACGGCGGTGATTTTGGCGATACG
 CCGAACGATCGCCAGTTCTGTATGAACGGTCTGGTCTTTGCCGACCGCACGCCGCATCCAGCGCTGACGG
 AAGCAAAACACCAGCAGCAGTTTTTCCAGTTCGGTTTATCCGGGCAAACCATCGAAGTGACCAGCGAATA
 CCTGTTCCGTCATAGCGATAACGAGCTCCTGCCTGGATGGTGGCGCTGGATGGTAAGCCGCTGGCAAGC
 GGTGAAGTGCCTCTGGATGTGCTCCACAAGGTAACAGTTGATTGAACTGCCTGAACTACCGCAGCCGG
 AGAGCGCCGGGCAACTCTGGCTCACAGTACGCGTAGTGCAACCGAACGCGACCGCATGGTCAGAAGCCGG
 ACACATCAGCGCCTGGCAGCAGTGGCGTCTGGCTGAAAACCTCAGCGTGACACTCCCCGCCGCGTCCCAC
 GCCATCCCGCATCTGACCACCAGCGAAATGGATTTTGCATCGAGCTGGGTAATAAGCGTGGCAATTTA
 ACCGCCAGTCCAGCTTTCTTTACAGATGTGGATTGGCGATAAAAAACAACCTGCTGACCCGCTGCGCGA
 TCAGTTTACCCGTCACCGCTGGATAACGACATTGGCGTAAGTGAAGCGACCCGCATTGACCCTAACGCC
 TGGGTGCAACGCTGGAAGGCGGCGGCCATTACCAGGCCGAAGCAGCGTTGTTGCAAGTGCACGGCAGATA
 CACTTGCTGATGCGGTGCTGATTACGACCGCTCACGCGTGGCAGCATCAGGGGAAAACCTTATTTATCAG
 CCGGAAAACCTACCGGATTGATGGTAGTGGTCAAATGGCGATTACCGTTGATGTTGAAGTGGCGAGCGAT
 ACACCGCATCCGGCGCGGATTGGCCTGAACTGCCAGCTGGCGCAGGTAGCAGAGCGGGTAAACTGGCTCG
 GATTAGGGCCGCAAGAAAATATCCCGACCGCTTACTGCCGCTGTTTTGACCGCTGGGATCTGCCATT
 GTCAGACATGTATAACCCGTACGTCTTCCCGAGCGAAAACGGTCTGCGCTGCGGGACGCGCGAATTGAAT
 TATGGCCACACCAGTGGCGCGGCGACTTCCAGTTCAACATCAGCCGCTACAGTCAACAGCAACTGATGG
 AAACCAGCCATCGCCATCTGCTGCACGCGGAAGAAGGCACATGGCTGAATATCGACGGTTTTCCATATGGG
 GATTGGTGGCGACGACTCCTGGAGCCCGTCAGTATCGGCGGAATTCCAGCTGAGCGCCGGTTCGCTACCAT
 TACCAGTTGGTCTGGTGTCAAAAAtaataaggatctgaagcttgggcccgaacaaaaactcatctcagaa
 gaggatctgaatagcgccgctcgaccatcatcatcatcattgagtttaaaccggtctccagcttggctg
 ttttggcgatgagagaagattttcagcctgatacagattaaatcagaacgcagaagcggctctgataaaa
 cagaatttgctggcgccagtagcgcggtggtcccacctgacctgaccgaactcagaagtgaacgccc
 gttagcgccgatggtagtgtggggtctccccatgagagtagggaaactgccaggcatcaataaaaacgaa
 aggctcagtcgaaagactgggcttttcgttttatctgttggttgtcggtgaactggatcgctcgaccggct
 gctaacaagcccgaaggaagctgagttggctgctgccaccgctgagcaataacc**tagcataaccctt**
ggggcctctaaacgggtcttgaggggttttttg

P _{T7} - <i>gfp</i>	Relevant part of the plasmid encoding super folder GFP expression under T7 promoter with a strong ribosomal binding site
T7 Promoter-Stability Hairpin-StrongRBS-gfp-T7 Terminator	

```

taatacgactcactataggggagaccacaacgggtttccctctagaaataatTTTTGTTTAACTTTAAGAAGG
agatatacatATGAGCAAAGGTGAAGAACTGTTTACCGGCGTTGTGCCGATTCTGGTGGAACTGGATGGC
GATGTGAACGGTCACAAATTCAGCGTGCCTGGTGAAGGTGAAGGCGATGCCACGATTGGCAAACCTGACGC
TGAAATTTATCTGCACCACCGCAAACCTGCCGGTGCCGTGGCCGACGCTGGTGACCACCCTGACCTATGG
CGTTCAGTGTTTTAGTCGCTATCCGGATCACATGAAACGTCACGATTTCTTTAAATCTGCAATGCCGGAA
GGCTATGTGCAGGAACGTACGATTAGCTTTAAAGATGATGGCAAATATAAAACGCGCGCCGTTGTGAAAT
TTGAAGGCGATACCCTGGTGAACCGCATTGAACTGAAAGGCACGGATTTTAAAGAAGATGGCAATATCCT
GGGCCATAAACTGGAATACAACCTTAAATAGCCATAATGTTTATATTACGGCGGATAAACAGAAAAATGGC
ATCAAAGCGAATTTTACCGTTCGCCATAACGTTGAAGATGGCAGTGTGCAGCTGGCAGATCATTATCAGC
AGAATACCCCGATTGGTGTGGTCCGGTGTCTGCTGCCGGATAATCATTATCTGAGCACGCAGACCGTTCT
GTCTAAAGATCCGAACGAAAAAGGCACGCGGGACCACATGGTTCTGCACGAATATGTGAATGCGGCAGGT
ATTACGTGGAGCCATCCGCAGTTCGAAAAATAAgtcgaccggctgctaacaagcccgaaggaagctga
gttggctgctgccaccgctgagcaataactagcataacccttggggcctctaacgggtcttgaggggt
tttttg

```

P _{T7} -MGA	Relevant part of the plasmid encoding malachite green RNA aptamer expression under the T7 promoter
T7 Promoter-MGA-T7 Terminator	
<pre> taatacgactcactatagggGGGATCCCGACTGGCGAGAGCCAGGTAACGAATGGATCGGGTCGGCATGG CATCTCCACCTCCTCGCGGTCCGACCTGGGCATCCGAAGGAGGACGTCGTCCACTCGGATGGCTAAGGGA GAGCTCGGATCCGGCTGCTAACAAAGCCCCGAAAGGAAGCTGAGTTGGCTGCTGCCACCGCTGAGCAATAA CTAGCATAAtagcataacccttggggcctctaacgggtcttgaggggttttttg </pre>	

B.3 CFE Reaction Conditions

Table 5. Description of lysate, plasmid concentrations, and reaction additives present in CFE reactions in each figure in CHAPTER 3

Figures	Detecting	Plasmids/ RNA Transcripts	Reaction Additives
Figure 3-2	N/A	N/A	0-25 mM glucose
Figure 3-2	N/A	0-2 nM P _{T7} - <i>lacZ</i>	
Figure 3-3	N/A	1 nM P _{T7} - <i>gfp</i>	-/+ 10 mM Naproxen sodium
Figure 3-3	N/A	N/A	5% BL21 Star (DE3) lysate containing LacZ 0.6 mg/mL CPRG
Figure 3-3	N/A	5 nM P _{T7} -MGA	1 mM Malachite Green dye -/+ 10 mM Naproxen sodium
Figure 3-3	N/A	0.5 μM <i>gfp</i> RNA	-/+ 10 mM Naproxen sodium
Figure 3-3	N/A	N/A	10 mM Naproxen sodium 0-25 mM glucose
Figure 3-4	Zinc in water	1 nM P _{T7} - <i>zntR</i> 2 nM P _{ZntA} - <i>lacZ</i>	
Figure 3-4	Zinc in serum	2 nM P _{T7} - <i>zntR</i> 8 nM P _{ZntA} - <i>lacZ</i>	1.5 % RNase Inhibitor Murine 25 % Pooled human serum
Figure 3-6	RNA <i>stx1</i> trigger	4 nM P _{T7} - <i>stx1</i> switch- <i>lacZ</i>	0.5 % RNase Inhibitor Murine
Figure 3-6	Linear DNA <i>stx2</i> trigger	5 nM P _{T7} - <i>stx2</i> switch- <i>lacZ</i>	4 μM GamS Protein
Figure 3-5	N/A	N/A	25% Pooled human serum with glucose dosed in
Figure 3-5	N/A	1 nM P _{T7} - <i>gfp</i>	1.5 % RNase Inhibitor Murine 25% Pooled human serum with glucose dosed in
Figure 13	Linear DNA <i>stx2</i> trigger	5 nM P _{T7} - <i>stx2</i> switch- <i>lacZ</i>	4 μM GamS Protein

B.4 Primers for Trigger DNA Amplification

Table 6. Primers for trigger DNA amplification from *E. coli* O157: H7 genomic DNA template in CHAPTER 3. Lowercase, unlabeled sequences are protective regions to decrease endonuclease degradation. Highlighted sequences indicate the T7 promoter, and uppercase sequences are primer annealing regions. Target-specific primers were designed to bind at least 20 base pairs before and after the actual trigger sequence to prevent unintended primer activation of switches.

Amplifying	Primer Sequence
<i>E. coli</i>	<p>Fwd: ggaaaaacgccagcaacgcgatcccgcgaaat taatacgactcactataggCAAAC TACGACGTCATCATTTAGC</p> <p>Rev: caaacgccgccgaaaggcggcggttttttttGTTGACGGTTCAAACGTGGAAA</p> <p>Genomic Target: AraC family transcriptional regulator. Accession # LR881938. Region: 315725...315888. TCAAAC TACGACGTCATCATTTAGCCAGATGTATGAAGAATTTTAAGACGGATATC TATTTTCGTTTCCACGTTTGAACCGTCAACAAAATCGGTTCGATTTGCTCACGGTTGA AACTTTTGCTGGTACGGTATGTGAATATGCTGACATGCCAAAAGAGTGGACA</p>
<i>stx1</i>	<p>Fwd: ggaaaaacgccagcaacgcgatcccgcgaaat taatacgactcactataggATAAA TCGCCATTCGTTGACTACT</p> <p>Rev: caaacgccgccgaaaggcggcggttttttttAAACCGTAACATCGCTCTTGCCA</p> <p>Genomic Target: Shiga Toxin 1. Accession #: BA000007. Region: 2924904...2925851. ATGAAAATAATTATTTTTAGAGTGCTAACTTTTTTCTTTGTTATCTTTTCAGTTAA TGTGGTTGCGAAGGAATTTACCTTAGACTTCTCGACTGCAAAGACGTATGTAGATT CGCTGAATGTCATTTCGCTCTGCAATAGGTAAGTCCATTACAGACTATTTTCATCAGGA GGTACGCTTTTACTGATGATTGATAGTGGCACAGGGGATAATTTGTTTGCAGTTGA TGTCAGAGGGATAGATCCAGAGGAAGGGCGGTTAATAATCTACGGCTTATTGTTG AACGAAATAATTTATATGTGACAGGATTTGTTAACAGGACAAATAATGTTTTTTAT CGCTTTGCTGATTTTTTACATGTTACCTTTCCAGGTACAACAGCGGTTACATTGTC TGGTGACAGTAGCTATAACCAGTTACAGCGTGTTCAGGGATCAGTCGTACGGGGA TGCAGATAAATCGCCATTCGTTGACTACTTCTTATCTGGATTTAATGTGCGCATAGT GGAACCTCACTGACGCAGTCTGTGGCAAGAGCGATGTTACGGTTTTGTTACTGTGAC AGCTGAAGCTTTACGTTTTTCGGCAAATACAGAGGGGATTTTCGTACAACACTGGATG ATCTCAGTGGGCGTCTTATGTAATGACTGCTGAAGATGTTGATCTTACATTGAAC TGGGGAAGGTTGAGTAGTGTCTGCCTGATTATCATGGACAAGACTCTGTTCGTGT AGGAAGAATTTCTTTTGAAGCATTAAATGCAATTCTGGGAAGCGTGGCATTAAATAC TGAATTGTCATCATCATGCATCGCGAGTTGCCAGAATGGCATCTGATGAGTTTCTCT TCTATGTGTCCGGCAGATGGAAGAGTCCGTGGGATTACGCACAATAAAAATTTGTG GGATTCATCCACTCTGGGGGCAATTCTGATGCGCAGAACTATTAGCAGTTG</p>
<i>stx2</i>	<p>Fwd:</p>

ggaaaaacgccagcaacgcgatcccgcgaaat**taatacgcactcactatagg**GTATC
CTATTCCCGGGAGTTTACGATAGACTTTTC

Rev:

caaacgccgccgaaaggcggcggttttttttGATATATGTTCAAGAGGGGTCGATAT
CTCTGTCCG

Genomic Target: Shiga Toxin 2.

Accession #: BA000007. Region: 1267107...1268066.

ATGAAGTGTATATTATTTAAATGGGTACTGTGCCTGTTACTGGGTTTTTCTTCGGT
ATCCTATTCCCGGGAGTTTACGATAGACTTTTCGACCCAACAAAGTTATGTCTCTT
CGTTAAATAGTATACGGACAGAGATATCGACCCCTCTTGAACATATATCTCAGGGG
ACCACATCGGTGTCTGTTATTAACCACACCCACCGGGCAGTTATTTTGCTGTGGA
TATACGAGGGCTTGATGTCTATCAGGCGCGTTTTGACCATCTTCGTCTGATTATTG
AGCAAAATAATTTATATGTGGCCGGTTTCGTTAATACGGCAACAAATACTTTCTAC
CGTTTTTTCAGATTTTACACATATATCAGTGCCCGGTGTGACAACGGTTTTCCATGAC
AACGGACAGCAGTTATACCACTCTGCAACGTGTCGCAGCGCTGGAACGTTCCGGAA
TGCAAATCAGTCGTCCTCACTCACTGGTTTTATCATATCTGGCGTTAATGGAGTTCAGT
GGTAATACAATGACCAGAGATGCATCCAGAGCAGTTCTGCGTTTTGTCACTGTCAC
AGCAGAAGCCTTACGCTTCAGGCAGATACAGAGAGAATTTTCGTAGGCCTGTCTG
AAACTGCTCCTGTGTATACGATGACCCGGGAGACGTGGACCTCACTCTGAACTGG
GGGCGAATCAGCAATGTGCTTCCGGAGTATCGGGGAGAGGATGGTGTGAGAGTGGG
GAGAATATCCTTTAATAATATATCAGCGATACTGGGGACTGTGGCCGTTATACTGA
ATTGCCATCATCAGGGGGCGGTTCTGTTTCGCGCCGTGAATGAAGAGAGTCAACCA
GAATGTCAGATAACTGGCGACAGGCCTGTTATAAAAATAAACAATACATTATGGGA
AAGTAATACAGCTGCAGCGTTTCTGAACAGAAAGTCACAGTTTTTATATACAACGG
GTAATAA

**APPENDIX C. SUPPLEMENTARY INFORMATION FOR CHAPTER
4: INTERFACING CELL-FREE EXPRESSION PLATFORMS WITH
IMMUNOASSAYS FOR SENSITIVE DETECTION OF PROTEIN
BIOMARKERS**

C.1 Sequence Information

Table 7. Description of plasmid parts and DNA sequences used in CHAPTER 4

Name	Construct Description
<i>P_{T7}-lacZ alpha</i>	200-nt linear DNA fragment encoding the 45 amino acids alpha fragment of β -galactosidase (LacZ) expression under the T7 promoter
T7 Promoter-StrongRBS-<i>lacZ alpha</i>	
<pre> aaaaaaaaataatacgactcactatagggagaccacaagaaggagatatacatatgACCATGATTACGGA TTCACTGGCCGTCGTTTTACAACGTCGTGACTGGGAAAACCCTGGCGTTACCCAACTTAATCGCCTTGCA GCACATCCCCCTTTCGCCAGCTGGCGTAATAGCGAAGAGGCCCGCACCTaaaaaaaaaaaa </pre>	
<i>P_{T7}-lacZ omega</i>	Relevant part of the plasmid encoding the omega fragment of β -galactosidase (LacZ) expression under the T7 promoter
T7 Promoter- Stability Hairpin-StrongRBS-<i>lacZ omega</i>-T7 Terminator	
<pre> taatacgactcactatagggagaccacaacgggtttccctctagaaataattttgtttaactttaagaagg agatatacatATGACCATGATTACGGATTCACTGGCCGTCGCCCGCACCGATCGCCCTTCCCAACAGTTG CGCAGCCTGAATGGCGAATGGCGCTTTGCCTGGTTTTCCGGCACCAGAAGCGGTGCCGGAAGCTGGCTGG AGTGCGATCTTCTGAGGCCGATACTGTCGTGCTCCCCTCAAACTGGCAGATGCACGGTTACGATGCGCC CATCTACACCAACGTGACCTATCCCATTACGGTCAATCCGCCGTTTGTTCCACGGAGAATCCGACGGGT TGTTACTCGCTCACATTTAATGTTGATGAAAGCTGGCTACAGGAAGGCCAGACGCGAATTATTTTTGATG GCGTTAACTCGCGCTTTCATCTGTGGTGCAACGGGCGCTGGGTCGGTTACGGCCAGGACAGTCGTTTGCC GTCTGAATTTGACCTGAGCGCATTTTTACGCGCCGGAGAAAACCGCCTCGCGGTGATGGTGCTGCGCTGG AGTGACGGCAGTTATCTGGAAGATCAGGATATGTGGCGGATGAGCGGCATTTTTCCGTGACGTCTCGTTGC TGCATAAACCGACTACACAAATCAGCGATTTCCATGTTGCCACTCGCTTTAATGATGATTTCAGCCGCGC TGTACTGGAGGCTGAAGTTCAGATGTGCGGCGAGTTGCGTGACTACCTACGGGTAACAGTTTCTTTATGG CAGGGTGAAACGCAGGTCGCCAGCGGCACCCGCCTTTCCGGCGGTGAAATTATCGATGAGCGTGGTGGTT ATGCCGATCGCGTCACACTACGTCTGAACGTCGAAAACCCGAAACTGTGGAGCGCCGAAATCCCGAATCT CTATCGTGCGGTGGTTGAACTGCACACCCCGACGGCAGCGCTGATTGAAGCAGAAGCCTGCGATGTCCGGT TTCCGCGAGGTGCGGATTGAAAATGGTCTGCTGCTGCTGAACGGCAAGCCGTTGCTGATTCGAGGCGTTA ACCGTCACGAGCATCATCCTCTGCATGGTCAGGTCATGGATGAGCAGACGATGGTGCAGGATATCCTGCT GATGAAGCAGAACAACTTTAACGCCGTGCGCTGTTCGCATTATCCGAACCATCCGCTGTGGTACACGCTG TGCGACCGCTACGGCCTGTATGTGGTGGATGAAGCCAATATTGAAACCCACGGCATGGTGCCAATGAATC GTCTGACCGATGATCCGCGCTGGCTACCGCGATGAGCGAACCGGTAACCGGAATGGTGCAGCGCGATCG </pre>	

TAATCACCCGAGTGTGATCATCTGGTCGCTGGGGAATGAATCAGGCCACGGCGCTAATCACGACGCGCTG
TATCGCTGGATCAAATCTGTGCATCCTTCCC GCCCGGTGCAGTATGAAGGCGGCGGAGCCGACACCACGG
CCACCGATATTATTTGCCGATGTACGCGCGCTGGATGAAGACCAGCCCTTCCC GGCTGTGCCGAAATG
GTCCATCAAAAAATGGCTTTCGCTACCTGGAGAGACGCGCCCGCTGATCCTTTGCGAATACGCCACGCG
ATGGGTAACAGTCTTGGCGGTTTTCGCTAAATACTGGCAGGCGTTTTCGTCAGTATCCCCGTTTACAGGGCG
GCTTCGCTCTGGGACTGGGTGGATCAGTCGCTGATTAATATGATGAAAACGGCAACCCGTGGTTCGGCTTA
CGGCGGTGATTTTGGCGATACGCCGAACGATCGCCAGTTCTGTATGAACGGTCTGGTCTTTGCCGACCGC
ACGCCGCATCCAGCGCTGACGGAAGCAAAACACCAGCAGCAGTTTTTCCAGTTCGGTTTATCCGGGCAAA
CCATCGAAGTGACCAGCGAATACCTGTTCCGTCATAGCGATAACGAGCTCCTGCCTGGATGGTGGCGCT
GGATGGTAAGCCGCTGGCAAGCGGTGAAGTGCCTCTGGATGTGCTCCACAAGGTAACAGATTGATTGAA
CTGCCTGAATACCCAGCCGAGAGCGCCGGCAACTCTGGCTCACAGTACGCTAGTGCAACCCGAACG
CGACCGCATGGTCAGAAGCCGGGCACATCAGCGCCTGGCAGCAGTGGCGTCTGGCGGAAAACCTCAGTGT
GACGCTCCCCGCCGCTCCACGCCATCCCGCATCTGACCACCAGCGAAATGGATTTTGCATCGAGCTG
GGTAATAAGCGTTGGCAATTTAACCGCCAGTCAGGCTTTCTTTACAGATGTGGATTGGCGATAAAAAAC
AACTGCTGACGCCGCTGCGCGATCAGTTCACCCGTGCACCGCTGGATAACGACATTGGCGTAAGTGAAGC
GACCCGCATTGACCCTAACGCCTGGGTGCAACGCTGGAAGGCGGCGGGCCATTACCAGGCCGAAGCAGCG
TTGTTGCAGTGCACGGCAGATACTTGTGATGCGGTGCTGATTACGACCGCTCACGCGTGGCAGCATC
AGGGGAAAACCTTATTTATCAGCCGAAAACCTACCGGATTGATGGTAGTGGTCAAATGGCGATTACCGT
TGATGTTGAAGTGGCGAGCGATACACCGCATCCGGCGCGGATTGGCCTGAACTGCCAGCTGGCGCAGGTA
GCAGAGCGGGTAAACTGGCTCGGATTAGGGCCGCAAGAAAACCTATCCCGACCGCCTTACTGCCGCTGTT
TTGACCGCTGGGATCTGCCATTGTCAGACATGTATAACCCGTACGCTTCCCGAGCGAAAACGGTCTGCG
CTGCGGGACGCGCAATTGAATTATGGCCACACCAGTGGCGCGGCGACTTCCAGTTC AACATCAGCCGC
TACAGTCAACAGCAACTGATGGAACCAGCCATCGCCATCTGCTGCACGCGGAAGAAGGCACATGGCTGA
ATATCGACGGTTTTCCATATGGGGATTGGTGGCGACGACTCCTGGAGCCCGTCAGTATCGGCGGAATTCCA
GCTGAGCGCCGGTCGCTACCATTACCAGTTGGTCTGGTGTCAAAAATAAgtcgcaccggctgctaacaaag
cccgaaaggaagctgagttggetgctgcccaccgctgagcaataac tagcataacccttggggcctctaa
acgggtcttgaggggttttttg

<i>P_{T7}-lacZ</i>	Relevant part of the plasmid encoding β -galactosidase (LacZ) expression under the T7 promoter
T7 Promoter- Stability Hairpin-StrongRBS-lacZ-T7 Terminator	
taatacgactcactatagggagaccacaacgggtttccctctagaaataattttgttttaactttaagaagg agatatacatatgACCATGATTACGGATTCACTGGCCGTCGTTTTACAACGTCGTGACTGGGAAAACCTT GGCGTTACCAACTTAATCGCCTTGAGCACATCCCCCTTTCGCCAGCTGGCGTAATAGCGAAGAGGCC GCACCGATCGCCCTTCCCAACAGTTGCGCAGCCTGAATGGCGAATGGCGCTTTGCCTGGTTTTCCGGCACC AGAAGCGGTGCCGAAAGCTGGCTGGAGTGCATCTTCTGAGGCCGATACTGTGCTCGTCCCCTCAAAC TGGCAGATGCACGGTTACGATGCGCCCATCTACACCAACGTGACCTATCCCATTACGGTCAATCCGCCGT TTGTTCCACGGAGAATCCGACGGGTGTTACTCGCTCACATTTAATGTTGATGAAAGCTGGCTACAGGA AGGCCAGACGCGAATTATTTTTGATGGCGTAACTCGGCGTTTCATCTGTGGTGAACGGGCGCTGGGTC GGTTACGGCCAGGACAGTCGTTTGGCGTCTGAATTTGACCTGAGCGCATTTTTACGCGCCGGAGAAAACC GCCTCGCGGTGATGGTGTGCTGCGCTGGAGTGACGGCAGTTATCTGGAAGATCAGGATATGTGGCGGATGAG CGGCATTTTCCGTGACGTCTCGTTGCTGCATAAACCAGCTACACAAATCAGCGATTTCCATGTTGCCACT CGCTTTAATGATGATTTTCAGCCGCGCTGACTGGAGGCTGAAGTTCAGATGTGCGGCGAGTTGCGTGACT ACCTACGGGTAACAGTTTTCTTTATGGCAGGGTGAAACGCAGGTCGCCAGCGGCACCGCGCCTTTCCGGCGG TGAAATTATCGATGAGCGTGGTGGTTATGCCGATCGCGTCACACTACGTCTGAACGTCGAAAACCCGAAA CTGTGGAGCGCCGAAATCCCGAATCTCTATCGTGCAGTGGTTGAACTGCACACCCGCCGACGGCAGCTGA TTGAAGCAGAAGCCTGCGATGTGCGTTTTCCGCGAGGTGCGGATTGAAAATGGTCTGCTGCTGCTGAACGG CAAGCCGTTGCTGATTGAGGCGTTAACCGTCACGAGCATCATCTCTGCATGGTCAGGTCAGTGGATGAG CAGACATGGTGCAGGATATCCTGCTGATGAAGCAGAACAACCTTAACGCCGTGCGCTGTTCCGATTTATC CGAACCATCCGCTGTGGTACACGCTGTGCGACCGCTACGGCCTGTATGTGGTGGATGAAGCCAATATTGA AACCCACGGCATGGTGCCAATGAATCGTCTGACCGATGATCCGCGCTGGCTACCGCGATGAGCGAACGC GTAACCGAATGGTGCAGCGCATCGTAATCACCCGAGTGTGATCATCTGGTCGCTGGGGAATGAA TCAGGCCACGGCGCTAATCACGACGCGCTGTATCGCTGGATCAAATCTGTGATCCTTCCC CCGGTGCAGTATGAAGGCGGCGGAGCCGACACCAGGCCACCGATATTATTTGCCGATGTAC	

GCGCGGTGGATGAAGACCAGCCCTTCCCGGCTGTGCCGAAATGGTCCATCAAAAAATGGCTT
 TCGCTACCTGGAGAGACGCGCCCGCTGATCCTTTGCGAATACGCCACGCGATGGGTAACAGT
 CTTGGCGGTTTTCGCTAAATACTGGCAGGCGTTTTGCTCAGTATCCCCGTTTACAGGGCGGCTTC
 GTCTGGGACTGGGTGGATCAGTCGCTGATTAAATATGATGAAAACGGCAACCCGTGGTCCGCT
 TACGGCGGTGATTTTGGCGATACGCCAACGATCGCCAGTTCTGTATGAACGGTCTGGTCTTT
 GCCGACCGCACGCCGCATCCAGCGCTGACGGAAGCAAACACCAGCAGCAGTTTTTCCAGTTC
 CGTTTTATCCGGGCAAACCATCGAAGTGACCAGCGAATACCTGTTCCGTCATAGCGATAACGAG
 CTCCTGCACTGGATGGTGGCGCTGGATGGTAAGCCGCTGGCAAGCGGTGAAGTGCCTCTGGAT
 GTCGCTCCACAAGGTAAACAGTTGATTGAACTGCCTGAACTACCGCAGCCGGAGAGCGCCGGG
 CAACTCTGGCTCACAGTACGCGTAGTGCAACCGAACGCGACCGCATGGTCAGAAGCCGGACAC
 ATCAGCGCCTGGCAGCAGTGGCGTCTGGCTGAAAACCTCAGCGTGACACTCCCCGCCGCTCC
 CACGCCATCCCCGCATCTGACCACCAGCGAAATGGATTTTTGCATCGAGCTGGGTAATAAGCGT
 TGGCAATTTAACCGCCAGTCAGGCTTTCTTTCACAGATGTGGATTGGCGATAAAAAACAACCTG
 CTGACGCCGCTGCGCGATCAGTTCACCCGTGCACCGCTGGATAACGACATTGGCGTAAGTGAA
 GCGACCCGCATTGACCCTAACGCCTGGGTGCAACGCTGGAAGGCGGCGGGCCATTACCAGGCC
 GAAGCAGCGTTGTTGCAGTGCACGGCAGATACTTGCTGATGCGGTGCTGATTACGACCGCT
 CACGCGTGGCAGCATCAGGGGAAAACCTTATTTATCAGCCGGAAAACCTACCGGATTGATGGT
 AGTGGTCAAATGGCGATTACCGTTGATGTTGAAGTGGCGAGCGATAACCGCATCCGGCGCGG
 ATTGGCCTGAACTGCCAGCTGGCGCAGGTAGCAGAGCGGGTAAACTGGCTCGGATTAGGGCCG
 CAAGAAAATATCCCGACCGCCTTACTGCCGCCTGTTTTGACCGCTGGGATCTGCCATTGTCA
 GACATGTATACCCCGTACGTCTTCCCGAGCGAAAACGGTCTGCGCTGCGGGACGCGCGAATTG
 AATTATGGCCACACCAGTGGCGCGGCGACTTCCAGTTC AACATCAGCCGCTACAGTCAACAG
 CAACTGATGGAAACCAGCCATCGCCATCTGCTGCACGCGGAAGAAGGCACATGGCTGAATATC
 GACGGTTTTCCATATGGGGATTGGTGGCGACGACTCCTGGAGCCCGTCAGTATCGGCGGAATTC
 CAGCTGAGCGCCGGTTCGCTACCATTACCAGTTGGTCTGGTGTCAAAAAaagtcgaccggctg
 ctaacaaagcccgaaggaagctgagttggctgctgccaccgctgagcaataac tagcataac
 cccttggggcctctaaacgggtcttgaggggtttttt

P _{T7} -c23do	Relevant part of the plasmid encoding the C23DO enzyme expression under the T7 promoter
T7 Promoter- Stability Hairpin- StrongRBS- c23do- T7 Terminator	
<p> taatacgactcactatagggaga ccacaacgggtttccctctagaaaataattttgtttaactttaa gaag agatatacatATGAACAAAGGTGTAATGCGACCGGGCCATGTGCAGCTGCGTGTACTGGACATGAGCAAG GCCCTGGAACACTACGTCGAGTTGCTGGCCCTGATCGAGATGGACCGTGACGACCAGGGCCGTGTCTATC TGAAGGCTTGGACCGAAGTGGATAAGTTTTCCCTGGTGTACGCGAGGCTGACGAGCCGGGCATGGATTT TATGGGTTTTCAAGGTTGTGGATGAGGATGCTCTCCGGCAACTGGAGCGGGATCTGATGGCATATGGCTGT GCCGTTGAGCAGCTACCCGCAGGTGAACTGAACAGTTGTGGCCGGCGCGTGCCTTCCAGGCCCCCTCCG GGCATCACTTCGAGTTGTATGCAGACAAGGAATATACTGGAAAGTGGGGTTTTGAATGACGTCAATCCCGA GGCATGGCCGCGCGATCTGAAAGGTATGGCGGCTGTGCGTTTTGACCACGCCCTCATGTATGGCGACGAA TTGCCGGCGACCTATGACCTGTTACCAAGGTGCTCGGTTTTCTATCTGGCCGAACAGGTGCTGGACGAAA ATGGCACGCGCGTCCGCCAGTTTTCTCAGTCTGTGACCAAGGCCACGACGTGGCCTTCATTACCATCC GGAAAAAGGCCGCCTCCATCATGTGTCTTCCACCTCGAAAACCTGGGAAGACTTGCTTCGCGCCGCCGAC CTGATCTCCATGACCGACACATCTATCGATATCGGCCAACCCGCCACGGCCTCACTACGGCAAGACCA TCTACTTCTTCGACCCGTCGGTAACCGCAACGAAAGTGTCTGCGGGGAGATTACAACCTACCCGACCA CAAACCGGTGACCTGGACCACCGACCTAGCTGGGCAAGGCGATCTTTTACCACGACCCGATTCTCAACGAA CGATTTCATGACCGTGTGACTGATAaagtcgaccggctgctaacaaagcccgaaggaagctgagttggc tgctgccaccgctgagcaataac tagcataacccttggggcctctaaacgggtcttgaggggtttttt </p>	

P _{T7} -trigger B (short)	Linear DNA encoding expression of RNA trigger B without stabilizing hairpins under a P _{T7} Promoter.
------------------------------------	--

P_{T7} Promoter-trigger B-T7 Terminator

cgaaat **taatac**gactcactataggg **TAACGACATACAGCAAGCGATT**TACTTATACTA **tagc**ataaacc
 cttggggcctctaaacgggtcttgaggggt

P _{T7} -switch B- <i>sfgfp</i>	Relevant part of the plasmid encoding sfGFP expression under P _{T7} promoter and toehold switch B
P_{T7} Promoter-switch B- <i>sfgfp</i>- TrnB-T7 Terminator	
<p>taatacgactcactataggggagaGGGTATAAGTAAATCGCTTGCTGTATGTCGTTAAACAGAGGAGATAA CGAATGACAGCAAGCAACCTGGCGGCAGCGCAAAAGATGCGTAAAGGAGAAGAAGCTTTTACTGGAGTTG TCCCAATTCTTGTTGAATTAGATGGTGTATGTTAATGGGCACAAATTTCTGTCCGTGGAGAGGGTGAAGG TGATGCTACAAACGGAAAACCTCACCTTAAATTTATTTGCACTACTGGAAAACCTACCTGTTCCGTGGCCA ACACCTTGCTACTACTCTGACCTATGGTGTTCATGCTTTTCCCCTTATCCGGATCACATGAAACGGCATG ACTTTTTCAAGAGTGCCATGCCCCGAAGGTTATGTACAGGAACGCACTATATCTTTCAAGATGACGGGAC CTACAAGACGCGTGCTGAAGTCAAGTTTGAAGGTGATACCCTTGTTAATCGTATCGAGTTAAAGGGTATT GATTTTAAAGAAGATGGAAACATTCTTGGACACAACTCGAGTACAACCTTAACTCACACAATGTATACA TCACGGCAGACAAAAGAAATGGAATCAAAGCTAACTTCAAATTCGCCACAACGTTGAAGATGGTTC CGTTCAACTAGCAGACCATTATCAACAAAATACTCAAATGGCGATGGCCCTGTCTTTTACCAGACAAC CATTAACTGTGACACAATCTGCTCTTTCGAAAGATCCCAACGAAAAGCGTGACCACATGGTCTCTCTG AGTTTGAACTGCTGCTGGGATTACACATGGCATGGATGAGCTCTACAAATAAgggatctgaagcttgggc ccgaacaaaaaactcatctcagaagaggatctgaatagcgccgctgaccatcatcatcatcattgagt ttaaacgggtctccagcttggtggttttggcgatgagagaagattttcagcctgatacagattaatcag aacgcagaagcggctcgataaaacagaatttgccctggcgagtagcgcgggtgggtccacactgacccat gccgaactcagaagtgaacgcgctgagcgcgatggtagtgtgggggtctcccatgagagtagggaac tgccaggcatcaataaaacgaaaggctcagtcgaaagactgggcctttcgtttatctggtgtttgtcg gtgaaactggatcgtagccggctgctaacaagcccgaaaggaagctgagttggctgctgccaccgctga gcaataacctagcataaacccttggggcctctaaacgggtcttgaggggttttttg</p>	

P _{T7} -switch B- <i>c23do</i>	Relevant part of the plasmid encoding C23DO expression under P _{T7} promoter and toehold switch B
P_{T7} Promoter-switch B- <i>c23do</i>- T7 Terminator	
<p>taatacgactcactataggggagaGGGTATAAGTAAATCGCTTGCTGTATGTCGTTAAACAGAGGAGATAA CGAATGACAGCAAGCAACCTGGCGGCAGCGCAAAAGATGAACAAAGGTGTAATGCGACCGGGCCATGTGC AGCTGCGTGTACTGGACATGAGCAAGGCCCTGGAACACTACGTCGAGTTGCTGGGCCTGATCGAGATGGA CCGTGACGACCAGGGCCGTGTCTATCTGAAGGCTTGGACCGAAGTGGATAAGTTTTCCCTGGTGTACGC GAGGCTGACGAGCCGGGCATGGATTTTATGGGTTTCAAGGTTGTGGATGAGGATGCTCTCCGGCAACTGG AGCGGGATCTGATGGCATATGGCTGTGCCGTTGAGCAGTACCCGCAGGTGAAGTGAACAGTTGTGGCCG GCGGTGCGCTTCCAGGCCCTCCGGGCATCACTCGAGTTGATGCAGACAAGGAATATACTGGAAAG TGGGGTTTGAATGACGTCAATCCCAGGCATGGCCGCGCATCTGAAAGGTATGGCGGCTGTGCGTTTCG ACCACGCCCTCATGTATGGCGACGAATTGCCGGCGACCTATGACCTGTTACCAAGGTGCTCGGTTTCTA TCTGGCCGAACAGGTGCTGGACGAAAATGGCACGCGCGTCCGCCAGTTTCTCAGTCTGTGACCAAGGCC CACGACGTGGCCTTCATTCACCATCCGAAAAAGGCCGCTCCATCATGTGTCTTCCACCTCGAAACCT GGGAAGACTTGCTTCGCGCCGCCGACCTGATCTCCATGACCGACACATCTATCGATATCGGCCCAACCCG CCACGGCCTCACTCACGGCAAGACCATCTACTTCTTCGACCCGTCCGGTAACCGCAACGAAGTGTCTGC GGGGGAGATTACAACCTACCCGGACCACAAACCGGTGACCTGGACCACCGACCAGCTGGGCAAGGCATCT TTTACCACGACCGCATTCTCAACGAACGATTCATGACCGTGCTGACCTGAgtcgaccggctgctaacaa gcccgaaaggaagctgagttggctgctgccaccgctgagcaataactagcataaacccttggggcctcta aacgggtcttgaggggttttttg</p>	

P _{T7} -switch B- <i>lacZ</i>	Relevant part of the plasmid encoding LacZ expression under P _{T7} promoter and toehold switch B
P _{T7} Promoter-switch B- <i>lacZ</i> -T7 Terminator	
<pre> taatacgcactcactatagggagaGGGTATAAGTAAATCGCTTGCTGTATGTCGTTAAACAGAGGAGATAA CGAATGACAGCAAGCAACCTGGCGGCAGCGCAAAAGatgACCATGATTACGGATTCACTGGCCGTCGTTT TACAACGTCGTGACTGGGAAAACCTGGCGTTACCCAACCTTAATCGCCTTGCAGCACATCCCCCTTTCGC CAGCTGGCGTAATAGCGAAGAGGCCCGCACCAGTTCGCCCTTCCCAACAGTTGCGCAGCCTGAATGGCGAA TGGCGCTTTCCTGGTTTCCGGCACCAAGCGGTGCCGAAAGCTGGCTGGAGTGCATCTTCTGAGG CCGATACTGTCGTCGTCCTCAAACCTGGCAGATGCACGGTTACGATGCGCCCATCTACACCAACGTGAC CTATCCCATTACGGTCAATCCGCCGTTTGTTCACCGGAGAATCCGACGGGTTGTTACTCGCTCACATTT AATGTTGATGAAAGCTGGCTACAGGAAGGCCAGACGCGAATTATTTTTGATGGCGTTAACTCGGCCTTTC ATCTGTGGTGCAACGGGCGCTGGGTTCGTTTACGGCCAGGACAGTCGTTTTCGCTGCTGAATTTGACCTGAG CGCATTTTTACGCGCCGGAGAAAACCGCCTCGCGGTGATGGTGCTGCGCTGGAGTGACGGCAGTTATCTG GAAGATCAGGATATGTGGCGGATGAGCGGCATTTTTCCGTGACGTCTCGTTGCTGCATAAACCGACTACAC AAATCAGCGATTTCCATGTTGCCACTCGCTTTAATGATGATTTTCCGCGCGCTGTACTGGAGGCTGAAGT TCAGATGTGCGGCGAGTTGCGTGACTACCTACGGGTAACAGTTTCTTTATGGCAGGGTGAACGCAGGTC GCCAGCGGCACCGCGCTTTCGGCGGTGAAATTATCGATGAGCGTGGTGGTTATGCCGATCGCGTCACAC TACGTCTGAACGTGAAAACCCGAAACTGTGGAGCGCCGAAATCCCGAATCTCTATCGTGCGGTGGTTGA ACTGCACACCGCCGACGGCAGCTGATTGAAGCAGAAGCCTGCGATGTCGGTTTCCGCGAGGTGCGGATT GAAAATGGTCTGCTGCTGCTGAACGGCAAGCCGTTGCTGATTTCGAGGCGTTAACCGTCACGAGCATCATC CTCTGCATGGTCAGGTCATGGATGAGCAGACGATGGTGCAGGATATCCTGCTGATGAAGCAGAACAACCTT TAACGCCGTCGCGCTGTTTCGATTATCCGAACCATCCGCTGTGGTACACGCTGTGCGACCGCTACGGCCTG TATGTGGTGGATGAAGCCAATATTGAAACCCACGGCATGGTGCCAATGAATCGTCTGACCGATGATCCGC GCTGGCTACCGGCGATGAGCGAACCGGTAACCGCAATGGTGCAGCGCGATCGTAATCACCCGAGTGTG ATCATCTGGTCGCTGGGGAATGAATCAGGCCACGGCGCTAATCACGACGCGCTGTATCGCTGG ATCAAATCTGTGATCCTTCCCGCCCGGTGCAGTATGAAGGCGGCGGAGCCGACACCACGGCC ACCGATATTATTTGCCGATGTACGCGCGCGTGGATGAAGACCAGCCCTTCCCGGCTGTGCCG AAATGGTCCATCAAAAAATGGCTTTCGCTACCTGGAGAGACGCGCCCGCTGATCCTTTGCGAA TACGCCACGCGATGGGTAACAGTCTTGGCGGTTTCGCTAAATACTGGCAGGCGTTTCGTGAG TATCCCCGTTTACAGGGCGGCTTCGTCTGGGACTGGGTGGATCAGTCGCTGATTAATATGAT GAAAACGGCAACCCGTGGTTCGGCTTACGGCGGTGATTTTGGCGATACGCCGAACGATCGCCAG TTCTGTATGAACGGTCTGGTCTTTGCCGACCGCACGCCGATCCAGCGCTGACGGAAGCAAAA CACCAGCAGCAGTTTTTCCAGTTCGTTTATCCGGGCAAACCATCGAAGTGACCAGCGAATAC CTGTTCCGTCATAGCGATAACGAGCTCCTGCACTGGATGGTGGCGCTGGATGGTAAGCCGCTG GCAAGCGGTGAAGTGCCTCTGGATGTCGCTCCACAAGGTAACAGTTGATTGAACTGCCTGAA CTACCGCAGCCGGAGAGCGCCGGCAACTCTGGCTCACAGTACGCGTAGTGCAACCGAACGCG ACCGCATGGTCAGAAGCCGGACACATCAGCGCCTGGCAGCAGTGGCGTCTGGCTGAAAACCTC AGCGTGACACTCCCCGCGCGTCCCACGCCATCCCGCATCTGACCACGCGAAATGGATTTT TGCATCGAGCTGGGTAATAAGCGTTGGCAATTTAACCGCCAGTCAGGCTTTCTTTCACAGATG TGGATTGGCGATAAAAAACAACCTGCTGACGCCGCTGCGCGATCAGTTCACCCGTGCACCGCTG GATAACGACATTGGCGTAAGTGAAGCGACCCGCATTGACCCTAACGCCTGGGTGCAACGCTGG AAGGCGGCGGGCCATTACCAGGCCGAAGCAGCGTTGTTGCAGTGCACGGCAGATACACTTGCT GATGCGGTGCTGATTACGACCGCTCACGCGTGGCAGCATCAGGGGAAAACCTTATTTATCAGC CGGAAAACCTACCGGATTGATGGTAGTGGTCAAATGGCGATTACCGTTGATGTTGAAGTGGCG AGCGATACACCGCATCCGGCGCGGATTGGCCTGAACTGCCAGCTGGCGCAGGTAGCAGAGCGG GTAAACTGGCTCGGATTAGGGCCGCAAGAAAACCTATCCCGACCGCCTTACTGCCGCTGTTTT GACCGCTGGGATCTGCCATTGTCAGACATGTATACCCCGTACGTCCTCCCGAGCGAAAACGGT CTGCGCTGCGGGACGCGCGAATTGAATTATGGCCACACCAGTGGCGCGGCGACTTCCAGTTC AACATCAGCCGCTACAGTCAACAGCAACTGATGGAAACCAGCCATCGCCATCTGCTGCACGCG GAAGAAGGCACATGGCTGAATATCGACGGTTTCCATATGGGGATTGGTGGCGACGACTCCTGG AGCCCGTCAGTATCGGCGGAATTCCAGCTGAGCGCCGTCGCTACCATTACCAGTTGGTCTGG </pre>	

TGTCAAAAAtaagtctgaccggctgctaacaaagcccgaaggaagctgagttggctgctgccaccgct
gagcaataac tagcataacccttggggcctctaaacgggtcttgaggggtttttttg

P _{T7} -S2 trigger	Linear DNA encoding expression of RNA S2 trigger without stabilizing hairpins under a P _{T7} Promoter.
T7 Promoter-S2 trigger	
cgaaat taatac gactcactat agg GACCCAACAAAGTTATGTCTCTTCGTTAAATAGTAT tagcataac cccttggggcctctaaacgggtcttgaggggt	

P _{T7} -switch S2-c23do	Relevant part of the plasmid encoding C23DO expression under P _{T7} promoter and toehold switch S2
P _{T7} Promoter-switch S2-c23do-T7 Terminator	
taatac gactcactat agggaga GGGATACTATTTAACGAAGAGACATAACTTTGTTGGGTCGGACTTTA GAACAGAGGAGATAAAGATGGACCCAACAAAGATGAACAAAGGTGTAATGCGACCCGGGCCATGTGCAGCT GCGTGTACTGGACATGAGCAAGGCCCTGGAACACTACGTCGAGTTGCTGGGCCTGATCGAGATGGACCGT GACGACTAGGCCCGTGTCTATCTGAAGGCTTGACCAGGATAAGTTTTCCCTGGTACTGCGGAGG CTGACGAGCCGGGCATGGATTTTTATGGGTTTTCAAGGTTGTGGATGAGGATGCTCTCCGGCAACTGGAGCG GGATCTGATGGCATATGGCTGTGCCGTTGAGCAGCTACCCGAGGTGAAGTGAACAGTTGTGGCCGGCGC GTGCGCTTCCAGGCCCCCTCCGGGCATCACTTCGAGTTGTATGCAGACAAGGAATATACTGGAAAGTGGG GTTTGAATGACGTCAATCCCGAGGCATGGCCGCGCGATCTGAAAGGTATGGCGGCTGTGCGTTTTCGACCA CGCCCTCATGTATGGCGACGAATTGCCGGCGACCTATGACCTGTTACCAAGGTGCTCGGTTTTCTATCTG GCCGAACAGGTGCTGGACGAAAATGGCAGCGCGCTCGCCAGTTTTCTCAGTCTGTGACCAAGGCCACG ACGTGGCCTTCATTACCATCCGAAAAAGGCCGCTCCATCATGTGTCTTCCACCTCGAAACCTGGGA AGACTTGCTTCGCGCCGCCGACCTGATCTCCATGACCGACACATCTATCGATATCGGCCCAACCCGCCAC GGCCTCACTCACGGCAAGACCATCTACTTCTTCGACCCGTCGGTAACCGCAACGAAGTGTCTGCGGGG GAGATTACAAC TACCCGGACCACAAACCGGTGACCTGGACCACCGACCAGCTGGGCAAGGCATCTTTTA CCACGACCGCATTCTCAACGAACGATTCATGACCGTGCTGACCTGAgctgaccggctgctaacaaagccc gaaaggaagctgagttggctgctgccaccgctgagcaataac tagcataacccttggggcctctaaacg ggtcttgaggggtttttttg	

P _{T7} -S2 switch-lacZ	Relevant part of the plasmid encoding LacZ expression under T7 promoter and S2 toehold switch
T7 Promoter-stx2 switch-lacZ-TrnB-T7 Terminator	
taatac gactcactat agggaga GGGATACTATTTAACGAAGAGACATAACTTTGTTGGGTCGGACTTTA GAACAGAGGAGATAAAGATGGACCCAACAAAGatgACCATGATTACGGATTCACTGGCCGTCGTTTTACA ACGTCGTGACTGGGAAAACCTGGCGTTACCCAACCTTAATCGCCTTGCAGCACATCCCCCTTTCGCCAGC TGGCGTAATAGCGAAGAGGCCCGCACCGATCGCCCTTCCAACAGTTGCGCAGCCTGAATGGCGAATGGC GCTTTGCCTGGTTTTCCGGCACCAAGCGGTGCCGAAAAGCTGGCTGGAGTGCGATCTTCTGAGGCCGA TACTGTGCTGTCCTCCCTCAAACCTGGCAGATGCACGGTTACGATGCGCCCATCTACACCAACGTGACCTAT CCCATTACGGTCAATCCGCCGTTTTGTTCCACGGAGAATCCGACGGGTTGTTACTCGCTCACATTTAATG TTGATGAAAGCTGGCTACAGGAAGGCCAGACGCGAATTATTTTTGATGGCGTTAACTCGCGTTTTCATCT GTGGTGAACGGGCGCTGGGTGCGTTACGGCCAGGACAGTCGTTTTGCCGCTGAAATTTGACCTGAGCGCA TTTTTACGCGCCGGAGAAAACCGCCTCGCGGTGATGGTGCTGCGCTGGAGTGACGGCAGTTATCTGGAAG ATCAGGATATGTGGCGGATGAGCGGCATTTTCCGTGACGTCGTTGCTGCATAAACCGACTACACAAAT CAGCGATTTCCATGTTGCCACTCGCTTTAATGATGATTTTACGCCGCGCTGACTGGAGGCTGAAGTTCAG ATGTGCGGCGAGTTGCGTGACTACCTACGGGTAACAGTTTCTTTATGGCAGGGTGAACGCAGGTGCCCA GCGGCACCGCGCTTTCGGCGGTGAAATTATCGATGAGCGTGGTGGTTATGCCGATCGCGTCACACTACG TCTGAACGTCGAAAACCCGAAACTGTGGAGCGCCGAAATCCCGAATCTCTATCGTGGGTGGTTGAACTG	

CACACCGCCGACGGCAGCCTGATTGAAGCAGAAGCCTGCGATGTCCGTTTCCGCGAGGTGCGGATTGAAA
ATGGTCTGCTGCTGCTGAACGGCAAGCCGTTGCTGATTTCGAGGCGTTAACCGTACAGAGCATCATCCTCT
GCATGGTCAGGTCATGGATGAGCAGACGATGGTGCAGGATATCCTGCTGATGAAGCAGAACAACCTTTAAC
GCCGTGCGCTGTTTCGATTATCCGAACCATCCGCTGTGGTACACGCTGTGCGACCGCTACGGCCTGTATG
TGGTGGATGAAGCCAATATTGAAACCCACGGCATGGTGCCAATGAATCGTCTGACCGATGATCCGCGCTG
GCTACCGGCGATGAGCGAACCGGTAACCGCAATGGTGCAGCGCGATCGTAATCACCCGAGTGTGATCATC
TGGTGCCTGGGGAATGAATCAGGCCACGGCGTAATCACGACGCGCTGTATCGCTGGATCAAATCTGTGCG
ATCCTTCCC GCCCGGTGCAGTATGAAGGCGGCGGAGCCGACACCACGGCCACCGATATTATTTGCCCGAT
GTACGCGCGCGTGGATGAAGACCAGCCCTTCCC GGCTGTGCCGAAATGGTCCATCAAAAAATGGCTTTCG
CTACCTGGAGAGACGCGCCCGCTGATCCTTTGCGAATACGCCACGCGATGGGTAACAGTCTTGGCGGTT
TCGTTAAATACTGGCAGGCGTTTCGTGAGTATCCCGTTTACAGGGCGGCTTCGTCTGGGATGGATGGA
TCAGTCGCTGATTAATAATGATGAAAACGGCAACCCGTTGGTCCGCTTACGGCGGTTGATTTTGGCGATA
CCGAACGATCGCCAGTCTGTATGAACGGTCTGGTCTTTGCCGACCGCACGCCGCATCCAGCGCTGACGG
AAGCAAAACACCAGCAGCAGTTTTTCCAGTTCGGTTTATCCGGGCAAACCATCGAAGTGACCAGCGAATA
CCTGTTCCGTCATAGCGATAACGAGCTCCTGCACTGGATGGTGGCGCTGGATGGTAAGCCGCTGGCAAGC
GGTGAAGTGCCTCTGGATGTGCTCCACAAGGTAACAGTTGATTGAACTGCCTGAACTACCGCAGCCGG
AGAGCGCCGGGCAACTCTGGCTCACAGTACGCGTAGTGCAACCGAACGCGACCGCATGGTCAGAAGCCGG
ACACATCAGCGCCTGGCAGCAGTGGCGTCTGGCTGAAAACCTCAGCGTGACACTCCCCGCCGCGTCCCAC
GCCATCCCGCATCTGACCACCAGCGAAATGGATTTTGCATCGAGCTGGGTAATAAGCGTTGGCAATTTA
ACCGCCAGTCAGGCTTTCTTTACAGATGTGGATTGGCGATAAAAAACAACCTGCTGACGCCGCTGCGCGA
TCAGTTACCCGCTGCACCGCTGGATAACGACATTGGCGTAAGTGAAGCGACCCGCATTGACCCTAACGCC
TGGGTGCAACGCTGGAAGGCGGCGGGCCATTACCAGGCCGAAGCAGCGTTGTTGCAGTGCACGGCAGATA
CACTTGCTGATGCGGTGCTGATTACGACCGCTCACGCGTGGCAGCATCAGGGGAAAACCTTATTTATCAG
CCGAAAACCTACCGGATTGATGGTAGTGGTCAAATGGCGATTACCGTTGATGTTGAAGTGGCGAGCGAT
ACACCGCATCCGGCGCGGATTGGCCTGAACTGCCAGCTGGCGCAGGTAGCAGAGCGGGTAAACTGGCTCG
GATTAGGGCCGCAAGAAAACCTATCCCGACCGCCTTACTGCCGCCTGTTTTGACCGCTGGGATCTGCCATT
GTCAGACATGTATACCCCGTACGTCTTCCCGAGCGAAAACGGTCTGCGCTGCGGGACGCGCGAATTGAAT
TATGGCCACACCAGTGGCGCGGCGACTTCCAGTTC AACATCAGCCGCTACAGTCAACAGCAACTGATGG
AAACCAGCCATCGCCATCTGCTGCACGCGGAAGAAGGCACATGGCTGAATATCGACGGTTTCCATATGG
GATTGGTGGCGACGACTCCTGGAGCCCGTCAGTATCGGCGGAATTCCAGCTGAGCGCCGGTTCGCTACCAT
TACCAGTTGGTCTGGTGTCAAAAAtaataaggatctgaagcttgggcccgaacaaaaactcatctcagaa
gaggatctgaatagcgccgtcgaccatcatcatcatcattgagtttaaacggtctccagcttggctg
tttggcgatgagagaagattttcagcctgatacagattaaatcagaacgcagaagcggctctgataaaa
cagaatttgctggcggcagtagcgcggtggtcccacctgacctgcccgaactcagaagtgaacgccc
gtagcgccgatggtagtgtggggtctccccatgagagtagggaactgccaggcatcaataaaaacgaa
aggctcagtcgaaagactgggcctttcgttttatctgttgggtgctggtgactggatcgtcgaccggct
gctaacaaagccccgaaaggaagctgagttggctgctgccaccgctgagcaataacc tagcataaccctt
ggggcctctaaacgggtcttgaggggttttttg

C.2 CFE Reaction Conditions

Table 8. Description of CFE system, plasmid concentrations, and reaction additives present used for each figure in CHAPTER 4

Figure	Detecting	CFE System	Plasmid	Reaction Additive
Figure 4-2	Free and antibody conjugated LacZ alpha	PURE <i>flex</i> ®	1 nM T7-LacZ omega	0.6 mg/mL CPRG
Figure 4-3	Antibody conjugated LacZ alpha	PURE <i>flex</i> ®	1 nM T7-LacZ omega	0.6 mg/mL CPRG
Figure 4-4	N/A	PURE <i>flex</i> ®	0-3 nM T7-LacZ omega	0.6 mg/mL CPRG
Figure 4-4	N/A	PURE <i>express</i> ®	0-4 nM T7-LacZ omega	0.6 mg/mL CPRG
Figure 4-6 A, B	N/A	PURE <i>express</i> ®	5 nM T7-C23DO	4 mM Catechol
Figure 4-6 B	N/A	PURE <i>express</i> ®	5 nM T7-C23DO	4 mM Catechol 1 mM FeSO ₄
Figure 4-6 C	N/A	PURE <i>express</i> ®	5 nM T7-LacZ	4 mM Catechol 1 w/v% X-gal 1 mM FeSO ₄
Figure 4-6 C	N/A	PURE <i>express</i> ®	5 nM T7-C23DO	4 mM Catechol 1 w/v% X-gal 1 mM FeSO ₄
Figure 4-7	N/A	PURE <i>express</i> ®	5 nM T7-C23DO	4 mM Catechol 0-0.5 mM FeSO ₄ 1 mM Ascorbic acid
Figure 4-7	N/A	PURE <i>express</i> ®	5 nM T7-C23DO	4 mM Catechol 0-0.5 mM FeSO ₄ 1 mM Ascorbic acid 1 mM Citric acid
Figure 4-8	0-5 nM T7-trigger B	PURE <i>express</i> ®	1.5 nM T7-switchB-C23DO	4 mM Catechol 1 mM FeSO ₄ 1 mM Ascorbic acid 1 mM Citric acid

Figure 4-9	5 nM T7-trigger B	T7 Induced Cell Lysate	2.5 nM T7-switchB-GFP	0-10 μ M χ DNA
Figure 4-10 A	5 nM T7-trigger B 5 nM T7-trigger B	T7 Induced Cell Lysate	0.5 nM T7-switch B-LacZ 2 nM T7-switch S2-C23DO	5 μ M χ DNA
Figure 4-10 B	5 nM T7-trigger B 5 nM T7-trigger B	T7 Induced Cell Lysate	0.75 nM T7-switch S2-LacZ 1.5 nM T7-switch B-C23DO	5 μ M χ DNA

REFERENCES

- 1 De Paepe, B., Peters, G., Coussement, P., Maertens, J. & De Mey, M. Tailor-made transcriptional biosensors for optimizing microbial cell factories. *J Ind Microbiol Biotechnol* **44**, 623-645, doi:10.1007/s10295-016-1862-3 (2017).
- 2 Vitreschak, A. G., Rodionov, D. A., Mironov, A. A. & Gelfand, M. S. Riboswitches: the oldest mechanism for the regulation of gene expression? *Trends Genet* **20**, 44-50, doi:10.1016/j.tig.2003.11.008 (2004).
- 3 Trausch, J. J., Ceres, P., Reyes, F. E. & Batey, R. T. The structure of a tetrahydrofolate-sensing riboswitch reveals two ligand binding sites in a single aptamer. *Structure* **19**, 1413-1423, doi:10.1016/j.str.2011.06.019 (2011).
- 4 Nahvi, A., Barrick, J. E. & Breaker, R. R. Coenzyme B12 riboswitches are widespread genetic control elements in prokaryotes. *Nucleic Acids Res* **32**, 143-150, doi:10.1093/nar/gkh167 (2004).
- 5 Townshend, B., Xiang, J. S., Manzanarez, G., Hayden, E. J. & Smolke, C. D. A multiplexed, automated evolution pipeline enables scalable discovery and characterization of biosensors. *Nat Commun* **12**, 1437, doi:10.1038/s41467-021-21716-0 (2021).
- 6 Green, A. A., Silver, P. A., Collins, J. J. & Yin, P. Toehold switches: de-novo-designed regulators of gene expression. *Cell* **159**, 925-939, doi:10.1016/j.cell.2014.10.002 (2014).
- 7 Pardee, K. *et al.* Rapid, Low-Cost Detection of Zika Virus Using Programmable Biomolecular Components. *Cell* **165**, 1255-1266, doi:10.1016/j.cell.2016.04.059 (2016).
- 8 Pardee, K. *et al.* Paper-based synthetic gene networks. *Cell* **159**, 940-954, doi:10.1016/j.cell.2014.10.004 (2014).
- 9 Takahashi, M. K. *et al.* A low-cost paper-based synthetic biology platform for analyzing gut microbiota and host biomarkers. *Nat Commun* **9**, 3347, doi:10.1038/s41467-018-05864-4 (2018).
- 10 McNerney, M. P., Michel, C. L., Kishore, K., Standeven, J. & Styczynski, M. P. Dynamic and tunable metabolite control for robust minimal-equipment assessment of serum zinc. *Nat Commun* **10**, 5514, doi:10.1038/s41467-019-13454-1 (2019).
- 11 McNerney, M. P., Piorino, F., Michel, C. L. & Styczynski, M. P. Active Analyte Import Improves the Dynamic Range and Sensitivity of a Vitamin B12 Biosensor. *ACS Synth Biol* **9**, 402-411, doi:10.1021/acssynbio.9b00429 (2020).

- 12 Holowko, M. B., Wang, H., Jayaraman, P. & Poh, C. L. Biosensing *Vibrio cholerae* with Genetically Engineered *Escherichia coli*. *ACS Synth Biol* **5**, 1275-1283, doi:10.1021/acssynbio.6b00079 (2016).
- 13 Daeffler, K. N. *et al.* Engineering bacterial thiosulfate and tetrathionate sensors for detecting gut inflammation. *Mol Syst Biol* **13**, 923, doi:10.15252/msb.20167416 (2017).
- 14 Gu, M. B., Mitchell, R. J. & Kim, B. C. Whole-cell-based biosensors for environmental biomonitoring and application. *Adv Biochem Eng Biotechnol* **87**, 269-305, doi:10.1007/b13533 (2004).
- 15 Silverman, A. D., Karim, A. S. & Jewett, M. C. Cell-free gene expression: an expanded repertoire of applications. *Nat Rev Genet* **21**, 151-170, doi:10.1038/s41576-019-0186-3 (2020).
- 16 Zubay, G. In vitro synthesis of protein in microbial systems. *Annu Rev Genet* **7**, 267-287, doi:10.1146/annurev.ge.07.120173.001411 (1973).
- 17 Kwon, Y. C. & Jewett, M. C. High-throughput preparation methods of crude extract for robust cell-free protein synthesis. *Sci Rep-Uk* **5**, doi:ARTN 8663
10.1038/srep08663 (2015).
- 18 Sun, Z. Z. *et al.* Protocols for Implementing an *Escherichia coli* Based TX-TL Cell-Free Expression System for Synthetic Biology. *Jove-J Vis Exp*, doi:ARTN e50762
10.3791/50762 (2013).
- 19 Silverman, A. D., Kelley-Loughnane, N., Lucks, J. B. & Jewett, M. C. Deconstructing Cell-Free Extract Preparation for in Vitro Activation of Transcriptional Genetic Circuitry. *ACS Synth Biol* **8**, 403-414, doi:10.1021/acssynbio.8b00430 (2019).
- 20 Jewett, M. C. & Swartz, J. R. Mimicking the *Escherichia coli* cytoplasmic environment activates long-lived and efficient cell-free protein synthesis. *Biotechnol Bioeng* **86**, 19-26, doi:10.1002/bit.20026 (2004).
- 21 Jung, J. K. *et al.* Cell-free biosensors for rapid detection of water contaminants. *Nat Biotechnol* **38**, 1451-1459, doi:10.1038/s41587-020-0571-7 (2020).
- 22 Liu, X. *et al.* Design of a Transcriptional Biosensor for the Portable, On-Demand Detection of Cyanuric Acid. *ACS Synth Biol* **9**, 84-94, doi:10.1021/acssynbio.9b00348 (2020).
- 23 Silverman, A. D., Akova, U., Alam, K. K., Jewett, M. C. & Lucks, J. B. Design and Optimization of a Cell-Free Atrazine Biosensor. *ACS Synth Biol* **9**, 671-677, doi:10.1021/acssynbio.9b00388 (2020).

- 24 Thavarajah, W. *et al.* Point-of-Use Detection of Environmental Fluoride via a Cell-Free Riboswitch-Based Biosensor. *ACS Synth Biol* **9**, 10-18, doi:10.1021/acssynbio.9b00347 (2020).
- 25 McNerney, M. P. *et al.* Point-of-care biomarker quantification enabled by sample-specific calibration. *Sci Adv* **5**, eaax4473, doi:10.1126/sciadv.aax4473 (2019).
- 26 Dincer, C., Bruch, R., Kling, A., Dittrich, P. S. & Urban, G. A. Multiplexed Point-of-Care Testing - xPOCT. *Trends Biotechnol* **35**, 728-742, doi:10.1016/j.tibtech.2017.03.013 (2017).
- 27 Gootenberg, J. S. *et al.* Multiplexed and portable nucleic acid detection platform with Cas13, Cas12a, and Csm6. *Science* **360**, 439-+, doi:10.1126/science.aaq0179 (2018).
- 28 Iyer, S., Karig, D. K., Norred, S. E., Simpson, M. L. & Doktycz, M. J. Multi-input regulation and logic with T7 promoters in cells and cell-free systems. *PLoS One* **8**, e78442, doi:10.1371/journal.pone.0078442 (2013).
- 29 Pandi, A. *et al.* Metabolic perceptrons for neural computing in biological systems. *Nat Commun* **10**, 3880, doi:10.1038/s41467-019-11889-0 (2019).
- 30 Sadat Mousavi, P. *et al.* A multiplexed, electrochemical interface for gene-circuit-based sensors. *Nat Chem* **12**, 48-55, doi:10.1038/s41557-019-0366-y (2020).
- 31 Ackerman, C. M. *et al.* Massively multiplexed nucleic acid detection using Cas13. *Nature*, doi:10.1038/s41586-020-2279-8 (2020).
- 32 Chao, Y. & Shum, H. C. Emerging aqueous two-phase systems: from fundamentals of interfaces to biomedical applications. *Chemical Society Reviews* **49**, 114-142, doi:10.1039/C9CS00466A (2020).
- 33 Iqbal, M. *et al.* Aqueous two-phase system (ATPS): an overview and advances in its applications. *Biol Proced Online* **18**, 18, doi:10.1186/s12575-016-0048-8 (2016).
- 34 Eiden, L., Yamanishi, C., Takayama, S. & Dishinger, J. F. Aqueous Two-Phase System Rehydration of Antibody–Polymer Microarrays Enables Convenient Compartmentalized Multiplex Immunoassays. *Analytical Chemistry* **88**, 11328-11334, doi:10.1021/acs.analchem.6b02960 (2016).
- 35 Frampton, J. P. *et al.* Aqueous two-phase system patterning of detection antibody solutions for cross-reaction-free multiplex ELISA. *Sci Rep* **4**, 4878, doi:10.1038/srep04878 (2014).
- 36 Tongdee, M. *et al.* One-incubation one-hour multiplex ELISA enabled by aqueous two-phase systems. *Analyst* **145**, 3517-3527, doi:10.1039/d0an00383b (2020).

- 37 Sokolova, E. *et al.* Enhanced transcription rates in membrane-free protocells formed by coacervation of cell lysate. *Proc Natl Acad Sci U S A* **110**, 11692-11697, doi:10.1073/pnas.1222321110 (2013).
- 38 Torre, P., Keating, C. D. & Mansy, S. S. Multiphase water-in-oil emulsion droplets for cell-free transcription-translation. *Langmuir* **30**, 5695-5699, doi:10.1021/la404146g (2014).
- 39 Lisi, F., Peterson, J. R. & Gooding, J. J. The application of personal glucose meters as universal point-of-care diagnostic tools. *Biosens Bioelectron* **148**, doi:ARTN 111835
10.1016/j.bios.2019.111835 (2020).
- 40 Xiang, Y. & Lu, Y. Using personal glucose meters and functional DNA sensors to quantify a variety of analytical targets. *Nature Chemistry* **3**, 697-703, doi:10.1038/Nchem.1092 (2011).
- 41 Bayat, P. *et al.* SELEX methods on the road to protein targeting with nucleic acid aptamers. *Biochimie* **154**, 132-155, doi:10.1016/j.biochi.2018.09.001 (2018).
- 42 Iyer, S. & Doktycz, M. J. Thrombin-mediated transcriptional regulation using DNA aptamers in DNA-based cell-free protein synthesis. *ACS Synth Biol* **3**, 340-346, doi:10.1021/sb4000756 (2014).
- 43 Niemeyer, C. M., Adler, M. & Wacker, R. Detecting antigens by quantitative immuno-PCR. *Nat Protoc* **2**, 1918-1930, doi:10.1038/nprot.2007.267 (2007).
- 44 Ruzicka, V., Marz, W., Russ, A. & Gross, W. Immuno-PCR with a commercially available avidin system. *Science* **260**, 698-699, doi:10.1126/science.8480182 (1993).
- 45 Wiener, J., Kokotek, D., Rosowski, S., Lickert, H. & Meier, M. Preparation of single- and double-oligonucleotide antibody conjugates and their application for protein analytics. *Sci Rep-Uk* **10**, doi:ARTN 1457
10.1038/s41598-020-58238-6 (2020).
- 46 Zhang, Y. *et al.* Protocell arrays for simultaneous detection of diverse analytes. *Nature Communications* **12**, 5724, doi:10.1038/s41467-021-25989-3 (2021).
- 47 Strulson, C. A., Molden, R. C., Keating, C. D. & Bevilacqua, P. C. RNA catalysis through compartmentalization. *Nature Chemistry* **4**, 941-946, doi:10.1038/Nchem.1466 (2012).
- 48 Simon, A. B. *et al.* Aqueous two-phase systems enable multiplexing of homogeneous immunoassays. *Technology (Singap World Sci)* **2**, 176, doi:10.1142/S2339547814500150 (2014).

- 49 Datsenko, K. A. & Wanner, B. L. One-step inactivation of chromosomal genes in *Escherichia coli* K-12 using PCR products. *Proc Natl Acad Sci U S A* **97**, 6640-6645, doi:10.1073/pnas.120163297 (2000).
- 50 Gibson, D. G. *et al.* Enzymatic assembly of DNA molecules up to several hundred kilobases. *Nat Methods* **6**, 343-345, doi:10.1038/nmeth.1318 (2009).
- 51 Gibson, E., Hong, L. & Leveille, J. CLiP'd: Characterizing Non-Lysosomal Inducible Protein Degradation. *PLOS iGEM* (2017).
- 52 Yamanishi, C., Oliver, C. R., Kojima, T. & Takayama, S. Stigmatic Microscopy Enables Low-Cost, 3D, Microscale Particle Imaging Velocimetry in Rehydrating Aqueous Two-Phase Systems. *Front Chem* **7**, 311, doi:10.3389/fchem.2019.00311 (2019).
- 53 Ge, X., Luo, D. & Xu, J. Cell-free protein expression under macromolecular crowding conditions. *PLoS One* **6**, e28707, doi:10.1371/journal.pone.0028707 (2011).
- 54 Kojima, T., Lin, C. C., Takayama, S. & Fan, S. K. Determination of Aqueous Two-Phase System Binodals and Tie-Lines by Electrowetting-on-Dielectric Droplet Manipulation. *Chembiochem* **20**, 270-275, doi:10.1002/cbic.201800553 (2019).
- 55 Balzer, S. *et al.* A comparative analysis of the properties of regulated promoter systems commonly used for recombinant gene expression in *Escherichia coli*. *Microb Cell Fact* **12**, 26, doi:10.1186/1475-2859-12-26 (2013).
- 56 Lobato, I. M. & O'Sullivan, C. K. Recombinase polymerase amplification: Basics, applications and recent advances. *Trac-Trend Anal Chem* **98**, 19-35, doi:10.1016/j.trac.2017.10.015 (2018).
- 57 Deiman, B., van Aarle, P. & Sillekens, P. Characteristics and applications of nucleic acid sequence-based amplification (NASBA). *Mol Biotechnol* **20**, 163-179, doi:10.1385/MB:20:2:163 (2002).
- 58 Karmali, M. A. Infection by Shiga toxin-producing *Escherichia coli*: an overview. *Mol Biotechnol* **26**, 117-122, doi:10.1385/MB:26:2:117 (2004).
- 59 Curtis, M. M. *et al.* The Gut Commensal *Bacteroides thetaiotaomicron* Exacerbates Enteric Infection through Modification of the Metabolic Landscape. *Cell Host Microbe* **16**, 759-769, doi:10.1016/j.chom.2014.11.005 (2014).
- 60 Makino, K. *et al.* Complete nucleotide sequence of the prophage VT2-Sakai carrying the verotoxin 2 genes of the enterohemorrhagic *Escherichia coli* O157:H7 derived from the Sakai outbreak. *Genes Genet Syst* **74**, 227-239, doi:10.1266/ggs.74.227 (1999).

- 61 Marshall, R., Maxwell, C. S., Collins, S. P., Beisel, C. L. & Noireaux, V. Short DNA containing chi sites enhances DNA stability and gene expression in E. coli cell-free transcription-translation systems. *Biotechnol Bioeng* **114**, 2137-2141, doi:10.1002/bit.26333 (2017).
- 62 Vancevska, A., Nikolic, A., Bonaci-Nikolic, B., Skiljevic, D. & Radojkovic, D. Assessment of Deoxyribonuclease Activity in Serum Samples of Patients With Systemic Lupus Erythematosus: Fluorescence-Based Method Versus ELISA. *J Clin Lab Anal* **30**, 797-803, doi:10.1002/jcla.21939 (2016).
- 63 Blank, A. & Dekker, C. A. Ribonucleases of human serum, urine, cerebrospinal fluid, and leukocytes. Activity staining following electrophoresis in sodium dodecyl sulfate-polyacrylamide gels. *Biochemistry* **20**, 2261-2267, doi:10.1021/bi00511a030 (1981).
- 64 Shiel, A. E., Barling, J., Orians, K. J. & Weis, D. Matrix effects on the multi-collector inductively coupled plasma mass spectrometric analysis of high-precision cadmium and zinc isotope ratios. *Anal Chim Acta* **633**, 29-37, doi:10.1016/j.aca.2008.11.026 (2009).
- 65 Taylor, P. J. Matrix effects: the Achilles heel of quantitative high-performance liquid chromatography-electrospray-tandem mass spectrometry. *Clin Biochem* **38**, 328-334, doi:10.1016/j.clinbiochem.2004.11.007 (2005).
- 66 Trufelli, H., Palma, P., Famigliani, G. & Cappiello, A. An overview of matrix effects in liquid chromatography-mass spectrometry. *Mass Spectrom Rev* **30**, 491-509, doi:10.1002/mas.20298 (2011).
- 67 Julin, D. A. in *Molecular Life Sciences: An Encyclopedic Reference* (eds Robert D. Wells, Judith S. Bond, Judith Klinman, & Bettie Sue Siler Masters) 72-73 (Springer New York, 2018).
- 68 Tavana, H. *et al.* Nanolitre liquid patterning in aqueous environments for spatially defined reagent delivery to mammalian cells. *Nat Mater* **8**, 736-741, doi:10.1038/nmat2515 (2009).
- 69 Poudyal, R. R. *et al.* Template-directed RNA polymerization and enhanced ribozyme catalysis inside membraneless compartments formed by coacervates. *Nat Commun* **10**, 490, doi:10.1038/s41467-019-08353-4 (2019).
- 70 Kojima, T. & Takayama, S. Membraneless Compartmentalization Facilitates Enzymatic Cascade Reactions and Reduces Substrate Inhibition. *ACS Appl Mater Interfaces* **10**, 32782-32791, doi:10.1021/acsami.8b07573 (2018).
- 71 Song, Y. *et al.* Budding-like division of all-aqueous emulsion droplets modulated by networks of protein nanofibrils. *Nat Commun* **9**, 2110, doi:10.1038/s41467-018-04510-3 (2018).

- 72 Tavana, H. *et al.* Polymeric Aqueous Biphasic System Rehydration Facilitates High Throughput Cell Exclusion Patterning For Cell Migration Studies. *Adv Funct Mater* **21**, 2920-2926, doi:10.1002/adfm.201002559 (2011).
- 73 Tian, L. *et al.* Spontaneous assembly of chemically encoded two-dimensional coacervate droplet arrays by acoustic wave patterning. *Nat Commun* **7**, 13068, doi:10.1038/ncomms13068 (2016).
- 74 Poudyal, R. R., Pir Cakmak, F., Keating, C. D. & Bevilacqua, P. C. Physical Principles and Extant Biology Reveal Roles for RNA-Containing Membraneless Compartments in Origins of Life Chemistry. *Biochemistry* **57**, 2509-2519, doi:10.1021/acs.biochem.8b00081 (2018).
- 75 Voyvodic, P. L. *et al.* Plug-and-play metabolic transducers expand the chemical detection space of cell-free biosensors. *Nat Commun* **10**, 1697, doi:10.1038/s41467-019-09722-9 (2019).
- 76 Wang, J. *et al.* A DNA Bubble-Mediated Gene Regulation System Based on Thrombin-Bound DNA Aptamers. *ACS Synth Biol* **6**, 758-765, doi:10.1021/acssynbio.6b00391 (2017).
- 77 Verosloff, M., Chappell, J., Perry, K. L., Thompson, J. R. & Lucks, J. B. PLANT-Dx: A Molecular Diagnostic for Point-of-Use Detection of Plant Pathogens. *ACS Synth Biol* **8**, 902-905, doi:10.1021/acssynbio.8b00526 (2019).
- 78 Dubuc, E. *et al.* Cell-free microcompartmentalised transcription-translation for the prototyping of synthetic communication networks. *Curr Opin Biotechnol* **58**, 72-80, doi:10.1016/j.copbio.2018.10.006 (2019).
- 79 Rampioni, G., D'Angelo, F., Leoni, L. & Stano, P. Gene-Expressing Liposomes as Synthetic Cells for Molecular Communication Studies. *Frontiers in Bioengineering and Biotechnology* **7**, doi:10.3389/fbioe.2019.00001 (2019).
- 80 Shin, J. & Noireaux, V. An E. coli cell-free expression toolbox: application to synthetic gene circuits and artificial cells. *ACS Synth Biol* **1**, 29-41, doi:10.1021/sb200016s (2012).
- 81 King, J. C. *et al.* Biomarkers of Nutrition for Development (BOND)-Zinc Review. *J Nutr* **146**, 858S-885S, doi:10.3945/jn.115.220079 (2015).
- 82 Allen, L. H. *et al.* Biomarkers of Nutrition for Development (BOND): Vitamin B-12 Review. *J Nutr* **148**, 1995S-2027S, doi:10.1093/jn/nxy201 (2018).
- 83 Gootenberg, J. S. *et al.* Multiplexed and portable nucleic acid detection platform with Cas13, Cas12a, and Csm6. *Science* **360**, 439-444, doi:10.1126/science.aag0179 (2018).

- 84 Fozouni, P. *et al.* Amplification-free detection of SARS-CoV-2 with CRISPR-Cas13a and mobile phone microscopy. *Cell* **184**, 323-333 e329, doi:10.1016/j.cell.2020.12.001 (2021).
- 85 Zhang, Y., Steppe, P. L., Kazman, M. W. & Styczynski, M. P. Point-of-Care Analyte Quantification and Digital Readout via Lysate-Based Cell-Free Biosensors Interfaced with Personal Glucose Monitors. *ACS Synth Biol* **10**, 2862-2869, doi:10.1021/acssynbio.1c00282 (2021).
- 86 Jang, Y. J., Lee, K. H., Yoo, T. H. & Kim, D. M. Interfacing a Personal Glucose Meter with Cell-Free Protein Synthesis for Rapid Analysis of Amino Acids. *Anal Chem* **91**, 2531-2535, doi:10.1021/acs.analchem.8b05526 (2019).
- 87 Amalfitano, E. *et al.* A glucose meter interface for point-of-care gene circuit-based diagnostics. *Nat Commun* **12**, 724, doi:10.1038/s41467-020-20639-6 (2021).
- 88 Xiang, Y., Lan, T. & Lu, Y. Using the widely available blood glucose meter to monitor insulin and HbA1c. *J Diabetes Sci Technol* **8**, 855-858, doi:10.1177/1932296814532875 (2014).
- 89 Xiang, Y. & Lu, Y. Portable and quantitative detection of protein biomarkers and small molecular toxins using antibodies and ubiquitous personal glucose meters. *Anal Chem* **84**, 4174-4178, doi:10.1021/ac300517n (2012).
- 90 Xiang, Y. & Lu, Y. Using commercially available personal glucose meters for portable quantification of DNA. *Anal Chem* **84**, 1975-1980, doi:10.1021/ac203014s (2012).
- 91 Yan, L. *et al.* Target-responsive "sweet" hydrogel with glucometer readout for portable and quantitative detection of non-glucose targets. *J Am Chem Soc* **135**, 3748-3751, doi:10.1021/ja3114714 (2013).
- 92 Zhang, J., Xiang, Y., Wang, M., Basu, A. & Lu, Y. Dose-Dependent Response of Personal Glucose Meters to Nicotinamide Coenzymes: Applications to Point-of-Care Diagnostics of Many Non-Glucose Targets in a Single Step. *Angew Chem Int Ed Engl* **55**, 732-736, doi:10.1002/anie.201507563 (2016).
- 93 Combs, G. F., Jr. *et al.* Biomarkers in nutrition: new frontiers in research and application. *Ann N Y Acad Sci* **1278**, 1-10, doi:10.1111/nyas.12069 (2013).
- 94 Goossens, N., Nakagawa, S., Sun, X. & Hoshida, Y. Cancer biomarker discovery and validation. *Transl Cancer Res* **4**, 256-269, doi:10.3978/j.issn.2218-676X.2015.06.04 (2015).
- 95 Vasan, R. S. Biomarkers of cardiovascular disease: molecular basis and practical considerations. *Circulation* **113**, 2335-2362, doi:10.1161/CIRCULATIONAHA.104.482570 (2006).

- 96 Calhoun, K. A. & Swartz, J. R. Energizing cell-free protein synthesis with glucose metabolism. *Biotechnol Bioeng* **90**, 606-613, doi:10.1002/bit.20449 (2005).
- 97 Caschera, F. & Noireaux, V. A cost-effective polyphosphate-based metabolism fuels an all E. coli cell-free expression system. *Metab Eng* **27**, 29-37, doi:10.1016/j.ymben.2014.10.007 (2015).
- 98 Karim, A. S., Rasor, B. J. & Jewett, M. C. Enhancing control of cell-free metabolism through pH modulation. *Synthetic Biology* **5**, doi:10.1093/synbio/ysz027 (2019).
- 99 Miguez, A. M., McNERney, M. P. & Styczynski, M. P. Metabolic Profiling of Escherichia coli-based Cell-Free Expression Systems for Process Optimization. *Ind Eng Chem Res* **58**, 22472-22482, doi:10.1021/acs.iecr.9b03565 (2019).
- 100 Miguez, A. M., Zhang, Y., Piorino, F. & Styczynski, M. P. Metabolic Dynamics in Escherichia coli-Based Cell-Free Systems. *ACS Synth Biol* **10**, 2252-2265, doi:10.1021/acssynbio.1c00167 (2021).
- 101 Bhutta, Z. A. *et al.* Evidence-based interventions for improvement of maternal and child nutrition: what can be done and at what cost? *Lancet* **382**, 452-477, doi:10.1016/S0140-6736(13)60996-4 (2013).
- 102 Carter, L. J. *et al.* Assay Techniques and Test Development for COVID-19 Diagnosis. *ACS Cent Sci* **6**, 591-605, doi:10.1021/acscentsci.0c00501 (2020).
- 103 Berger, A., Braner, J., Doerr, H. W. & Weber, B. Quantification of viral load: clinical relevance for human immunodeficiency virus, hepatitis B virus and hepatitis C virus infection. *Intervirology* **41**, 24-34, doi:10.1159/000024912 (1998).
- 104 Cole, S. D. *et al.* Quantification of Interlaboratory Cell-Free Protein Synthesis Variability. *ACS Synth Biol* **8**, 2080-2091, doi:10.1021/acssynbio.9b00178 (2019).
- 105 Gayet, R. V. *et al.* Creating CRISPR-responsive smart materials for diagnostics and programmable cargo release. *Nat Protoc* **15**, 3030-3063, doi:10.1038/s41596-020-0367-8 (2020).
- 106 English, M. A. *et al.* Programmable CRISPR-responsive smart materials. *Science* **365**, 780-785, doi:10.1126/science.aaw5122 (2019).
- 107 Aleem, A., Akbar Samad, A. B. & Slenker, A. K. in *StatPearls* (2022).
- 108 Callaway, E. Heavily mutated Omicron variant puts scientists on alert. *Nature* **600**, 21, doi:10.1038/d41586-021-03552-w (2021).
- 109 Poudel, S. *et al.* Highly mutated SARS-CoV-2 Omicron variant sparks significant concern among global experts - What is known so far? *Travel Med Infect Dis* **45**, 102234, doi:10.1016/j.tmaid.2021.102234 (2022).

- 110 Wang, H. *et al.* Mutation-Specific SARS-CoV-2 PCR Screen: Rapid and Accurate Detection of Variants of Concern and the Identification of a Newly Emerging Variant with Spike L452R Mutation. *J Clin Microbiol* **59**, e0092621, doi:10.1128/JCM.00926-21 (2021).
- 111 Harvey, W. T. *et al.* SARS-CoV-2 variants, spike mutations and immune escape. *Nat Rev Microbiol* **19**, 409-424, doi:10.1038/s41579-021-00573-0 (2021).
- 112 Chapman, A. P. *et al.* Rapid development of neutralizing and diagnostic SARS-COV-2 mouse monoclonal antibodies. *Sci Rep* **11**, 9682, doi:10.1038/s41598-021-88809-0 (2021).
- 113 Mitchell, S. L. *et al.* Performance of SARS-CoV-2 antigen testing in symptomatic and asymptomatic adults: a single-center evaluation. *BMC Infect Dis* **21**, 1071, doi:10.1186/s12879-021-06716-1 (2021).
- 114 Dahotre, S. N., Chang, Y. M., Wieland, A., Stammen, S. R. & Kwong, G. A. Individually addressable and dynamic DNA gates for multiplexed cell sorting. *Proc Natl Acad Sci U S A* **115**, 4357-4362, doi:10.1073/pnas.1714820115 (2018).
- 115 Nishiyama, K., Ichihashi, N., Kazuta, Y. & Yomo, T. Development of a reporter peptide that catalytically produces a fluorescent signal through alpha-complementation. *Protein Sci* **24**, 599-603, doi:10.1002/pro.2667 (2015).
- 116 Junker, F., Leisinger, T. & Cook, A. M. 3-Sulphocatechol 2,3-dioxygenase and other dioxygenases (EC 1.13.11.2 and EC 1.14.12.-) in the degradative pathways of 2-aminobenzenesulphonic, benzenesulphonic and 4-toluenesulphonic acids in *Alcaligenes* sp. strain 0-1. *Microbiology* **140**, 1713-1722, doi:https://doi.org/10.1099/13500872-140-7-1713 (1994).
- 117 Suzuki, T., Clydesdale, F. M. & Pandolf, T. Solubility of Iron in Model Systems Containing Organic Acids and Lignin. *J Food Prot* **55**, 893-898, doi:10.4315/0362-028X-55.11.893 (1992).
- 118 Cohen, J. D. *et al.* Detection and localization of surgically resectable cancers with a multi-analyte blood test. *Science* **359**, 926-930, doi:10.1126/science.aar3247 (2018).
- 119 Day, A. S. *et al.* Contamination-resistant, rapid emulsion-based isothermal nucleic acid amplification with Mie-scatter inspired light scatter analysis for bacterial identification. *Sci Rep* **11**, 19933, doi:10.1038/s41598-021-99200-4 (2021).
- 120 Libicher, K., Hornberger, R., Heymann, M. & Mutschler, H. In vitro self-replication and multicistronic expression of large synthetic genomes. *Nat Commun* **11**, 904, doi:10.1038/s41467-020-14694-2 (2020).

- 121 Sakatani, Y., Ichihashi, N., Kazuta, Y. & Yomo, T. A transcription and translation-coupled DNA replication system using rolling-circle replication. *Sci Rep* **5**, 10404, doi:10.1038/srep10404 (2015).
- 122 Kim, T. H., Hahn, Y. K. & Kim, M. S. Recent Advances of Fluid Manipulation Technologies in Microfluidic Paper-Based Analytical Devices (muPADs) toward Multi-Step Assays. *Micromachines (Basel)* **11**, doi:10.3390/mi11030269 (2020).
- 123 Nabatiyan, A., Parpia, Z. A., Elghanian, R. & Kelso, D. M. Membrane-based plasma collection device for point-of-care diagnosis of HIV. *J Virol Methods* **173**, 37-42, doi:10.1016/j.jviromet.2011.01.003 (2011).
- 124 Scudellari, M. How the coronavirus infects cells - and why Delta is so dangerous. *Nature* **595**, 640-644, doi:10.1038/d41586-021-02039-y (2021).
- 125 Welch, S. R. *et al.* Analysis of Inactivation of SARS-CoV-2 by Specimen Transport Media, Nucleic Acid Extraction Reagents, Detergents, and Fixatives. *J Clin Microbiol* **58**, doi:10.1128/JCM.01713-20 (2020).